The Syntheses and Reactivity of Heavier Group 14 Element-Transition Metal Heterobimetallic Complexes and their Catalytic Applications

By

QIHAO ZHU

DISSERTATION

Submitted in partial satisfaction of the requirements for the degree of

DOCTOR OF PHILOSOPHY

in

Chemistry

in the

OFFICE OF GRADUATE STUDIES

of the

UNIVERSITY OF CALIFORNIA

DAVIS

Approved:

Philip P. Power, Chair

Frank E. Osterloh

Louise A. Berben

Committee in Charge

2022

List of Symbols, Nomenclature, or Abbreviations

Å	Angstrom (10^{-10} m)
Ar^{Me_6}	C_6H_3-2,6-(C_6H_2-2,4,6-Me_3)$_2$
Ar^{iPr_4}	C_6H_3-2,6-(C_6H_3-2,6-$^{i}Pr_2$)$_2$
Ar^{iPr_6}	C_6H_3-2,6-(C_6H_2-2,4,6-$^{i}Pr_3$)$_2$
Ar^{iPr_8}	C_6H-2,6-(C_6H_2-2,4,6-$^{i}Pr_3$)$_2$-3,5-$^{i}Pr_2$
Ar^{tBu_6}	C_6H_3-2,6-(C_6H_2-2,4,6-$^{t}Bu_3$)$_2$
κ	denticity
η	hapticity
ca.	approximately
cf.	comparison
DFT	Density Functional Theory
Dipp	C_6H_3-2,6-$^{i}Pr_2$
Ether	Diethyl Ether
IR	Infrared
Pr	n-propyl
^{i}Pr	isopropyl
Mes	C_6H_2-2,4,6-Me_3
^{n}Bu	n-butyl

^{t}Bu	t-butyl
Cp	Cyclopentadienyl
Cp*	Pentamethylcyclopentadienyl
Trip	C_6H_2-2,4,6-$^{i}Pr_3$
THF	Tetrahydrofuran
Py	Pyridine
Ph	Phenyl
pin	pinacolato
NMR	Nuclear Magnetic Resonance
COSY	correlation spectroscopy
HSQC	heteronuclear single quantum coherence
DOSY	diffusion-ordered spectroscopy
NOESY	nuclear Overhauser effect spectroscopy
UV-vis	Ultraviolet–visible
ΔG	Gibbs Free-Energy Change
ΔH	Enthalpy Change
ΔS	Entropy Change
δ	chemical shift
ε	molar absorption coefficient
ν	frequency

Abstract

This dissertation describes the reactivity of a terphenyl-substituted heavier group 14 dimetallyne, and a diplumbyne with dinuclear transition metal carbonyls, as well as the synthesis and reactivity of certain divalent tin hydrides. The solid-state structures of the reaction products of these preparations are determined by single X-ray crystallography. Other characterization methods include nuclear magnetic resonance spectroscopy, UV-visible spectroscopy, infrared spectroscopy.

A summary of the previous investigations of the synthesis and reactivity of heavy group 14 dimetallynes and the prior studies on the synthesis and reactivity of divalent tin hydrides are described in **Chapter 1**.

Chapter 2: In this chapter, it is shown that the metathesis reactions of the diplumbyne $Ar^{iPr6}Pb{\equiv}PbAr^{iPr6}$ (Ar^{iPr6} = $-C_6H_3$–2,6-(C_6H_2–2,4,6-$^{i}Pr_3$)$_2$) with the dinuclear metal carbonyls $Mn_2(CO)_{10}$, $Fe_2(CO)_9$, and $Co_2(CO)_8$ under mild conditions afford the complexes $Mn(CO)_5(PbAr^{iPr}{}_6)$ (**1**), $Fe(CO)_4(PbAr^{iPr}{}_6)_2$ (**2**), and $Co_4(CO)_9(PbAr^{iPr}{}_6)_2$ (**3**), respectively. Complexes **1**–**3** are structurally characterized by single-crystal X-ray diffraction and spectroscopically characterized by ^{1}H, $^{13}C\{^{1}H\}$, $^{59}Co\{^{1}H\}$, and $^{207}Pb\{^{1}H\}$ NMR; UV–vis; and IR methods. They are rare examples of species formed by the direct reaction of a group 14 dimetallyne with transition metal carbonyls. Complexes **1** and **2** feature Mn–Pb or Fe–Pb single bonds, whereas in **3** a Co–Pb cluster is formed in which the plumbylidyne moiety bridges either an edge or a face of a Co_4 carbonyl cluster.

Chapter 3: In this chapter, it is shown that the reaction of the aryltin(II) hydrides $\{Ar^{iPr4}Sn(\mu\text{-}H)\}_2$ or $\{Ar^{iPr6}Sn(\mu\text{-}H)\}_2$ (Ar^{iPr4} = –C_6H_3-2,6-(C_6H_3-2,6-$^{i}Pr_2$)$_2$, Ar^{iPr6} = –C_6H_3-2,6-(C_6H_2-2,4,6-$^{i}Pr_3$)$_2$) with two equivalents of the molybdenum carbonyl [$Mo(CO)_5$(THF)] yields the divalent tin hydride transition metal complexes, $Mo(CO)_5\{Sn(Ar^{iPr}{}_6)H\}$, (**1**), or

$Mo(CO)_5\{Sn(Ar^{iPr}{}_4)(THF)H\}$ (**2**), respectively. Complex **1** effects the facile hydrostannylation of carbon dioxide, to yield $Mo(CO)_5\{Sn(Ar^{iPr}{}_6)(\kappa^2\text{-}O,O'\text{-}O_2CH)\}$, (**3**), which features a bidentate formate ligand coordinating to the tin atom. Reaction of **3** with the pinacolborane, HBpin (pin = pinacolato), in benzene regenerates **1** in quantitative yield by NMR spectroscopy. All complexes are characterized by X-ray crystallography, as well as by UV-visible, IR, and multinuclear NMR spectroscopies. The isolation of **1** and **2** is consistent with the existence of monomeric forms of $\{Ar^{iPr}{}_4Sn(\mu\text{-}H)\}_2$ and $\{Ar^{iPr}{}_6Sn(\mu\text{-}H)\}_2$ in solution. Regeneration of **1** from **3** *via* reaction with pinacolborane as the hydrogen source shows the catalytic potential of **1** in the hydrogenation of CO_2.

Chapter 4: In this chapter, it is shown that reaction of the aryltin(II) hydride $\{Ar^{iPr6}Sn(\mu\text{-}H)\}_2$ (Ar^{iPr6} = -C_6H_3-2,6-(C_6H_2-2,4,6-$^i Pr_3$)$_2$) with two equivalents of the tungsten carbonyl THF complex, $[W(CO)_5(THF)]$, gives the divalent tin hydride transition metal complex, $W(CO)_5\{Sn(Ar^{iPr6})H\}$, (**1**). Complex **1** reacts rapidly with ethylene, or propylene under ambient conditions to yield the corresponding hydrostannylated organometallic species, $W(CO)_5\{Sn(Ar^{iPr6})(Et)\}$ (**2**), or $W(CO)_5\{Sn(Ar^{iPr6})(^n Pr)\}$ (**3**), via olefin insertion into the Sn-H bond. Treatment of **1** with the Lewis base dbu (dbu = 1,8-diazabicycloundec-7-ene) yields the Lewis acid-base complex, $W(CO)_5\{Sn(Ar^{iPr6})(dbu)H\}$ (**4**), indicating that the Lewis acidity of the tin atom is preserved in **4**. The complexes were characterized by X-ray crystallography, and by UV-visible, FT-IR, and multinuclear NMR spectroscopies. DFT calculations by Dr. Petra Vasko suggest hydrostannylation of ethylene with **1** proceeds via coordination of ethylene to the tin atom, then insertion into the Sn-H bond. Further computational study on the reactivity of **1** towards Ph_3SiH indicated that the rate-determining step involves the metathesis reaction of a Sn-C/Si-H bond with a very high energy barrier being 71.3 kcal/mol. The calculated proton abstraction product of **1** with dbu, $[W(CO)_5\{Sn(Ar^{iPr6})\}]^+[H(dbu)]^-$, is 18.2 kcal/mol less stable than the observed coordination product **4**.

Acknowledgments

First, I would like to express my deep gratitude to my advisor, Prof. Philip Power. It was a great honor to have worked alongside a highly respected scholar, and I thank him for his support and encouragement throughout my Ph.D., and his expertise in the field of organometallic chemistry. His dedication and passion for science will always be an inspiration to me. I thank Dr. James Fettinger and Dr. Marilyn Olmstead for assistance in X-ray crystallography throughout this work. I thank Dr. Petra Vasko for providing the computational results for chapter 2 & 4.

I would like to thank Prof. James Ames, Dr. Jeffrey Walton, Dr. Derrick Kaseman, and Dr. Ping Yu for their mentorship throughout my time as an NMR facility teaching assistant, and their assistance in NMR spectroscopy.

I thank Prof. Frank Osterloh, and Prof. Louise Berben for their time and support as my dissertation committee.

I would like to thank all the Power group members for maintaining a friendly & cooperative atmosphere in the lab and for their useful feedback on my work. The lab members include (in no particular order): Prof. Clifton Wagner, Jade Pratt, Dr, Madison McCrea-Hendrick, Dr. Cary Stennett, Joshua Queen, Dr. Shuai Wang, Dr. Kristian Mears, Dr. Ting-Yi Lai, Dr. Pei Zhao, Robert Tureski, Jan Kulenkampff, Wenxing Zou, Alice Phung, Connor McLoughlin, Sam Cao, Chia-Yuan Chen, Dr. Luis Perla, Dr. Beate Steller, Prof. Chun-Yi Lin, Prof. David Manke, and Dr. Hannah Sullivan. Special thanks to Prof. Clifton Wagner for teaching me all the Schlenk techniques upon my arrival in the group, and proofreading several manuscripts; Dr. Cary Stennett, for his kind help in maintaining the laboratory, and proofreading several manuscripts; Josh Queen, for his useful suggestions on laboratory work, and proofreading several manuscripts; Dr. Kristian Mears, for his kind help with laboratory

maintenance, and useful suggestions on laboratory work; Dr. Ting-Yi Lai, for his useful suggestions for experimental work; Wenxing Zou, for her useful suggestions on laboratory work, and her kind help with laboratory maintenance.

I would like to thank my friends that I have met at UC Davis (in no particular order), Allan He, Zheng Ju, and Wen Fu, for all the joys and fun we shared throughout my time at Davis.

Finally, I would like to express my deep gratitude to my parents and other family members, especially my parents: Weisheng Zhu, and Aiwen Li for their continuous support, unconditional love, and encouragement. I could not have done this without them.

Table of Contents

Chapter 1: The Synthesis and Reactivity of group 14 Dimetallynes and Divalent Tin Hydrides

1.1: General Introduction

Recent advances in main group organometallic chemistry stem from the early investigations of the validity of the "double bond rule" for heavier congeners of carbon which commenced in the mid-1970s.[1-3] The "double bond rule" states that heavy p-block elements, with having a principal quantum number greater than two, cannot form stable multiple bonds.[4,5] However, the rule was unequivocally disproved with the synthesis and isolation of the first heavy alkene analogues of germanium and tin, R_2EER_2 (E = Ge, Sn), by Lappert and coworkers in 1976.[6-8] This discovery was soon followed by the isolation of doubly bonded disilene, $Mes_2Si{=}SiMes_2$ (Mes = C_6H_2- 2,4,6-Me_3) in 1981, by West and coworkers,[9] and the isolation of doubly bonded diphosphene, ArP=PAr (Ar = C_6H_2-2,4,6-$^tBu_3$), by Yoshifuji and coworkers in 1981.[10] This confirmed that the use of sterically bulky substituents enabled the stabilization of reactive multiply bonded species of heavy main group elements.[11-13]

In addition to the breakthroughs in the synthesis of the rare heavy main group compounds, numerous efforts were also made in reactivity studies with important small molecules, such as dihydrogen,[14-17] and ethylene.[18-21] The theme of these studies was focused on comparisons between transition metals and heavy main group metals in the catalytic applications of organic transformation, where the key steps involving reactions such as oxidative addition or reductive elimination cycles can be readily observed at low valent main group metal centers.[22-25]

This chapter will serve as general introduction and motivation on the reactivity of multiple-bonded dimetallynes, RE≡ER (E = Sn, Pb), and on the reactivity of divalent tin hydrides, respectively.

1.2: Synthesis of Heavy Group 14 Elements Dimetallynes

The heavy group 14 alkyne analogues, distannynes and diplumbynes, are compounds of the general formula, RE≡ER. The remarkable chemical differences between the alkynes and their heavier congeners arise from the difference in their E-E bonding, whereas alkynes mostly feature linear structures, their heavier analogues display trans-bent structures.[11,12] The conventional valence orbital hybridization, which is used to explain the geometries of alkanes (sp^3), alkenes (sp^2), and alkynes (sp),[26] fails when the orbitals to be hybridized have different probable radii, as in the heavier tetrel atoms Si-Pb. The lower tendency to hybridize tends to preserve the distinctive features of the valence s and p orbitals in which the s electrons remain unhybridized and often occupied by a pair of valence electrons, also known as the inert pair effect, which is reflected in their trans-bent structures. The bent geometry creates both electronic unsaturation and electronic richness which results in increased reactivity at the heavier element centers.[11] The molecular orbital (MO) analysis of the bonding in heavier group 14 element alkyne analogues can also be explained on the basis of a second order Jahn–Teller effect,[27-33] which arises from a symmetry allowed, intramolecular mixing of an unoccupied non-bonding or anti-bonding orbital with a bonding orbital. The consequent orbital mixing introduces non-bonding electron character in a HOMO which can drastically affect the degree of trans-bending on molecular shape. (Figure 1.1)

The isolation of the first heavy alkene analogues of germanium and tin by Lappert and coworkers[7,8] led to the recognition that the use of sterically encumbering substituents can be used to provide kinetic stabilization to these compounds. Generally, the absence of steric

encumbering substituents will lead to thermodynamically favored oligomerization or isomerization of the corresponding species, as predicted by quantum chemical calculations.[11]

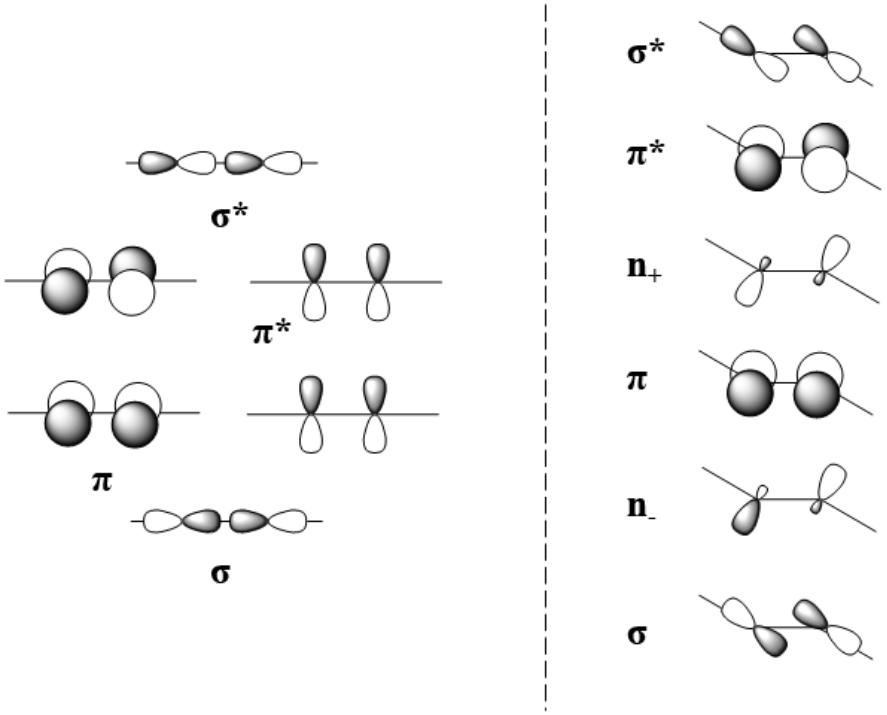

Figure 1.1: Illustration of orbital scheme of the conventional bonding model for alkyne (left) vs. second order Jahn-Teller distortion in HE≡EH (E = Si, Ge, Sn, Pb) (right).[27-33]

The sterically crowding substituents can also generate London dispersion effects, arising from attraction between the ligand C-H moieties which can produce counterintuitive steric effects.[34,35] London dispersion interaction is a weak force between atoms or molecules with induced dipoles, such as the H atoms from the ligand C−H moieties. These London dispersion effects are not as widely recognized as key factors in the stabilization of low-coordination number or rare oxidation state complexes due to the relative weakness (ca. 1 kcal/mol, between two hydrogen atoms) of individual London dispersion interactions owing to their heavy dependence on distance. However, accumulation of numerous H···H interactions can collectively give rise to an energy of several tens of kcal/mol. Throughout this dissertation,

however, the main focus is on the application of terphenyl ligands, which are a type of monoanionic aryl ligand that was earlier known to display London dispersion effects.[35] These ligands are used in the stabilization of low-valent and low-coordinate heavy group 14 element compounds, and investigations on their reactivity. In Figure 1.2, the listed terphenyl ligands are in the order of increasing steric bulkiness from left to right, Ar^{iPr4} and Ar^{iPr6} are used throughout this work.

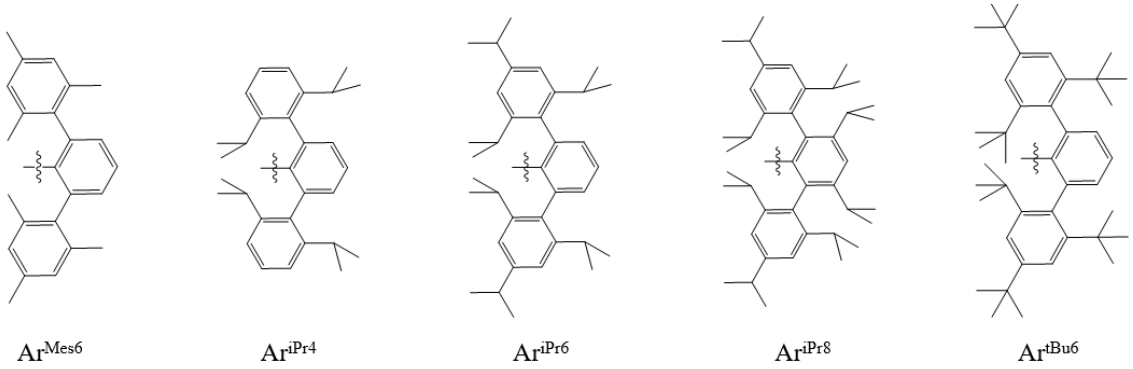

Figure 1.2: Examples of sterically encumbering terphenyl groups.

The synthesis and characterization of the first stable, heavy group 14 element alkyne analogue, the diplumbyne $Ar^{iPr6}Pb{\equiv}PbAr^{iPr6}$, was reported in 2000 by our group.[36] The syntheses of similar derivatives of remaining of heavier group 14 elements were later accomplished.[37-40] The syntheses of the series included two major pathways: reductive dehalogenation, and hydrogen elimination (only known for E = Sn, Pb).[11] The $Ar^{iPr6}Pb{\equiv}PbAr^{iPr6}$ was synthesized by addition of $LiAlH_4$ ether solution into the ether solution of $\{Ar^{iPr6}Pb(\mu\text{-}Br)\}_2$ at ca. -78 °C,[36] where it was believed to proceed via the hydrogen elimination of the hydrido-plumbylene intermediate, $\{Ar^{iPr6}Pb(\mu\text{-}H)\}_2$ which was later isolated by Wesemann and coworkers.[41] The molecular structure of diplumbyne, (Figure 1.3) $Ar^{iPr6}Pb{\equiv}PbAr^{iPr6}$, featured a long Pb−Pb bond, 3.1881(1) Å, cf. 2.9 Å predicted from the sum of the covalent radii,[42] and the Pb−Pb−C angle, 94.26(4)°. The observed Pb−Pb−C angle, which is relatively close to 90°, is consistent with the increasing nonbonding electron pair character at the group 14 element descending the group.

The long Pb-Pb bond can be considered as a single bond with two non-bonding electron pairs, one of each lead, which consist of mostly 6s character, and the remaining single bond is a result of head-to-head overlap of a 6p orbital from each lead atom. This result is accounted for the decreasing hybridization of the elements that occurs upon descending the group.[27-33]

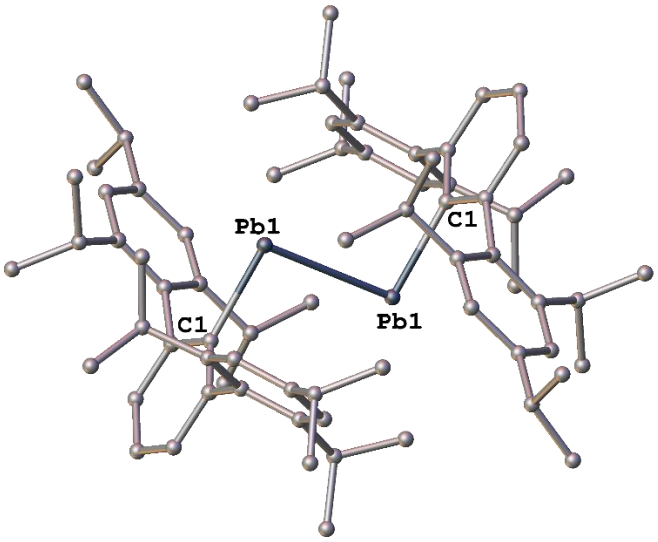

Figure 1.3: Solid-state molecular structure of $Ar^{iPr6}Pb{\equiv}PbAr^{iPr6}$ (hydrogen atoms are not shown for clarity. Thermal ellipsoids are shown at 30% probability).[36]

1.3: Reactivity of Dimetallynes of Sn and Pb with Transition Metals

The heavy group 14 element dimetallynes RE≡ER (M = Sn, Pb; R = aryl group) are stable compounds with formal triple bonds between heavier group 14 elements. In a recent study from this group, the reversible dissociation of the distannyne into the corresponding Sn(I) radicals in toluene was detected by EPR spectroscopy, which suggested bond metathesis reactions featuring the heavier group 14 elements might be feasible.[43] Van 't Hoff analysis estimated the enthalpy of dissociation of the Sn≡Sn bond to be ΔH_{diss} = 17.2 ± 1.7 kcal/mol (scheme 1.1).[43]

Scheme 1.1: Reversible dissociation of Sn-Sn triple bond in a distannyne.[43]

The reactions of distannyne, $Ar^{iPr4}Sn{\equiv}SnAr^{iPr4}$ with the group 6 transition-metal carbonyls $M(CO)_6$ (M = Cr, Mo, W) under UV irradiation led to the cleavage of the E–E triple bond and the formation of the complexes $\{Ar^{iPr4}SnM(CO)_4\}_2$ (M = Cr, Mo, W).[44] Structural analyses of the products showed that these have a nearly planar rhomboid M_2E_2 core with three-coordinate group 14 atoms. In addition, the reaction of the molybdenum−molybdenum triple-bonded dimer $(CO)_2CpMo{\equiv}MoCp(CO)_2$ with the dimetallynes $ArM{\equiv}MAr$ (Ar = Ar^{iPr4} or Ar^{iPr6}; M = Sn or Pb) afforded $ArM{\equiv}MoCp(CO)_2$ (Ar = Ar^{iPr4} or Ar^{iPr6}; M = Sn or Pb), where the reactions represent the first example for metathesis between two metal−metal triple bonds to afford isolable products.[45] Theses investigation led to the further exploration on the metathesis reactions of the diplumbyne $Ar^{iPr6}PbPbAr^{iPr6}$ with the dinuclear metal carbonyls $Mn_2(CO)_{10}$, $Fe_2(CO)_9$, and $Co_2(CO)_8$ that are described in **Chapter 2**.

1.4: Synthesis of Divalent Tin Hydrides

Tetravalent heavier group 14 element hydrides are widely used in numerous organic transformations under mild conditions.[46-54] However, the corresponding reactions of their divalent hydride congeners remained underexplored. Low coordinate divalent tin(II) hydrides have attracted increasing interest due to their potential catalytic applications. These reactivities are largely due to their coordinative unsaturation and their hydridic reactivity with unsaturated molecules.[55-57]

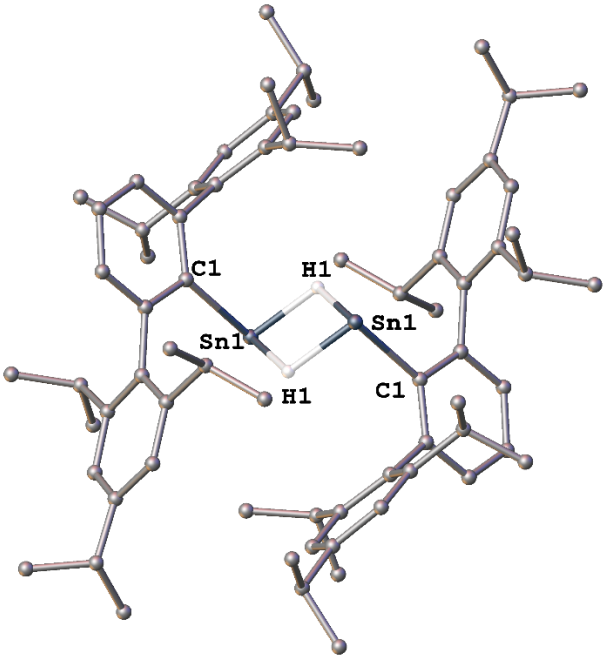

Figure 1.4: Solid-state molecular structure of $Ar^{iPr6}Sn(\mu\text{-}H)$ (hydrogen atoms are not shown for clarity, except hydrogens bonded to tin. Thermal ellipsoids are shown at 30% probability).

In 2000, the first stable tin(II) hydride, $\{Ar^{iPr6}Sn(\mu\text{-}H)\}_2$ (Ar^{iPr6} = -C_6H_3-2,6-(C_6H_2-2,4,6-$^i Pr_3$)$_2$), was reported, which featured a dimeric hydrogen bridged structure (Figure 1.4).[58] This was synthesized by addition of diisobutylaluminum hydride ether solution into ether solution of $\{Ar^{iPr6}Sn(\mu\text{-}Cl)\}_2$ at ca. -78°C. Later, Roesky and coworkers reported the monomeric tin(II) hydrides [{HC(CMeNAr)$_2$}SnH] (Figure 1.5),[59] and [{ArN=C(Me)]$_2C_6H_3SnH$][60] (Ar = 2,6-$iPr_2C_6H_3$). These compounds featured terminal Sn-H bonds with the support of electron-rich donor ligands. Synthetic methods to access divalent tin hydrides can be categorized in either salt-metathesis[58] or an oxidative route;[61] the salt-metathesis reaction generally involves reaction between a chlorostannylene species and a hydride derivative of an electropositive element which drives the reaction by salt elimination, whereas the oxidative route involves the facile activation of dihydrogen by the distannyne and results in the isolation of the corresponding hydride species.

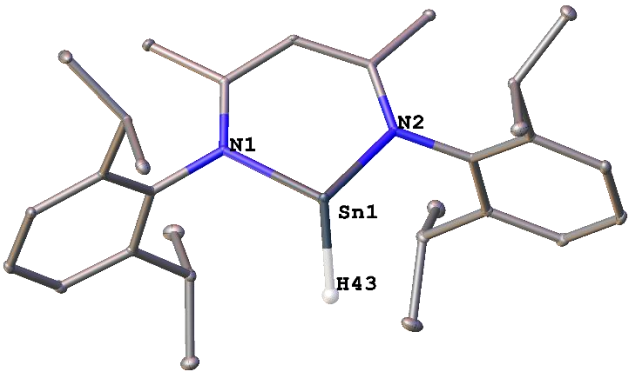

Figure 1.5: Solid-state molecular structure of [{HC(CMeNAr)$_2$}SnH] (hydrogen atoms are not shown for clarity, except hydrogens bonded to tin. Thermal ellipsoids are shown at 30% probability).[59]

1.5: Reactivity of Divalent Tin Hydrides

There has been a growing interest in the reactivity of tin(II) hydrides with important small molecules (e.g. dihydrogen, alkenes, alkynes, ketones, etc.),[62-66] and transition metal complexes.[67,68] The structure of {Ar^{iPr6}Sn(μ-H)}$_2$ (Ar^{iPr6} = -C$_6$H$_3$-2,6-(C$_6$H$_2$-2,4,6-^{i}Pr$_3$)$_2$) can be considered as a dimeric hydrido-stannylene, and it is very likely that this dimer will dissociate into monomer in solution, despite no success in the isolation of such species. The interactions between hydrido-tetrylenes and unsaturated small molecules can be explained by the singlet electronic ground-state for heavier tetrylenes. The singlet electronic ground-state indicates the presence of a vacant p orbital and lone pair electrons in their valence s shell, which allows for interactions with unsaturated small molecules.[69] This reactivity is similar to the Dewar-Chatt-Duncason model for transition metals,[70,71] which provides the theoretical foundation for further investigation on reactivity of heavier tetrylenes.[22] However, the lone pair on heavier tetrel atoms is relatively inert, hence most tetrylene reactivity is initiated by the interaction of the reagents with the vacant p orbitals. Examples include activation of NH$_3$ with Ge(Ar^{Me6})$_2$ and Ge(Ar^{iPr4})$_2$ to afford the respective oxidative addition product, (Ar^{Me6})$_2$GeH(NH$_2$) and

$(Ar^{iPr4})_2GeH(NH_2)$, where the reaction was initiated by the coordination of the ammonia to the empty p-orbital of the germanium atom,[72] as well as the isolations of Lewis base-stabilized hydrido-stannylenes reported by Wesemann and coworkers.[73-75] Despite of the inertness of the lone pair on heavier tetrel atom in tetrylene, probing the Lewis basicity of heavier tetrylenes is also of vital significance, early examples of their Lewis basic reactivity can be described in the coordination reactions of tetrylene to transition metal complexes as summarized by Petz.[76]

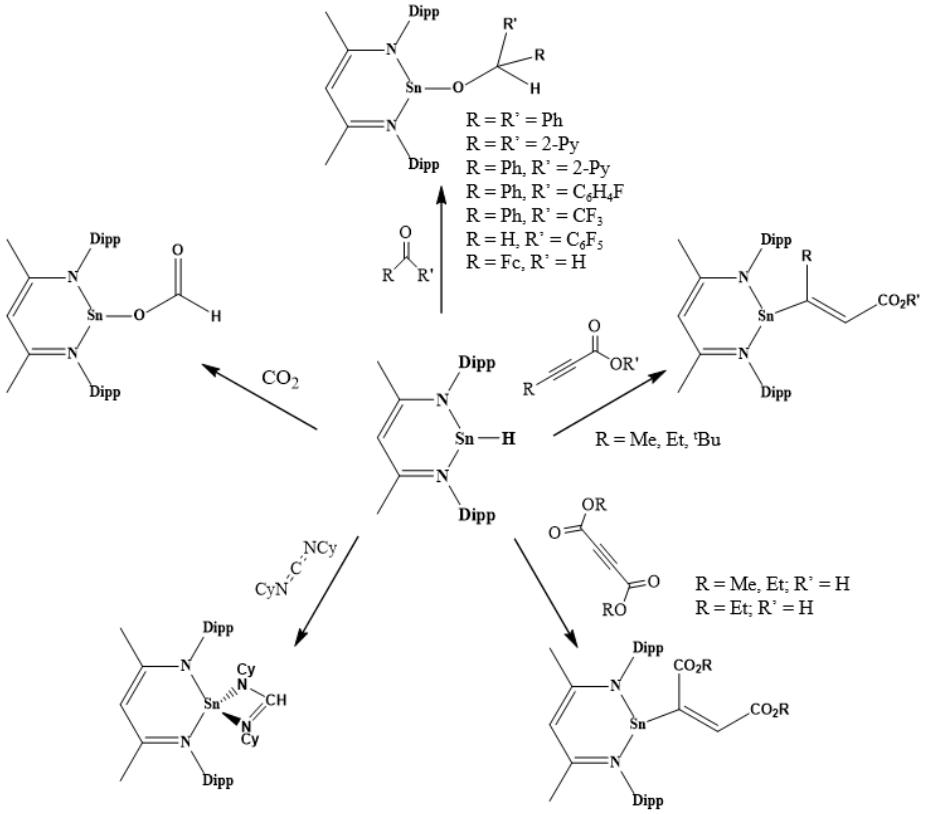

Scheme 1.2: Reactivity of [{HC(CMeNAr)$_2$}SnH] towards unsaturated molecules.[63,77]

As mentioned above, low-valent group 14 element hydrides showed significantly improved hydridic reactivity compared to their tetravalent congeners. For example, the hydridic reactivity of divalent tin hydride, [{HC(CMeNAr)$_2$}SnH] (Ar = 2,6-$iPr_2C_6H_3$), has been thoroughly studied by Roesky and coworkers (Scheme 1.2), as it displayed rapid hydrostannylation towards unactivated ketones under ambient conditions.[63] Additionally, reactivity of this tin hydride towards activated alkynes and a carboimide was also investigated.

In **Chapter 3**, we investigated the reaction of the aryltin(II) hydrides $\{Ar^{iPr4}Sn(\mu\text{-}H)\}_2$ or $\{Ar^{iPr6}Sn(\mu\text{-}H)\}_2$ (Ar^{iPr4} = $-C_6H_3$-2,6-(C_6H_3-2,6-$^{i}Pr_2)_2$, Ar^{iPr6} = $-C_6H_3$-2,6-(C_6H_2-2,4,6-$^{i}Pr_3)_2$) with two equivalents of the molybdenum carbonyl $[Mo(CO)_5(THF)]$ which yielded the divalent tin hydride transition metal complexes. The catalytic potential of this complex towards carbon dioxide was examined.

Recent work in our group has shown that $\{Ar^{iPr4}Sn(\mu\text{-}H)\}_2$ and $\{Ar^{iPr6}Sn(\mu\text{-}H)\}_2$ can rapidly hydrostannylate norbornene and norbornadiene as well as other alkenes at ambient temperature. These results suggested that the monomeric $Ar^{iPr4}SnH$/$Ar^{iPr6}SnH$ unit, which is in equilibrium with the dimer, is the reactive species in hydrostannylation reactions. The rearrangement of norbornadiene to the nortricyclic group can also be accessed via thermolysis of the mono-hydrostannylation product of norbornadiene with the tin hydrides (Scheme 1.3).[62] In **Chapter 4**, we investigated the reaction of the aryltin(II) hydride $\{Ar^{iPr6}Sn(\mu\text{-}H)\}_2$ (Ar^{iPr6} = $-C_6H_3$-2,6-(C_6H_2-2,4,6-$^{i}Pr_3)_2$) with two equivalents of the tungsten carbonyl $[W(CO)_5(THF)]$ which yielded the divalent tin hydride transition metal complex. The catalytic application of this complex towards olefins was examined. The Lewis acidity of this complex was also studied with the Lewis base dbu (dbu = 1,8-diazabicycloundec-7-ene). DFT calculations were used to give mechanistic insights on hydrostannylation of ethylene with the synthesized complex.

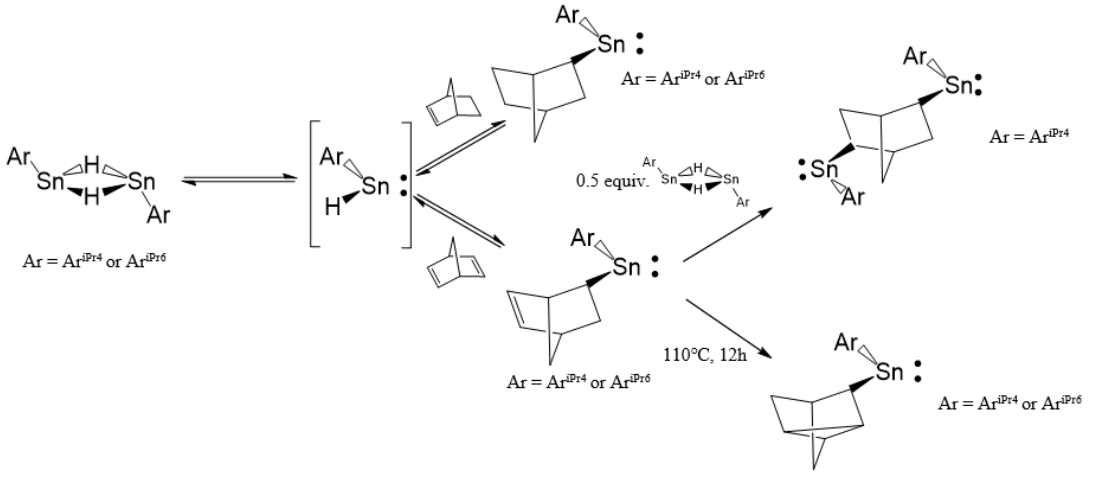

Scheme 1.3: Reactivity of $\{Ar^{iPr4}Sn(\mu\text{-}H)\}_2$ and $\{Ar^{iPr6}Sn(\mu\text{-}H)\}_2$ towards norbornene or norbornadiene.[62]

1.6: Discussion

In order to further investigate the metathesis reaction between the diplumbyne $Ar^{iPr6}PbPbAr^{iPr6}$ and metal-metal bonded species, we examined the reactions of the diplumbyne $Ar^{iPr6}PbPbAr^{iPr6}$ with the dinuclear metal carbonyls $Mn_2(CO)_{10}$, $Fe_2(CO)_9$, and $Co_2(CO)_8$ in **Chapter 2**. The isolated compounds are rare examples of species formed by the direct reaction of a group 14 dimetallyne with transition metal carbonyls.

The hydridic reactivity of $\{Ar^{iPr4}Sn(\mu\text{-}H)\}_2$ or $\{Ar^{iPr6}Sn(\mu\text{-}H)\}_2$ has been extensively studied, as it can readily hydrostannylate alkenes or carbon dioxide under ambient conditions, which suggest the presence of reactive monomer, ArSnH (Ar = Ar^{iPr4} or Ar^{iPr6}), in solution.[62] However, no further exploration on the catalytic application of relevant species has been done. In **Chapters 3** and **4**, it is shown that the reactive monomer, ArSnH (Ar = Ar^{iPr4} or Ar^{iPr6}) can be stabilized by Lewis acidic moieties, $M(CO)_5$ (M = Mo, W), and the reactivity of consequent products were explored towards unsaturated compounds such as carbon dioxide or olefins, and their potentials in catalytic applications were investigated.

1.7: References

1. Dasent, W. E. (1965). *Nonexistent Compounds and Compounds of Low Stability*. Marcel Dekker: New York, 1965.
2. Pitzer, K. S., The Thermodynamic and Physical Properties of the Elements. *J. Am. Chem. Soc.,* **1948,** *70*, 2140–2145.
3. Mulliken, R. S., Overlap Integrals and Chemical Binding. *J. Am. Chem. Soc.,* **1950**, *72*, 4493–4503.

4. Pettit, L. D., Multiple Bonding and Back-co-ordination in Inorganic Compounds. *Q. Rev. Chem. Soc.*, **1971**, *25*, 1-29.

5. Jutzi, P., New Element-Carbon (p-p)n Bonds. *Angew. Chem. Int. Ed. Engl.*, **1975**, *14*, 232-245.

6. Davidson, P.J.; Lappert, M.F., Stabilisation of metals in a low co-ordinative environment using the bis(trimethylsilyl)methyl ligand; coloured Sn^{II} and Pb^{II} alkyls, $M[CH(SiMe_3)_2]_2$ *J. Chem. Soc., Chem. Commun.*, **1973**, 317a-317a.

7. Goldberg, D. E.; Harris, D. H.; Lappert, M. F.; Thomas, K. M., A New Synthesis of Divalent Group 4B Alkyls $M[CH(SiMe_2)_2]_2$ (M=Ge or Sn), and the Crystal and Molecular Structure of the Tin Compound *J. Chem. Soc., Chem. Commun.*, **1976**, 261-262.

8. Goldberg, D.E.; Hitchcock, P.B.; Lappert, M.F.; Thomas, K.M.; Thorne, A.J., Subvalent Group 4B metal alkyls and amides. Part 9. Germanium and tin alkene analogues, the dimetallenes M_2R_4[M = Ge or Sn, R = $CH(SiMe_3)_2$]: X-ray structures, molecular orbital calculations for M_2H_4, and trends in the series $M_2R'_4$[M = C, Si, Ge, or Sn; R′= R, Ph, $C_6H_2Me_3$-2,4,6, or $C_6H_3Et_2$-2,6] *J. Chem. Soc., Dalton Trans.*, **1986**, 2387-2394

9. West, R.; Fink M. J. ; Michl, J., Tetramesityldisilene, a Stable Compound Containing a Silicon-Silicon Double Bond. *Science*, **1981**, *214*, 1343– 1344

10. Yoshifuji, M. ; Shima, I. ; Inomoto, N. ; Hirotsu, K. ; Higuchi T., Synthesis and structure of bis(2,4,6-tri-tert-butylphenyl)diphosphene: isolation of a true phosphobenzene. *J. Am. Chem. Soc.*, **1981**, *103*, 4587− 4589.

11. Hanusch, F.; Groll, L.; Inoue, S., Recent Advances of Group 14 Dimetallenes and Dimetallynes in Bond Activation and Catalysis. *Chem. Sci.* **2021**, *12*, 2001–2015.

12. Kutzelnigg, W., Chemical Bonding in Higher Main Group Elements. *Angew. Chem. Int. Ed.* **1984**, *23*, 272–295.

13. West, R., Multiple Bonds to Silicon: 20 Years Later. *Polyhedron* **2002**, *21*, 467–472.

14. Spikes, G. H.; Fettinger, J. C.; Power, P. P., Facile Activation of Dihydrogen by an Unsaturated Heavier Main Group Compound. *J. Am. Chem. Soc.* **2005**, *127*, 12232–12233.

15. Peng, Y.; Brynda, M.; Ellis, B. D.; Fettinger, J. C.; Rivard, E.; Power, P. P., Addition of H_2 to Distannynes under Ambient Conditions. *Chem. Commun.* **2008**, 6042-6044.

16. Li, J.; Schenk, C.; Goedecke, C.; Frenking, G.; Jones, C., A Digermyne with a Ge–Ge Single Bond That Activates Dihydrogen in the Solid State. *J. Am. Chem. Soc.* **2011**, *133*, 18622–18625.

17. Protchenko, A. V.; Birjkumar, K. H.; Dange, D.; Schwarz, A. D.; Vidovic, D.; Jones, C.; Kaltsoyannis, N.; Mountford, P.; Aldridge, S., A Stable Two-Coordinate Acyclic Silylene. *J. Am. Chem. Soc.* **2012**, *134*, 6500–6503.

18. Peng, Y.; Ellis, B. D.; Wang, X.; Fettinger, J. C.; Power, P. P., Reversible Reactions of Ethylene with Distannynes under Ambient Conditions. *Science* **2009**, *325*, 1668–1670.

19. Rodriguez, R.; Gau, D.; Kato, T.; Saffon-Merceron, N.; De Cózar, A.; Cossío, F. P.; Baceiredo, A., Reversible Binding of Ethylene to Silylene-Phosphine Complexes at Room Temperature. *Angew. Chem. Int. Ed.* **2011**, *50*, 10414–10416.

20. Hadlington, T. J.; Li, J.; Hermann, M.; Davey, A.; Frenking, G.; Jones, C., Reactivity of Amido-Digermynes, LGeGeL (L = Bulky Amide), toward Olefins and Related Molecules: Facile Reduction, C–H Activation, and Reversible Cycloaddition of Unsaturated Substrates. *Organometallics* **2015**, *34*, 3175–3185.

21. Sasamori, T.; Sugahara, T.; Agou, T.; Sugamata, K.; Guo, J.-D.; Nagase, S.; Tokitoh, N., Reaction of a Diaryldigermyne with Ethylene. *Chem. Sci.* **2015**, *6*, 5526–5530.

22. Power, P. P., Main-Group Elements as Transition Metals. *Nature* **2010**, *463*, 171–177.

23. Peng, Y.; Ellis, B. D.; Wang, X.; Power, P. P., Diarylstannylene Activation of Hydrogen or Ammonia with Arene Elimination. *J. Am. Chem. Soc.* **2008**, *130*, 12268–12269.

24. Peng, Y.; Guo, J.-D.; Ellis, B. D.; Zhu, Z.; Fettinger, J. C.; Nagase, S.; Power, P. P., Reaction of Hydrogen or Ammonia with Unsaturated Germanium or Tin Molecules under Ambient Conditions: Oxidative Addition versus Arene Elimination. *J. Am. Chem. Soc.* **2009**, *131*, 16272–16282.

25. Rodriguez, R.; Contie, Y.; Nougué, R.; Baceiredo, A.; Saffon-Merceron, N.; Sotiropoulos, J.-M.; Kato, T., Reversible Silylene Insertion Reactions into Si−H and P−H σ-Bonds at Room Temperature. *Angew. Chem. Int. Ed.* **2016**, *55*, 14355–14358.

26. Pauling, L. The Nature of the Chemical Bond 3rd ed., *Cornell University Press: Ithaca*, 1960, p.111–120

27. Cherry, W.; Epiotis, N.; Borden, W. T., Effects of filled pi and unfilled sigma molecular orbital interactions on molecular structures. *Acc. Chem. Res.* 1977, 10, 167−173.

28. Albright, T. A.; Burdett, J. K.; Whangbo, M.-H. Orbital Interactions in Chemistry; *Wiley: New York*, 1985.

29. Kira, M., Distortion Modes of Heavy Ethylenes and Their Anions: π–* Mixing Model. *Organometallics* 2011, 30, 4459−4465.

30. Wedler, H. B.; Wendelboe, P.; Power, P. P., Second Order Jahn-Teller Structural Distortions in Multiple Bonded Higher Main Group Compounds. *Organometallics* 2018, 37, 2929−2936.

31. Power, P. P., An Update on Multiple Bonding between Heavier Main Group Elements: The Importance of Pauli Repulsion, Charge-Shift Character, and London Dispersion Force Effects. *Organometallics* **2020**, *39*, 4127–4138.

32. Fischer, R. C.; Power, P. P., π-Bonding and the Lone Pair Effect in Multiple Bonds Involving Heavier Main Group Elements: Developments in the New Millennium. *Chem. Rev.* **2010**, *110*, 3877–3923.

33. Power, P. P., Bonding and Reactivity of Heavier Group 14 Element Alkyne Analogues. *Organometallics* **2007**, *26*, 4362–4372.

34. Liptrot, D. J.; Power, P. P., London Dispersion Forces in Sterically Crowded Inorganic and Organometallic Molecules. *Nat. Rev. Chem.* **2017**, *1* ,0004.

35. Mears, K. L.; Power, P. P., Beyond Steric Crowding: Dispersion Energy Donor Effects in Large Hydrocarbon Ligands. *Acc. Chem. Res.* **2022**, *55*, 1337–1348.

36. Pu, L.; Twamley, B.; Power, P. P., Synthesis and Characterization of 2,6-$Trip_2H_3C_6PbPbC_6H_3$-2,6-$Trip_2$ (Trip = C_6H_2-2,4,6-*i*-Pr_3): a Stable Heavier Group 14 Element Analogue of an Alkyne. *J. Am. Chem. Soc.* **2000**, *122*, 3524–3525.

37. Phillips, A. D.; Wright, R. J.; Olmstead, M. M.; Power, P. P., Synthesis and Characterization of 2,6-$Dipp_2$-$H_3C_6SnSnC_6H_3$-2,6-$Dipp_2$ (Dipp = C_6H_3-2,6-Pr^i_2): a Tin Analogue of an Alkyne. *J. Am. Chem. Soc.* **2002**, *124*, 5930–5931.

38. Stender, M.; Phillips, A. D.; Wright, R. J.; Power, P. P., Synthesis and Characterization of a Digermanium Analogue of an Alkyne. *Angew. Chem. Int. Ed.* **2002**, *41*, 1785–1787.

39. Sekiguchi, A.; Kinjo, R.; Ichinohe, M. A Stable Compound Containing a Silicon-Silicon Triple Bond. *Science* **2004**, *305*, 1755–1757.

40. Queen, J. D.; Bursch, M.; Seibert, J.; Maurer, L. R.; Ellis, B. D.; Fettinger, J. C.; Grimme, S.; Power, P. P., Isolation and Computational Studies of a Series of Terphenyl Substituted Diplumbynes with Ligand Dependent Lead–Lead Multiple-Bonding Character. *J. Am. Chem. Soc.* **2019**, *141*, 14370–14383.

41. Pyykkö, P., Additive Covalent Radii for Single-, Double-, and Triple-Bonded Molecules and Tetrahedrally Bonded Crystals: A Summary. J. Phys. Chem. A 2015, 119, 2326−2337.

42. Schneider, J.; Sindlinger, C. P.; Eichele, K.; Schubert, H.; Wesemann, L., Low-Valent Lead Hydride and Its Extreme Low-Field ^{1}H NMR Chemical Shift. *J. Am. Chem. Soc.* **2017**, *139*, 6542–6545.

43. Lai, T. Y.; Tao, L.; Britt, R. D.; Power, P. P., Reversible Sn–Sn Triple Bond Dissociation in a Distannyne: Support for Charge-Shift Bonding Character. *J. Am. Chem. Soc.* **2019**, *141*, 12527–12530.

44. McCrea-Hendrick, M. L.; Caputo, C. A.; Linnera, J.; Vasko, P.; Weinstein, C. M.; Fettinger, J. C.; Tuononen, H. M.; Power, P. P., Cleavage of Ge–Ge and Sn–Sn Triple Bonds in Heavy Group 14 Element Alkyne Analogues $(EAr^{iPr4})_2$ (E = Ge, Sn; Ar^{iPr4} = C_6H_3-2,6(C_6H_3-2,6-$^{i}Pr_2$)$_2$) by Reaction with Group 6 Carbonyls. *Organometallics* **2016**, *35*, 2759–2767.

45. Queen, J. D.; Phung, A. C.; Caputo, C. A.; Fettinger, J. C.; Power, P. P., Metathetical Exchange between Metal–Metal Triple Bonds. *J. Am. Chem. Soc.* **2020**, *142*, 2233–2237.

46. Attrill, R. P.; Blower, M. A.; Mulholland, K. R.; Roberts, J. K.; Richardson, J. E.; Teasdale, M. J.; Wanders, A., Development of a Catalytic Tributyltin Hydride Cyclisation Process. *Org. Process Res. Dev.* **2000,** *4*, 98-101.

47. Dobbs, A. P.; Chio, F. K. I., 8.25 Hydrometallation Group 4 (Si, Sn, Ge, and Pb). In *Comprehensive Organic Synthesis II (Second Edition)*, Knochel, P., Ed. Elsevier: Amsterdam, 2014; pp 964-998.

48. Caprio, V., 3.04 - Ketones: Dialkyl Ketones. In *Comprehensive Organic Functional Group Transformations II*, Katritzky, A. R.; Taylor, R. J. K., Eds. Elsevier: Oxford, 2005; pp 135-214.

49. Bradley, G. F.; Stobart, S. R., Reaction of octacarbonyldicobalt with organo-silanes, -germanes, and -stannanes: formation, properties, and vibrational spectra of trimethylgermyltetracarbonylcobalt and related complexes. *J. Chem. Soc., Dalton Trans.* **1974**, 264-269.

50. Saegusa, T.; Ito, Y.; Kobayashi, S.; Hirota, K., Synthetic Reactions by a Complex Catalyst. VI. A Novel Hydrosilation of Isocyanide by Copper Catalyst. *J. Am. Chem. Soc.* **1967,** *89*, 2240-2241.

51. Beard, C. D.; Craig, J. C., Insertion of vinylidene carbenes into carbon-hydrogen and silicon-hydrogen bonds. *J. Am. Chem. Soc.* **1974,** *96*, 7950-7954.

52. Adams, R. D.; Cotton, F. A.; Cullen, W. R.; Hunter, D. L.; Mihichuk, L., Fluxional behavior of some dinuclear iron and cobalt hexacarbonyl compounds with alkylsulfur and dialkylphosphorus, -arsenic, -germanium, and -tin bridges. *Inorg. Chem.* **1975,** *14*, 1395-1399.

53. Manuel, G.; Bertrand, G.; Mazerolles, P., Synthese et rearrangements de cycles α-fonctionnels du germanium: oxa-6 diphenyl-2,2 germa-2 bicyclo[3.1.0] hexane et diphenyl-1,1 germa-1 cyclopentanol-2. etude comparative avec les derives isologues du silicium. *J. Organomet. Chem.* **1978,** *146*, 7-16.

54. Walling, C.; Cooley, J. H.; Ponaras, A. A.; Racah, E. J., Radical Cyclizations in the Reaction of Trialkyltin Hydrides with Alkenyl Halides1. *J. Am. Chem. Soc.* **1966,** *88*, 5361-5363.

55. Hadlington, T. J.; Driess, M.; Jones, C., Low-valent group 14 element hydride chemistry: towards catalysis. *Chem. Soc. Rev.* **2018,** *47*, 4176-4197.

56. Rivard, E.; Power, P. P., Recent developments in the chemistry of low valent Group 14 hydrides. *Dalton Trans.* **2008**, 4336-4343.

57. Aldridge, S.; Downs, A. J., Hydrides of the Main-Group Metals: New Variations on an Old Theme. *Chem. Rev.* **2001,** *101*, 3305-3366.

58. Eichler, B. E.; Power, P. P., [2,6-$Trip_2H_3C_6Sn(\mu$-H)]$_2$ (Trip = C_6H_2-2,4,6-*i*-Pr_3): Synthesis and Structure of a Divalent Group 14 Element Hydride. *J. Am. Chem. Soc.* **2000,** *122*, 8785-8786.

59. Pineda, L. W.; Jancik, V.; Starke, K.; Oswald, R. B.; Roesky, H. W., Stable Monomeric Germanium(II) and Tin(II) Compounds with Terminal Hydrides. *Angew. Chem. Int. Ed.* **2006,** *45*, 2602-2605.

60. Khan, S.; Samuel, P. P.; Michel, R.; Dieterich, J. M.; Mata, R. A.; Demers, J.-P.; Lange, A.; Roesky, H. W.; Stalke, D., Monomeric Sn(II) and Ge(II) hydrides supported by a tridentate pincer-based ligand. *Chem. Commun.* **2012,** *48*, 4890-4892.

61. Wang, S.; Sherbow, T. J.; Berben, L. A.; Power, P. P., Reversible Coordination of H_2 by a Distannyne. *J. Am. Chem. Soc.* **2018,** *140*, 590-593.

62. Wang, S.; McCrea-Hendrick, M. L.; Weinstein, C. M.; Caputo, C. A.; Hoppe, E.; Fettinger, J. C.; Olmstead, M. M.; Power, P. P., Tin(II) Hydrides as Intermediates in Rearrangements of Tin(II) Alkyl Derivatives. *J. Am. Chem. Soc.* **2017,** *139*, 6596-6604.

63. Jana, A.; Roesky, H. W.; Schulzke, C.; Döring, A., Reactions of Tin(II) Hydride Species with Unsaturated Molecules. *Angew. Chem. Int. Ed.* **2009,** *48*, 1106-1109.

64. Jana, A.; Roesky, H. W.; Schulzke, C.; Samuel, P. P., Reaction of Tin(II) Hydride with Compounds Containing Aromatic C−F Bonds. *Organometallics* **2010,** *29*, 4837-4841.

65. Hadlington, T. J.; Hermann, M.; Frenking, G.; Jones, C., Two-coordinate group 14 element(II) hydrides as reagents for the facile, and sometimes reversible,

hydrogermylation/hydrostannylation of unactivated alkenes and alkynes. *Chem. Sci.* **2015,** *6*, 7249-7257.

66. Hadlington, T. J.; Kefalidis, C. E.; Maron, L.; Jones, C., Efficient Reduction of Carbon Dioxide to Methanol Equivalents Catalyzed by Two-Coordinate Amido–Germanium(II) and −Tin(II) Hydride Complexes. *ACS Catal.* **2017,** *7*, 1853-1859.

67. Al-Rafia, S. M. I.; Malcolm, A. C.; Liew, S. K.; Ferguson, M. J.; Rivard, E., Stabilization of the Heavy Methylene Analogues, GeH_2 and SnH_2, within the Coordination Sphere of a Transition Metal. *J. Am. Chem. Soc.* **2011,** *133*, 777-779.

68. Maudrich, J.-J.; Widemann, M.; Diab, F.; Kern, R. H.; Sirsch, P.; Sindlinger, C. P.; Schubert, H.; Wesemann, L., Hydridoorganostannylene Coordination: Group 4 Metallocene Dichloride Reduction in Reaction with Organodihydridostannate Anions. *Chem. Eur. J.* **2019,** *25*, 16081-16087.

69. Mizuhata, Y.; Sasamori, T.; Tokitoh, N., Stable heavier carbene analogues. *Chem. Rev.* **2009**, *109*, 3479–3511

70. Dewar, M. J. S. "A review of π Complex Theory", *Bull. Soc. Chim. Fr.*, **1951**, *18*, C79.

71. Chatt, J.; Duncanson, L.A. 586. Olefin co-ordination compounds. Part III. Infra-red spectra and structure: attempted preparation of acetylene complexes. *J. Chem. Soc.***, 1953**, 2939-2947

72. Peng, Y.; Guo, J.-D.; Ellis, B. D.; Zhu, Z.; Fettinger, J. C.; Nagase, S.; Power, P. P. Reaction of Hydrogen or Ammonia with Unsaturated Germanium or Tin Molecules under Ambient Conditions: Oxidative Addition versus Arene Elimination. *J. Am. Chem. Soc.* **2009** *131*, 16272–16282.

73. Sindlinger, C. P.; Wesemann, L., Hydrogen abstraction from organotin di- and trihydrides by N-heterocyclic carbenes: a new method for the preparation of NHC

adducts to tin(II) species and observation of an isomer of a hexastannabenzene derivative [R_6Sn_6]. *Chem. Sci.* **2014,** *5*, 2739-2746.

74. Sindlinger, C. P.; Stasch, A.; Bettinger, H. F.; Wesemann, L., A nitrogen-base catalyzed generation of organotin(II) hydride from an organotin trihydride under reductive dihydrogen elimination. *Chem. Sci.* **2015,** *6*, 4737-4751.
75. Sindlinger, C. P.; Grahneis, W.; Aicher, F. S. W.; Wesemann, L., Access to Base Adducts of Low-Valent Organotin-Hydride Compounds by Controlled, Stepwise Hydrogen Abstraction from a Tetravalent Organotin Trihydride. *Chem. Eur. J.* **2016,** *22*, 7554-7566.
76. Petz, W., Transition-metal complexes with derivatives of divalent silicon, germanium, tin, and lead as ligands. *Chem. Rev.* **1986,** *86*, 1019-1047.
77. Mandal, S. K.; Roesky, H. W., Group 14 Hydrides with Low valent Elements for activation of Small Molecules. *Acc. Chem. Res.*, **2012**, 45, 298-307.

Chapter 2

Interactions of a Diplumbyne with Dinuclear Transition Metal Carbonyls to Afford Metalloplumbylenes

This work is published in Organometallics, DOI: 10.1021/acs.organomet.0c00659

Zhu, Q.; Fettinger J. C.; Vasko, P.; Power, P. P. *Organometallics* **2020**, *39*, 4629-4636.

2.1 Introduction

Organometallic complexes containing bonds between transition metals and low oxidation state group 14 element moieties are of interest because of their potential for a diverse reactivity which arises mainly from the unsaturated character of the group 14 element bound directly to the transition metal.[1] For the heavier group 14 elements, early work by Marks[2] and Lappert[3] reported the synthesis of the first isolable stannylene-transition metal complexes which were characterized spectroscopically[2-3] and structurally.[3] These initial examples have been followed by numerous other L_nMER_2 (L = ligand; M = transition metal; E = heavier group 14 element; R= organic & related substituents) complexes that have incorporated the other heavier group 14 elements and various transition metals.[4-6] Related to these complexes are species of formula L_nM-ER in which the transition metal is σ-bonded directly to a low-valent group 14 element. The first such complex, Mes*GeFe$(CO)_2$R (Mes* = supermesityl, i.e. C_6H_2-2,4,6-$^tBu_3$; R = Cp/Cp*), which was reported by Jutzi and Leue in 1994, was characterized spectroscopically.[7] Later Power and coworkers reported the synthesis of metallostannylene[8], $Cp(CO)_3MSnAr^{Me6}$, and metalloplumbylene[9], $Cp(CO)_3MSnAr^{iPr6}$ (M = Cr, Mo, or W; Ar^{Me6} = -C_6H_3-2,6-(C_6H_2-2,4,6-Me_3)$_2$; Ar^{iPr6} = -C_6H_3-2,6-(C_6H_2-2,4,6-$^iPr_3$)$_2$), analogues, and related species[10]. Attempts to generate the corresponding metallogermylenes led to the fortuitous discovery of a metallogermylyne featuring a molybdenum-germanium triple bond[11] via carbon monoxide

elimination (Scheme 2.1). In contrast, the corresponding chemistry with the chromium or tungsten species afforded several examples of the desired singly bonded metallogermylenes.[12] Work by Filippou and coworkers disclosed other routes to the metallogermylynes[13] and metallogermylenes (Scheme 2.1) and expanded their results to include the corresponding complexes with triple bonds to tin[14] and lead.[15]

***Power** et. al*[11]

$$Ar^{Me6}GeCl + Na[Mo(\eta^5\text{-}C_5H_5)(CO)_3] \xrightarrow[-CO]{THF,\ 50\ ^\circ C} (\eta^5\text{-}C_5H_5)(CO)_2Mo{\equiv}GeAr^{Me6} + NaCl$$

***Filippou** et. al*[13]

$$trans\text{-}[W(dppe)_2(N_2)_2] + Cp^*GeX \xrightarrow[-2N_2]{toluene,\ 110\ ^\circ C} trans\text{-}[(X)(dppe)_2W{\equiv}Ge\text{-}Cp^*]$$

X = halide; Ar^{Me6} = -C_6H_3-2,6-(C_6H_2-2,4,6-Me_3)$_2$
Cp* = C_5Me_5; dppe = $Ph_2PCH_2CH_2PPh_2$

Scheme 2.1: Synthetic routes to metallogermylynes.

More recent work[16] has shown that the above species can be synthesized by metathesis of the dimetallynes REER (R = terphenyl; E = Ge,[17] Sn,[18] or Pb[19]) with the single or triple bonded transition metal species, $(CO)_3CpMo\text{-}MoCp(CO)_3$ or $(CO)_2CpMo{\equiv}MoCp(CO)_2$.[16] In addition, the distannyne and digermyne were reacted with the group 6 carbonyls $M(CO)_6$ to form the cluster species, $\{Ar^{iPr4}EM(CO)_4\}_2$ (E = Ge, Sn; Ar^{iPr4} = -C_6H_3-2,6-(C_6H_3-2,6-$^iPr_3$)$_2$).[20] However, the reactivity of diplumbynes towards simple transition metal carbonyls remains hardly explored. Herein, we report the syntheses and characterizations of metalloplumbylenes $Mn(CO)_5(PbAr^{iPr6})$ (**1**), $Fe(CO)_4(PbAr^{iPr6})_2$ (**2**), $Co_4(CO)_9(PbAr^{iPr6})_2$ (**3**) by reactions of the diplumbyne, $Ar^{iPr6}PbPbAr^{iPr6}$, with the dinuclear metal carbonyls, $Mn_2(CO)_{10}$, $Fe_2(CO)_9$, $Co_2(CO)_8$.

2.2 Experimental Details

General Procedures. All operations were carried out by using modified Schlenk techniques or in a Vacuum Atmospheres OMNI-Lab drybox under an atmosphere of dry argon

or nitrogen. The lead compounds were manipulated with careful exclusion of light due to the tendency of low-valent lead compounds to decompose or disproportionate under illumination. Solvents were dried over an alumina column and degassed prior to use.[21] The compound $Ar^{iPr6}PbPbAr^{iPr6}$ was prepared according to literature procedures.[19, 22] Metal carbonyls were used as purchased without further purification. $Na[Mn(CO)_5]$ was prepared by a modified literature procedure (see SI).[23-25] The ^{1}H, $^{13}C\{^{1}H\}$, $^{59}Co\{^{1}H\}$, and $^{207}Pb\{^{1}H\}$ NMR spectra were recorded on a Varian Inova 600 MHz spectrometer. The ^{1}H and $^{13}C\{^{1}H\}$NMR spectra were referenced to the residual solvent signals in C_6D_6. The $^{59}Co\{^{1}H\}$ NMR spectrum was referenced to an external standard of a saturated solution of $K_3Co(CN)_6$ (δ 0.0 ppm) in D_2O. The $^{207}Pb\{^{1}H\}$ NMR spectra were referenced to an external standard of $PbMe_4$ (δ 0.0 ppm) in $CDCl_3$. UV-Visible spectra were recorded in dilute hexane solutions in 3.5 mL quartz cuvettes using an Olis 17 Modernized Cary 14 UV-Vis/NIR spectrophotometer. Infrared spectra were collected on a Bruker Tensor 27 ATR-FTIR spectrometer.

$Mn(CO)_5(PbAr^{iPr6})$ (**1**). Method A: ca. 50 mL of THF were added to a heavy-walled Teflon tapped Schlenk flask charged with 0.395 g (0.29 mmol) $Ar^{iPr6}PbPbAr^{iPr6}$ and 0.122 g (0.31 mmol) $Mn_2(CO)_{10}$. The flask was then sealed, and the solution was stirred at ambient temperature for 2 days, and then heated to ca. 50 ^{o}C for 5 days, during which time the color changed from dark brown to dark green. The solution was cooled to room temperature, and filtered. The filtrate was then concentrated under reduced pressure to ca. 10 mL, and cooled to a ca. -18 °C for one week to afford the product as teal colored crystals of $Mn(CO)_5(PbAr^{iPr6})$ (**1**). Yield: 0.098 g, 19 %.

Method B: 0.46 g (2.11 mmol) $Na[Mn(CO)_5]$ in ca. 40 mL Et_2O solution was added dropwise over 15 minutes to a Schlenk flask charged with 1.472 g (0.96 mmol) $[Ar^{iPr6}Pb(\mu\text{-}Br)]_2$ and ca. 30 mL of Et_2O at 0 ^{o}C,. After stirring for 2 days, during which time the color changed from yellow to teal, solvent was removed and the residue was extracted with hexanes,

and filtered. The hexanes were removed under reduced pressure and ca. 20 mL of Et_2O was added. Storage of the solution at room temperature overnight afforded teal crystals of $Mn(CO)_5(PbAr^{iPr6})$ (**1**) that were suitable for X-ray diffraction studies. Yield: 1.392 g, 82 %. ^{1}H NMR (600 MHz, C_6D_6, 298K, ppm): δ = 1.09 (br, 12H, p-$CH(CH_3)_2$), 1.19 (d, 12H, o-$CH(CH_3)_2$), $^3J_{H,H}$ = 6.6 Hz, 1.38 (d, 12H, o-$CH(CH_3)_2$), $^3J_{H,H}$ = 6.6 Hz, 2.77 (sept, 2H, p-$CH(CH_3)_2$), $^3J_{H,H}$ = 7.2 Hz, 3.40 (br, 4H, o-$CH(CH_3)_2$) $^3J_{H,H}$ = 5.8 Hz; 7.12 (br, 4H, m-Trip); 7.55 (t, 1H, p-C_6H_3) $^3J_{H,H}$ = 7.3 Hz, 8.03 (d, 2H, m-C_6H_3) $^3J_{H,H}$ = 7.3 Hz. $^{13}C\{^1H\}$ NMR (151 MHz, C_6D_6, 298K, ppm): δ = 23.54 (o-$CH(CH_3)_2$), 23.95 (o-$CH(CH_3)_2$), 27.44 (p-$CH(CH_3)_2$), 30.90 (o-$CH(CH_3)_2$), 34.78 (p-$CH(CH_3)_2$), 122.49 (br, m-Trip), 125.30 (p-C_6H_3), 128.30 (m-C_6H_3), 133.02 (i-Trip), 140.54 (p-Trip), 146.38 (o-Trip), 149.17 (o-C_6H_3), 210.94 (br, CO), 282.93 (br, CO). $^{207}Pb\{^1H\}$ NMR (125 MHz, C_6D_6, 298K, ppm): δ = 8007. ATR-FTIR: $\tilde{\nu}_{CO}$ (cm^{-1}): 1958(s), 2060(m). UV-vis (hexane) λ_{max} = nm (ε = $M^{-1}\cdot cm^{-1}$): 332 (13700), 671 (1640).

$Fe(CO)_4(PbAr^{iPr6})_2$ (**2**). ca. 50 mL of Et_2O was added to a Schlenk flask charged with 0.452 g (0.33 mmol) $Ar^{iPr6}PbPbAr^{iPr6}$ and 0.132 g (0.36 mmol) $Fe_2(CO)_9$. The solution was stirred for 2 days, during which time the color changed from dark brown to green. The solution was filtered, concentrated under reduced pressure to ca. 10 mL, and cooled to ca. -18 ℃ for one week to afford crystals of $Fe(CO)_4(PbAr^{iPr6})_2$ (**2**) as green needles that were suitable for X-ray diffraction studies. Yield: 0.295 g, 58 %. ^{1}H NMR (600 MHz, C_6D_6, 298K, ppm): δ = 1.13 (d, 12H, p-$CH(CH_3)_2$), $^3J_{H,H}$ = 5.5 Hz. 1.28 (d, 12H, o-$CH(CH_3)_2$), $^3J_{H,H}$ = 6.2 Hz, 1.36 (d, 12H, o-$CH(CH_3)_2$), $^3J_{H,H}$ = 7.0 Hz, 2.85 (sept, 2H, p-$CH(CH_3)_2$), $^3J_{H,H}$ = 6.6 Hz, 3.46 (broad, 4H, o-$CH(CH_3)_2$) $^3J_{H,H}$ = 5.8 Hz; 7.12 (s, 4H, m-Trip); 7.51 (t, 1H, p-C_6H_3) $^3J_{H,H}$ = 7.1 Hz, 8.06 (d, 2H, m-C_6H_3) $^3J_{H,H}$ = 7.9 Hz. $^{13}C\{^1H\}$ NMR (151 MHz, C_6D_6, 298K, ppm): δ = 23.46 (o-$CH(CH_3)_2$), 24.24 (o-$CH(CH_3)_2$), 27.14 (p-$CH(CH_3)_2$), 30.66 (o-$CH(CH_3)_2$), 34.73 (p-$CH(CH_3)_2$), 120.73 (m-Trip), 124.99 (p-C_6H_3), 128.29 (m-C_6H_3), 133.60 (i-Trip), 141.21 (p-Trip), 145.95 (o-Trip), 149.00 (o-C_6H_3), 295.48 (br, CO). $^{207}Pb\{^1H\}$ NMR (125 MHz, C_6D_6,

298K, ppm): not observed. ATR-FTIR: $\tilde{\nu}_{CO}$ (cm^{-1}): 1889(m), 1958(m), 2005(m), 2041(w). UV-vis (hexane) λ_{max} = nm ($\varepsilon = M^{-1}\cdot cm^{-1}$): 341 (22700), 505 (3140), 641 (3000).

$Co_4(CO)_9(PbAr^{iPr6})_2$ (**3**). ca. 50 mL of hexane was added to a Schlenk flask charged with 0.330 g (0.24 mmol) $Ar^{iPr6}PbPbAr^{iPr6}$ and 0.168 g (0.49 mmol) $Co_2(CO)_8$. After stirring overnight, during which time the color changed from dark brown to dark red, the solution was filtered, concentrated under reduced pressure to ca. 15 mL, and cooled to ca. -30 ℃ for one week to afford crystals of $Co_4(CO)_9(PbAr^{iPr6})_2$ (**3**) as dark maroon blocks that were suitable for X-ray diffraction studies. Yield: 0.299 g, 67 %. ^{1}H NMR (600 MHz, C_6D_6, 298K, ppm): δ = 1.11 (d, 12H, p-$CH(CH_3)_2$), $^3J_{H,H}$ = 6.6 Hz. 1.38 (d, 12H, o-$CH(CH_3)_2$), $^3J_{H,H}$ = 6.9 Hz, 1.56 (d, 12H, o-$CH(CH_3)_2$), $^3J_{H,H}$ = 6.9 Hz, 2.92 (sept, 2H, p-$CH(CH_3)_2$), $^3J_{H,H}$ = 7.1 Hz, 3.16 (broad, 4H, o-$CH(CH_3)_2$) $^3J_{H,H}$ = 7.4 Hz; 7.26 (s, 4H, m-Trip); 7.38 (t, 1H, p-C_6H_3) $^3J_{H,H}$ = 5.9 Hz, 7.88 (d, 2H, m-C_6H_3) $^3J_{H,H}$ = 7.3 Hz. ^{13}C{^{1}H} NMR (151 MHz, C_6D_6, 298K, ppm): δ = 23.47 (o-$CH(CH_3)_2$), 24.05 (o-$CH(CH_3)_2$), 26.14 (p-$CH(CH_3)_2$), 31.08 (o-$CH(CH_3)_2$), 34.92 (p-$CH(CH_3)_2$), 123.15 (m-Trip), 128.89 (p-C_6H_3), 134.74 (m-C_6H_3), 138.52 (i-Trip), 143.57 (p-Trip), 146.42 (o-Trip), 149.99 (o-C_6H_3), 213.17 (br, CO). ^{59}Co NMR (142 MHz, C_6D_6, 298K, ppm): δ = -173 (Co(1), relative intensity = 1), -654 (Co(2) and Co(3), relative intensity = 2), -2016 (Co(4), relative intensity = 1). ^{207}Pb{^{1}H} NMR (125 MHz, C_6D_6, 298K, ppm): δ = 9010. ATR-FTIR: $\tilde{\nu}_{CO}$ (cm^{-1}): 1820(m), 1849(m), 1948(m), 1972(s), 2008(m), 2035(m). UV-vis (hexane) λ_{max} = nm ($\varepsilon = M^{-1}\cdot cm^{-1}$): 368 (shoulder, 57700).

2.3 Results and Discussion

Synthesis. Metathetical exchange between group 14 dimetallynes, $Ar^{iPr4}MMAr^{iPr4}$ or $Ar^{iPr6}MMAr^{iPr6}$ (M= Ge, Sn, or Pb) and $(CO)_3CpMo\text{-}MoCp(CO)_3$ or $(CO)_2CpMo{\equiv}MoCp(CO)_2$, was shown earlier to afford $Ar^{iPr4}M{\equiv}MoCp(CO)_2$, $Ar^{iPr6}M{\equiv}MoCp(CO)_2$, and $Ar^{iPr4}M\text{-}MoCp(CO)_3$ or $Ar^{iPr6}M\text{-}MoCp(CO)_3$.[16] In particular, the relatively weak Pb-Pb bond of the

diplumbyne[22] is expected to facilitate these reactions with metal-metal (M-M) bonded transition metal carbonyl dimers, hence we studied the reactions of the nominally M-M bonded dinuclear metal carbonyls $Mn_2(CO)_{10}$, $Fe_2(CO)_9$, $Co_2(CO)_8$ with the diplumbyne, $Ar^{iPr6}PbPbAr^{iPr6}$. Compounds $Mn(CO)_5(PbAr^{iPr6})$ (**1**), $Fe(CO)_4(PbAr^{iPr6})_2$ (**2**), $Co_4(CO)_9(PbAr^{iPr6})_2$ (**3**) were attained by the reaction of the diplumbyne with the dinuclear metal carbonyls either in ethereal solvents (Et_2O or THF) or in hexanes (Scheme 2.2). For compounds **2** and **3**, the syntheses

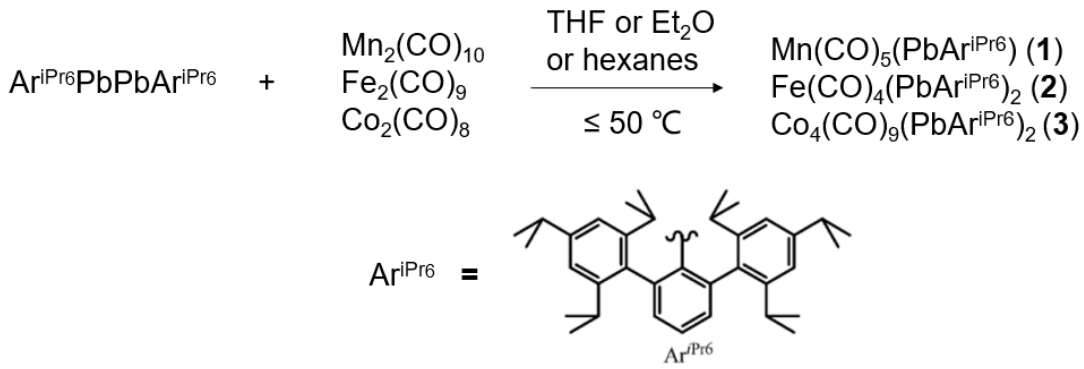

Scheme 2.2: Reactions of $Ar^{iPr6}PbPbAr^{iPr6}$ with metal carbonyls.

were carried out at ambient temperature, and the products were isolated in moderate to good yields. A similar approach to the synthesis of **1** afforded a color change from dark brown to green. However, the major signals in the ^1H NMR spectrum of the residue after removal of solvent were attributed to the unreacted starting materials. To avoid the propensity for decomposition of the diplumbyne under irradiation, gentle heating was applied to the reaction solution after stirring at room temperature for two days. This approach afforded **1** in low (ca. 20%) yield. In contrast, an alternative approach to the synthesis of **1** via salt metathesis of $[Ar^{iPr6}Pb(\mu\text{-}Br)]_2$ and $Na[Mn(CO)_5]$ afforded **1** in a much higher (82%) yield.

The synthesis of **1** by reaction of $Ar^{iPr6}PbPbAr^{iPr6}$ and $Mn_2(CO)_{10}$ is formally a metathetical exchange between the Pb≡Pb 'triple' bond and the Mn-Mn single bond. However,

for steric reasons it seems unlikely that this reaction proceeds via intact dinuclear metal carbonyls. In the cases of **1-3**, it is proposed that the diplumbyne, $Ar^{iPr6}PbPbAr^{iPr6}$, dissociates into $Ar^{iPr6}Pb\cdot$ radical fragments[16, 26], followed by subsequent reaction with $Mn_2(CO)_{10}$, $Fe_2(CO)_9$, or $Co_2(CO)_8$.

The yields of the reactions between diplumbyne and metal carbonyls are probably affected by the transition metal-metal (M-M) bond strength. Recently, Shaik and coworkers presented computational studies on the M-M bonds in transition metal complexes using of ab initio valence-bond methods, in which the M-M bonds of the 3d-series (group 3-10) are considered as pure charge shift bonds.[27] The Mn-Mn bond in $Mn_2(CO)_{10}$ is calculated to have a bond dissociation energy of 22.9 kcal/mol with a charge-shift resonance energy of 24.5 kcal/mol (experimental 38.0 ± 5 kcal/mol)[28] suggesting that the Mn-Mn bond is the strongest M-M bond among $Mn_2(CO)_{10}$,[27] $Fe_2(CO)_9$ (no Fe-Fe bond),[29] and $Co_2(CO)_8$ (9.8 kcal/mol),[27] which may account for the relatively low yield of **1** in the reaction between $Ar^{iPr6}PbPbAr^{iPr6}$ and $Mn_2(CO)_{10}$.

Both the teal crystals of **1**, and green crystals of **2** are highly air-sensitive, and an immediate color change is observed upon their exposure to air. In contrast, dark maroon crystals of **3** can be briefly handled in air without displaying significant color change. Hydrocarbon solutions of **1**, **2**, and **3** were prone to decomposition by light over time, with lead metal deposition and a lightening of the color of the solution.

Structures. The solid-state molecular structures of compounds **1**, **2**, and **3** were determined by single crystal X-ray crystallography. Selected bond distances and bond angles are given in Table 2.1, and the molecular structures of **1**, **2**, and **3** are illustrated in Figures 2.1-2.3, respectively.

Compound **1** crystallized in the I2/a space group. The manganese atom in compound **1** is six-coordinate with a near-octahedral coordination geometry (Figure 2.1). The Pb- Mn distance is 2.838(4) Å, which is slightly longer than the Pb-Mn bonds in $[Pb\{Mn(CO)_5\}_3][AlCl_4]$ [30] (2.750(1)-2.785(1) Å), and the Pb-Mn single bond in the dimetalloborylene complex, $(Ph_3Pb)[Mn(\eta^5\text{-}C_5H_5)(CO)_2]_2B$, 2.703(7) Å.[31] The Pb-Mn bond distance in **1** is slightly shorter than the sum (2.85 Å) of the covalent radii of Mn(1.39 Å) and Pb(1.46 Å).[32-34] The interligand angles at the Mn atom range from 82.65(8)° to 96.75(11)° which deviate somewhat (<7.5°) from the 90° value expected for idealized octahedral coordination. The C(1)-Pb(1)-Mn(1) angle at the lead atom is 106.45(5)°.

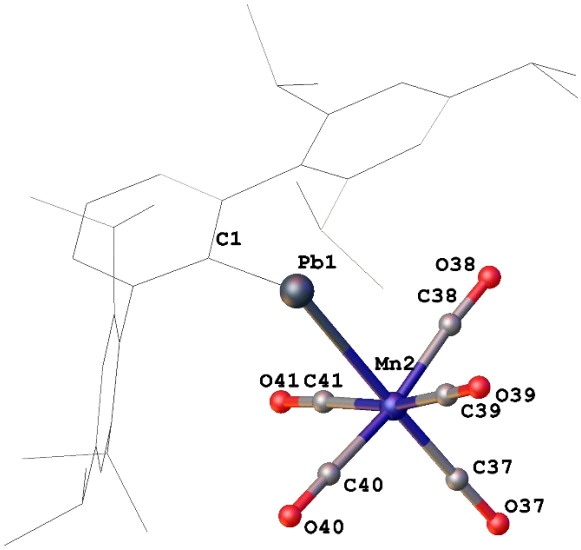

Figure 2.1: Thermal ellipsoid (50%) plot of **1**. H atoms and disordered groups are not shown for clarity, the organic substituents are shown as wire frames.

The molecular structure of **2** (Figure 2.2) showed that it has a six-coordinated iron atom with four carbonyl ligands and two mutually cis-$PbAr^{iPr6}$ moieties, which afford distorted octahedral coordination at iron. The interligand angles at the iron atom range from 75.0(5)° to 106.5(7)°. The deviation of interligand angles from ideal octahedral geometry at iron is probably due to the steric hindrance between the two cis-$PbAr^{iPr6}$ moieties. The two Pb- Fe

bond distances are 2.830(3) Å, and 2.804(3) Å, which are slightly longer than the sum (2.78 Å) of the covalent radii of Pb(1.46 Å) and Fe(1.32 Å).[32-34] The Pb-Fe bond lengths in **2** are slightly longer than the Pb-Fe distances, (2.736(2) Å and 2.728(2) Å), observed in $[Et_2PbFe(CO)_4]_2$ by Wrackmeyer and coworkers.[35] The relatively long Fe-Pb and Mn-Pb bond lengths in **1** and **2** are consistent with a +2 oxidation state of lead as the σ-bonds are likely to be dominated by the

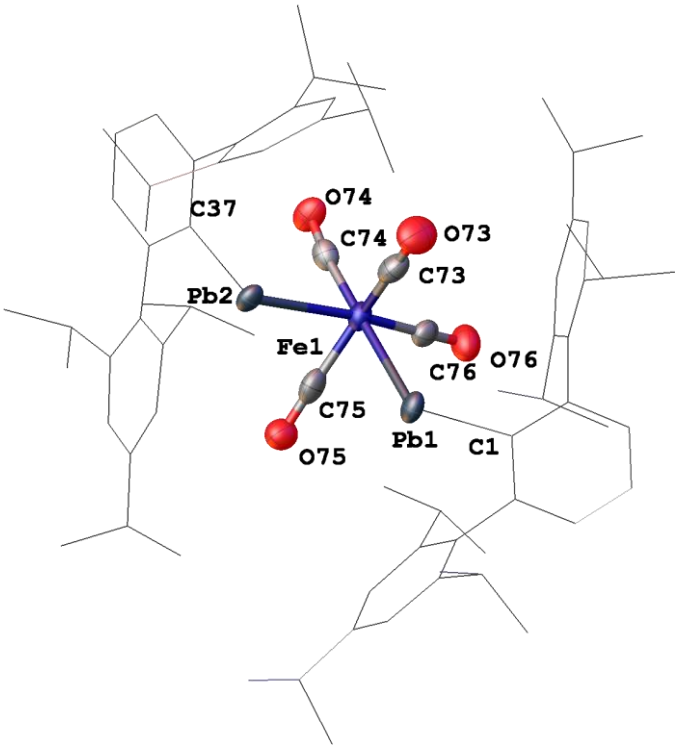

Figure 2.2: Thermal ellipsoid (50%) plot of **2**. H atoms and disordered groups are not shown for clarity, the organic substituents are shown as wire frames.

p-orbital character from the Pb(II) atom, assuming that the transition metal carbonyl fragment carries a negative charge.[9] The interligand angles at the lead atom(s) of **1** (106.45(5)°) and **2** (100.50(3)°, 102.70(3)°) are slightly narrower than those in the $Cp(CO)_3M\text{-}PbAr^{iPr6}$ (M=Cr, Mo, W) complexes (108.6(2)°-113.58(9)°)[9], possibly due to the steric differences between carbonyl groups and cyclopentadienyl group. The structures of **1** and **2** can also be rationalized by the 18-electron rule where the $PbAr^{iPr6}$ moieties are 1-electron ligands bound to the transition metals.[9]

Compound **3** crystallized as dark maroon blocks in the $P2_1/c$ space group. The molecular structure of **3** (Figure 2.3) displays a near-tetrahedral Co_4 core bonded to a total of nine carbonyls and two $PbAr^{iPr6}$ moieties. Seven of the carbonyls are terminally bound, with the remaining two carbonyls and one of the $PbAr^{iPr6}$ moieties each bridging one of the three edges linking the apical cobalt atom with the three basal cobalt atoms. The remaining $PbAr^{iPr6}$ moiety bridges the face formed from the three basal cobalt atoms. The apical cobalt atom carries only one terminal carbonyl, while each of the basal cobalt atoms carry two terminal carbonyls. The structure of **3** therefore differs from that of $Co_4(CO)_{12}$, where the apical atom is connected to three terminal carbonyls. The structure of compound **3** conforms to Wade's rules which predict a *nido* structure for the tetracobalt tetrahedron core as it has n+2 (n=no. of vertices) skeletal electron pairs for cluster bonding.[36-37] The edge-bridging Pb-Co bonds are 2.5008(7) Å and 2.5150(6) Å, while the average of the face-bridging Pb-Co distances is 2.5750(8) Å, which is slightly longer than the edge-bridging distance as expected for the higher coordination number. The Co-Co lengths are similar to those of the Co-Co bonds (2.441(14) Å to 2.527(10) Å) in cobalt carbonyl clusters[38] except that the Co(1)-Co(4) distance bridged by the $PbAr^{iPr6}$ moiety which is 2.7472(9) Å, much longer than an average Co-Co bond, 2.499(1) Å.[39-41] The calculated structure of the unsaturated compound $Co_4(CO)_{11}$ reported by King and coworkers[42] was predicted to have a μ_4-CO group bridging all four cobalt atoms, where the structure of **3** resembles one of the predicted structures with a butterfly array of cobalt atoms.

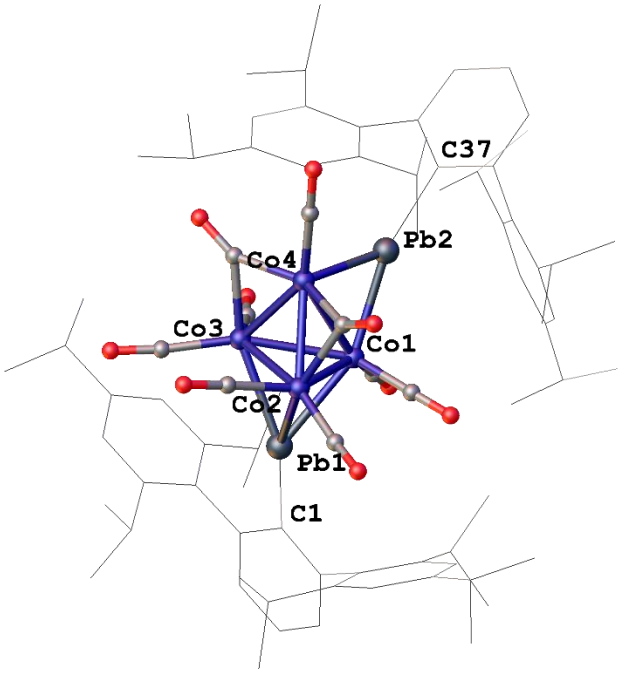

Figure 2.3: Thermal ellipsoid (50%) plot of **3**. H atoms and disordered groups are not shown for clarity, the organic substituents are shown as wire frames.

	1 (M = Mn)	**2** (M = Fe)	**3** (M = Co)
Pb-C	2.288(2)	Pb(1)-C(1) 2.313(13) Pb(2)-C(37) 2.307(13)	Pb(1)-C(1) 2.229(2) Pb(2)-C(37) 2.214(2)
Pb-M	2.8376(4)	Pb(1)-Fe(1) 2.800(2) Pb(2)-Fe(1) 2.829(2)	2.5078(4) (average of edge-bridging) 2.5735(4) (average of face-bridging)
M-CO (average)	1.839(3)	1.772(19)	1.775(3) (terminal) 1.932(3) (bridging)
M-Pb-C	106.45(5)	C(1)-Pb(1)-Fe(1) 102.70(3) C(37)-Pb(2)-Fe(1) 100.50(3)	C(37)-Pb(2)-Co(4) 130.44(7) C(37)-Pb(2)-Co(1) 162.43(7) (edge-bridging) C(1)-Pb(1)-Co(1) 128.18(6) C(1)-Pb(1)-Co(2) 153.22(6) C(1)-Pb(1)-Co(3) 146.90(6) (face-bridging)

Table 2.1. Selected bond distances (Å) and angles (°) for **1-3**.

The calculated structure indicated a long Co···Co distance between the two wingtips cobalt atoms of 2.974 Å (B3LYP) or 3.105 Å (BP86), in the Co_4 butterfly, 0.2~0.3 Å longer than Co(1)-Co(4) in the structure of **3**.[42] The structure of **3** displays wide interligand angles at the lead atoms (see Table 2.1) thus arises from the bridging nature of the $PbAr^{iPr6}$ moieties and the higher coordination number at lead atom. In addition, the sum of the angles at Pb(2) is 359.26(7)°, consistent with a planar coordination geometry. The Pb-C distances in **1-3** range from 2.214(2) Å to 2.313(13) Å which are within the range of reported divalent aryllead species.[43-45] The transition metal-carbon distances to the carbonyl groups are comparable to their parent metal carbonyls.[46]

Spectroscopy. ^{1}H and $^{13}C\{^1H\}$ NMR spectra of **1**, **2**, and **3** are consistent with high sample purity. The ^{1}H NMR spectra of **1** and **2** each displayed a set of signals which correspond to the ligand, Ar^{iPr6}.[45] Peak broadenings were observed in the ^{1}H NMR spectrum of **1** possibly due to restricted rotations of the flanking rings, which has been noted previously.[22] The ^{1}H NMR spectrum of **3** displayed two sets of peaks attributable to the ligand which differ by approximately 0.01 ppm due to the two slightly different environments of the face-bridging and edge-bridging lead atoms.

The $^{13}C\{^1H\}$ NMR spectra of **1**, **2**, and **3** displayed signals similar to those in the previously reported complexes, $(\eta^5\text{-}C_5H_5)(CO)_3M\text{-}PbAr^{iPr6}$ (M=Cr, Mo, W), including **3** where there was only one set of signals from the ligand Ar^{iPr6} moieties. The $^{13}C\{^1H\}$ NMR spectrum of **1** displayed two peaks attributable to the carbonyl groups at 210.94 ppm, and 282.93 ppm (Table 2.2) in an approximate integration ratio of 4:1, which correspond to the COs cis and trans to the $PbAr^{iPr6}$ substituents. There is no indication of restricted rotation around the Pb(1)-Mn(1) axis in the $^{13}C\{^1H\}$ NMR spectrum of **1**, consistent with a single bond between Pb and Mn. The $^{13}C\{^1H\}$ NMR spectra of **2** and **3** each showed a single broad signal at 295.48 ppm, and 213.17 ppm for the carbonyl groups, respectively. (see Table 2.2) The $^{13}C\{^1H\}$ NMR

spectrum of **2** can be understood by having an overall C_{2v} symmetry for its solid-state structure. The single broad peak for the carbonyl groups in the $^{13}C\{^{1}H\}$ NMR spectra of **2** and **3** can be attributed to its fluxional solution behavior of carbonyl ligands and possibly restricted rotation around the transition metal-lead bond.[9] In addition, it has also been previously reported of missing apical ^{13}C signal in the $^{13}C\{^{1}H\}$ NMR spectrum of $Co_4(CO)_{12}$.[47]

The $^{207}Pb\{^{1}H\}$ NMR spectra of **1** and **3** displayed broad signals at 8007 ppm, and 9010 ppm (Table 2.2) which are in fair agreement with ^{207}Pb NMR signals observed for $(\eta^5\text{-}C_5H_5)(CO)_3M\text{-}PbAr^{iPr6}$ (M=Cr, Mo, W), 9374-9659 ppm,[9] are also within the chemical shift range for two-coordinated lead.[44] The absence of signal in the $^{207}Pb\{^{1}H\}$ NMR spectrum of **2** can be explained by its possible fluxional solution behavior, which therefore resulted in the ^{207}Pb signals broadening.[72,73] Signal broadening in $^{207}Pb\{^{1}H\}$ NMR spectrum of **3** could be caused by coupling to multiple ^{59}Co atoms as ^{59}Co is a 7/2 spin nucleus and is thus quadrupolar.[48] The $^{59}Co\{^{1}H\}$ NMR spectrum of **3** displayed three signals at -173 ppm, -654 ppm, and -2016 ppm, respectively. The intensity ratio of the three signals is 1:2:1 which corresponds to the three different chemical environments for the cobalt atoms seen in the crystal structure of **3**. The chemical shifts in the ^{59}Co NMR spectrum of tetrahedral clusters supported by carbonyl ligands are generally unaffected by edge-bridging or face-bridging metals.[48] The signal at -173 ppm can be assigned to Co(1), the more intense signal at -654 ppm can be assigned to both Co(2) and Co(3) where Co(1), Co(2) and Co(3) are all bonded to two terminal carbonyl ligands in its solid state, and the signal at -2016 ppm to Co(4), which is bonded to two bridged carbonyl ligands and one terminal carbonyl ligand, respectively, suggesting that solid-state structure of **3** is also present in the solution structure. The chemical shifts of the signals are close to those chemical shifts reported for $Co_4(CO)_{12}$, -668 ppm (apical Co), and -2032 ppm (basal Co) in $CDCl_3$.[48]

The UV-vis spectra of **1** and **2** showed absorptions at 671 nm and 641 nm (Table 2.2), respectively, which are attributed to the n-p transitions of the lead atoms as depicted in DFT calculations (Figure 2.4). These absorptions are close to the reported values for (η^5-C_5H_5)$(CO)_3$M-PbAr^{iPr6} 611-624 nm.[9] However, the UV-vis spectrum of **3** displayed an absorption at 368 nm that is blue-shifted compared to the absorptions for plumbylenes, possibly due to the large extinction coefficient of cobalt-centered electronic transition where the absorption is very similar to what was reported for $Co_4(CO)_{12}$ (372 nm).[49]

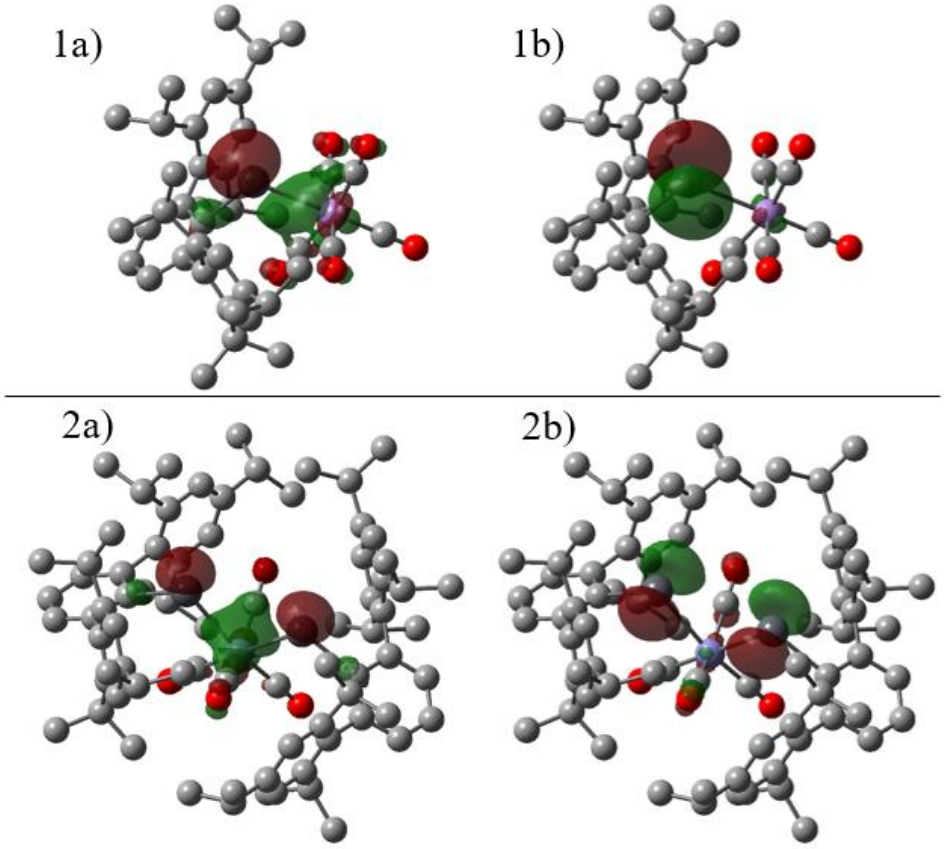

Figure 2.4: Depiction of calculated HOMO (1a) and LUMO (1b) of **1**, calculated HOMO (2a) and LUMO (2b) of 2. HOMO-LUMO gap of **1** is calculated at 340 kJ/mol, and 325 kJ/mol for **2**, hydrogens are not shown for clarity and the isovalue is set at 0.05.

Compounds **1-3** were also characterized by IR spectroscopy. The IR spectrum of **1** displayed a similar pattern to that of the corresponding complex, $(Ph_3PAu)Mn(CO)_5$ (1961(vs) cm^{-1}, 2062(s) cm^{-1}).[50] The IR spectrum of **1** showed two vibrational modes for the carbonyl groups, A_1 (1958(s) cm^{-1}), and E (2060(m) cm^{-1}), which correspond to axial and equatorial CO stretching modes, respectively. The 4-band ($2A_1+B_1+B_2$) pattern in the IR spectrum of **2** is similar to what was reported for (NHC)Al(Br)[$(Fe(CO)_4)$[51] (NHC = N-heterocyclic carbene) and cis-$Fe(CO)_4(SnR_3)_2$[52]. CO stretching frequencies of **1** were calculated to be 1974 cm^{-1} for axial, 1975 cm^{-1} for equatorial, and 2055 cm^{-1} for axial + equatorial. CO stretching frequencies of **2** were calculated to be 1893 cm^{-1}, 1921 cm^{-1}, 1967 cm^{-1}, and 2008 cm^{-1}. The IR spectrum of **3** showed similarities with the calculated (BP86) vibrational frequencies of the theoretical butterfly complex $Co_4(CO)_{11}$, where the vibrational frequencies have relatively low wavenumber values of 1820 cm^{-1} and 1849 cm^{-1}, which can be attributed to the bridging

	1 (M = Mn)	**2** (M = Fe)	**3** (M = Co)
UV-vis (nm)[a]	332, 671	341, 505, 641	368
IR($\tilde{\nu}_{CO}$) cm^{-1})	1958(s), 2060(m)	1889(m), 1958(m), 2005(m), 2041(w)	1820(m), 1849(m), 1948(m), 1972(s), 2008(m), 2035(m).
^{13}C NMR (CO) (ppm)[b]	210.94, 282.93	295.48	213.17
^{207}Pb NMR (ppm)[c]	8007.2	-	9010.4

Table 2.2. Selected spectroscopic data for **1-3**. (a. UV-vis spectra were collected in hexanes at 298K. b. $^{13}C\{^{1}H\}$ NMR spectra were collected in C_6D_6 at 298K. c. $^{207}Pb\{^{1}H\}$ NMR spectra were collected in C_6D_6 at 298K.)

carbonyl groups, and that 2008(m) cm^{-1} and 2035(m) cm^{-1} to the terminal carbonyl groups(2020(s), 2026(s), 2032(s)).[42]

2.4 Conclusions

In conclusion, the syntheses and characterizations of complexes $Mn(CO)_5(PbAr^{iPr6})$ (**1**), $Fe(CO)_4(PbAr^{iPr6})_2$ (**2**), $Co_4(CO)_9(PbAr^{iPr6})_2$ (**3**), have been described. They are rare examples of complexes synthesized by interaction of group 14 dimetallyne and dinuclear transition metal carbonyls. The reactivities of diplumbyne and dinuclear metal carbonyls can be attributed to the charge-shift bond character of Pb≡Pb triple bond and M-M single bond. The syntheses of **1-3** are postulated to proceed via the reactions of $Ar^{iPr6}Pb\cdot$ radical fragment from the dissociation of $Ar^{iPr6}PbPbAr^{iPr6}$ with $Mn_2(CO)_{10}$, $Fe_2(CO)_9$, or $Co_2(CO)_8$.

2.5 Supporting Information

$Na[Mn(CO)_5]$.[53-55] To a Schlenk flask charged with 6.734 g (mmol) Na/NaCl (5% wt.), 1.68 g (4.3 mmol) $Mn_2(CO)_{10}$ in ca. 60 mL of THF was added. After stirring overnight, during which the color changed from yellow to grey, the solution was filtered. Removal of solvent afforded $Na[Mn(CO)_5]$ as a grey powder. Yield: 1.685 g, 89.9 %.

Computational details. The geometry optimizations were performed with the Gaussian16 (Revision C.01) program[56] using the PBE1PBE hybrid exchange functional[57] and Def2-TZVP basis set.[58] For Pb, the effective core potential (ECP) basis set with similar valence quality was used.[59] In addition, Grimme's empirical dispersion correction with Becke-Johnson damping (GD3BJ)[60] was used as well as an ultrafine integration grid. Full analytical frequency

calculations were performed for the optimized structures to ensure the nature of the stationary points found (minima, no imaginary frequencies). The reported IR frequencies are scaled by 0.950 as suggested by Truhlar.[61] Calculated Mulliken charges for **1**: -0.229 (Mn) and 0.708 (Pb) and for **2**: -0.042 (Fe), 0.636 (Pb1) and 0.652 (Pb2).

1 (cm^{-1})	**2** (cm^{-1})
1974 (ax)	1893 (ax)
1975 (2 eq)	1921 (ax+eq)
1984 (weak)	1967 (eq)
1988 (eq)	2008 (ax+eq)
2055 (ax+eq)	

Table 2.S1: Scaled CO stretching frequencies (scaled by 0.950).

Compound	**1**	**2**	**2**
Empirical formula	$C_{41}H_{49}MnO_5Pb$	$C_{76}H_{98}FeO_4Pb_2$	$C_{93}H_{126}Co_4O_9Pb_2$
Formula weight	883.93	1545.77	2038.03
Temperature	100(2) K	90(2) K	100(2) K
Wavelength	0.71073 Å	0.71073 Å	0.71073 Å
Crystal system	Monoclinic	Orthorhombic	Monoclinic
Space group	I2/a	$P2_12_12_1$	$P2_1/c$
Crystal color and habit	Blue block	Green needle	Brown block
a(Å)	24.7432(16)	13.7838(10)	15.2271(15)
b(Å)	9.8984(7)	b = 19.2541(14)	18.2682(17)
c(Å)	32.595(2)	c = 53.714(4)	33.059(3)
a(°)	90	90	90
b(°)	107.862(2)	90	101.381(2)

g(°)	90	90	90
Density (calculated) (Mg/m^3)	1.545	1.440	1.502
F(000)	3536	6208	4112
Crystal size(mm^3)	0.334 x 0.304 x 0.304	0.425 x 0.195 x 0.064	0.442 x 0.330 x 0.318
Crystal color and habit	Blue Block	Green Needle	Brown Block
θ range(°)	2.160 to 27.619	1.661 to 25.250	1.778 to 27.500
Reflections collected	33339	102889	80707
Independent reflections	8814 [R(int) = 0.0252]	25829 [R(int) = 0.1292]	20693 [R(int) = 0.0206]
Observed reflections (I > 2σ(I))	8509	19116	18426
Completeness to 2θ= 25.242°	99.9 %	100.0 %	99.9 %
Goodness-of-fit on F^2	1.055	1.026	1.025
Final R indices (I>2σ(I))	R1 = 0.0229, wR2 = 0.0558	R1 = 0.0521, wR2 = 0.0882	R1 = 0.0243, wR2 = 0.0543
R indices (all data)	R1 = 0.0239, wR2 = 0.0564	R1 = 0.0864, wR2 = 0.0966	R1 = 0.0294, wR2 = 0.0559

Table 2.S2: Selected X-ray Crystallographic data for **1-3.**[62-70]

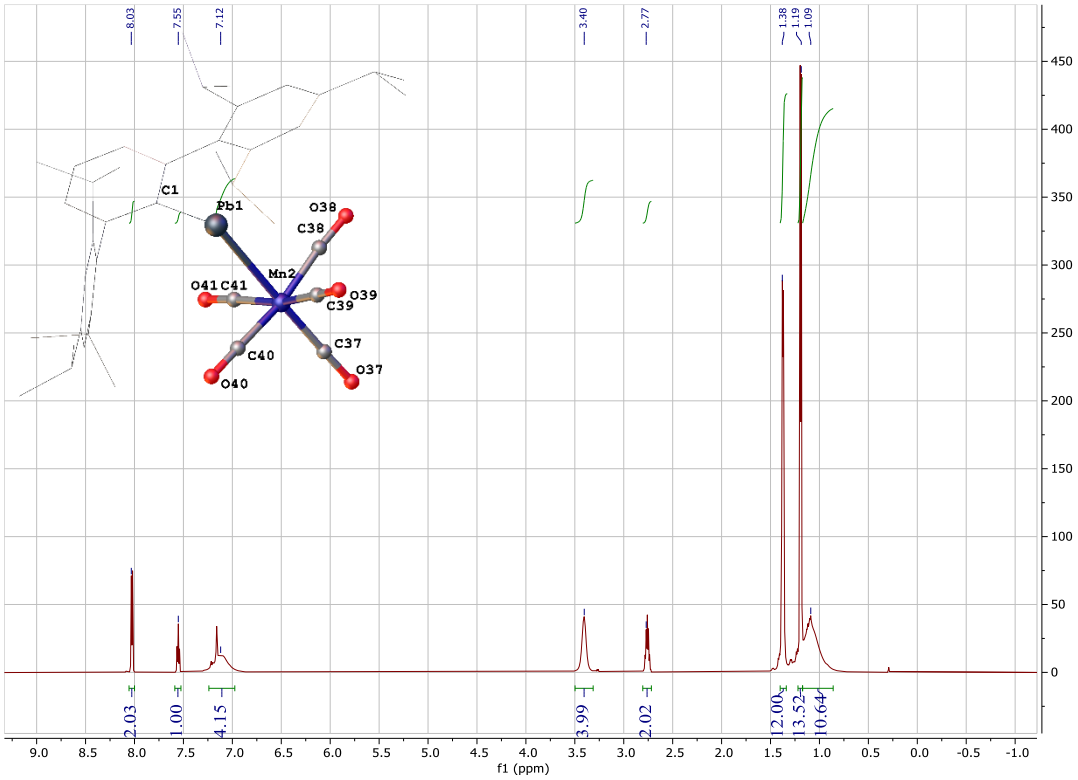

Figure 2.S1: ^{1}H NMR spectrum of **1** in C_6D_6 at 298K.

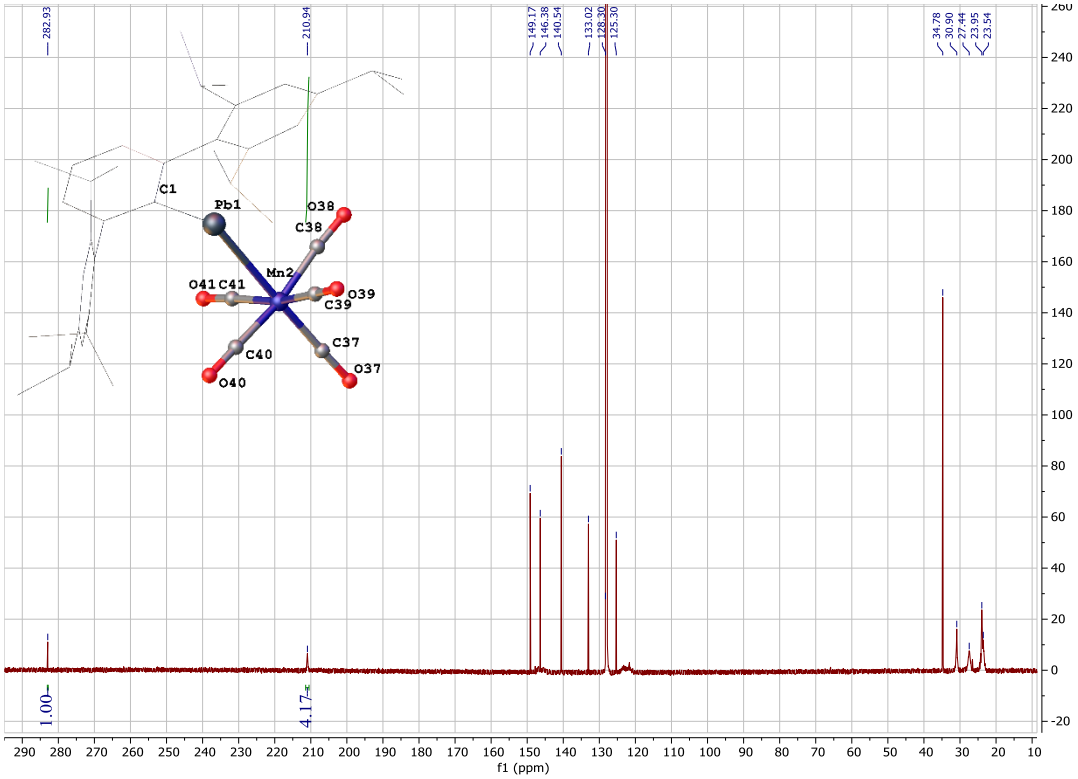

Figure 2.S2: $^{13}C\{^{1}H\}$ NMR spectrum of **1** in C_6D_6 at 298K.

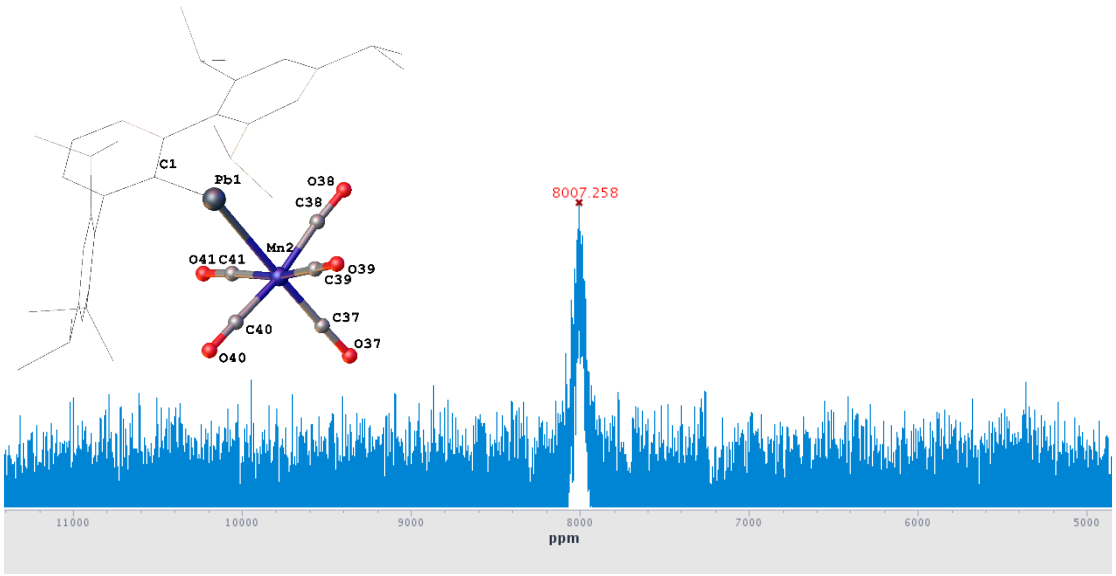

Figure 2.S3: $^{207}Pb\{^{1}H\}$ NMR spectrum of **1** in C_6D_6 at 298K.

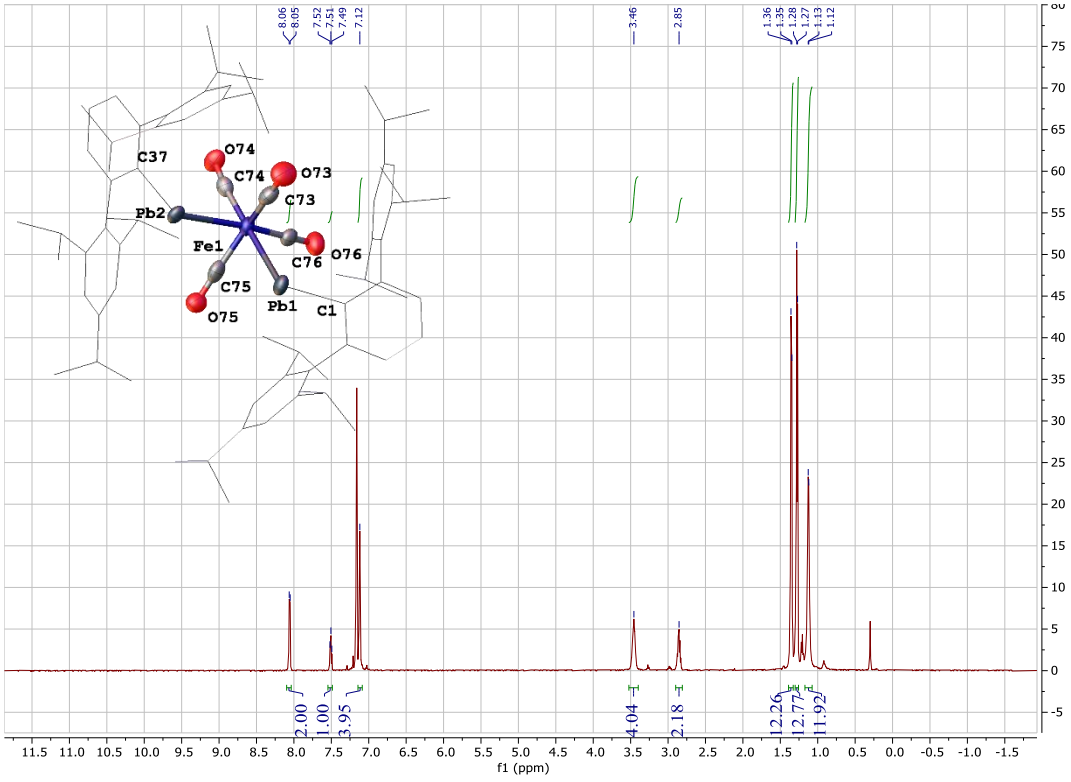

Figure 2.S4: ^{1}H NMR spectrum of **2** in C_6D_6 at 298K.

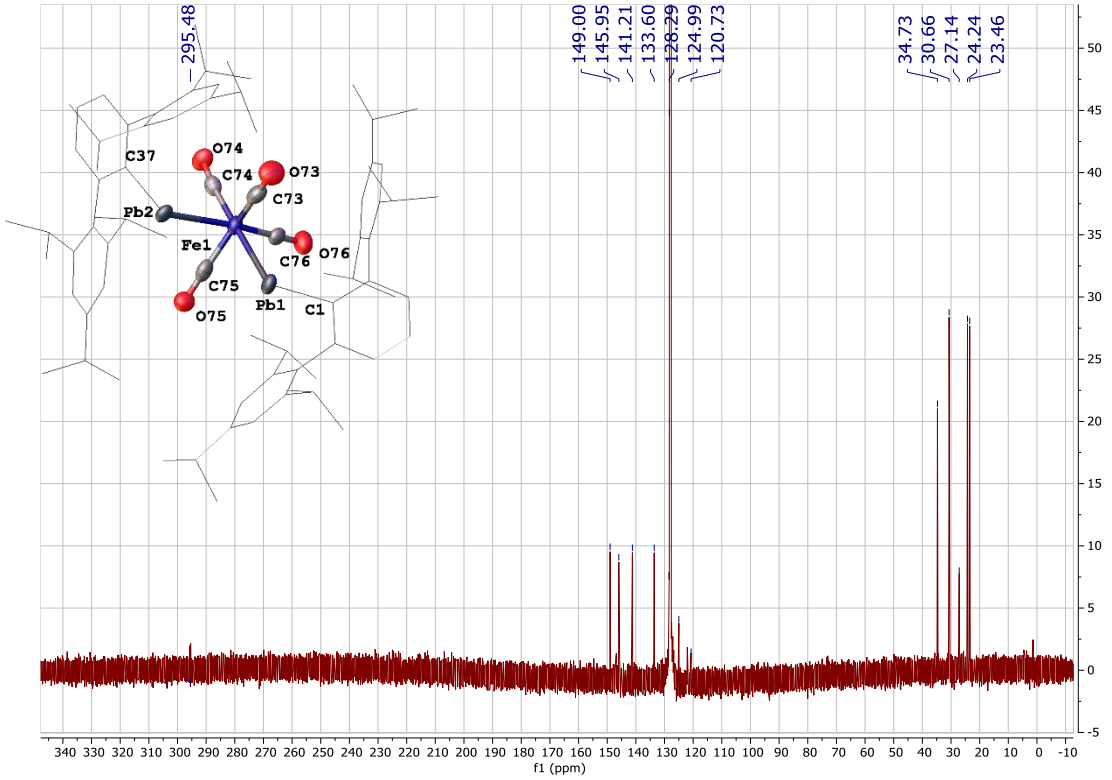

Figure 2.S5: $^{13}C\{^{1}H\}$ NMR spectrum of **2** in C_6D_6 at 298K.

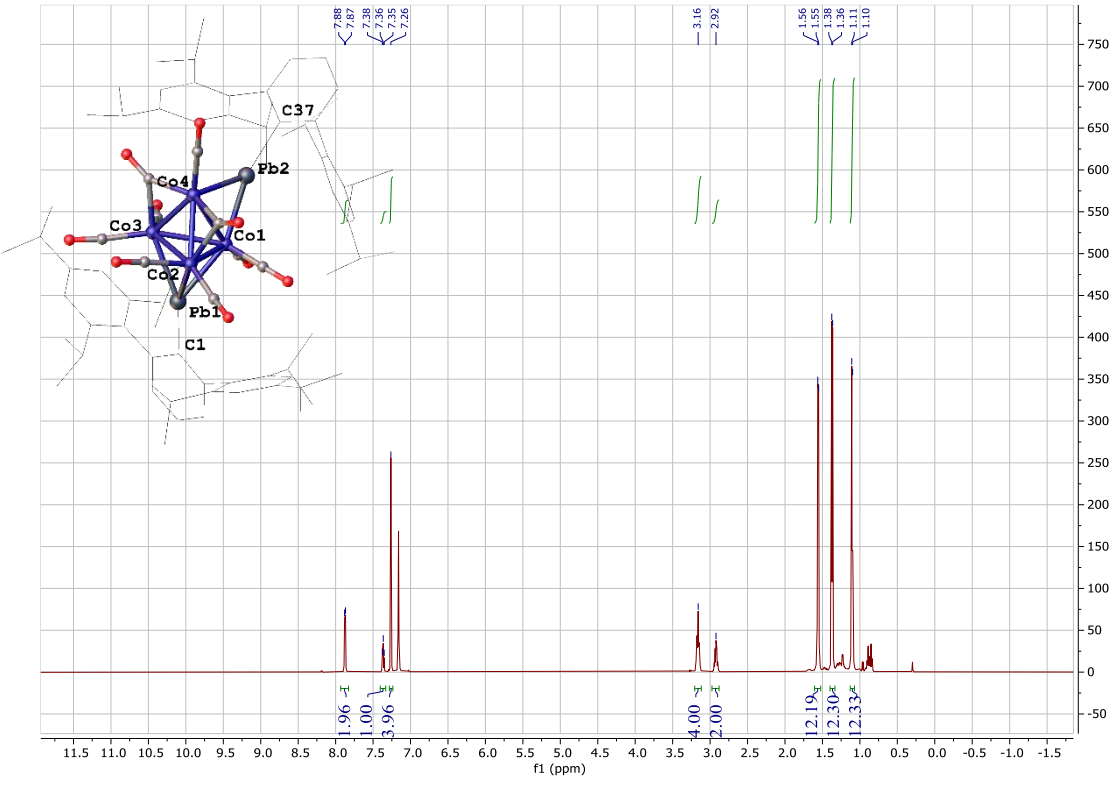

Figure 2.S6: ^{1}H NMR spectrum of **3** in C_6D_6 at 298K.

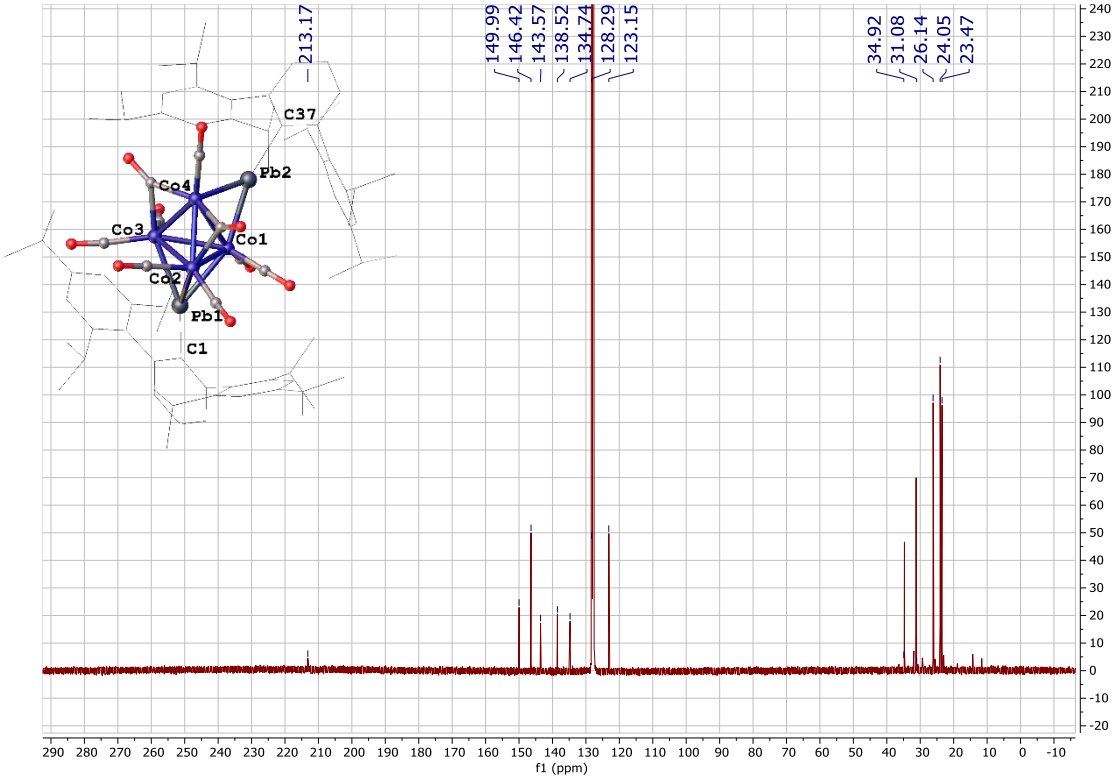

Figure 2.S7: $^{13}C\{^{1}H\}$ NMR spectrum of **3** in C_6D_6 at 298K.

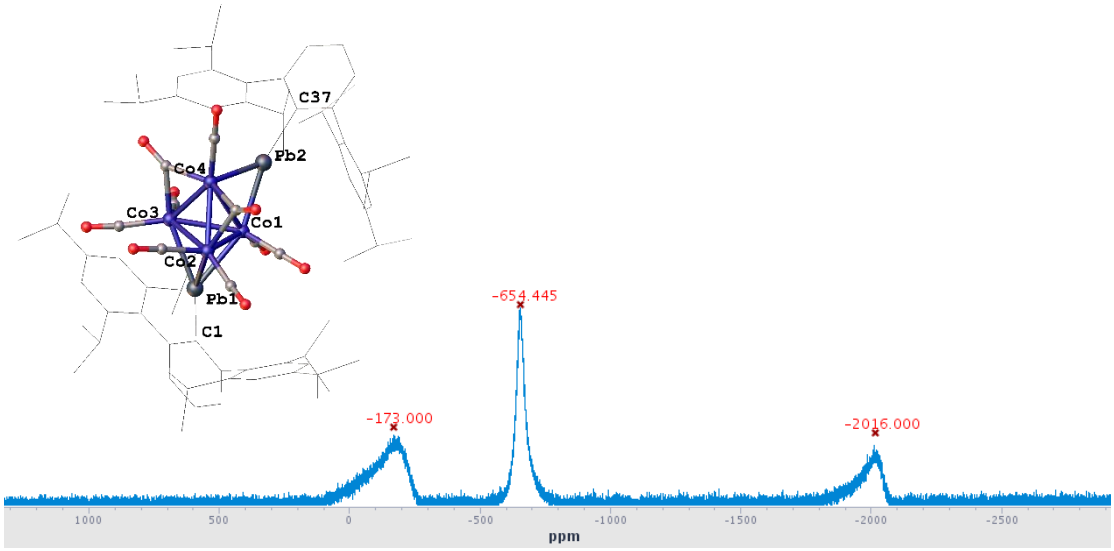

Figure 2.S8: $^{59}Co\{^{1}H\}$ NMR spectrum of **3** in C_6D_6 at 298K.

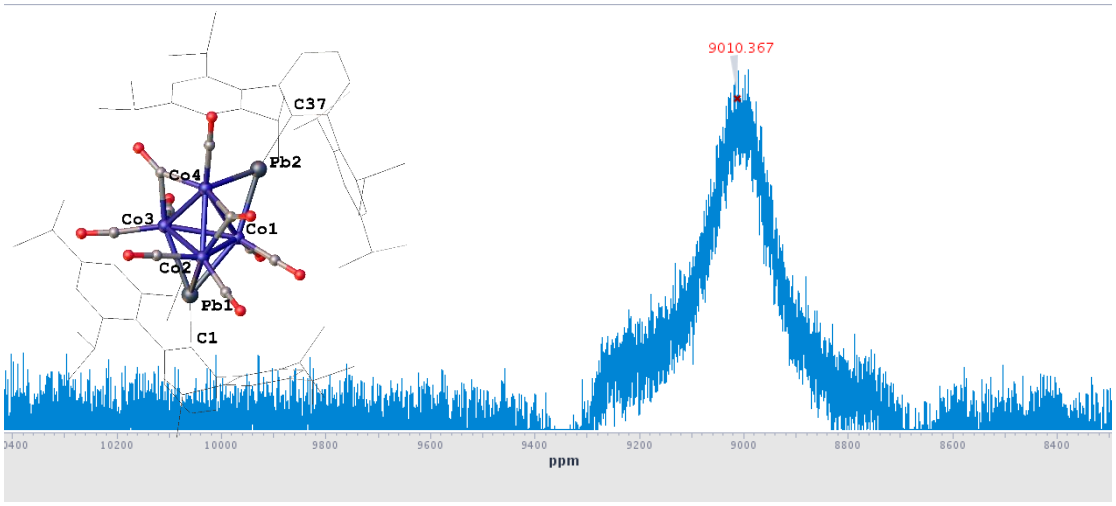

Figure 2.S9: $^{207}Pb\{^{1}H\}$ NMR spectrum of **3** in C_6D_6 at 298K.

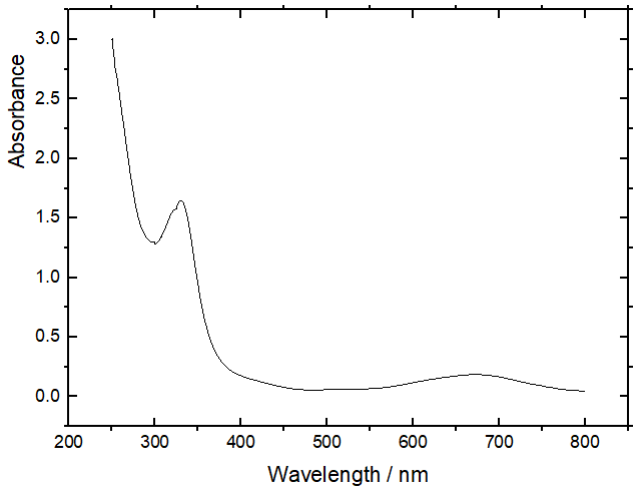

Figure 2.S10: UV-vis spectrum of **1** in hexanes at 298K.

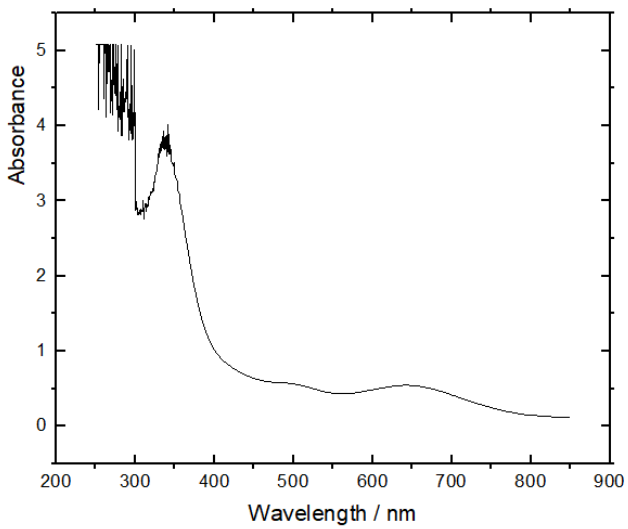

Figure 2.S11: UV-vis spectrum of **2** in hexanes at 298K.

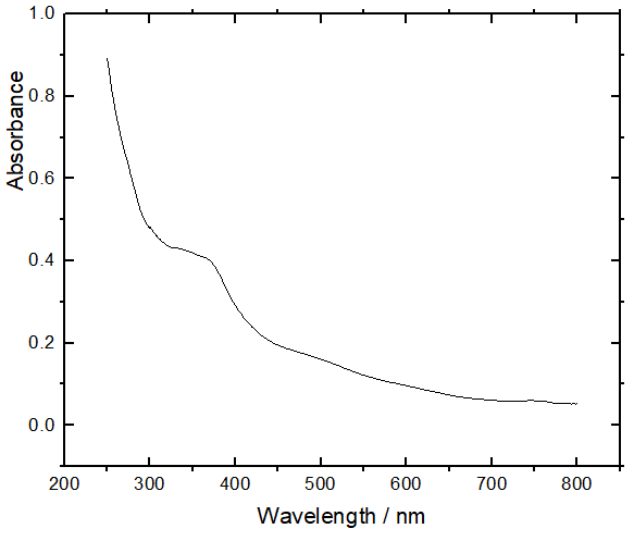

Figure 2.S12: UV-vis spectrum of **3** in hexanes at 298K.

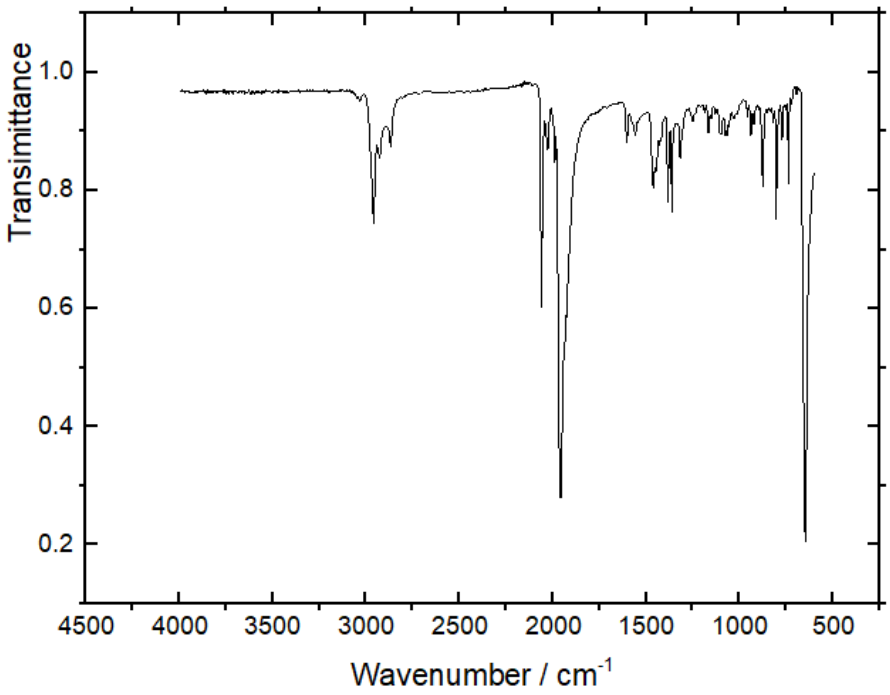

Figure 2.S13: ATR-FTIR spectrum of **1** at 298K.

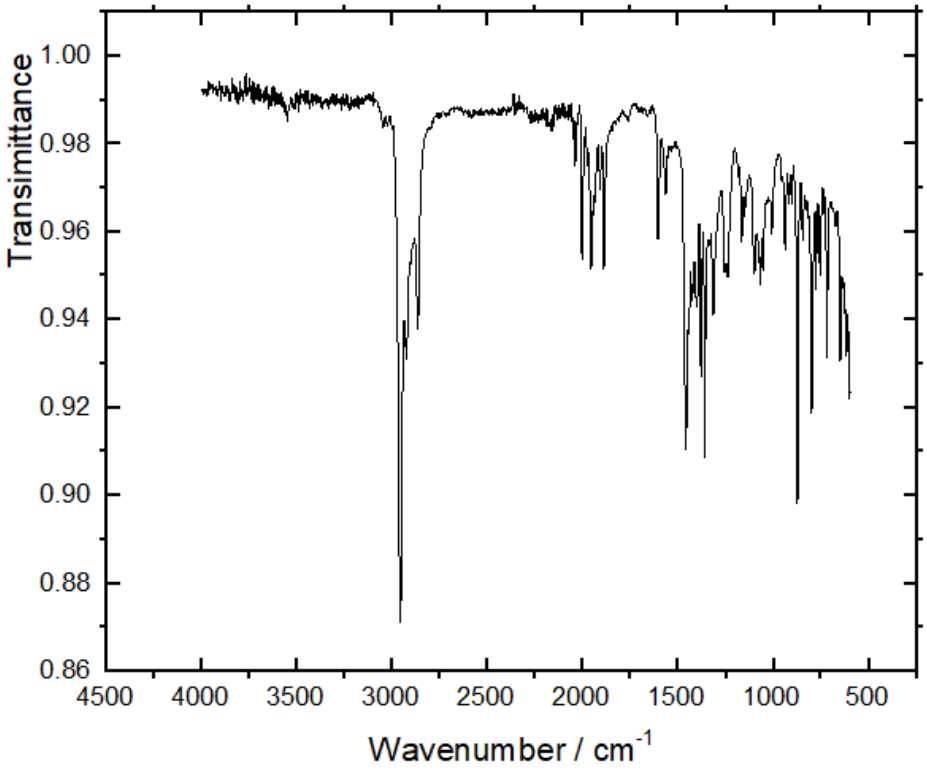

Figure 2.S14: ATR-FTIR spectrum of **2** at 298K.

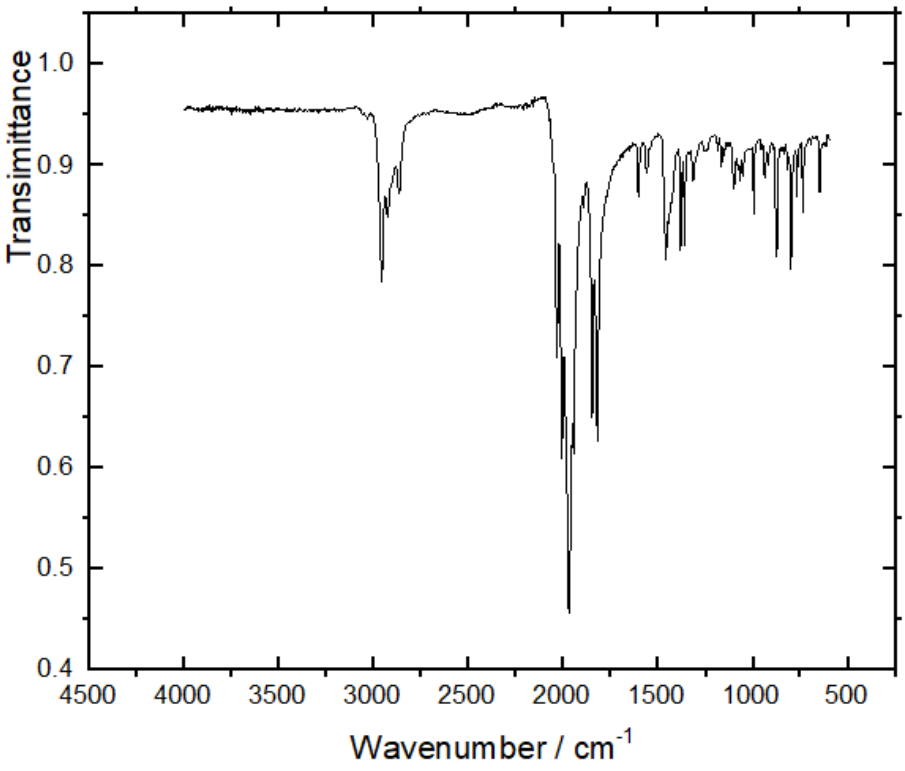

Figure 2.S15: ATR-FTIR spectrum of **3** at 298K.

Optimized xyz-coordinates

97

1

Pb	-0.00012	-0.01001	-0.99984
Mn	0.00017	2.73806	-0.18928
O	-0.00005	5.53616	0.68942
O	2.95551	2.64558	-0.44092
O	0.00046	3.17921	-3.12320
O	-2.95509	2.64542	-0.44161
O	0.00003	1.61279	2.56103
C	-0.00002	-1.20466	0.95957
C	1.20924	-1.67219	1.47700
C	1.20188	-2.57653	2.53559
H	2.13887	-2.94867	2.93493
C	-0.00007	-3.01944	3.06638
H	-0.00010	-3.72762	3.88710
C	-1.20201	-2.57642	2.53562
H	-2.13901	-2.94849	2.93500
C	-1.20932	-1.67209	1.47704
C	2.47106	-1.21537	0.82896
C	2.79800	-1.70565	-0.45640
C	3.91790	-1.19947	-1.10625
H	4.16092	-1.56837	-2.09582
C	4.75117	-0.26232	-0.51090

C	4.44755	0.15443	0.77480
H	5.10149	0.87709	1.25110
C	3.32202	-0.29340	1.45765
C	2.05974	-2.89168	-1.04741
H	1.02618	-2.85357	-0.69540
C	2.03341	-2.92439	-2.56841
H	1.65486	-1.98949	-2.98926
H	1.38366	-3.73310	-2.91019
H	3.02458	-3.10982	-2.98978
C	2.66522	-4.18253	-0.49545
H	3.71483	-4.26839	-0.78960
H	2.12895	-5.05386	-0.88050
H	2.61489	-4.20576	0.59430
C	3.07087	0.18108	2.87242
H	2.02619	-0.03087	3.11003
C	3.29698	1.67631	3.06433
H	4.35181	1.94348	2.96393
H	2.98012	1.97318	4.06663
H	2.73376	2.27146	2.34618
C	3.94553	-0.60147	3.85156
H	3.77719	-1.67655	3.77377
H	3.73769	-0.29708	4.88063
H	5.00457	-0.41647	3.65071
C	-2.47109	-1.21518	0.82899
C	-3.32200	-0.29312	1.45762
C	-4.44749	0.15475	0.77474
H	-5.10138	0.87748	1.25100
C	-4.75114	-0.26205	-0.51094
C	-3.91794	-1.19930	-1.10623
H	-4.16099	-1.56824	-2.09578
C	-2.79807	-1.70551	-0.45636
C	-3.07081	0.18134	2.87239
H	-2.02612	-0.03057	3.10995
C	-3.29699	1.67656	3.06436
H	-2.73387	2.27176	2.34616
H	-2.98005	1.97342	4.06663
H	-4.35185	1.94367	2.96407
C	-3.94541	-0.60128	3.85153
H	-5.00446	-0.41632	3.65071
H	-3.73754	-0.29690	4.88061
H	-3.77701	-1.67635	3.77371
C	-5.95813	0.27962	-1.23564
H	-6.43473	1.00219	-0.56412
C	-5.55819	1.01906	-2.50873
H	-4.85411	1.82399	-2.29132
H	-6.43638	1.45078	-2.99549
H	-5.08325	0.34022	-3.22233
C	-6.97213	-0.82031	-1.53527
H	-6.55180	-1.56558	-2.21597
H	-7.86460	-0.40388	-2.00926

H	-7.27708	-1.33666	-0.62259
C	-2.05987	-2.89161	-1.04729
H	-1.02631	-2.85352	-0.69529
C	-2.03356	-2.92444	-2.56829
H	-3.02474	-3.10985	-2.98964
H	-1.38387	-3.73323	-2.91001
H	-1.65495	-1.98960	-2.98921
C	-2.66542	-4.18238	-0.49522
H	-2.61509	-4.20552	0.59453
H	-2.12919	-5.05378	-0.88020
H	-3.71503	-4.26821	-0.78936
C	0.00010	4.44844	0.34434
C	1.82225	2.63492	-0.30841
C	0.00043	3.01642	-1.99352
C	-1.82187	2.63479	-0.30875
C	0.00014	2.00570	1.48971
C	5.95815	0.27937	-1.23561
C	6.97191	-0.82061	-1.53585
H	7.86437	-0.40414	-2.00980
H	6.55136	-1.56553	-2.21678
H	7.27691	-1.33738	-0.62342
C	5.55808	1.01935	-2.50835
H	6.43500	1.00162	-0.56392
H	5.08284	0.34084	-3.22208
H	6.43625	1.45107	-2.99516
H	4.85420	1.82433	-2.29051

181

2

Fe	-0.03373	0.01009	-1.21585
Pb	1.71320	0.96325	0.80243
Pb	-1.76811	-0.86939	0.83753
C	3.45084	1.76866	-0.46925
C	4.52535	1.01566	-0.94611
C	5.58459	1.66983	-1.57441
H	6.42869	1.09246	-1.93581
C	5.57759	3.04791	-1.72374
H	6.40853	3.54184	-2.21443
C	4.52299	3.79812	-1.22524
H	4.53525	4.87882	-1.31498
C	3.46248	3.16139	-0.58983
C	4.56942	-0.46018	-0.73838
C	4.41293	-1.34565	-1.81594
C	4.47273	-2.71475	-1.58352
H	4.33817	-3.38738	-2.42196
C	4.66716	-3.24083	-0.31807
C	4.82791	-2.35249	0.73517
H	4.99097	-2.75379	1.72971

C	4.79600	-0.97614	0.55402
C	4.19017	-0.86179	-3.23172
H	3.93887	0.19907	-3.18511
C	5.46423	-1.00577	-4.06146
H	5.76309	-2.05561	-4.13062
H	6.29597	-0.45276	-3.62155
H	5.30592	-0.63196	-5.07650
C	3.03422	-1.58348	-3.91829
H	2.80330	-1.10169	-4.87105
H	2.13165	-1.57019	-3.30605
H	3.27800	-2.62790	-4.12892
C	4.73981	-4.72700	-0.06462
H	4.37894	-4.88743	0.95796
C	6.18764	-5.21017	-0.12611
H	6.25391	-6.27686	0.10515
H	6.81670	-4.66542	0.58094
H	6.59857	-5.05313	-1.12727
C	3.85848	-5.54040	-1.00166
H	4.25011	-5.53943	-2.02224
H	2.84371	-5.13976	-1.03339
H	3.81243	-6.58211	-0.67486
C	5.12300	-0.06631	1.72043
H	4.65129	0.89967	1.52898
C	4.60931	-0.57028	3.06220
H	5.14002	-1.46618	3.39351
H	3.54303	-0.80873	3.02421
H	4.75636	0.19361	3.82902
C	6.62885	0.18427	1.77464
H	7.16730	-0.75326	1.93873
H	6.87823	0.86945	2.58964
H	6.98606	0.62119	0.84030
C	2.33504	3.90226	0.05183
C	1.28781	4.45866	-0.70170
C	0.20820	5.02670	-0.03347
H	-0.60945	5.44071	-0.61235
C	0.12236	5.05547	1.35023
C	1.18611	4.54589	2.08106
H	1.15557	4.59250	3.16288
C	2.30109	3.98978	1.46467
C	1.35011	4.50828	-2.21198
H	2.06274	3.74654	-2.53529
C	1.88209	5.86972	-2.66040
H	1.98300	5.90215	-3.74827
H	2.85667	6.08760	-2.22094
H	1.19598	6.66636	-2.35889
C	0.01956	4.22351	-2.89747

H	-0.41837	3.28287	-2.56697
H	0.16789	4.16394	-3.97793
H	-0.71056	5.01535	-2.71164
C	-1.10579	5.59581	2.04000
H	-1.71282	6.08775	1.27316
C	-0.77315	6.63665	3.10256
H	-0.20693	6.19831	3.92837
H	-1.68965	7.05833	3.52261
H	-0.17998	7.45325	2.68559
C	-1.92939	4.45225	2.62961
H	-2.21289	3.72993	1.86150
H	-2.83983	4.83334	3.10018
H	-1.35567	3.92068	3.39421
C	3.51891	3.63003	2.29240
H	4.05557	2.83636	1.76792
C	4.45747	4.83555	2.34935
H	4.75329	5.15079	1.34743
H	5.36275	4.59057	2.91091
H	3.96664	5.67994	2.84100
C	3.20257	3.13198	3.69491
H	4.11791	2.78279	4.17799
H	2.49169	2.30204	3.67956
H	2.78937	3.92292	4.32597
C	-3.47515	-1.82036	-0.37428
C	-3.44391	-3.21758	-0.40635
C	-4.50080	-3.92769	-0.96565
H	-4.47842	-5.01176	-0.98485
C	-5.59410	-3.24631	-1.47870
H	-6.42286	-3.79743	-1.90839
C	-5.63908	-1.86220	-1.42476
H	-6.50959	-1.33553	-1.80053
C	-4.58406	-1.13520	-0.87373
C	-2.26863	-3.88498	0.22805
C	-1.24325	-4.45705	-0.54237
C	-0.12143	-4.96214	0.10483
H	0.67896	-5.38996	-0.48753
C	0.03457	-4.90262	1.48031
C	-1.00605	-4.37587	2.23265
H	-0.92018	-4.35422	3.31257
C	-2.16585	-3.88741	1.64050
C	-1.35720	-4.57329	-2.04596
H	-2.09876	-3.84232	-2.37544
C	-1.86571	-5.96411	-2.42466
H	-1.15201	-6.73080	-2.10975
H	-1.99327	-6.04373	-3.50731
H	-2.82307	-6.18749	-1.95158

C	-0.05580	-4.28106	-2.78354
H	0.37906	-3.32860	-2.48382
H	-0.24169	-4.24184	-3.85904
H	0.69253	-5.05910	-2.61124
C	1.30897	-5.37451	2.13513
H	1.93481	-5.79954	1.34327
C	1.05499	-6.46716	3.16768
H	0.45366	-6.09254	4.00028
H	1.99885	-6.83164	3.58106
H	0.52426	-7.31347	2.72645
C	2.06692	-4.19976	2.74890
H	2.28934	-3.44032	1.99770
H	3.00930	-4.53620	3.19020
H	1.47806	-3.73028	3.54202
C	-3.35569	-3.51215	2.50278
H	-3.92805	-2.74922	1.96897
C	-4.27049	-4.72841	2.64918
H	-3.74435	-5.54397	3.15280
H	-4.60411	-5.08907	1.67498
H	-5.15456	-4.47425	3.23968
C	-2.99169	-2.95153	3.86970
H	-2.54570	-3.71135	4.51655
H	-3.89189	-2.59099	4.37256
H	-2.29140	-2.11605	3.79258
C	-4.67209	0.35015	-0.78277
C	-4.89807	0.96606	0.46103
C	-5.00469	2.35338	0.52723
H	-5.17753	2.81576	1.49028
C	-4.92593	3.14890	-0.60365
C	-4.72319	2.51858	-1.82300
H	-4.66288	3.12825	-2.71901
C	-4.58109	1.14525	-1.93934
C	-5.16268	0.14774	1.70893
H	-4.67353	-0.82065	1.58108
C	-6.65898	-0.13196	1.83634
H	-7.21582	0.80346	1.93967
H	-6.86408	-0.75119	2.71404
H	-7.03479	-0.65427	0.95456
C	-4.61883	0.77347	2.98655
H	-3.56308	1.04060	2.89039
H	-4.71359	0.06995	3.81705
H	-5.16675	1.67708	3.26485
C	-5.02137	4.65703	-0.56788
H	-5.74432	4.94520	-1.34168
C	-5.51317	5.21825	0.75567
H	-6.47612	4.79122	1.04475

H	-5.63219	6.30161	0.68368
H	-4.79907	5.02063	1.55973
C	-3.67363	5.27116	-0.94263
H	-2.91089	4.95810	-0.22794
H	-3.72734	6.36340	-0.94111
H	-3.34521	4.94470	-1.93086
C	-4.34597	0.55471	-3.31185
H	-4.03414	-0.48239	-3.17864
C	-5.62970	0.55632	-4.13866
H	-5.99069	1.57767	-4.28933
H	-6.42516	-0.00804	-3.64921
H	-5.45335	0.11204	-5.12182
C	-3.23644	1.28196	-4.06697
H	-3.54844	2.28405	-4.37233
H	-2.97207	0.73021	-4.97182
H	-2.33675	1.38522	-3.45853
C	-0.96885	1.41864	-0.70131
O	-1.58861	2.32872	-0.35918
C	1.01314	0.77603	-2.41396
O	1.62357	1.27565	-3.24129
C	-1.06622	-0.82257	-2.38054
O	-1.66225	-1.37752	-3.18269
C	0.88702	-1.37715	-0.62888
O	1.49273	-2.27730	-0.23896

2.6 References

(1) Fischer, E. O., On the Way to Carbene and Carbyne Complexes. Advances in Organometallic Chemistry, 14; Elsevier: Burlington, 1976; pp 1-32.

(2) Marks, T. J., Dialkylgermylene- and -stannylene-pentacarbonylchromium complexes. *J. Am. Chem. Soc.* **1971,** *93*, 7090-7091.

(3) Cotton, J. D.; Davison, P. J.; Goldberg, D. E.; Lappert, M. F.; Thomas, K. M., Co-ordination chemistry of heavy-atom group IV donors, and the crystal and molecular structure of $[(Me_3Si)_2CH]_2SnCr(CO)_5$. *J. Chem. Soc., Chem. Commun.* **1974**, 893-895.

(4) Petz, W., Transition-metal complexes with derivatives of divalent silicon, germanium, tin, and lead as ligands. *Chem. Rev.* **1986,** *86*, 1019-1047.

(5) Hashimoto, H.; Tobita, H., Recent advances in the chemistry of transition metal–silicon/germanium triple-bonded complexes. *Coord. Chem. Rev.* **2018,** *355*, 362-379.

(6) Álvarez-Rodríguez, L.; Cabeza, J. A.; García-Álvarez, P.; Polo, D., The transition-metal chemistry of amidinatosilylenes, -germylenes and -stannylenes. *Coord. Chem. Rev.* **2015,** *300*, 1-28.

(7) Jutzi, P.; Leue, C., (Supermesityl)chlorogermylene (Supermesityl = Mes* = 2,4,6-$tBu_3C_6H_2$): Synthesis and Derivatization to (Supermesityl)ferriogermylenes. *Organometallics* **1994,** *13*, 2898-2899.

(8) Eichler, B. E.; Phillips, A. D.; Haubrich, S. T.; Mork, B. V.; Power, P. P., Synthesis, Structures, and Spectroscopy of the Metallostannylenes $(\eta^5\text{-}C_5H_5)(CO)_3M{-}\ddot{S}n{-}C_6H_3\text{-}2,6\text{-}Ar_2$ (M = Cr, Mo, W; Ar = C_6H_2-2,4,6-Me_3, C_6H_2-2,4,6-Pr^i_3). *Organometallics* **2002,** *21*, 5622-5627.

(9) Pu, L.; Power, P. P.; Boltes, I.; Herbst-Irmer, R., Synthesis and Characterization of the Metalloplumbylenes $(\eta^5\text{-}C_5H_5)(CO)_3M\text{-}\ddot{P}b\text{-}C_6H_3\text{-}2,6\text{-}Trip_2$ (M = Cr, Mo, or W; Trip = $-C_6H_2$-2,4,6-i-Pr_3). *Organometallics* **2000,** *19*, 352-356.

(10) Lei, H.; Guo, J.-D.; Fettinger, J. C.; Nagase, S.; Power, P. P., Synthesis, Characterization, and CO Elimination of Ferrio-Substituted Two-Coordinate Germylenes and Stannylenes. Organometallics **2011**, 30, 6316-6322.

(11) Simons, R. S.; Power, P. P., $(\eta^5\text{-}C_5H_5)(CO)_2MoGeC_6H_3\text{-}2,6\text{-}Mes_2$: A Transition-Metal Germylyne Complex. *J. Am. Chem. Soc.* **1996,** *118*, 11966-11967.

(12) Pu, L.; Twamley, B.; Haubrich, S. T.; Olmstead, M. M.; Mork, B. V.; Simons, R. S.; Power, P. P., Triple Bonding to Germanium: Characterization of the Transition Metal Germylynes $(\eta^5\text{-}C_5H_5)(CO)_2M{\vdots}Ge\text{-}C_6H_3\text{-}2,6\text{-}Mes_2$ (M = Mo, W; Mes = $-C_6H_2$-2,4,6-

Me_3) and (η^5-C_5H_5)$(CO)_2$M⋮Ge-C_6H_3-2,6-$Trip_2$ (M = Cr, Mo, W; Trip = −C_6H_2-2,4,6-i-Pr_3) and the Related Single Bonded Metallogermylenes (η^5-C_5H_5)$(CO)_3$M-G̈e-C_6H_3-2,6-$Trip_2$ (M = Cr, W). *J. Am. Chem. Soc.* **2000,** *122*, 650-656.

(13) Filippou, A. C.; Philippopoulos, A. I.; Portius, P.; Neumann, D. U., Synthesis and Structure of the Germylyne Complexes trans-[X$(dppe)_2$W≡Ge(η^1-Cp*)] (X=Cl, Br, I) and Comparison of the W≡E Bonds (E=C, Ge) by Density Functional Calculations. *Angew. Chem. Int. Ed.* **2000,** *39*, 2778-2781.

(14) Filippou, A. C.; Portius, P.; Philippopoulos, A. I.; Rohde, H., Triple Bonding to Tin: Synthesis and Characterization of the Stannylyne Complex trans-[Cl$(PMe_3)_4$W≡Sn-C_6H_3-2,6-Mes_2]. *Angew. Chem. Int. Ed.* **2003,** *42*, 445-447.

(15) Filippou, A. C.; Weidemann, N.; Schnakenburg, G.; Rohde, H.; Philippopoulos, A. I., Tungsten–Lead Triple Bonds: Syntheses, Structures, and Coordination Chemistry of the Plumbylidyne Complexes trans-[X$(PMe_3)_4$W≡Pb(2,6-$Trip_2C_6H_3$)]. *Angew. Chem. Int. Ed.* **2004,** *43*, 6512-6516.

(16) Queen, J. D.; Phung, A. C.; Caputo, C. A.; Fettinger, J. C.; Power, P. P., Metathetical Exchange between Metal-Metal Triple Bonds. *J. Am. Chem. Soc.* **2020,** *142*, 2233-2237.

(17) Stender, M.; Phillips, A. D.; Wright, R. J.; Power, P. P., Synthesis and Characterization of a Digermanium Analogue of an Alkyne. *Angew. Chem. Int. Ed.* **2002,** *41*, 1785-1787.

(18) Phillips, A. D.; Wright, R. J.; Olmstead, M. M.; Power, P. P., Synthesis and Characterization of 2,6-$Dipp_2$-$H_3C_6SnSnC_6H_3$-2,6-$Dipp_2$ (Dipp = C_6H_3-2,6-Pr^i_2): A Tin Analogue of an Alkyne. *J. Am. Chem. Soc.* **2002,** *124*, 5930-5931.

(19) Pu, L.; Twamley, B.; Power, P. P., Synthesis and Characterization of 2,6-$Trip_2H_3C_6PbPbC_6H_3$-2,6-$Trip_2$ (Trip = C_6H_2-2,4,6-i-Pr_3): A Stable Heavier Group 14 Element Analogue of an Alkyne. *J. Am. Chem. Soc.* **2000,** *122*, 3524-3525.

(20) McCrea-Hendrick, M. L.; Caputo, C. A.; Linnera, J.; Vasko, P.; Weinstein, C. M.; Fettinger, J. C.; Tuononen, H. M.; Power, P. P., Cleavage of Ge–Ge and Sn–Sn Triple Bonds in Heavy Group 14 Element Alkyne Analogues $(EAr^{iPr}{}_4)_2$ (E = Ge, Sn; $Ar^{iPr}{}_4$ = C_6H_3-2,6(C_6H_3-2,6-$^iPr_2$)$_2$) by Reaction with Group 6 Carbonyls. *Organometallics* **2016,** *35*, 2759-2767.

(21) Pangborn, A. B.; Giardello, M. A.; Grubbs, R. H.; Rosen, R. K.; Timmers, F. J., Safe and Convenient Procedure for Solvent Purification. *Organometallics* **1996,** *15*, 1518-1520.

(22) Queen, J. D.; Bursch, M.; Seibert, J.; Maurer, L. R.; Ellis, B. D.; Fettinger, J. C.; Grimme, S.; Power, P. P., Isolation and Computational Studies of a Series of Terphenyl Substituted Diplumbynes with Ligand Dependent Lead–Lead Multiple-Bonding Character. *J. Am. Chem. Soc.* **2019,** *141*, 14370-14383.

(23) King R. B., Stone F. G. A., Sodium Salts of Carbonyl Hydrides Prepared in Ethereal Media. In *Inorg. Synth.*; McGraw-Hill book: New-York, 1963; Vol. 7, pp 196-201.

(24) Reimer, K. J., Shaver, A., Quick, M.H. and Angelici, R.J., Pentacarbonylmanganese Halides. In *Inorg. Synth.*, Reagents for Transition Metal Complex and Organometallic Syntheses; Wiley-Interscience: Hoboken, 2006; pp 154-159.

(25) Hicks, J.; Juckel, M.; Paparo, A.; Dange, D.; Jones, C., Multigram Syntheses of Magnesium(I) Compounds Using Alkali Metal Halide Supported Alkali Metals as Dispersible Reducing Agents. *Organometallics* **2018,** *37*, 4810-4813.

(26) Lai, T. Y.; Tao, L.; Britt, R. D.; Power, P. P., Reversible Sn–Sn Triple Bond Dissociation in a Distannyne: Support for Charge-Shift Bonding Character. *J. Am. Chem. Soc.* **2019,** *141*, 12527-12530.

(27) Joy, J.; Danovich, D.; Kaupp, M.; Shaik, S., Covalent vs Charge-Shift Nature of the Metal–Metal Bond in Transition Metal Complexes: A Unified Understanding. *J. Am. Chem. Soc.* **2020,** *142*, 12277-12287.

(28) Goodman, J. L.; Peters, K. S.; Vaida, V., The determination of the manganese-manganese bond strength in $Mn_2(CO)_{10}$ using pulsed time-resolved photoacoustic calorimetry. *Organometallics* **1986,** *5*, 815-816.

(29) Pan, S.; Zhao, L.; Dias, H. V. R.; Frenking, G., Bonding in Binuclear Carbonyl Complexes $M_2(CO)_9$ (M = Fe, Ru, Os). *Inorg. Chem.* **2018,** *57*, 7780-7791.

(30) Wolf, S.; Fenske, D.; Klopper, W.; Feldmann, C., $[Pb\{Mn(CO)_5\}_3][AlCl_4]$: a lead-manganese carbonyl with $AlCl_4$-linked $PbMn_3$ clusters. *Dalton Trans.* **2019,** *48*, 4696-4701.

(31) Braunschweig, H.; Damme, A.; Dewhurst, R. D.; Kramer, T.; Östreicher, S.; Radacki, K.; Vargas, A., Ditopic Ambiphilicity of an Anionic Dimetalloborylene Complex. *J. Am. Chem. Soc.* **2013,** *135*, 2313-2320.

(32) Clementi, E.; Raimondi, D. L.; Reinhardt, W. P., Atomic Screening Constants from SCF Functions. II. Atoms with 37 to 86 Electrons. *J. Chem. Phys.* **1967,** *47*, 1300-1307.

(33) Pyykkö, P.; Atsumi, M., Molecular Single-Bond Covalent Radii for Elements 1–118. *Chem. Eur. J.* **2009,** *15*, 186-197.

(34) Cordero, B.; Gómez, V.; Platero-Prats, A. E.; Revés, M.; Echeverría, J.; Cremades, E.; Barragán, F.; Alvarez, S., Covalent radii revisited. *Dalton Trans.* **2008**, 2832-2838.

(35) Herberhold, M.; Tröbs, V.; Milius, W.; Wrackmeyer, B., Carbonyliron-Lead Complexes: Multinuclear Magnetic Resonance Study in Solution and X-Ray Structure Determination of $[Et_2PbFe(CO)_4]_2$. *Z. Naturforsch. B* **1994,** *49*, 1781.

(36) Wade, K., The structural significance of the number of skeletal bonding electron-pairs in carboranes, the higher boranes and borane anions, and various transition-metal carbonyl cluster compounds. *J. Chem. Soc. D* **1971**, 792-793.

(37) Mingos, D. M. P., A General Theory for Cluster and Ring Compounds of the Main Group and Transition Elements. *Nat. Phys.* **1972,** *236*, 99-102.

(38) Wei, C. H., Structural analyses of tetracobalt dodecacarbonyl and tetrarhodium dodecacarbonyl. Crystallographic treatments of a disordered structure and a twinned composite. *Inorg. Chem.* **1969,** *8*, 2384-2397.

(39) Plečnik, C. E.; Liu, S.; Chen, X.; Meyers, E. A.; Shore, S. G., Lanthanide−Transition-Metal Carbonyl Complexes: New $[Co_4(CO)_{11}]^{2-}$ Clusters and Lanthanide(II) Isocarbonyl Polymeric Arrays. *J. Am. Chem. Soc.* **2004,** *126*, 204-213.

(40) Chini, P., The closed metal carbonyl clusters. *Inorg. Chim. Acta* **1968,** *2*, 31-51.

(41) Farrugia, L. J.; Braga, D.; Grepioni, F., A structural redetermination of $Co_4(CO)_{12}$: evidence for dynamic disorder and the pathway of metal atom migration in the crystalline phase. *J. Organomet. Chem.* **1999,** *573*, 60-66.

(42) Zhang, X.; Li, Q.-s.; Xie, Y.; King, R. B.; Schaefer, H. F., A Carbonyl Group Bridging Four Metal Atoms in a Homoleptic Carbonylmetal Cluster: The Remarkable Case of -$Co_4(CO)_{11}$. *Eur. J. Inorg. Chem.* **2008**, 2158-2164.

(43) Simons, R. S.; Pu, L.; Olmstead, M. M.; Power, P. P., Synthesis and Characterization of the Monomeric Diaryls $M\{C_6H_3\text{-}2,6\text{-}Mes_2\}_2$ (M = Ge, Sn, or Pb; Mes = 2,4,6-

$Me_3C_6H_2$−) and Dimeric Aryl−Metal Chlorides [M(Cl){C_6H_3-2,6-Mes_2}]$_2$ (M = Ge or Sn). *Organometallics* **1997,** *16*, 1920-1925.

(44) Kano, N.; Tokitoh, N.; Okazaki, R., Synthesis and X-ray Crystal Structure of Bis{2,4,6-tris[bis(trimethylsilyl)methyl]phenyl}dibromoplumbane: The First Monomeric Diorganodihaloplumbane in the Crystalline State. *Organometallics* **1997,** *16*, 2748-2750.

(45) McCrea-Hendrick, M.; Bursch, M.; Gullett, K.; Maurer, L.; Fettinger, J.; Grimme, S.; Power, P., Counterintuitive Interligand Angles in the Diaryls E{C_6H_3-2,6-(C_6H_2-2,4,6-iPr_3)$_2$}$_2$ (E = Ge, Sn, or Pb) and Related Species: The Role of London Dispersion Forces. *Organometallics* **2018,** *37*.

(46) Elschenbroich, C., *Organometallic*. Wiley-VCH: Weinheim, 2006; pp. 356-372.

(47) Aime, S.; Gobetto, R.; Osella, D.; Milonej, L.; Hawkes, G. E.; Randall, E. W., Reinvestigation of the solution structure of $Co_4(CO)_{12}$ by ^{13}C and ^{59}Co NMR. 2. *J. Magn. Reson. (1969)* **1985,** *65*, 308-315.

(48) Richert, T.; Elbayed, K.; Raya, J.; Granger, P.; Braunstein, P.; Rosé, J., ^{59}Co NMR in Tetrahedral Clusters. *Magn. Reson. Chem.* **1996,** *34*, 689-696.

(49) Friedel, R. A.; Wender, I.; Shufler, S. L.; Sternberg, H. W., Spectra and Structures of Cobalt Carbonyls1. *J. Am. Chem. Soc.* **1955,** *77*, 3951-3958.

(50) Coffey, C. E.; Lewis, J.; Nyholm, R. S., 339. Metal–metal bonds. Part I. Compounds of gold(0) with the carbonyls of manganese, iron, and cobalt. *J. Chem. Soc.* **1964**, 1741-1749.

(51) Tan, G.; Szilvási, T.; Inoue, S.; Blom, B.; Driess, M., An Elusive Hydridoaluminum(I) Complex for Facile C–H and C–O Bond Activation of Ethers and Access to Its Isolable

Hydridogallium(I) Analogue: Syntheses, Structures, and Theoretical Studies. *J. Am. Chem. Soc.* **2014,** *136*, 9732-9742.

(52) Pomeroy, R. K.; Vancea, L.; Calhoun, H. P.; Graham, W. A. G., Stereochemically nonrigid six-coordinate metal carbonyl complexes. 3. The series cis-$Fe(CO)_4(SnR_3)_2$ (R = methyl, ethyl, propyl, butyl, phenyl, chloro) and the x-ray structure of tetracarbonylbis(triphenylstannyl)iron(II). *Inorg. Chem.* **1977,** *16*, 1508-1514.

(53) R. B. King, F. G. A. S., Sodium Salts of Carbonyl Hydrides Prepared in Ethereal Media. In *Inorganic Syntheses*, 1963; Vol. 7, pp 196-201.

(54) Reimer, K. J., Shaver, A., Quick, M.H. and Angelici, R.J., Pentacarbonylmanganese Halides. In *Inorganic Syntheses*, 1990; Vol. 28, pp 154-159.

(55) Hicks, J.; Juckel, M.; Paparo, A.; Dange, D.; Jones, C., Multigram Syntheses of Magnesium(I) Compounds Using Alkali Metal Halide Supported Alkali Metals as Dispersible Reducing Agents. *Organometallics* **2018,** *37*, 4810-4813.

(56) Gaussian 16, Revision C.01, M. J. Frisch, G. W. Trucks, H. B. Schlegel, G. E. Scuseria, M. A. Robb, J. R. Cheeseman, G. Scalmani, V. Barone, G. A. Petersson, H. Nakatsuji, X. Li, M. Caricato, A. V. Marenich, J. Bloino, B. G. Janesko, R. Gomperts, B. Mennucci, H. P. Hratchian, J. V. Ortiz, A. F. Izmaylov, J. L. Sonnenberg, D. Williams-Young, F. Ding, F. Lipparini, F. Egidi, J. Goings, B. Peng, A. Petrone, T. Henderson, D. Ranasinghe, V. G. Zakrzewski, J. Gao, N. Rega, G. Zheng, W. Liang, M. Hada, M. Ehara, K. Toyota, R. Fukuda, J. Hasegawa, M. Ishida, T. Nakajima, Y. Honda, O. Kitao, H. Nakai, T. Vreven, K. Throssell, J. A. Montgomery, Jr., J. E. Peralta, F. Ogliaro, M. J. Bearpark, J. J. Heyd, E. N. Brothers, K. N. Kudin, V. N. Staroverov, T. A. Keith, R. Kobayashi, J. Normand, K. Raghavachari, A. P. Rendell, J. C. Burant, S. S. Iyengar, J. Tomasi, M. Cossi, J. M. Millam, M. Klene, C. Adamo, R. Cammi, J. W. Ochterski, R. L. Martin, K. Morokuma, O. Farkas, J. B. Foresman, and D. J. Fox, Gaussian, Inc.,

Wallingford CT, 2019.

(57) a) J. P. Perdew, K. Burke, and M. Ernzerhof, Generalized Gradient Approximation Made Simple. *Phys. Rev. Lett.*, **1996**, *77*, 3865-68. b) J. P. Perdew, K. Burke, and M. Ernzerhof, Generalized Gradient Approximation Made Simple. *Phys. Rev. Lett.*, **1997**, *78*, 1396. c) C. Adamo and V. Barone, Toward reliable density functional methods without adjustable parameters: The PBE0 model. *J. Chem. Phys.*, **1999**, *110*, 6158-69.

(58) a) F. Weigend and R. Ahlrichs, Balanced basis sets of split valence, triple zeta valence and quadruple zeta valence quality for H to Rn: Design and assessment of accuracy. *Phys. Chem. Chem. Phys.*, **2005**, *7*, 3297-305. b) F. Weigend, Accurate Coulomb-fitting basis sets for H to Rn, *Phys. Chem. Chem. Phys.*, **2006**, *8*, 1057-65.

(59) B. Metz, H. Stoll, and M. Dolg, Small-core multiconfiguration-Dirac–Hartree–Fock-adjusted pseudopotentials for post-d main group elements: Application to PbH and PbO. *J. Chem. Phys.*, **2000**, *113*, 2563-2569.

(60) S. Grimme, S. Ehrlich and L. Goerigk, Effect of the damping function in dispersion corrected density functional theory. *J. Comp. Chem*. **2011**, *32*, 1456-65.

(61) I. M. Alecu, J. Zheng, Y. Zhao, and D. G. Truhlar, Computational Thermochemistry: Scale Factor Databases and Scale Factors for Vibrational Frequencies Obtained from Electronic Model Chemistries. *J. Chem. Theory Comput.*, **2010**, *6*, 2872-2887.

(62) Bruker (2019) APEX3 (Version 2019.1) and (2016) SAINT (Version 8.37a). Bruker AXS Inc., Madison, Wisconsin, USA.

(63) Blessing, R. H., An Empirical Correction for Absorption Anisotropy, *Acta Cryst.*, **1995**, A51, 33-38.

(64) Sheldrick, G.M., SADABS (2016) Version 2016/2, 'Siemens Area Detector Absorption Correction' Universität Göttingen: Göttingen, Germany.

(65) Sheldrick, G.M., (2002). SHELXTL. Version 6.1. Bruker AXS Inc., Madison, Wisconsin, USA.

(66) Sheldrick, G. M., (2017). SHELXL2017/1. Universität Göttingen: Göttingen, Germany.

(67) Sheldrick, G. M., (2014) SHELXT, Universität Göttingen: Göttingen, Germany. Structure determination program. Private communication.

(68) Sheldrick, G. M., (2018). SHELXL2018/3. Universität Göttingen: Göttingen, Germany.

(69) Flack, H.D., On Enantiomorph-Polarity Estimation. *Acta Cryst.*, **1983**, A39, 876-881.

(70) Hooft, R.W.W, Straver, L.H. & Spek, A.L. Determination of absolute structure using Bayesian statistics on Bijvoet differences, J. Appl, Cryst., **2008**, 41, 96-103.

(71) Thompson,A.L. & Watkin, D.J., X-ray crystallography and chirality: understanding the limitations. *Tetrahedron: Asymmetry*, **2009**, 20, 712-717.

(72) Berry, R. S., Correlation of Rates of Intramolecular Tunneling Processes, with Application to Some Group V Compounds. *J. Chem. Phys.*, **1960**, *32*, 933–938.

(73) Vancea, L.; Bennett, M. J.; Jones C. E.; Smith, R. A.; Graham, W. A. G., Stereochemically nonrigid six-coordinate metal carbonyl complexes. 1. Polytopal rearrangement and x-ray structure of tetracarbonylbis(trimethylsilyl)iron. *Inorg. Chem.* **1977,** *16*, 897-902.

Chapter 3

Hydrostannylation of Carbon Dioxide by a Hydrido-stannylene Molybdenum Complex

This work is published in Dalton Transactions, DOI: 10.1039/D1DT02473F

Zhu, **Q**.; Fettinger, J.C.; Power, P.P. *Dalton Trans.* **2021**, *50*, 12555-12562.

3.1 Introduction

Tetravalent heavier group 14 element hydrides are well-known as reagents that effect numerous organic transformations under mild conditions. In contrast, the corresponding reactions of their divalent hydride congeners are much less explored although they have been shown to display catalytic potential as a result of their coordinative unsaturation and their hydridic reactivity with unsaturated molecules.[10-12] The first stable divalent organotin hydride, $\{Ar^{iPr6}Sn(\mu\text{-}H)\}_2$ (Ar^{iPr6} = -C_6H_3-2,6-(C_6H_2-2,4,6-$^i Pr_3$)$_2$),[13] was reported in 2000. This was followed by further examples[14-20] from a number of groups which included the three-coordinate organotin(II) hydride [{HC(CMeNAr)$_2$}SnH] (Ar = 2,6-i$Pr_2C_6H_3$) containing a terminal Sn-H bond as reported by Roesky and coworkers in 2006,[14] and the amido species $[LSn(\mu\text{-}H)]_2$ (L=-N(Ar)($SiPr^i_3$) Ar = C_6H_2{C(H)Ph_2}$_2Pr^i$-2,6,4) as described by Jones and coworkers in 2013.[19] In addition, there has been a growing interest in the reactivity of these hydrides with important small molecules (e.g. alkenes, alkynes, ketones, etc.),[21-27] transition metal complexes,[28-31] and their recently discovered involvement in equilibria between the multiply bonded group 14 species and hydrogen.[32]

Recent work in this group has shown that the aryltin(II) hydrides $\{Ar^{iPr4}Sn(\mu\text{-}H)\}_2$ and $\{Ar^{iPr6}Sn(\mu\text{-}H)\}_2$ react rapidly with norbornene and norbornadiene as well as other alkenes to afford the similar hydrostannylation products ArSn(norbornyl) and ArSn(norbornenyl) at ambient temperature.[33] These results suggested that the reactive tin species is a monomeric

$Ar^{iPr4}SnH/Ar^{iPr6}SnH$ unit that is in equilibrium with the dimer. Although a ^1H NMR calculation of the chemical shift of Sn-H in $Ar^{iPr6}SnH$, which resonates at δ=25.4 ppm, suggests the presence of monomeric $Ar^{iPr6}SnH$, no structurally characterized two-coordinate divalent tin(II) hydride has been reported to date.[34] Wesemann and coworkers reported a series of Lewis base-complex of $Ar^{iPr6}SnH$, which is the monomeric unit of $\{Ar^{iPr6}Sn(\mu\text{-}H)\}_2$, including NHCs, and DMAP, indicating the Lewis acidic nature of $Ar^{iPr6}SnH$ moiety.[35-37] On the other hand, isolation of $Cp_2M(Ar^{iPr6}SnH)_2$ (M = Ti, Zr, Hf) complexes via reaction of organodihydridostannate with group 4 metallocene dichloride highlighted the Lewis basicity of $Ar^{iPr6}SnH$.[31]

In addition to reactivity with alkenes, workers have also examined the reactivity of low-valent group 14 element hydrides with carbonyl compounds and carbon dioxide, as conversions of CO_2 into useful chemicals are of broad interest. However, examples of Sn(II) hydrides in these processes remain scarce. In 2009, Roesky and coworkers reported hydrostannylation of CO_2 with the organotin(II) hydride, $[\{HC(CMeNAr)_2\}SnH]$ (Ar = 2,6-$iPr_2C_6H_3$), as well as activated alkynes and a carbodiimide.[21] Computational studies by Toro-Labbé and coworkers on the hydroboration of CO_2 using $[\{HC(CMeNAr)_2\}EH]$ (E = Si(II), Ge(II), Sn(II), and Pb(II), Ar = 2,6-$iPr_2C_6H_3$) as catalysts demonstrated that activation energies for the catalytic cycle become lower as group 14 is descended.[38] However, reduction of CO_2 to formic acid and methanol by germanium hydride $[\{HC(CMeNAr)_2\}GeH]$ (Ar = 2,6-$iPr_2C_6H_3$) using ammonia borane as the hydrogen source is the sole reported example among these complexes.[39] A recent study by Wesemann and coworkers reported the reaction of $\{Ar^{iPr6}Sn(\mu\text{-}H)\}_2$ and CO_2, wherein a hydride was transferred to the carbon atom and the resulting formate anion displayed bridging coordination at two tin atoms.[40] Earlier, Jones and coworkers reported that catalytic hydroboration of carbonyl compounds and CO_2 reduction were achieved via the two-coordinated amidotin hydride $[LSn(\mu\text{-}H)]_2$ (L=-N(Ar)($SiPr^i_3$) Ar = $C_6H_2\{C(H)Ph_2\}_2Pr^i$-2,6,4)

in solution, using boranes as the hydrogen source, with their turnover frequencies rivaling those of transition metal-based catalysts.[41]

Herein, we report the reactions of $\{Ar^{iPr4}Sn(\mu\text{-}H)\}_2$ and $\{Ar^{iPr6}Sn(\mu\text{-}H)\}_2$ with the molybdenum carbonyl $[Mo(CO)_5(THF)]$, which afforded the complexes $Mo(CO)_5\{Sn(Ar^{iPr6})H\}$, (**1**), and $Mo(CO)_5\{Sn(Ar^{iPr4})(THF)H\}$, (**2**), respectively. Reactions of **1** or **2** with CO_2 were then explored. Hydrostannylation of CO_2 with **1** was observed to result in the formation of $Mo(CO)_5\{Sn(Ar^{iPr6})(\kappa^2\text{-}O,O'\text{-}O_2CH)\}$, (**3**), in which a bidentate formate anions coordinated to the tin. The Lewis basic nature of $Ar^{iPr6}SnH$ was shown by the isolation of the Lewis acid-base complex $[(Ar^{iPr6})(H)Sn\text{-}Mo(CO)_5]$, **1**, which results from the dissociation of $\{Ar^{iPr6}Sn(\mu\text{-}H)\}_2$ to monomers and its subsequent complexation with a Lewis acidic $[Mo(CO)_5]$ moiety (Scheme 3.1). The catalytic potential of **1** for CO_2 reduction was also investigated by reacting **3** with pinacolborane in C_6D_6, where quantitative conversion of **3** to **1** and formation of a methanol equivalent was observed.

3.2 Experimental Details

General considerations. All operations were carried out under anaerobic & anhydrous conditions by using modified Schlenk techniques or in a Vacuum Atmospheres OMNI-Lab drybox under an atmosphere of dry argon or nitrogen. All solvents were dried over alumina columns and degassed prior to use.[42] $Mo(CO)_6$ was used as purchased without further purification. ^1H, ^{13}C, and ^{119}Sn NMR spectra were collected on a Varian 600 MHz spectrometer. ^{11}B NMR spectra were collected on a 500 MHz Bruker Avance DRX spectrometer. The ^{11}B NMR data were referenced to the external standard BF_3OEt_2. The ^{119}Sn NMR spectra were referenced to an external standard of $SnMe_4$. UV-Visible spectra were recorded in dilute hexane solutions in 3.5 mL quartz cuvettes using an Olis 17 Modernized Cary 14 UV-Vis/NIR spectrophotometer. Infrared spectra were collected on a Bruker Tensor 27 ATR-FTIR

spectrometer. $\{Ar^{iPr4}Sn(\mu\text{-}H)\}_2$,[43] $\{Ar^{iPr6}Sn(\mu\text{-}H)\}_2$[13] and $[Mo(CO)_5(THF)]$[44] were synthesized via literature methods.

$Mo(CO)_5\{Sn(Ar^{iPr6})H\}$ (1). A solution of $[Mo(CO)_5(THF)]$ (0.55 mmol, from 0.144 g $Mo(CO)_6$) in THF (ca. 30 mL) was added to a heavy-walled Teflon tapped Schlenk flask along with $\{Ar^{iPr6}SnH\}_2$ (0.327 g, 0.272 mmol) in THF (ca. 20 mL). Upon addition of $[Mo(CO)_5(THF)]$, the color of the solution changed from blue to green, and then to a brownish yellow color after heating at 50 °C for 1 day. The flask was then heated at this temperature for 2 additional days. The solution was cooled to room temperature, the solvent was removed under reduced pressure and the yellow residue was extracted with ca. 50 mL of hexanes and filtered. Storage of the solution in a ca. -30 °C freezer for 2 weeks afforded pale yellow crystals of **1** that were suitable for single crystal X-ray diffraction studies. Yield: 40.7% (0.186 g). ^{1}H NMR (C_6D_6, 600 MHz, 298 K): δ 1.06 (d, 12 H, J_{HH} = 6.7 Hz, o-$CH(CH_3)_2$), 1.21 (d, 12 H, J_{HH} = 7.1 Hz, o-$CH(CH_3)_2$), 1.40 (d, 12 H, J_{HH} = 6.7 Hz, p-$CH(CH_3)_2$), 2.78 (hept., 2 H, J_{HH} = 6.3 Hz, p-$CH(CH_3)_2$), 3.09 (hept., 4 H, J_{HH} = 6.7 Hz, o-$CH(CH_3)_2$), 7.14-7.19 (m, 5H, m-C_6H_2 and p-C_6H_3), 7.28 (d, 2H, m-C_6H_3), 18.00 (s, 1 H, $J_{Sn\text{-}H}$ = 647 Hz, Sn-H); $^{13}C\{^1H\}$ NMR (C_6D_6, 150.6 MHz, 298 K): δ 23.46 , 24.00, 26.24, 31.14, 34.77, 122.57, 128.73, 129.85, 133.56, 145.19, 147.47, 150.60, 163.10, 206.15, 212.97; $^{119}Sn\{^1H\}$ NMR (C_6D_6, 223.6 MHz, 298 K): δ 1324 (d, $J_{Sn\text{-}H}$ = 669 Hz). λ_{max} (ε): 395.8 nm (2550 L mol^{-1} cm^{-1}). IR (ν, cm^{-1}): 2073 (m), 2057 (m), 1923 (vs), 1751 (w).

$Mo(CO)_5\{Sn(Ar^{iPr4})(THF)H\}$ (2). Using a procedure similar to that used for the preparation of **1**, $[Mo(CO)_5(THF)]$ (0.845 mmol, from 0.223 g $Mo(CO)_6$) was treated with $\{Ar^{iPr6}SnH\}_2$ (0.365 g, 0.353 mmol) to afford pale yellow crystals suitable for single crystal X-ray studies. Yield: 46.7% (0.272 g). ^{1}H NMR (C_6D_6, 600 MHz, 298 K): δ 1.00 (d, 12 H, J_{HH} = 6.8 Hz, o-$CH(CH_3)_2$), 1.33 (d, 16 H, J_{HH} = 6.9 Hz, o-$CH(CH_3)_2$ overlapped with CH_2 from THF), 3.04 (hept., 2 H, J_{HH} = 6.9 Hz, o-$CH(CH_3)_2$), 3.43 (t, 4 H, J_{HH} =5.4 Hz, THF), 7.12 (d,

4H, J_{HH} = 7.8 Hz, m-C_6H_3), 7.19 (t, 2H, J_{HH} = 7.4 Hz, p-C_6H_3), 7.23 (m, 3H, m-C_6H_3 overlapped with p- C_6H_3), 17.09 (s, 1 H, J_{Sn-H} = 704 Hz, Sn-H); $^{13}C\{^1H\}$ NMR (C_6D_6, 150.6 MHz, 298 K): δ 23.32, 25.72, 26.10, 31.01, 69.22, 124.36, 127.98, 128.34, 129.98, 130.21, 136.62, 145.30, 147.26, 206.78, 212.79; $^{119}Sn\{^1H\}$ NMR (C_6D_6, 223.6 MHz, 298 K): δ 1102. λ_{max} (ε): 402 nm (11800 L mol^{-1} cm^{-1}). IR (ν, cm^{-1}): 2059 (m), 1982 (m), 1913.63 (vs), 1795 (w).

$Mo(CO)_5\{Sn(Ar^{iPr6})(\kappa^2\text{-}O,O'\text{-}O_2CH)\}$ (3). THF (ca. 30 mL) was added to a heavy-walled Teflon tapped Schlenk flask charged with 0.435 g of **1**. Then, the solution was frozen, and the flask was evacuated and refilled with CO_2, repeated three times. The reaction was then allowed to warm to room temperature, where the color of the solution changed from yellow to pale yellow. After stirring overnight, the solvent was removed under reduced pressure and the residue was extracted with diethyl ether. Storage of the solution in a ca. -30 °C freezer for 1 week afforded colorless crystals suitable for single crystal X-ray studies. Yield: 83.2% (0.381 g). ^1H NMR (C_6D_6, 600 MHz, 298 K): δ 1.06 (d, 12 H, J_{HH} = 6.9 Hz, o-$CH(CH_3)_2$), 1.27 (d, 12 H, J_{HH} = 7.1 Hz, o-$CH(CH_3)_2$), 1.45 (d, 12 H, J_{HH} = 7.1 Hz, p-$CH(CH_3)_2$), 2.85 (hept., 2 H, J_{HH} = 6.9 Hz, p-$CH(CH_3)_2$), 2.93 (hept., 4 H, J_{HH} = 6.8 Hz, o-$CH(CH_3)_2$), 7.18 (t, 1H, J_{HH} = 7.6 Hz, p-C_6H_3), 7.29 (s, 4H, m-C_6H_2), 7.30 (d, 2H, J_{HH} = 7.6 Hz, m-C_6H_3), 8.07 (s, 1 H, CO_2H); $^{13}C\{^1H\}$ NMR (C_6D_6, 150.6 MHz, 298 K): δ 22.85, 24.06, 26.62, 31.44, 34.83, 121.99, 128.35, 131.33, 134.72, 145.74, 147.50, 150.33, 164.43, 174.01, 205.58, 210.21; $^{119}Sn\{^1H\}$ NMR (C_6D_6, 223.6 MHz, 298 K): δ 606. λ_{max} (ε): 341.8 nm (shoulder, 7500 L mol^{-1} cm^{-1}). IR (ν, cm^{-1}): 2072 (m), 1969 (w), 1934 (vs), 1605 (w), 1560 (w), 1533 (m), 1352 (m).

Catalytic studies. To a J Young's tube containing 20 mg of **3**, was added 0.6 mL of C_6D_6, then 140 μL (five equivalents) of HBpin (pin = pinacolato) was added to the tube. The reactions were monitored by ^1H, and ^{11}B NMR spectroscopies. ^1H and ^{11}B NMR spectra were recorded after a brief sonication (less than 30 seconds) of the mixture. ^1H NMR spectra

of the mixture solution of **3** and HBpin in C_6D_6 were recorded 5 min, 3 hours after mixing in glove box, separately. A distinct color change from almost colorless to yellow was observed upon addition of HBpin to the C_6D_6 solution of **3** (see SI).

3.3 Result and Discussion

Syntheses. Compound **1** was synthesized by gently heating 1 equivalent of $\{Ar^{iPr6}Sn(\mu\text{-}H)\}_2$[10] THF solution with 2 equivalents of $[Mo(CO)_5(THF)]$[34] in a Schlenk flask for 3 days. (Scheme 3.1) The resulting solution was extracted with hexanes, and storage of the solution in a ca. -30 °C freezer for 2 weeks afforded pale yellow crystal of **1** in moderate yield. Compound **2** was synthesized analogously using $\{Ar^{iPr4}Sn(\mu\text{-}H)\}_2$.[33] Initial attempts involved either using $Mo(CO)_6$ instead of $[Mo(CO)_5(THF)]$ or performing the above reactions at room temperature (298K) and 0 °C (273K), and ^1H NMR spectra of the crude product revealed low conversion to the product, although gentle heating to 50 °C overnight significantly improved the product yield. The moderate yield may be associated with the tendency of the $\{Ar^{iPr6}Sn(\mu\text{-}H)\}_2$ or $\{Ar^{iPr4}Sn(\mu\text{-}H)\}_2$, to exist in equilibrim with multiply bonded species and hydrogen.[32] Also, the formation of tin clusters was reported from heating the organotin(II) hydrides in toluene, which also may account for the low overall yield.[43, 45] Attempts in removing the coordinated THF in **2** by heating **2** at 80 °C under reduced pressure were unsuccessful.

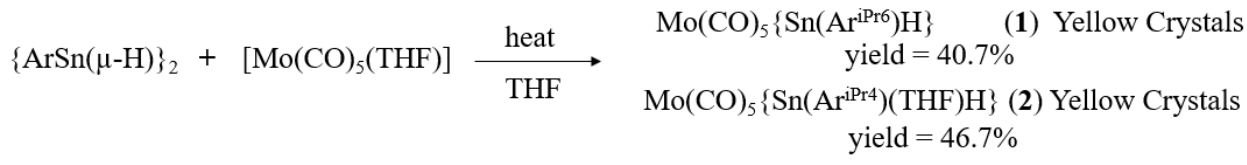

Scheme 3.1: Syntheses of **1** and **2**

For the synthesis of **3** (see Scheme 3.2 below), a solution of **1** in THF was frozen, and the flask was evacuated under reduced pressure and refilled with CO_2, repeated three times. The reaction flask was then allowed to warm to room temperature, whereupon the color of the

solution changed from yellow to pale yellow, and overnight stirring resulted in quantitative conversion of **1** to **3** based on the ^{1}H NMR spectrum of the crude product. Extraction with diethyl ether and storage of the solution in a ca. -30 °C freezer for 1 week afforded colorless crystals of **3** in good yield. Similar reactions were also attempted with **2**, but only a very limited reaction was observed, possibly due to lack of a coordination site at the tin atom in **2**.

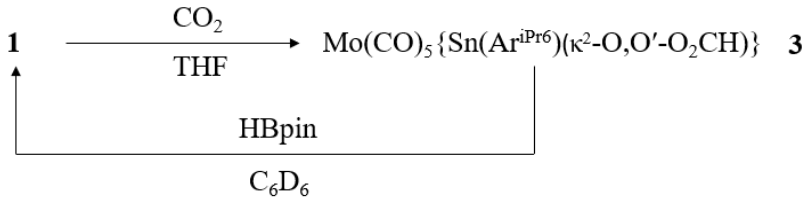

Scheme 3.2: Reaction of **1** with CO_2, and reaction of **3** with boranes

Structures. The molecular structures of **1**, **2**, and **3** are shown in Figure 3.1, 3.2, and 3.3.

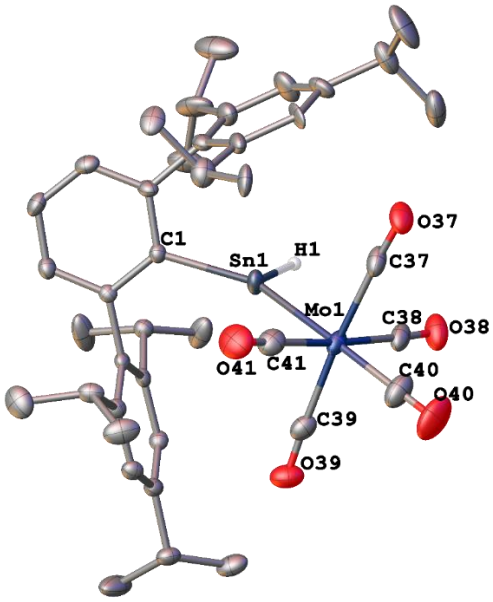

Figure 3.1: Solid-state molecular structure of **1** (hydrogen atoms and disorder not shown, thermal ellipsoids are shown at 50% probability. Selected bond lengths (Å) and angles (deg.): Sn(1)-C(1) 2.158(2), Sn(1)-Mo(1) 2.7157(4), Sn(1)-H(1) 1.93(2), Mo(1)-C(40) 2.018(3), Mo(1)-C(41) 2.050(3), Mo(1)-C(38) 2.050(3), Mo(1)-C(37) 2.053(3), Mo(1)-C(39) 2.053(3), C(37)-O(37) 1.143(3), C(38)-O(38) 1.139(3), C(39)-O(39) 1.143(3), C(40)-O(40) 1.135(4), C(41)-O(41) 1.140(4); C(1)-Sn(1)-Mo(1) 140.11(6), C(1)-Sn(1)-H(1)

108.3(6), Mo(1)-Sn(1)-H(1) 111.4(6).

Compound **1** features almost trigonal planar three-coordination at the tin atom, where the sum of C(1)-Sn(1)-Mo(1), C(1)-Sn(1)-H(1), and Mo(1)-Sn(1)-H(1) angles around tin is 359.81(8)^{o} in **1**, with a terminal Sn-H bond. In contrast, compound **2** features a four-coordinate tin atom to which THF is also coordinated. In both complexes the aryltin hydride unit acts as a Lewis base via the tin lone pair, forming donor/acceptor complex with a $Mo(CO)_5$ unit to yield a distorted octahedral coordination geometry at molybdenum. The almost planar coordination environment generated at Sn by these ligands is consistent with a vacant p orbital located perpendicularly to the coordination plane in the structure of **1**. In **2**, the p orbital is likely to be occupied by THF coordination but the Sn(1)-O(1) bond in the structure of **2** is not perpendicular to the coordination plane, as the O(1)-Sn(1)-H(1) angle is 62.9(19)^{o}. The sum of the angles at tin associated with the hydride and terphenyl ligand in **2** is 359.0(19)^{o}. In the structure of **1**, the C(1)-Sn(1)-H(1) unit is almost coplanar with that of molybdenum and the three carbonyl groups of C(38), C(40), and C(41). The C(38)-Mo(1)-Sn(1)-C(1) torsion angle is 1.2(4)^{o}, and Sn(1)-Mo(1)-C(40) array is almost linear (176.49(8)^{o}), whereas in the structure of **2**, the C(1)-Sn(1)-H(1) plane deviates somewhat from the molybdenum carbonyl plane, and the C(32)-Mo(1)-Sn(1)-C(1) torsion angle is 17(2)^{o}. The Sn-H distance in **1** is 1.93(2) Å, and 1.82(6) Å for **2**. These values may be compared to that of the terminal Sn-H bond, 1.74(3) Å, in [{$HC(CMeNAr)_2$}SnH] reported by Roesky and coworkers,[14] and Sn-H bonds in $Cp_2M(Ar^{iPr6}SnH)_2$ (M = Ti, Zr, Hf) complexes reported by Wesemann and coworkers, which range from 1.69(2) to 1.776(18) Å.[31] The Mo-C bond lengths in **1** and **2**, Mo(1)-C(40) for **1** and Mo(1)-C(35) for **2**, which are trans to $Ar^{iPr6}SnH$ ligand, are 2.018(3) Å for **1**, 1.999(7) Å for **2**, respectively, showing little variation. In the structure of **1**, the average Mo-C bond length of other four carbonyls is 2.052(3) Å, suggesting stronger pi-back bonding for Mo(1)-C(40) bond, where in the structure of **2**, the average bond length of other four carbonyls is 2.037(6)

Å. This is likely a result of the increased electron density at molybdenum due to the favorable sigma-donor properties of the $Ar^{iPr6}SnH$ ligand and its relatively weak π-acceptor character.[46] The Sn(1)-Mo(1) bond length is 2.716(4) Å in **1**, and 2.756(6) Å in **2**, which are similar to the Sn-Mo bond length (2.784(17) Å) in $(CO)_5MoSn(\mu_2\text{-}O^tBu)_3Ce(O^tBu)_3$ reported by Mathur and coworkers.[47] The sum of the covalent radii of Mo and Sn is 2.93(5) Å,[48] which is longer than Sn-Mo single bonds in **1** and **2**. The Sn-Mo triple bond in $Ar^{iPr6}SnMo(\eta^5\text{-}C_5H_5)(CO)_2$ results from metathetical exchange reaction between the distannyne, $Ar^{iPr6}Sn{\equiv}SnAr^{iPr6}$, and $(CO)_2(\eta^5\text{-}C_5H_5)Mo{\equiv}Mo(\eta_5\text{-}C_5H_5)(CO)_2$, is 2.4691(7) Å.[49]

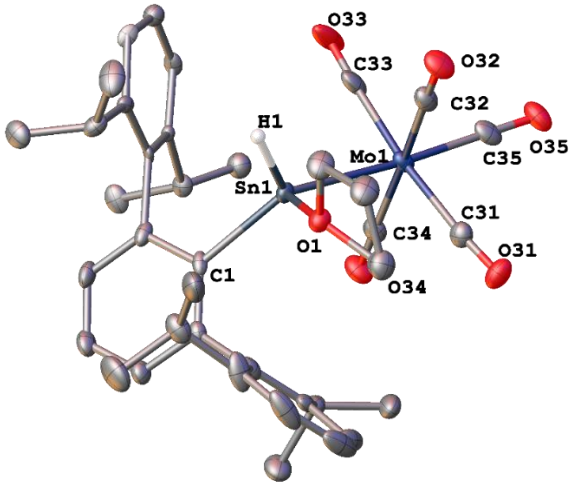

Figure 3.2: Solid-state molecular structure of **2** (hydrogen atoms and disorder are not shown, thermal ellipsoids are shown at 30% probability. Selected bond lengths (Å) and angles (deg.): Sn(1)-C(1) 2.198(5), Sn(1)-Mo(1) 2.7563(6), Sn(1)-H(1) 1.82(6), Mo(1)-C(35) 1.999(6), Mo(1)-C(31) 2.024(6), Mo(1)-C(32) 2.025(6), Mo(1)-C(33) 2.053(6), Mo(1)-C(34) 2.046(6), C(31)-O(31) 1.149(6), C(32)-O(32) 1.157(6), C(33)-O(33) 1.147(7), C(34)-O(34) 1.146(6), C(35)-O(35) 1.153(6); C(1)-Sn(1)-Mo(1) 134.31(11), C(1)-Sn(1)-H(1) 105.9(19), Mo(1)-Sn(1)-H(1) 118.8(19), O(1)-Sn(1)-H(1) 62.9(19).

The molecular structure of **3** features a four-coordinate tin atom that is coordinated by a bidentate formate ligand, a terphenyl group, and $Mo(CO)_5$ moiety. Complex **3** possesses an internal mirror plane incorporating the C(1)-Sn(1)-Mo(1) array. The formate ligand is

symmetrically bound to the tin atom, and the two Sn-O bonds being equal, 2.2228(12) Å, underlying the resonance structure of formate anion. These may be compared to the Sn-O bonds in LSn (κ^2-O,O′-O_2CH)} (L=-N(Ar)($SiPr^i_3$) Ar = C_6H_2{C(H)Ph_2}$_2Pr^i$-2,6,4) reported by Jones and coworkers are 2.353(2), and 2.333(2), respectively.[41] The Mo(1)-C(21) bond, 2.011(3) Å in **3** is slightly shortened in comparison to the Mo(1)-C(40), 2.018(3) Å, bond in the structure of **1**, suggesting similar sigma-donor properties of the Ar^{iPr6}Sn(κ^2-O,O′-O_2CH) moiety and Ar^{iPr6}SnH.

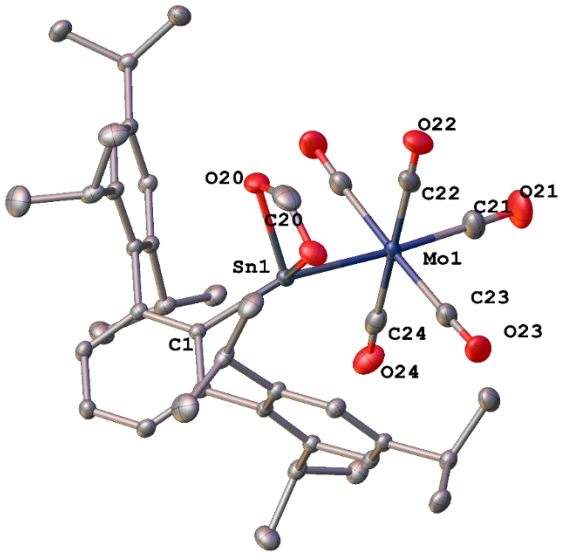

Figure 3.3. Solid-state molecular structure of **3** (hydrogen atoms and disorder are not shown, thermal ellipsoids are shown at 50% probability. Selected bond lengths (Å) and angles (deg.): Sn(1)-Mo(1) 2.158(2), Sn(1)-Mo(1) 2.723(3), Mo(1)-C(21) 2.011(3), Mo(1)-C(22) 2.036(3), Mo(1)-C(23) 2.054(3), Mo(1)-C(24) 2.062(3), C(21)-O(21) 1.140(4), C(22)-O(22) 1.147(3), C(23)-O(23) 1.138(2), C(24)-O(24) 1.142(3); C(1)-Sn(1)-Mo(1) 152.54(5), C(1)-Sn(1)-O(20) 98.18(6).

NMR Spectroscopy. The solution ^{1}H NMR spectra of **1**, **2**, and **3** displayed signals due to the Ar^{iPr4} or Ar^{iPr6} ligands with diastereotopic isopropyl methyl groups and septet methine signals, and showed little difference from those reported for {Ar^{iPr4}Sn(μ-H)}$_2$ or {Ar^{iPr6}Sn(μ-H)}$_2$.[13,43] The Sn-H signal is however observed at δ = 18.03 ppm for **1**, and at δ = 17.09 ppm for **2**, which are much further downfield than the Sn-H signal at δ = 7.87 ppm for {Ar^{iPr6}Sn(μ-

H)}$_2$, and δ = 9.13 ppm for {Ar^{iPr4}Sn(μ-H)}$_2$. The downfield shift of the signals can be attributed to the terminal nature of the Sn-H bonds in each compound, and the coordination of the transition metal to the tin atom.[46] Compared to **1**, the Sn-H signal in **2** is shifted slightly upfield, possibly as a result of the THF coordination and consequent increased electron density at the tin atom in **2**. The calculated ^{1}H NMR chemical shift of the Sn-H hydrogen of the hypothetical monomeric unit of {Ar^{iPr6}Sn(μ-H)}$_2$ is δ=25.4 ppm,[34] and coordination of transition metal carbonyl moiety should result in further a downfield shift[46] of the Sn-H signal which contradicts to the experimentally observed shifts of the hydrogens for Sn-H in **1** and **2**. The Sn-H chemical shifts of **1** and **2** are in good agreement with that seen for the hydride-bridged tin(II) species, {LSn(μ-H)}$_2$ (L=-N(Ar)(SiPr$^i_3$) Ar = C$_6$H$_2${C(H)Ph$_2$}$_2$Pr^i-2,6,4), which dissociated to monomers when dissolved in an aromatic solvent, as reported by Jones and coworkers (Sn-H δ=17.20 ppm at 298 K, broad Sn-H at δ=19.20 ppm at 313K),[19] and δ=19.4 ppm observed for a hydrogen-substituted stannylene complex, Cp*(^{i}Pr$_3$P)(H)Os=SnH(trip) (trip = 2,4,6-triisopropylphenyl), of Tilley and coworkers.[50] $^{117/119}$Sn satellites were also observed for the Sn-H signal with a coupling constant of 647 Hz for **1** and 704 Hz for **2**. The ^{1}H NMR signal of the formate hydrogen in **3** was observed at downfield region, 8.07 ppm. The ^{13}C{^{1}H} NMR spectra of **1**, **2** and **3** displayed two distinct chemical shifts for the carbonyl resonances in an approximate 1:4 ratio, which is consistent with their structures data for **1**, **2,** and **3** (see above), while ^{13}C-$^{117/119}$Sn coupling was not observed. The carbonyl resonances suggest that the rotations around Mo-Sn bond in **1** and **2** are not restricted, and thus the monomeric unit, Ar^{iPr6}SnH, is a better σ-donor than it is a π-acceptor despite the presence of an empty p-orbital on the Sn atom, which is further demonstrated in calculations (vide infra).

The ^{119}Sn{^{1}H} NMR spectra of **1**, **2**, and **3** were recorded in C$_6$D$_6$ and referenced to the external standard SnMe$_4$ in CDCl$_3$. The ^{119}Sn signal of **1** appeared at δ = 1324 ppm, which is slightly further downfield than the range of three-coordinated tin-transition metal complexes

(673-1231 ppm).[51-56] The ^{1}H-coupled ^{119}Sn NMR spectrum of **1** displayed a doublet signal (J_{Sn-H} = 649 Hz) which matches both the ^{1}H NMR spectrum and is consistent with molecular structure of **1**. The ^{119}Sn spectrum of **2** displayed one signal at δ = 1102 ppm, which is slightly more upfield than that of **1**, likely a result of the increased electron density due to the coordinated THF molecule. Both the ^{119}Sn{^{1}H} NMR spectra of **1** and **2** agree well with the ^{119}Sn NMR chemical shift of $Cp_2M(Ar^{iPr6}SnH)_2$ (M = Ti, Zr, Hf) complexes reported by Wesemann and coworkers, which ranged from 1060 to 1250 ppm.[31]

The ^{119}Sn NMR signal of **3** appeared at δ = 606 ppm, which is further downfield than those of other divalent or tetravalent tin formates[57], as reported by Roesky and coworkers for [{HC(CMeNAr)$_2$}Sn-OC(O)H] (Ar = 2,6-iPr$_2$C$_6$H$_3$) at -360 ppm.[21] Jones and coworkers reported the ^{119}Sn{^{1}H} NMR chemical shift of LSn (κ^2-O,O′-O$_2$CH)} (L=-N(Ar)(SiPr$^{i}_3$) Ar = C$_6$H$_2${C(H)Ph$_2$}$_2$Pr^{i}-2,6,4) at -134 ppm, where the formate has the same bidentate coordination as **3.**[41] The ^{119}Sn{^{1}H} NMR chemical shift of $Ar^{iPr6}Sn(H)OC(H)OSnAr^{iPr6}$ was reported at 113.4 ppm by Wesemann and coworkers.[40] The downfield shift of ^{119}Sn NMR of **3** is likely due to the coordination of [Mo(CO)$_5$] fragment at the tin atom[46], compared to those reported for organotin formates.[57]

We investigated the catalytic potential of **1** towards hydrogenation of CO_2, which is enabled at the tin atom in **1** by its coordinative unsaturation. Initial attempts using dihydrogen gas or NaH as the hydrogen source in the regeneration of **1** were unsuccessful, however, using HBpin (pin = pinacolato) as the hydrogen source resulted in quantitative conversion from **3** to **1**. The ^{1}H NMR spectrum of a mixture of **3** and HBpin showed signals attributable to the unreacted species, **3** and HBpin, 5 min after mixing in glove box. Then, after 3 hours at room temperature, the ^{1}H NMR spectrum indicated complete conversion of **3** to **1**, as evidenced by the disappearance of the 8.07 ppm signal of the formate in **3**, and the appearance of a new signal which corresponded to the Sn-H hydrogen of **1** at 18.07 ppm emerged. (Scheme 3.2) ^{11}B

NMR spectroscopy of the reaction between **3** and pinacolborane showed two additional signals apart from the excess amount of HBpin, which are attributed to $(pinB)_2O$, and MeOBpin[58, 59], which is considered as a methanol equivalent (see Scheme 3.3).

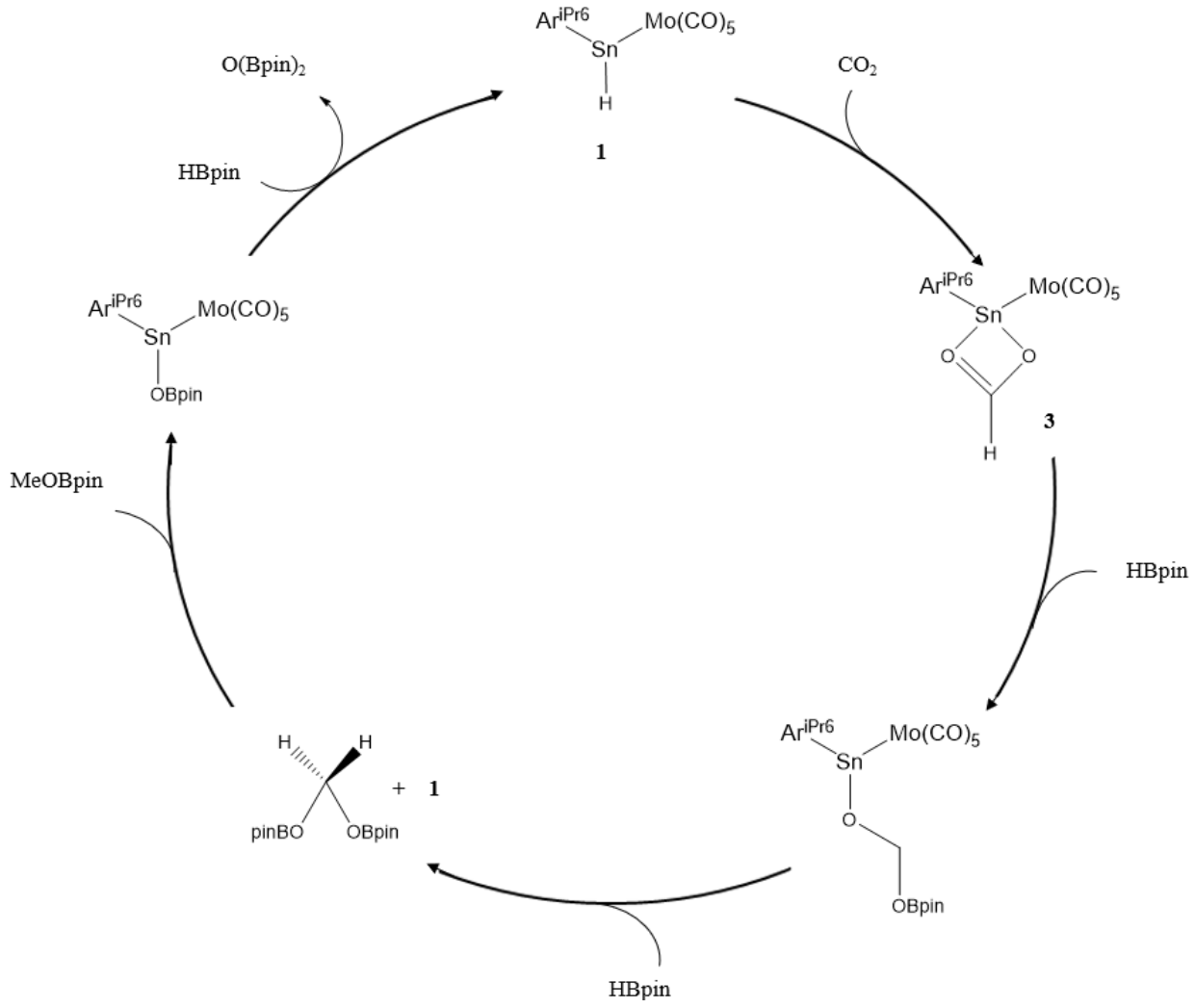

Scheme 3.3: Proposed cycle for the reduction of CO_2, catalyzed by **1**

IR spectroscopy. Compounds **1** and **2** displayed three ν_{CO} stretching bands and one Sn-H stretching band in their FT-IR spectra. The weak absorption at 1752 (w) cm^{-1} for **1** and 1795 (w) cm^{-1} for **2** were assigned to the Sn-H stretching mode, while the other three bands at, 2074 (m), 2058 (m), and 1924 (vs) cm^{-1} for **1**, 2059 (m), or 1982 (m), and 1913 (vs) cm^{-1} for **2** are attributed to the three CO stretching bands. This three-band pattern is considered to be characteristic of a $[LM(CO)_5]$ species.[60] The ν_{co} stretching frequencies of **1** are lower than those

of $[Mo(CO)_5PPh_3]$ and other molybdenum phosphine complexes as reported by Cotton and coworkers,[61] which suggests that the $Ar^{iPr6}SnH$ unit is a weaker π-acceptor than a phosphine ligand. The Sn-H stretching frequencies of **1** and **2** differ from those of the previously reported bridged-hydride Sn(II) species, $\{Ar^{iPr6}Sn(\mu\text{-}H)\}_2$ ($\nu_{Sn\text{-}H}$=1828, 1771 cm^{-1}), which are due to the asymmetric isomeric $\{Ar^{iPr6}SnSn(H)_2Ar^{iPr6}\}$.[13, 16] The Sn-H stretching frequencies of the terminal Sn-H bonds were reported to be $[\{HC(CMeNAr)_2\}SnH]$ (Ar = 2,6-$iPr_2C_6H_3$) $\nu_{Sn\text{-}H}$= 1849 cm^{-1},[14] and $[\{2,6\text{-}iPr_2C_6H_3NCMe\}_2C_6H_3SnH]$ $\nu_{Sn\text{-}H}$= 1826 cm^{-1}.[15] The Sn-H stretching frequency, however is in close agreement with those of $Cp_2M(Ar^{iPr6}SnH)_2$ (M = Ti, Zr, Hf) complexes, from 1741 to 1749 cm^{-1},[31] and calculated stretching frequency for the $Ar^{iPr4}SnH$ monomer, 1734 cm^{-1}.[16]

The IR spectrum of compound **3** displayed CO stretching bands that are similar to those of **1** and **2**. The Sn-H stretching band at 1752 cm^{-1} is no longer apparent. However, another absorbance appeared at 1533 cm^{-1} which arises from the carbonyl group of the formate, HCO_2^-. The carbonyl stretching frequency of $[\{HC(CMeNAr)_2\}Sn\text{-}OC(O)H]$ (Ar = 2,6-$iPr_2C_6H_3$) was reported to be 1641 cm^{-1}.[21] Jones and coworkers reported carbonyl stretching frequency of LSn(κ^2-O,O′-O_2CH)} (L=-N(Ar)($SiPr^i_3$) Ar = $C_6H_2\{C(H)Ph_2\}_2Pr^i$-2,6,4) at 1549 cm^{-1},[41] which agrees well with the carbonyl stretching frequency of the bidentate formate in **3**.

Computational Analysis.

The structure of **1** was subjected to refinement at the DFT level of theory (B3LYP, see computational details). Overall, the calculated and experimental bond angles of compound **1** agree well, and the slight deviations between the experimental and calculated bond angles could be a result of intermolecular interactions for the former in the solid state. The calculated length of the Sn-Mo bond is 2.723 Å, which is in close agreement to that observed in the crystal

structure of **1**, 2.7157(4) Å. However, the calculated bond length of Sn-H bond, 1.750 Å, deviates from the experimentally observed, 1.93(2) Å.

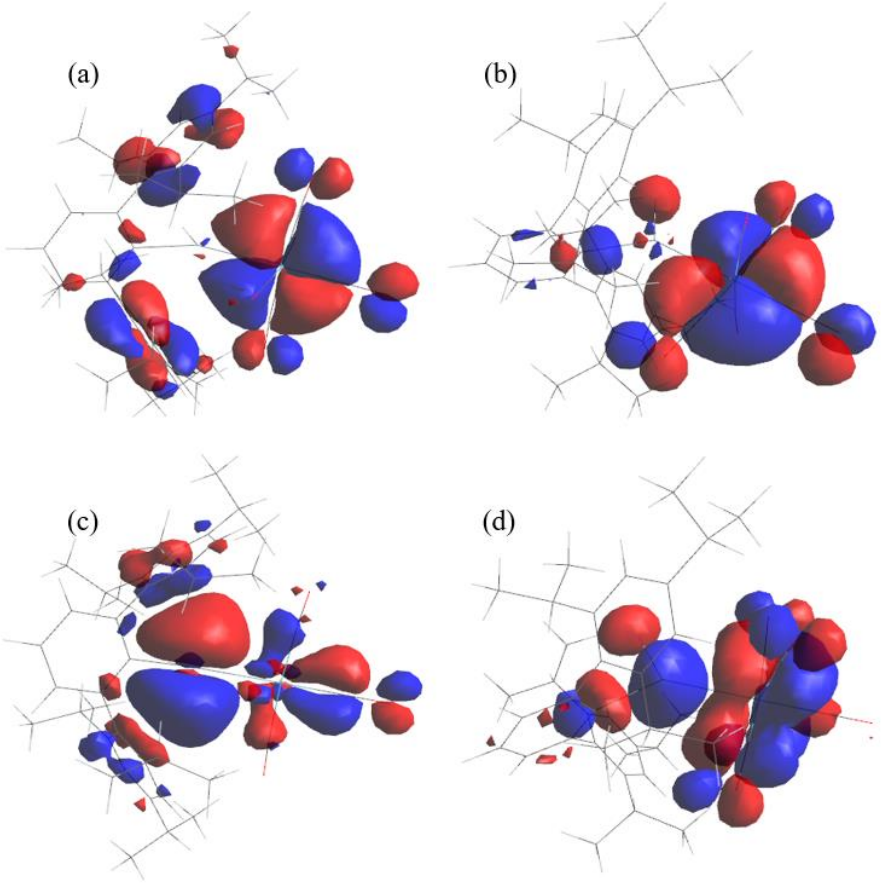

Figure 3.4: (a) HOMO-1 (-5.801 eV), (b) HOMO (-5.655 eV), (c) LUMO (-3.115 eV), (d) LUMO+1 (-2.319 eV)

Analysis of the frontier orbitals (Figure 3.4) of **1** reveals no significant π-back bonding between molybdenum and tin, despite having an available p-orbital at the tin. The major component of the HOMO is located on molybdenum, and illustrating pi-back bonding between Mo(1)-C(40), while the LUMO is located largely on tin, where a p-orbital is centered at tin, lying perpendicular to the C(1)-Sn(1)-H(1) plane. The LUMO indicates a coordinative unsaturation at tin, likely resulted from steric shielding exerted by the terphenyl ligand. For simplicity, a phenyl group has been used in place of Ar^{iPr6} group to calculate vibrational

frequencies of **1**. The terminal Sn-H bond is calculated to have a stretching frequency of 1762 cm^{-1}, which is in close agreement with what was observed experimentally, 1752 cm^{-1}.

3.4 Conclusions

We have shown that reactions of aryltin(II) hydrides $\{Ar^{iPr4}Sn(\mu\text{-}H)\}_2$ or $\{Ar^{iPr6}Sn(\mu\text{-}H)\}_2$ with two equivalents of the group 6 carbonyls, $[Mo(CO)_5(THF)]$, yield either a stable, monomeric, three coordinate, divalent tin hydride transition metal complex, $Mo(CO)_5\{Sn(Ar^{iPr6})H\}$, (**1**), or a four coordinate tin hydride species $Mo(CO)_5\{Sn(Ar^{iPr4})(THF)H\}$, (**2**). Hydrostannylation of carbon dioxide by **1** afforded the complex, $Mo(CO)_5\{Sn(Ar^{iPr6})(\kappa^2\text{-}O,O'\text{-}O_2CH)\}$, (**3**), incorporating a bidentate formate anion coordinated to the tin atom. The catalytic potential of **1** was investigated by reaction of **3** with pinacolborane in C_6D_6, where **1** was generated in nearly quantitative yield. The complexes were characterized by single crystal X-ray diffraction, UV-Visible, IR, and multinuclear NMR spectroscopy. The isolation of **1** and **2** gives supporting evidence to the existence of monomeric form of $\{Ar^{iPr4}Sn(\mu\text{-}H)\}_2$ and $\{Ar^{iPr6}Sn(\mu\text{-}H)\}_2$ in solution by its trapping as a donor ligand in complexation to $[Mo(CO)_5]$ moiety to afford an acid-base complex. Regeneration of **1** from **3** via reaction with pinacolborane as a hydrogen source suggests the promising catalytic potential of **1** in the hydrogenation of CO_2.

3.5 Supporting Information

Computational details. The structure was subjected to refinement at the DFT level of theory, with the B3LYP hybrid exchange functional[62-65] using Ahlrichs polarized basis set def2-TZVP.[66] For Sn, the effective core potential (ECP) basis set[67] with similar valence quality was used. In addition, dispersion correction with Becke-Johnson damping (D3BJ)[68,69] was used. The resolution of identity approximation was employed with auxiliary basis set def2-TZVP/C[70,71] in order to speed up the calculations. Phenyl was used in substitution of Ar^{iPr6} in

the calculation of IR frequencies to speed up calculation. The reported IR frequencies are scaled by 0.986 as suggested by Truhlar. All calculations were carried out using the ORCA 4.2.1 quantum chemistry package.[72]

Compound **1**	Bond lengths (Å) Expt.	Bond lengths (Å) Calc.	Compound **1**	Bond angles (°) Expt.	Bond angles (°) Calc.
Sn(1)-C(1)	2.158(2)	2.16853	Mo(1)-Sn(1)-C(1)	140.11(6)	135.0253
Sn(1)-Mo(1)	2.7157(4)	2.72286	H(1)-Sn(1)-C(1)	108.3(6)	100.3012
Sn(1)-H(1)	1.93(2)	1.74977	H(1)-Sn(1)-Mo(1)	111.4(6)	124.6165
Mo(1)-C(38)	2.050(3)	2.04503	Sn(1)-Mo(1)-C(40)	176.48(9)	179.1233
Mo(1)-C(39)	2.053(3)	2.05207	C(38)-Mo(1)-C(40)	91.25(12)	92.8569
Mo(1)-C(40)	2.018(3)	2.00717	Sn(1)-Mo(1)-C(38)	86.08(8)	86.5436
Mo(1)-C(41)	2.050(3)	2.04461	Mo(1)-C(40)-O(40)	179.5(4)	179.8013

Table 3.S1: Experimental and Calculated Bond Lengths and Bond Angles of **1**

1 (cm^{-1})
607
1762
1998
2013
2104

Table 3.S2: Scaled CO stretching frequencies (scaled by 0.986).

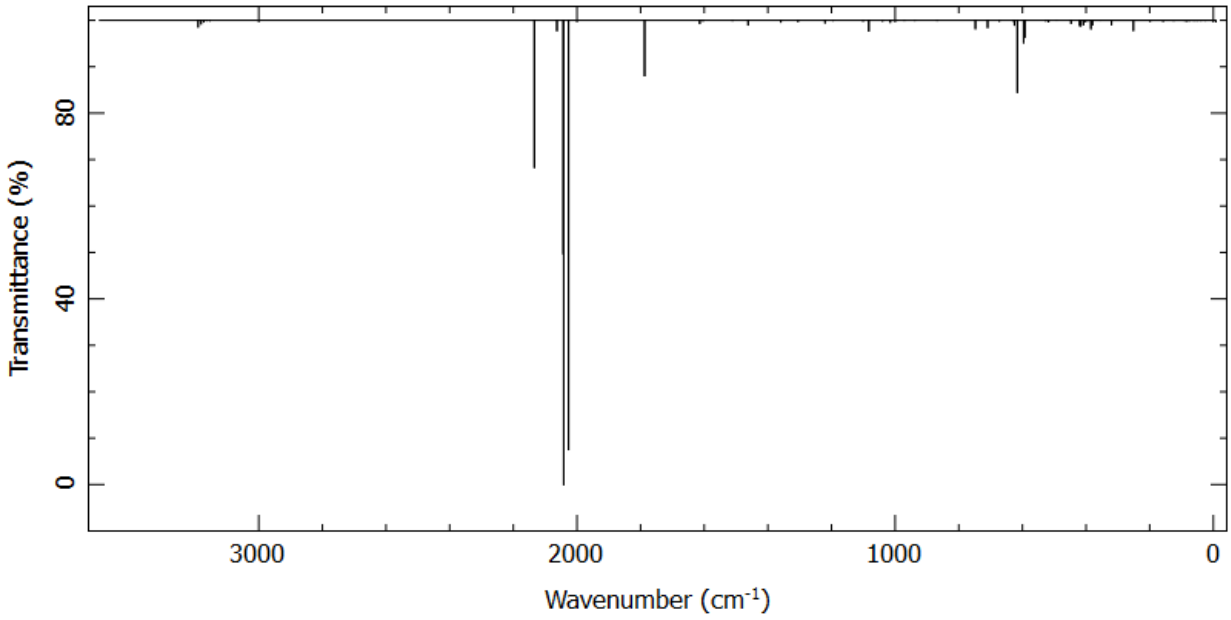

Figure 3.S1: Calculated IR spectrum of **1**.

Compound	**1**	**2**	**2**
Empirical formula	$C_{41}H_{50}MoO_5Sn$	$C_{39}H_{46}MoO_6Sn$	$C_{42}H_{50}MoO_7Sn$
Formula weight	837.44	825.39	881.45
Temperature	90(2) K	90(2) K	90(2) K
Wavelength	0.71073 Å	0.71073 Å	0.71073 Å
Crystal system	Triclinic	Monoclinic	Monoclinic
Space group	P-1	$P2_1/c$	$P2_1/m$
Crystal color and habit	Yellow block	Yellow plate	Colorless block
a(Å)	10.0036(9)	14.7682(5)	8.6205(6)
b(Å)	13.2565(12)	10.7848(4)	18.6744(13)
c(Å)	15.0972(13)	23.6781(10)	12.8381(9)
α(°)	94.4823(14)	90	90
β(°)	92.9268(14)	95.0100(10)	90.8178(10)

γ(°)	96.3788(14)	90	90
Density (calculated) (Mg/m^3)	1.405	1.459	1.417
F(000)	856	1680	900
Crystal size(mm^3)	0.522 x 0.368 x 0.354	0.334 x 0.288 x 0.285	0.476 x 0.456 x 0.268
θ range(°)	1.972 to 27.487°	2.076 to 25.249°	1.925 to 30.631°
Reflections collected	17915	16327	24632
Independent reflections	9055 [R(int) = 0.0163]	6802 [R(int) = 0.0549]	6555 [R(int) = 0.0281]
Observed reflections (I > 2σ(I))	7878	4769	5706
Completeness to 2θ= 25.242°	99.9 %	100.0 %	100.0 %
Goodness-of-fit on F^2	1.045	1.018	1.078
Final R indices (I>2σ(I))	R1 = 0.0313, wR2 = 0.0794	R1 = 0.0417, wR2 = 0.0829	R1 = 0.0248, wR2 = 0.0607
R indices (all data)	R1 = 0.0368, wR2 = 0.0817	R1 = 0.0702, wR2 = 0.0954	R1 = 0.0313, wR2 = 0.0642

Table 3.S3: Selected X-ray Crystallographic data for **1-3.**

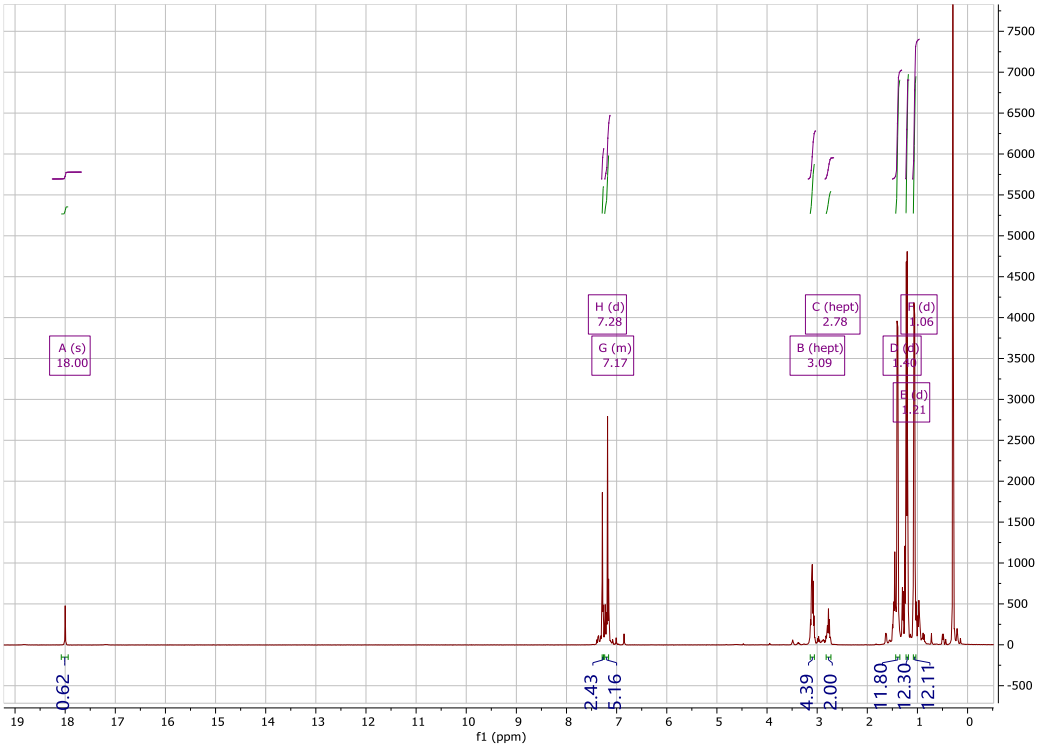

Figure 3.S2: ^{1}H NMR spectrum of **1** in C_6D_6 at 298K.

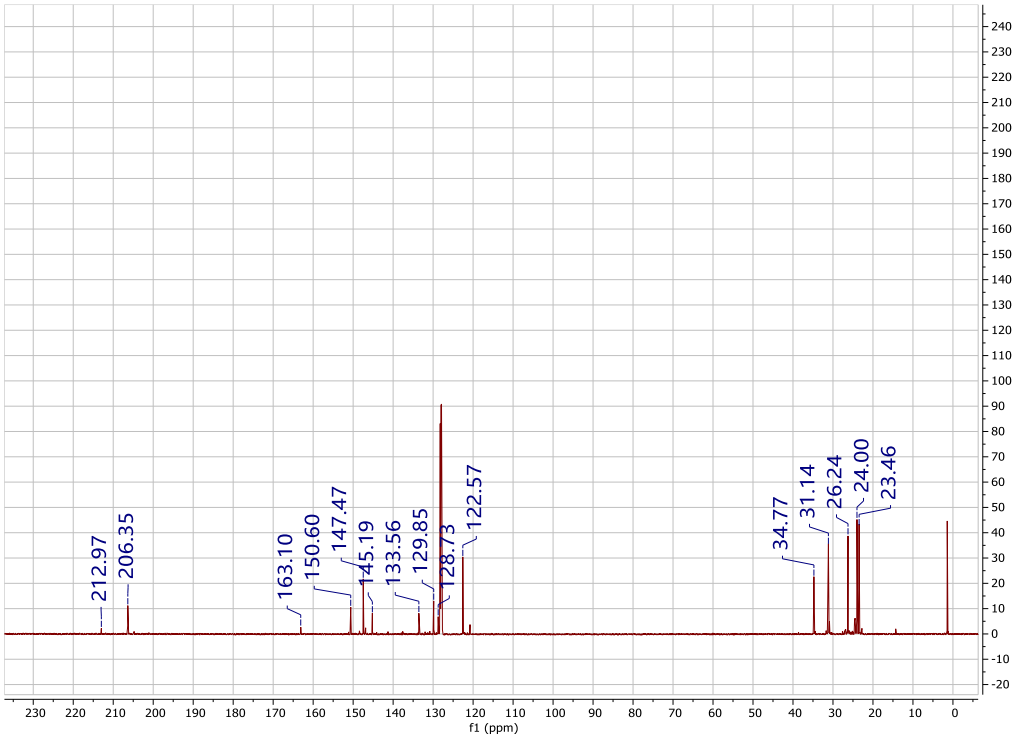

Figure 3.S3: ^{13}C{^{1}H} NMR spectrum of **1** in C_6D_6 at 298K.

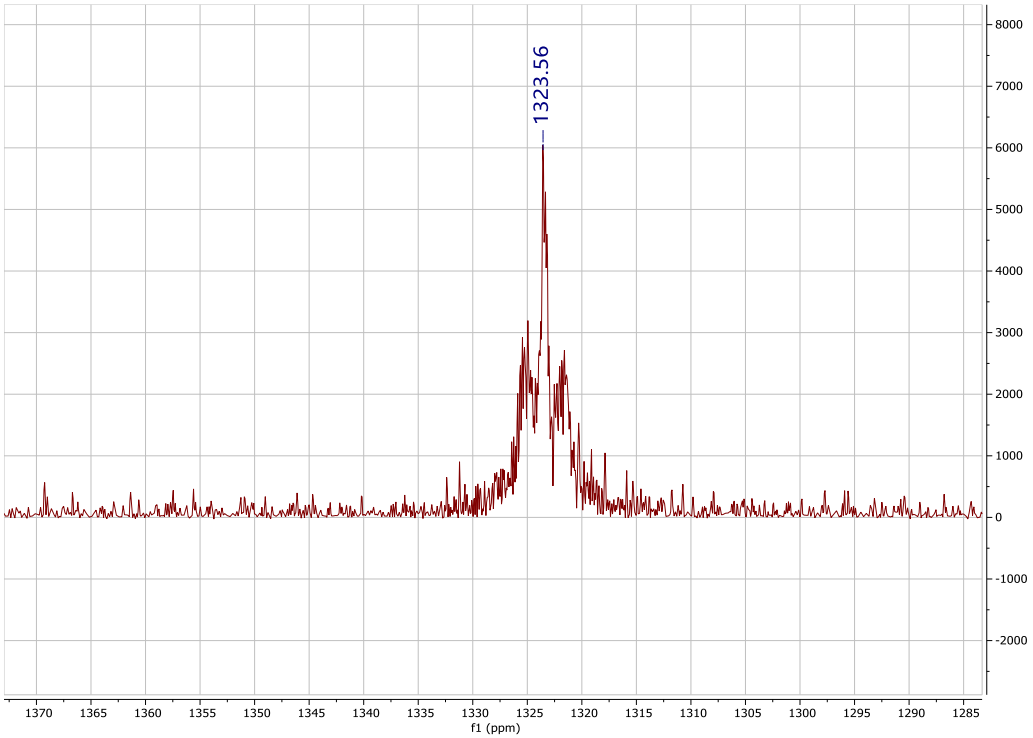

Figure 3.S4: $^{119}Sn\{^{1}H\}$ NMR spectrum of **1** in C_6D_6 at 298K.

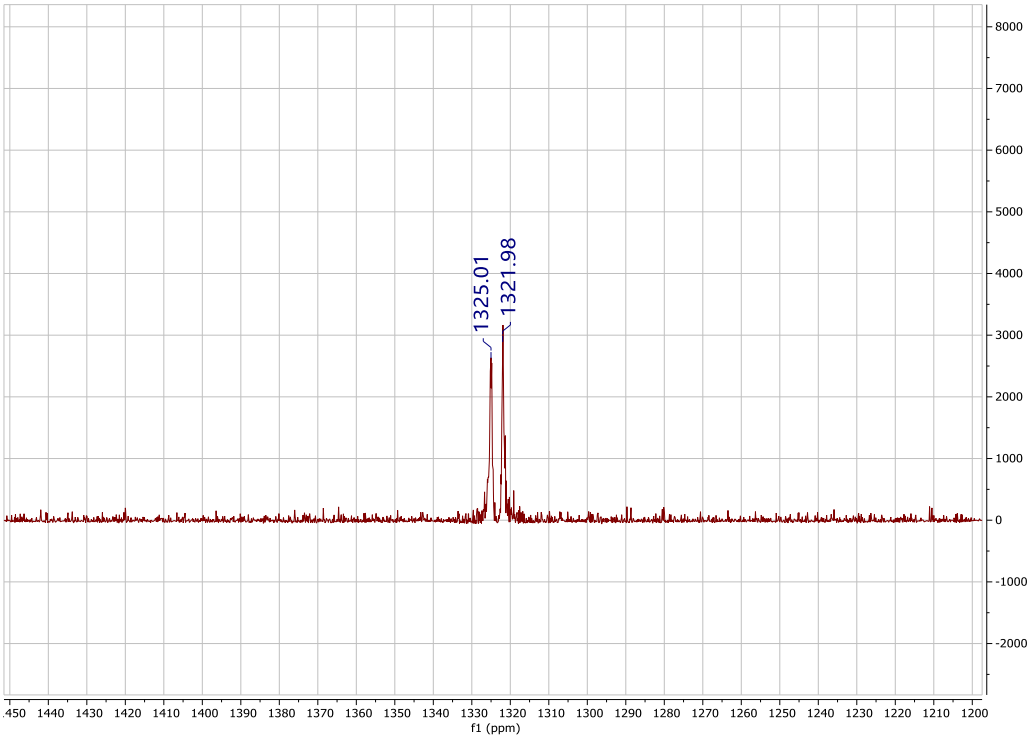

Figure 3.S5: ^{119}Sn NMR spectrum of **1** in C_6D_6 at 298K.

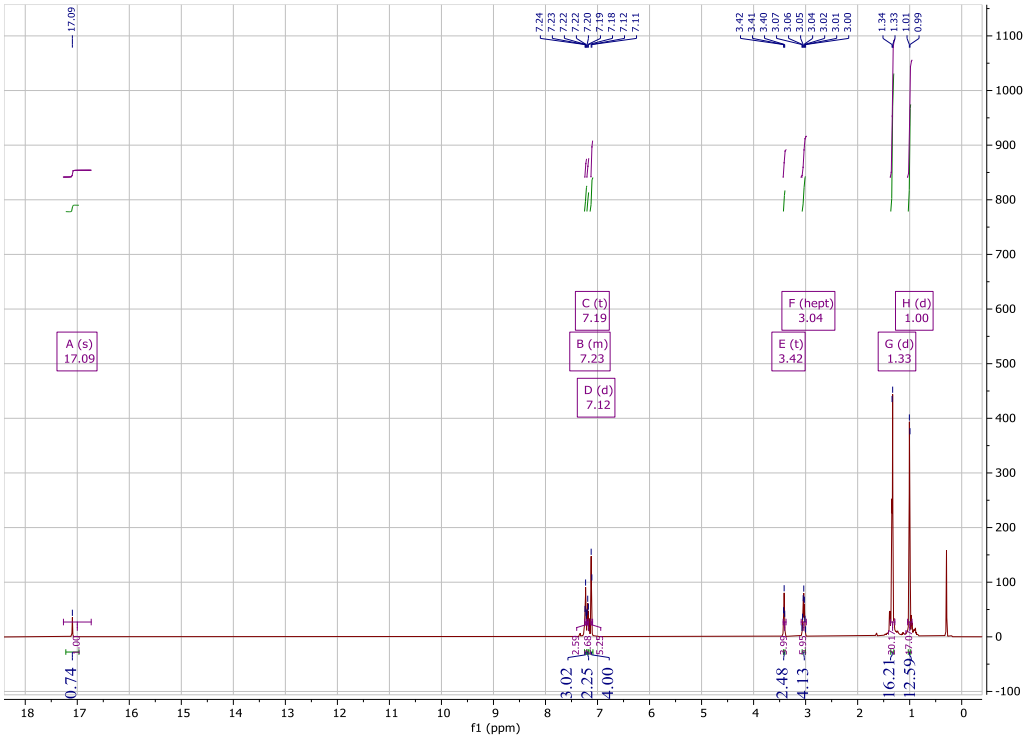

Figure 3.S6: ^{1}H NMR spectrum of **2** in C_6D_6 at 298K.

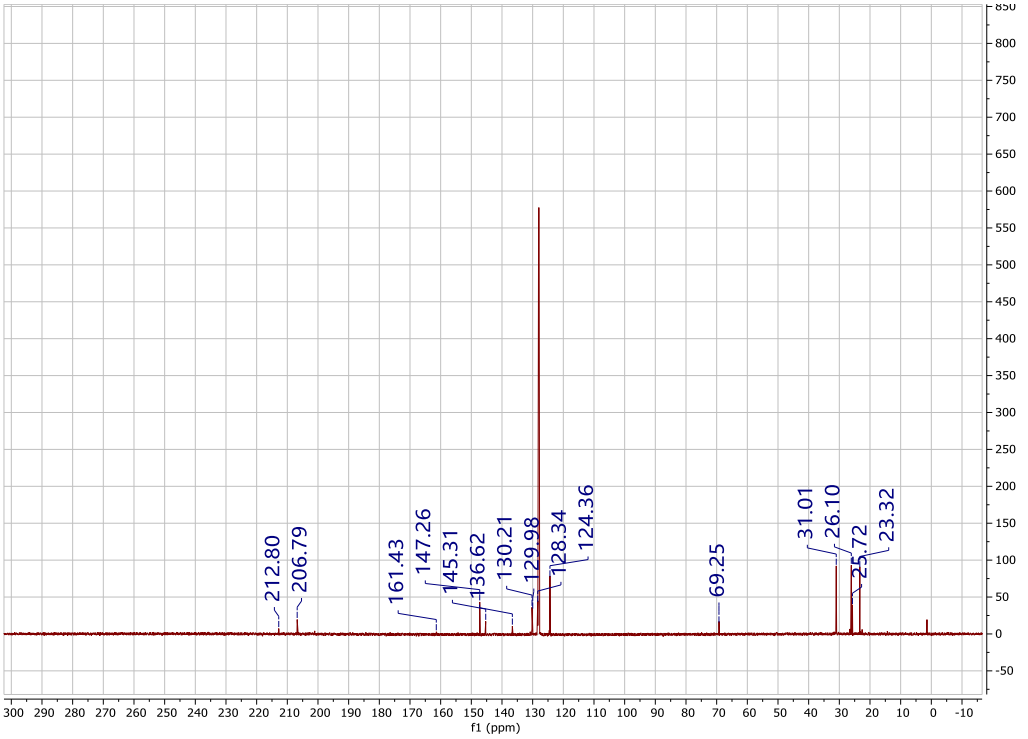

Figure 3.S7: $^{13}C\{^{1}H\}$ NMR spectrum of **2** in C_6D_6 at 298K.

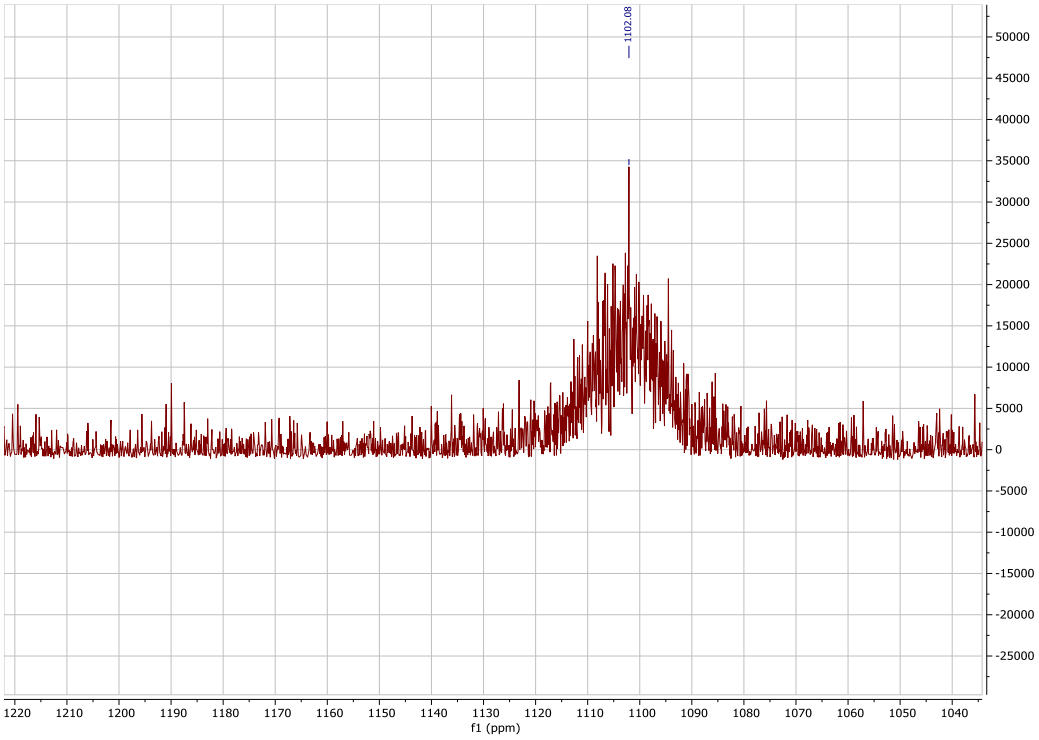

Figure 3.S8: $^{119}Sn\{^{1}H\}$ NMR spectrum of **2** in C_6D_6 at 298K.

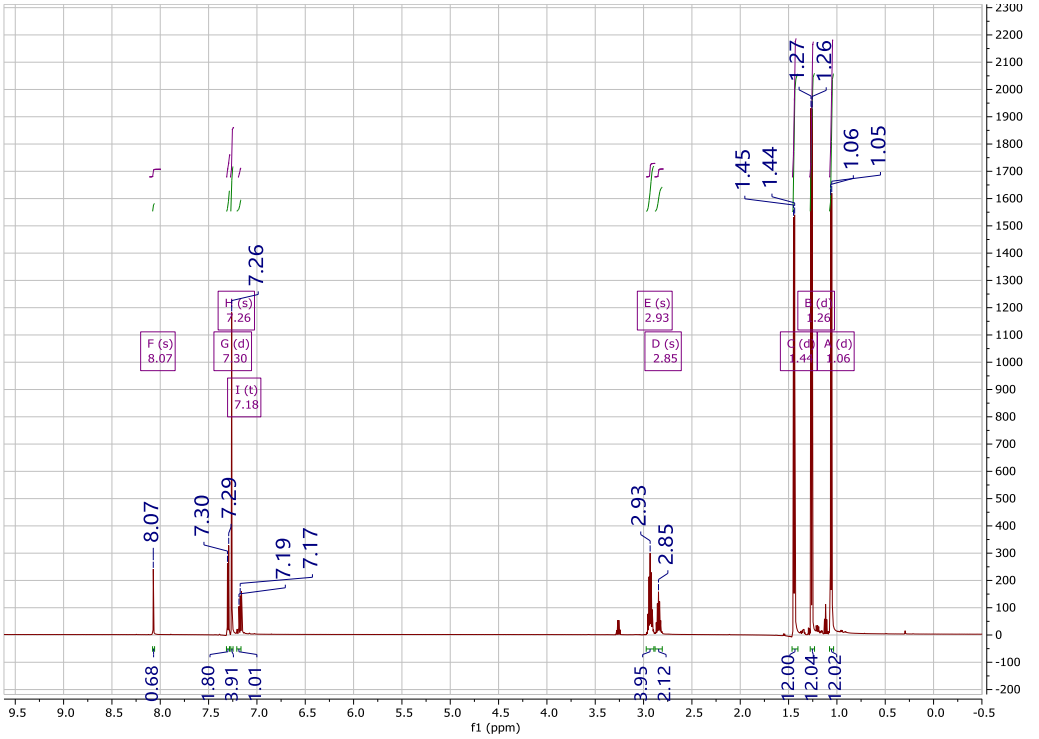

Figure 3.S9: ^{1}H NMR spectrum of **3** in C_6D_6 at 298K.

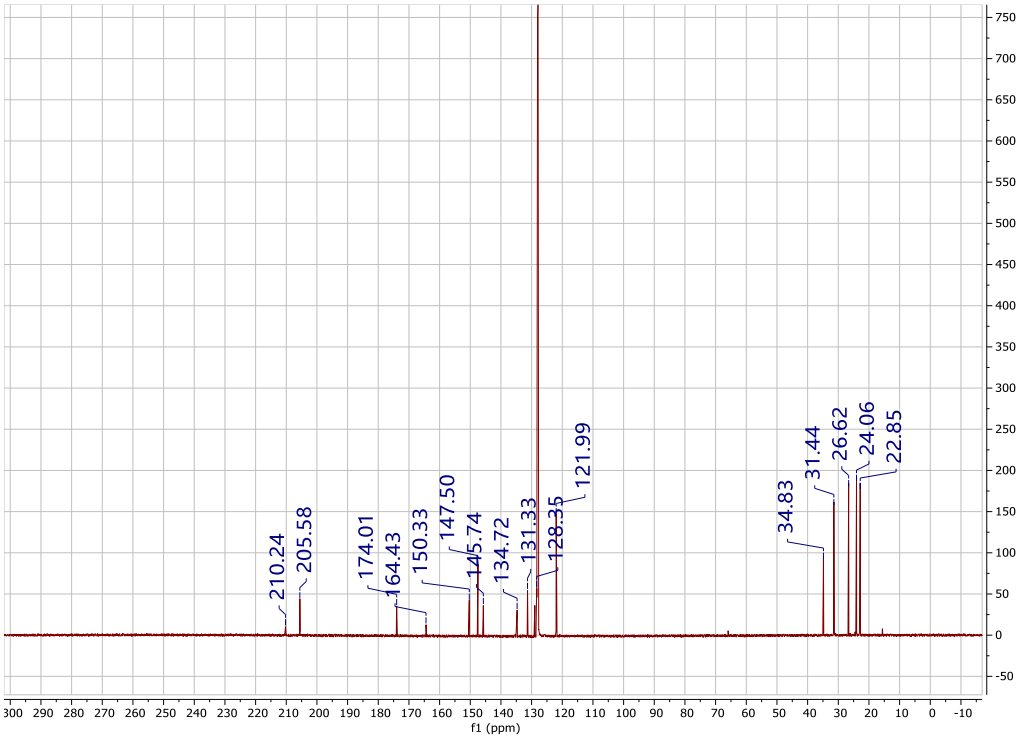

Figure 3.S10: $^{13}C\{^{1}H\}$ NMR spectrum of **3** in C_6D_6 at 298K.

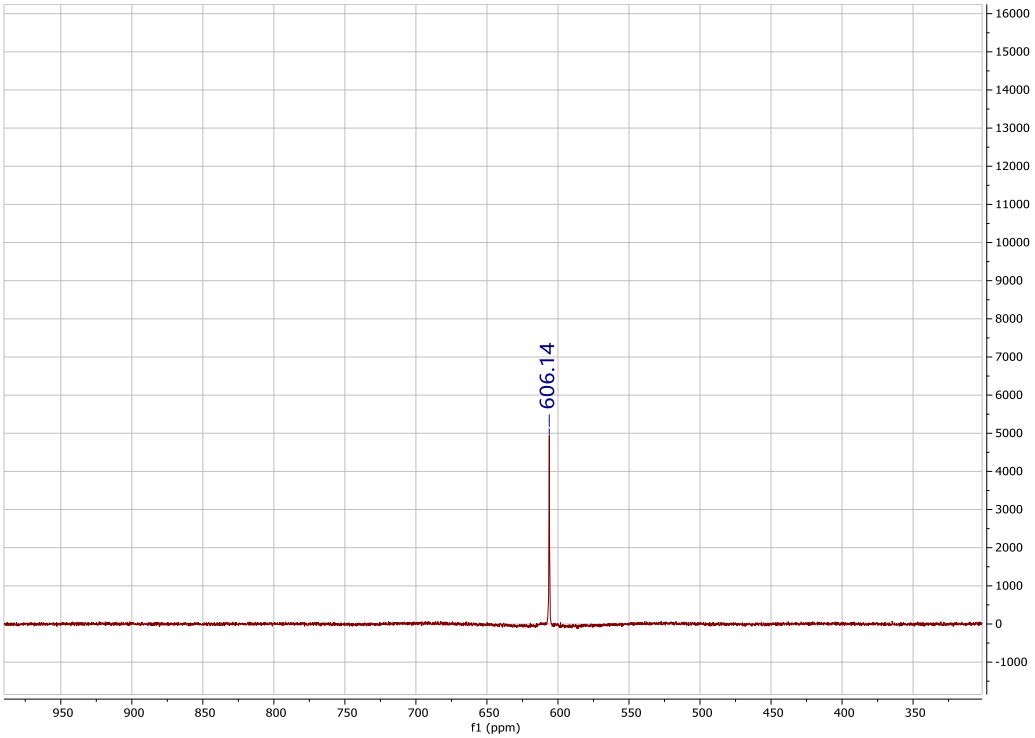

Figure 3.S11: $^{119}Sn\{^{1}H\}$ NMR spectrum of **3** in C_6D_6 at 298K.

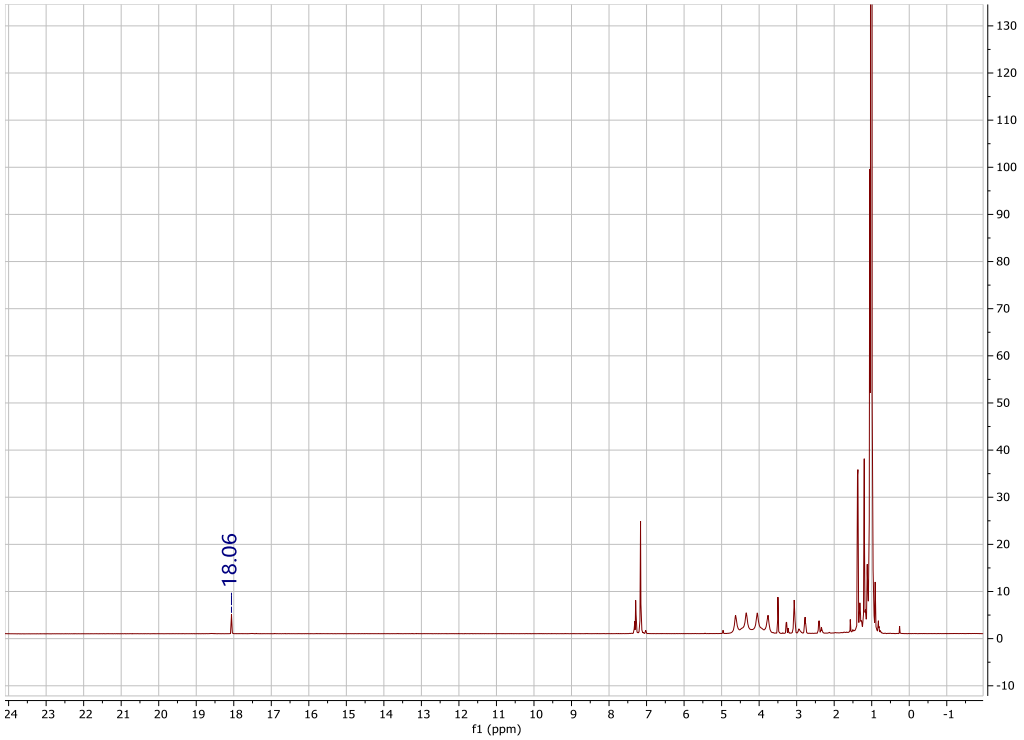

Figure 3.S12: ^{1}H NMR spectrum of **3** with HBpin (3 hours after mixing) in C_6D_6 at 298K.

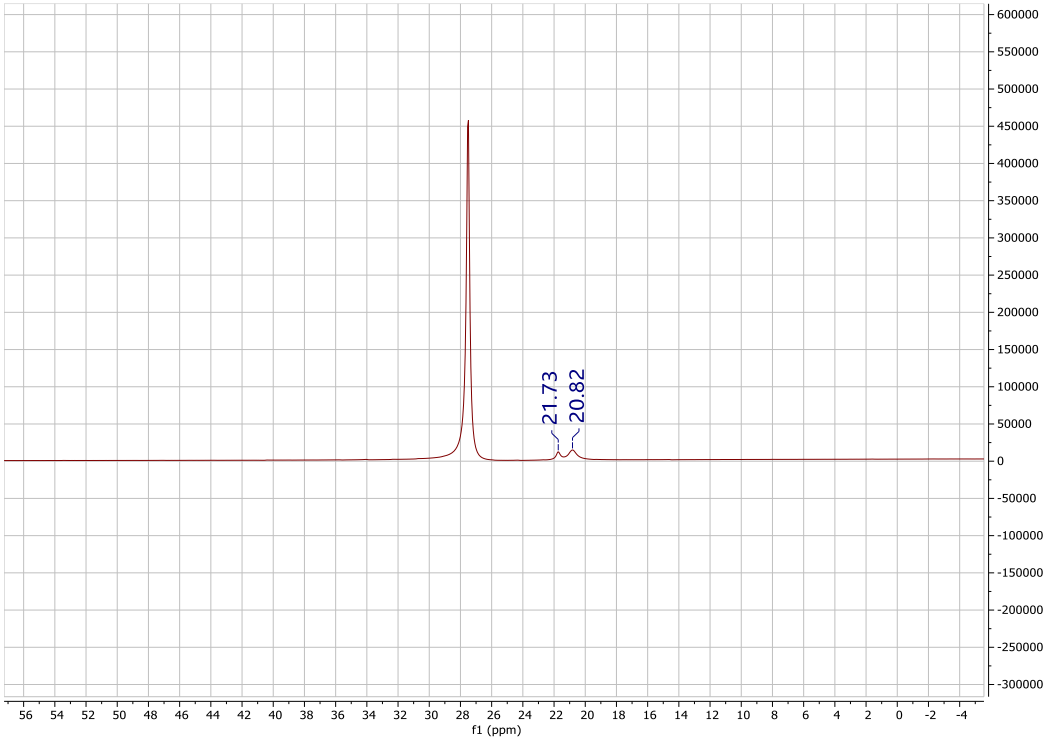

Figure 3.S13: $^{11}B\{^{1}H\}$ NMR spectrum of **3** with HBpin (3 hours after mixing) in C_6D_6 at 298K.

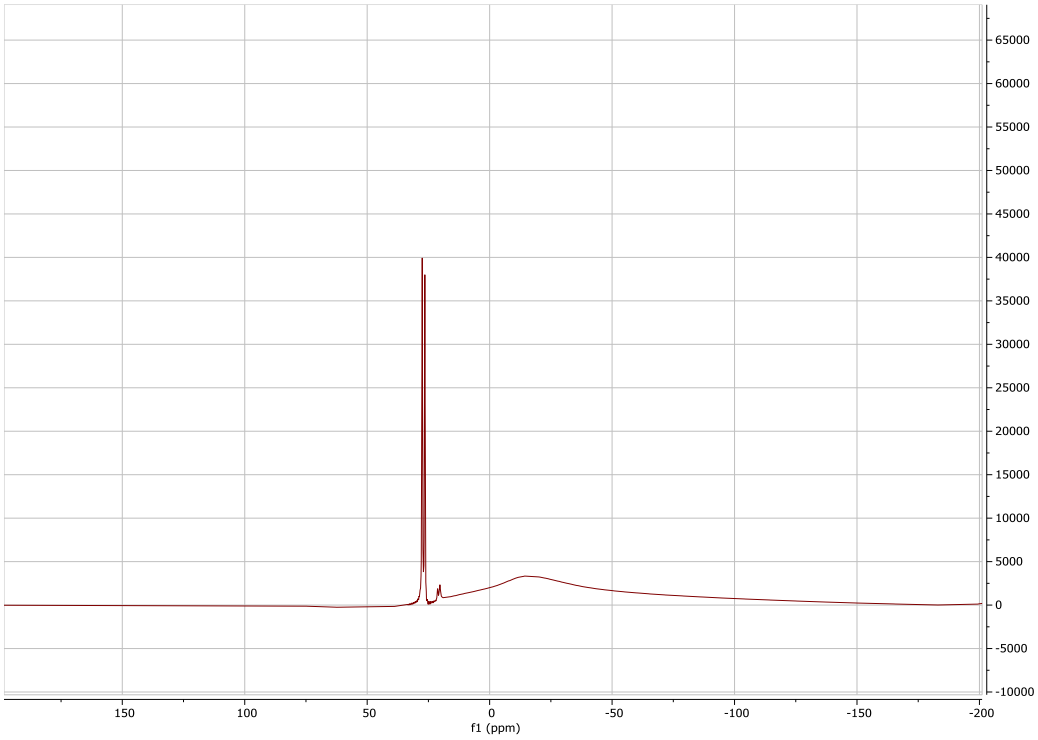

Figure 3.S14: ^{11}B NMR spectrum of **3** with HBpin (3 hours after mixing) in C_6D_6 at 298K.

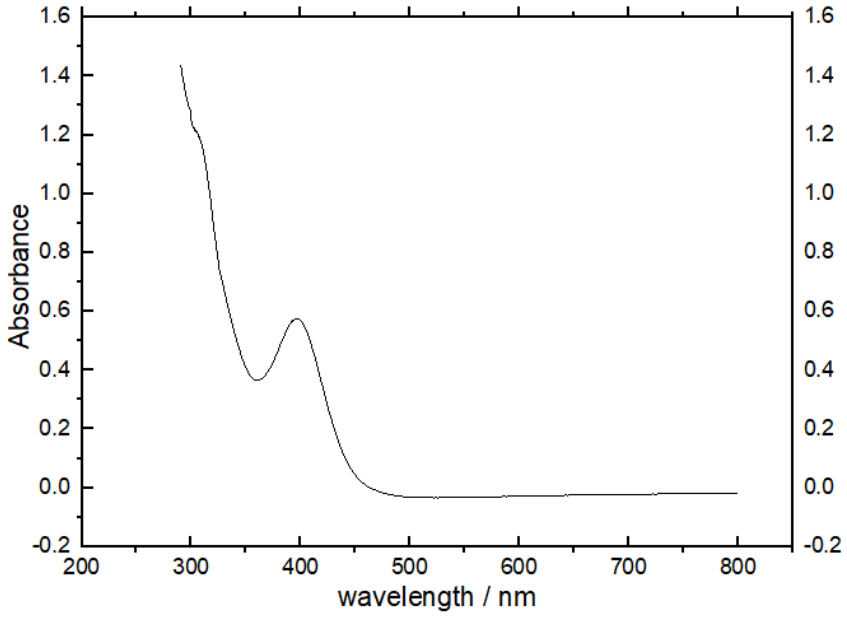

Figure 3.S15: UV-vis spectrum of **1** in hexanes ($2.3*10^{-4}$ M) at 298K.

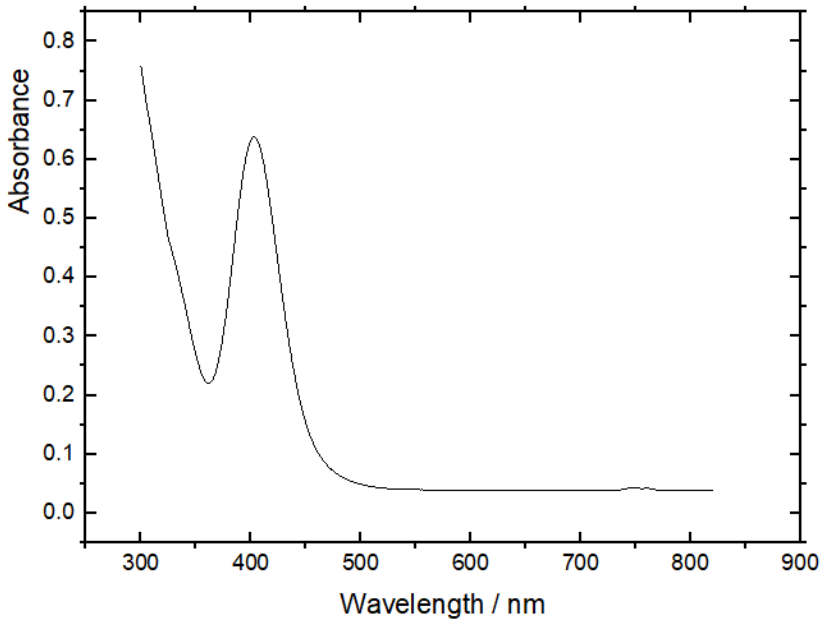

Figure 3.S16: UV-vis spectrum of **2** in hexanes ($6.0*10^{-5}$ M) at 298K.

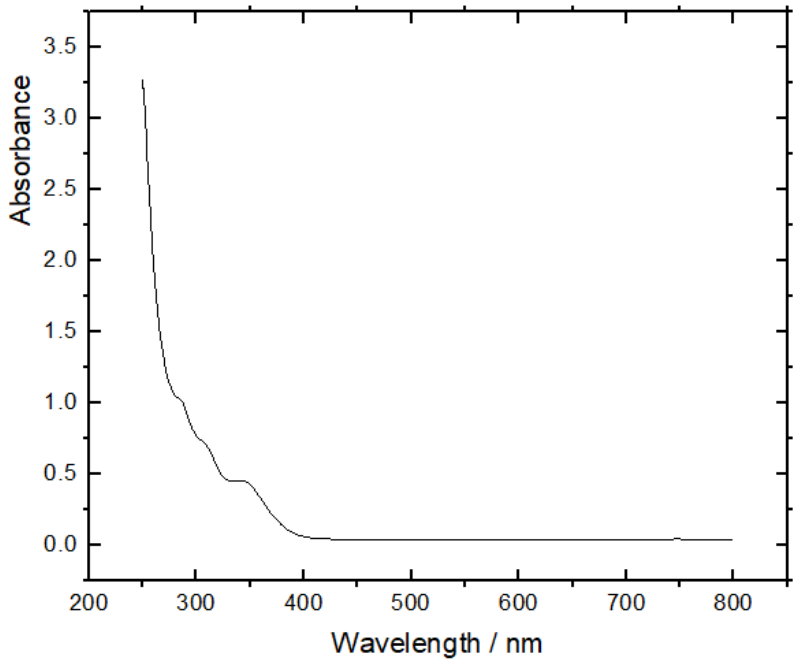

Figure 3.S17: UV-vis spectrum of **3** in hexanes ($5.4*10^{-5}$ M) at 298K.

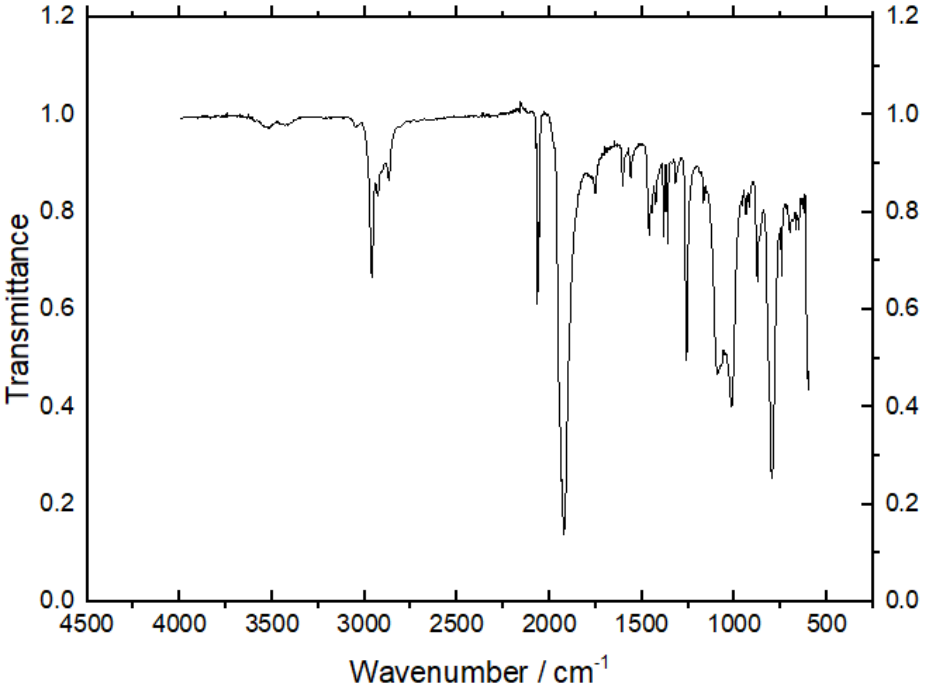

Figure 3.S18: ATR-FTIR spectrum of **1** at 298K.

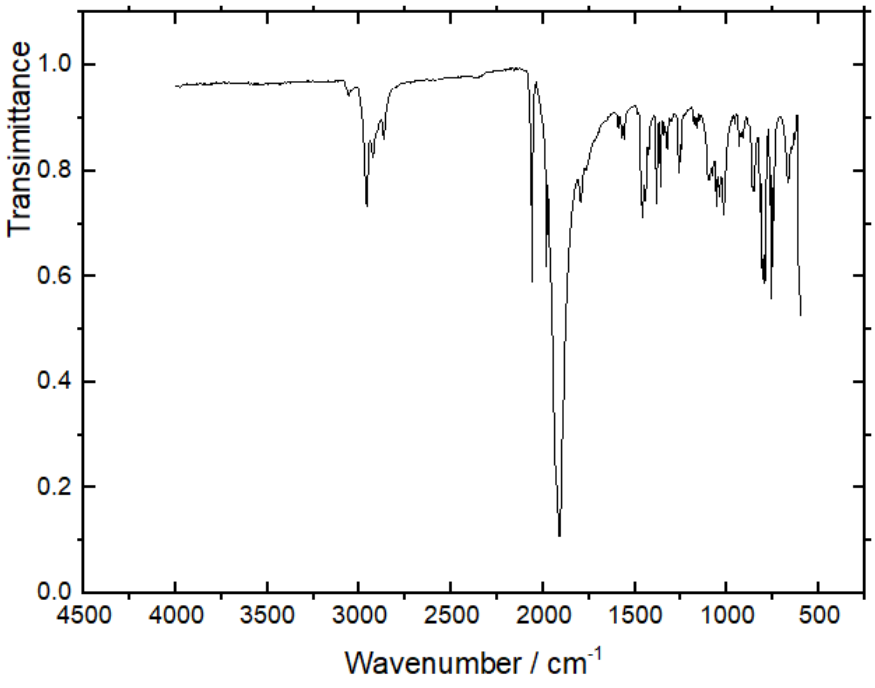

Figure 3.S19: ATR-FTIR spectrum of **2** at 298K.

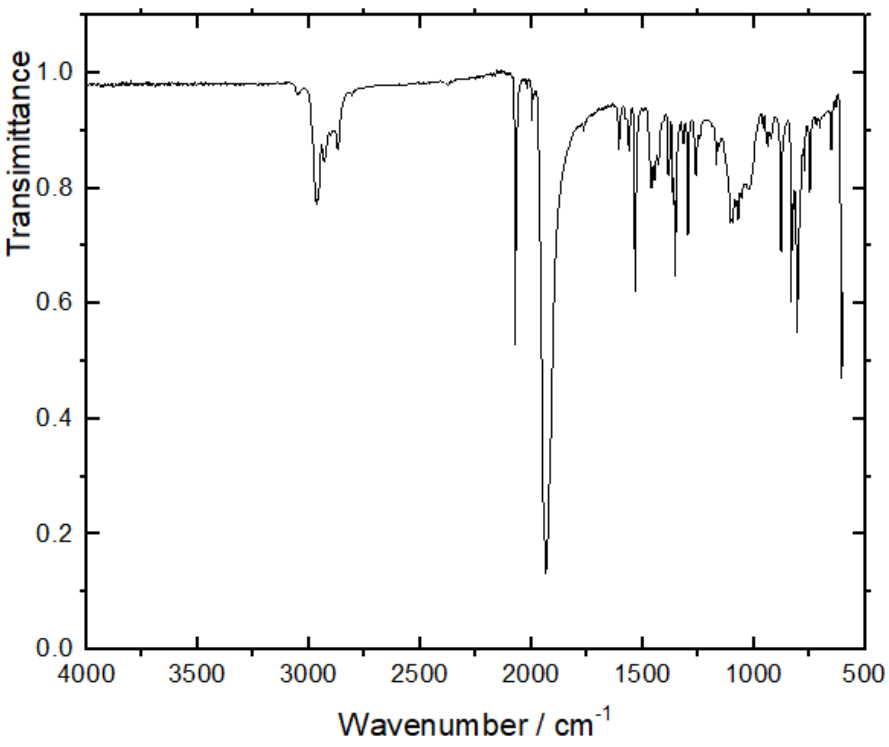

Figure 3.S20: ATR-FTIR spectrum of **3** at 298K.

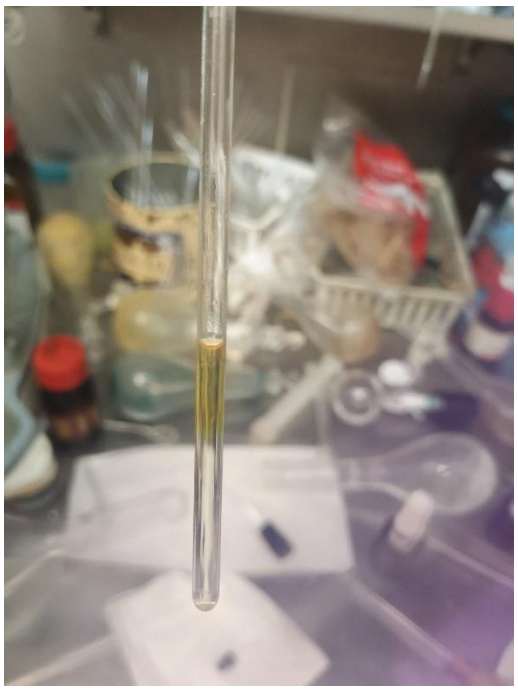

Figure 3.S21: Photo of addition HBpin to **3** in C_6D_6 at 298K.

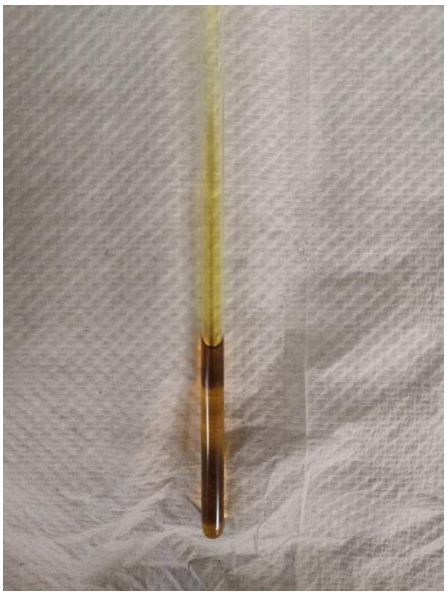

Figure 3.S22: Photo of addition HBpin to **3** (3 hours later) in C_6D_6 at 298K.

Optimized xyz-coordinates

98
1

Sn	2.21762028558569	9.30954850110434	4.22161284102014
H	3.27273423271752	10.46702876335059	5.00011020020318
Mo	2.40639677281093	6.59008066499129	4.18452291102161
C	0.78201216864648	10.63471928834753	3.27131881225944
C	-0.36239376876747	11.01024745588481	3.98916071398442
C	-1.25867017195876	11.91400506216061	3.40243132507208
H	-2.14336963196065	12.23716331452508	3.95171148688636
C	-1.00060251128387	12.42452576874601	2.12600904883565
H	-1.69899546117922	13.13170803738650	1.67737034622698
C	0.15667459339489	12.06033170717750	1.42992826595489
H	0.36558945957472	12.49491909333025	0.45190405809303
C	1.06542952622760	11.16004189858276	2.00305024872466
C	-0.48012929441443	10.46780788518204	5.38068130208668
C	-1.23858468257048	9.30025694370469	5.64762888398361
C	-1.21051802591826	8.76635850252737	6.94095286703315
H	-1.76823301942812	7.85435039108284	7.15388291690352
C	-0.45027840507965	9.33336775601134	7.96737343052517
C	0.27825360710224	10.49414521480783	7.68830914873824
H	0.86663518885395	10.95415429926442	8.48243872272641
C	0.27691455820622	11.08298627562189	6.41826262159458

C	-2.07778633735511	8.64943455560843	4.55584530254646
H	-1.56036516097442	8.82482471666074	3.59908298525597
C	-2.25008892933281	7.13332956537756	4.72441902252576
H	-1.29233652959890	6.62764442920920	4.89276556770077
H	-2.70097439566289	6.70709621428207	3.81883495716087
H	-2.91342966416596	6.89226880439336	5.56751035761300
C	-3.46314186150806	9.32148880604842	4.47351854220317
H	-4.00433614468592	9.19035509325280	5.42212145973125
H	-4.06369718883493	8.87017931005889	3.67078442596170
H	-3.38290917123901	10.39685528342906	4.27568978362281
C	-0.40487775121273	8.69355641059069	9.34412777937637
H	-1.02483661943420	7.78363119443640	9.29790780988503
C	1.02549948292849	8.26581633821218	9.71709924515672
H	1.69064524656832	9.13803187364103	9.79652264230663
H	1.44351671467521	7.58745126015923	8.96248819543727
H	1.03425581245203	7.75018200388871	10.68793483924518
C	-1.00406570283419	9.62102102458421	10.41628134874142
H	-1.01703877283306	9.12380010809908	11.39670647095656
H	-2.03255392881785	9.91121536240387	10.16177915244342
H	-0.41016691858071	10.54139229458606	10.51607842771917
C	0.99233648592640	12.40910938743334	6.18073788187150
H	1.29241661878088	12.44130259624359	5.12260407309385
C	2.26146860496551	12.60076507875236	7.02086827271926
H	2.79405664442281	13.50313291461710	6.69047928899528
H	2.94498034271600	11.74754692538017	6.91714735151734
H	2.03273813143938	12.73237126838060	8.08833989296068
C	0.00702501882756	13.57228030548053	6.41098159472983
H	-0.34615035547098	13.57382492597144	7.45257569243142
H	-0.86887033596041	13.48720968689952	5.75473942584647
H	0.49334554656979	14.53786827042633	6.21077252662676
C	2.38158602231860	10.77620054621444	1.39930418221577
C	2.48249695495804	9.68167368896322	0.50449873172630
C	3.75290838580365	9.29256851435401	0.06440397251888
H	3.84689656757746	8.43682459581289	-0.60426650608130
C	4.91841251098214	9.93919527609812	0.48380502649084
C	4.79592862508002	11.02799450968603	1.35361698814462
H	5.69675280659051	11.54787531383918	1.68079308563554
C	3.55205566547997	11.46769762277206	1.81999150680272
C	1.23401993070713	8.96523565504147	0.00712151341784
H	0.48455147761208	9.01426228974953	0.81308709696580
C	1.45941936099252	7.48600992976206	-0.33504655719313
H	2.06307546448231	7.36736935862171	-1.24633765618859
H	0.49479275582000	6.99319467144752	-0.51281608351482
H	1.96546751040925	6.95070810579169	0.47660455003426
C	0.65450515125797	9.70009947920073	-1.21850295023871
H	0.41558120499722	10.74547207723448	-0.98930912451730

H	-0.26466110515220	9.20683637617648	-1.56571392478469
H	1.38195532864335	9.69162221217860	-2.04351102165757
C	6.28255576147708	9.45703174938252	0.02153828959974
H	6.11200390651436	8.59858711740663	-0.64825922313581
C	7.12989847541264	8.96430199029166	1.20824163251685
H	7.33975601950360	9.78633355941782	1.90819501762890
H	8.09387017580259	8.56775752511109	0.85877663478030
H	6.61002295446173	8.17143010403845	1.76103477565546
C	7.02644286217577	10.53979340452999	-0.77969735337288
H	6.42787143887514	10.88443011804140	-1.63393756350347
H	7.98212862719968	10.15220336997225	-1.16058464297216
H	7.24875212967702	11.41425255434269	-0.15077120641241
C	3.44989654220737	12.71624867411227	2.68968581257663
H	2.54460443158482	12.61789996723691	3.30760712852494
C	3.25748834879483	13.95470281760419	1.79240274502153
H	4.12747224336276	14.08742941730217	1.13275409042831
H	3.14577192579519	14.86287835419107	2.40210310548696
H	2.36495570300833	13.85334940904191	1.16129067124916
C	4.63519042559713	12.91748723124008	3.64276255992872
H	4.82517006250097	12.01743932351172	4.24257844339647
H	4.42367484229360	13.74643217097003	4.33233802383153
H	5.55830023131078	13.17334702324418	3.10279567728765
C	1.26103026508009	6.36976490091210	5.87236202746035
O	0.65968931940538	6.17018197117374	6.83991363236768
C	4.03840365219932	6.77156009062908	5.40644669038556
O	4.95526459684289	6.90451451067612	6.09915283816050
C	3.68603751545510	6.63585519784340	2.58177599603247
O	4.44147916107913	6.59234107105910	1.70701910461221
C	2.51153481205278	4.58625907653141	4.09900753816708
O	2.56987948378215	3.43031496233690	4.04607648154449
C	0.75536039090834	6.66379040761919	2.98282165121397
O	-0.18282522525019	6.74372887498903	2.30857212350710

3.6 References

(1) Attrill, R. P.; Blower, M. A.; Mulholland, K. R.; Roberts, J. K.; Richardson, J. E.; Teasdale, M. J.; Wanders, A., Development of a Catalytic Tributyltin Hydride Cyclisation Process. *Org. Process Res. Dev.* **2000,** *4*, 98-101.

(2) Dobbs, A. P.; Chio, F. K. I., 8.25 Hydrometallation Group 4 (Si, Sn, Ge, and Pb). In *Comprehensive Organic Synthesis II (Second Edition)*, Knochel, P., Ed. Elsevier: Amsterdam, 2014; pp 964-998.

(3) Caprio, V., 3.04 - Ketones: Dialkyl Ketones. In *Comprehensive Organic Functional Group Transformations II*, Katritzky, A. R.; Taylor, R. J. K., Eds. Elsevier: Oxford, 2005; pp 135-214.

(4) Bradley, G. F.; Stobart, S. R., Reaction of octacarbonyldicobalt with organo-silanes, -germanes, and -stannanes: formation, properties, and vibrational spectra of trimethylgermyltetracarbonylcobalt and related complexes. *J. Chem. Soc., Dalton Trans.* **1974**, 264-269.

(5) Saegusa, T.; Ito, Y.; Kobayashi, S.; Hirota, K., Synthetic Reactions by a Complex Catalyst. VI. A Novel Hydrosilation of Isocyanide by Copper Catalyst. *J. Am. Chem. Soc.* **1967,** *89*, 2240-2241.

(6) Beard, C. D.; Craig, J. C., Insertion of vinylidene carbenes into carbon-hydrogen and silicon-hydrogen bonds. *J. Am. Chem. Soc.* **1974,** *96*, 7950-7954.

(7) Adams, R. D.; Cotton, F. A.; Cullen, W. R.; Hunter, D. L.; Mihichuk, L., Fluxional behavior of some dinuclear iron and cobalt hexacarbonyl compounds with alkylsulfur and dialkylphosphorus, -arsenic, -germanium, and -tin bridges. *Inorg. Chem.* **1975,** *14*, 1395-1399.

(8) Manuel, G.; Bertrand, G.; Mazerolles, P., Synthese et rearrangements de cycles α-fonctionnels du germanium: oxa-6 diphenyl-2,2 germa-2 bicyclo[3.1.0] hexane et diphenyl-1,1 germa-1 cyclopentanol-2. etude comparative avec les derives isologues du silicium. *J. Organomet. Chem.* **1978,** *146*, 7-16.

(9) Walling, C.; Cooley, J. H.; Ponaras, A. A.; Racah, E. J., Radical Cyclizations in the Reaction of Trialkyltin Hydrides with Alkenyl Halides. *J. Am. Chem. Soc.* **1966,** *88*, 5361-5363.

(10) Hadlington, T. J.; Driess, M.; Jones, C., Low-valent group 14 element hydride chemistry: towards catalysis. *Chem. Soc. Rev.* **2018,** *47*, 4176-4197.

(11) Rivard, E.; Power, P. P., Recent developments in the chemistry of low valent Group 14 hydrides. *Dalton Trans.* **2008**, 4336-4343.

(12) Aldridge, S.; Downs, A. J., Hydrides of the Main-Group Metals: New Variations on an Old Theme. *Chem. Rev.* **2001,** *101*, 3305-3366.

(13) Eichler, B. E.; Power, P. P., $[2,6\text{-Trip}_2H_3C_6Sn(\mu\text{-}H)]_2$ (Trip = C_6H_2-2,4,6-*i*-Pr_3): Synthesis and Structure of a Divalent Group 14 Element Hydride. *J. Am. Chem. Soc.* **2000,** *122*, 8785-8786.

(14) Pineda, L. W.; Jancik, V.; Starke, K.; Oswald, R. B.; Roesky, H. W., Stable Monomeric Germanium(II) and Tin(II) Compounds with Terminal Hydrides. *Angew. Chem. Int. Ed.* **2006,** *45*, 2602-2605.

(15) Khan, S.; Samuel, P. P.; Michel, R.; Dieterich, J. M.; Mata, R. A.; Demers, J.-P.; Lange, A.; Roesky, H. W.; Stalke, D., Monomeric Sn(II) and Ge(II) hydrides supported by a tridentate pincer-based ligand. *Chem. Commun.* **2012,** *48*, 4890-4892.

(16) Rivard, E.; Fischer, R. C.; Wolf, R.; Peng, Y.; Merrill, W. A.; Schley, N. D.; Zhu, Z.; Pu, L.; Fettinger, J. C.; Teat, S. J.; Nowik, I.; Herber, R. H.; Takagi, N.; Nagase, S.; Power, P. P., Isomeric Forms of Heavier Main Group Hydrides: Experimental and Theoretical Studies of the $[Sn(Ar)H]_2$ (Ar = Terphenyl) System. *J. Am. Chem. Soc.* **2007,** *129*, 16197-16208.

(17) Richards, A. F.; Phillips, A. D.; Olmstead, M. M.; Power, P. P., Isomeric Forms of Divalent Heavier Group 14 Element Hydrides: Characterization of

Ar‘(H)GeGe(H)Ar‘ and Ar‘(H)$_2$GeGeAr‘·PMe$_3$ (Ar‘ = C$_6$H$_3$-2,6-Dipp$_2$; Dipp = C$_6$H$_3$-2,6-Pr$^i_2$). *J. Am. Chem. Soc.* **2003,** *125*, 3204-3205.

(18) Schneider, J.; Sindlinger, C. P.; Eichele, K.; Schubert, H.; Wesemann, L., Low-Valent Lead Hydride and Its Extreme Low-Field 1H NMR Chemical Shift. *J. Am. Chem. Soc.* **2017,** *139*, 6542-6545.

(19) Hadlington, T. J.; Hermann, M.; Li, J.; Frenking, G.; Jones, C., Activation of H_2 by a Multiply Bonded Amido–Digermyne: Evidence for the Formation of a Hydrido–Germylene. *Angew. Chem. Int. Ed.* **2013,** *52*, 10199-10203.

(20) Queen, J. D.; Fettinger, J. C.; Power, P. P., Two quasi-stable lead(II) hydrides at ambient temperature. *Chem. Commun.* **2019,** *55*, 10285-10287.

(21) Jana, A.; Roesky, H. W.; Schulzke, C.; Döring, A., Reactions of Tin(II) Hydride Species with Unsaturated Molecules. *Angew. Chem. Int. Ed.* **2009,** *48*, 1106-1109.

(22) Jana, A.; Roesky, H. W.; Schulzke, C.; Samuel, P. P., Reaction of Tin(II) Hydride with Compounds Containing Aromatic C−F Bonds. *Organometallics* **2010,** *29*, 4837-4841.

(23) Rodriguez, R.; Gau, D.; Contie, Y.; Kato, T.; Saffon-Merceron, N.; Baceiredo, A., Synthesis of a Phosphine-Stabilized Silicon(II) Hydride and Its Addition to Olefins: A Catalyst-Free Hydrosilylation Reaction. *Angew. Chem. Int. Ed.* **2011,** *50*, 11492-11495.

(24) Hadlington, T. J.; Hermann, M.; Frenking, G.; Jones, C., Two-coordinate group 14 element(II) hydrides as reagents for the facile, and sometimes reversible, hydrogermylation/hydrostannylation of unactivated alkenes and alkynes. *Chem. Sci.* **2015,** *6*, 7249-7257.

(25) Power, P. P., Main-group elements as transition metals. *Nature* **2010,** *463*, 171-177.

(26) Frey, G. D.; Lavallo, V.; Donnadieu, B.; Schoeller, W. W.; Bertrand, G., Facile Splitting of Hydrogen and Ammonia by Nucleophilic Activation at a Single Carbon Center. *Science* **2007,** *316*, 439.

(27) Roy, M. M. D.; Fujimori, S.; Ferguson, M. J.; McDonald, R.; Tokitoh, N.; Rivard, E., Neutral, Cationic and Hydride-substituted Siloxygermylenes. *Chem. Eur. J.* **2018,** *24*, 14392-14399.

(28) Al-Rafia, S. M. I.; Malcolm, A. C.; Liew, S. K.; Ferguson, M. J.; Rivard, E., Stabilization of the Heavy Methylene Analogues, GeH_2 and SnH_2, within the Coordination Sphere of a Transition Metal. *J. Am. Chem. Soc.* **2011,** *133*, 777-779.

(29) Dhungana, T. P.; Hashimoto, H.; Tobita, H., An iron germylene complex having Fe–H and Ge–H bonds: synthesis, structure and reactivity. *Dalton Trans.* **2017,** *46*, 8167-8179.

(30) Inomata, K.; Watanabe, T.; Miyazaki, Y.; Tobita, H., Insertion of a Cationic Metallogermylene into E–H Bonds (E = H, B, Si). *J. Am. Chem. Soc.* **2015,** *137*, 11935-11937.

(31) Maudrich, J.-J.; Widemann, M.; Diab, F.; Kern, R. H.; Sirsch, P.; Sindlinger, C. P.; Schubert, H.; Wesemann, L., Hydridoorganostannylene Coordination: Group 4 Metallocene Dichloride Reduction in Reaction with Organodihydridostannate Anions. *Chem. Eur. J.* **2019,** *25*, 16081-16087.

(32) Wang, S.; Sherbow, T. J.; Berben, L. A.; Power, P. P., Reversible Coordination of H_2 by a Distannyne. *J. Am. Chem. Soc.* **2018,** *140*, 590-593.

(33) Wang, S.; McCrea-Hendrick, M. L.; Weinstein, C. M.; Caputo, C. A.; Hoppe, E.; Fettinger, J. C.; Olmstead, M. M.; Power, P. P., Tin(II) Hydrides as Intermediates in Rearrangements of Tin(II) Alkyl Derivatives. *J. Am. Chem. Soc.* **2017,** *139*, 6596-6604.

(34) Vícha, J.; Marek, R.; Straka, M., High-Frequency ^{1}H NMR Chemical Shifts of Sn^{II} and Pb^{II} Hydrides Induced by Relativistic Effects: Quest for Pb^{II} Hydrides. *Inorg. Chem.* **2016,** *55*, 10302-10309.

(35) Sindlinger, C. P.; Wesemann, L., Hydrogen abstraction from organotin di- and trihydrides by N-heterocyclic carbenes: a new method for the preparation of NHC adducts to tin(II) species and observation of an isomer of a hexastannabenzene derivative [R_6Sn_6]. *Chem. Sci.* **2014,** *5*, 2739-2746.

(36) Sindlinger, C. P.; Stasch, A.; Bettinger, H. F.; Wesemann, L., A nitrogen-base catalyzed generation of organotin(II) hydride from an organotin trihydride under reductive dihydrogen elimination. *Chem. Sci.* **2015,** *6*, 4737-4751.

(37) Sindlinger, C. P.; Grahneis, W.; Aicher, F. S. W.; Wesemann, L., Access to Base Adducts of Low-Valent Organotin-Hydride Compounds by Controlled, Stepwise Hydrogen Abstraction from a Tetravalent Organotin Trihydride. *Chem. Eur. J.* **2016,** *22*, 7554-7566.

(38) Villegas-Escobar, N.; Schaefer, H. F.; Toro-Labbé, A., Formation of Formic Acid Derivatives through Activation and Hydroboration of CO_2 by Low-Valent Group 14 (Si, Ge, Sn, Pb) Catalysts. *J. Phys. Chem. A* **2020,** *124*, 1121-1133.

(39) Jana, A.; Tavčar, G.; Roesky, H. W.; John, M., Germanium(II) hydride mediated reduction of carbon dioxide to formic acid and methanol with ammonia borane as the hydrogen source. *Dalton Trans.* **2010,** *39*, 9487-9489.

(40) Weiß, S.; Widemann, M.; Eichele, K.; Schubert, H.; Wesemann, L., Low valent lead and tin hydrides in reactions with heteroallenes. *Dalton Trans.* **2021,** *50*, 4952-4958.

(41) Hadlington, T. J.; Kefalidis, C. E.; Maron, L.; Jones, C., Efficient Reduction of Carbon Dioxide to Methanol Equivalents Catalyzed by Two-Coordinate Amido–Germanium(II) and −Tin(II) Hydride Complexes. *ACS Catal.* **2017,** *7*, 1853-1859.

(42) Pangborn, A. B.; Giardello, M. A.; Grubbs, R. H.; Rosen, R. K.; Timmers, F. J., Safe and Convenient Procedure for Solvent Purification. *Organometallics* **1996,** *15*, 1518-1520.

(43) Rivard, E.; Steiner, J.; Fettinger, J. C.; Giuliani, J. R.; Augustine, M. P.; Power, P. P., Convergent syntheses of [Sn_7{C_6H_3-2,6-(C_6H_3-2,6-$^iPr_2$)$_2$}$_2$]: a cluster with a rare pentagonal bipyramidal motif. *Chem. Commun.* **2007**, 4919-4921.

(44) Boylan, M. J.; Braterman, P. S.; Fullarton, A., Metal carbonyl photolysis and its reversal;probable spurious nature of "trigonal bipyramidal $Mo(CO)_5$". *J. Organomet. Chem.* **1971,** *31*, C29-C30.

(45) Richards, A. F.; Eichler, B. E.; Brynda, M.; Olmstead, M. M.; Power, P. P., Metal-Rich, Neutral and Cationic Organotin Clusters. *Angew. Chem. Int. Ed.* **2005,** *44*, 2546-2549.

(46) Petz, W., Transition-metal complexes with derivatives of divalent silicon, germanium, tin, and lead as ligands. *Chem. Rev.* **1986,** *86*, 1019-1047.

(47) Schläfer, J.; Stucky, S.; Tyrra, W.; Mathur, S., Heterobi- and Trimetallic Cerium(IV) tert-Butoxides with Mono-, Di-, and Trivalent Metals (M = K(I), Ge(II), Sn(II), Pb(II), Al(III), Fe(III)). *Inorg. Chem.* **2013,** *52*, 4002-4010.

(48) Pyykkö, P.; Atsumi, M., Molecular Single-Bond Covalent Radii for Elements 1–118. *Chem. Eur. J.* **2009,** *15*, 186-197.

(49) Queen, J. D.; Phung, A. C.; Caputo, C. A.; Fettinger, J. C.; Power, P. P., Metathetical Exchange between Metal-Metal Triple Bonds. *J. Am. Chem. Soc.* **2020,** *142*, 2233-2237.

(50) Hayes, P. G.; Gribble, C. W.; Waterman, R.; Tilley, T. D., A Hydrogen-Substituted Osmium Stannylene Complex: Isomerization to a Metallostannylene Complex via an Unusual α-Hydrogen Migration from Tin to Osmium. *J. Am. Chem. Soc.* **2009,** *131*, 4606-4607.

(51) Weidenbruch, M.; Stilter, A.; Schlaefke, J.; Peters, K.; Schnering, H. G. v., Compounds of germanium and tin XIV. Rearrangement of bis(2,4,6-tri-tert-

butylphenyl)stannylene: synthesis and structure of a donor-free alkylarylstannylene-tungsten complex. *J. Organomet. Chem.* **1995,** *501*, 67-70.

(52) Weidenbruch, M.; Stilter, A.; Peters, K.; von Schnering, H. G., Verbindungen des Germainums und Zinns. 17. Alkylarylstannylen-Komplexe des Chroms und Molybdäns ohne Donorstabilisierung. *Z. Anorg. Allg. Chem.* **1996,** *622*, 534-538.

(53) Weidenbruch, M.; Stilter, A.; Saak, W.; Peters, K.; von Schnering, H. G., An octahedral stannylmanganese stannylene complex. *J. Organomet. Chem.* **1998,** *560*, 125-129.

(54) Schneider, J. J.; Czap, N.; Bläser, D.; Boese, R., Metal Atom Synthesis of (η^6-Toluene)(η^2-ethene)iron(σ^1-stannandiyls): Unusual Iron(0) Complexes. *J. Am. Chem. Soc.* **1999,** *121*, 1409-1410.

(55) Bareš, J.; Richard, P.; Meunier, P.; Pirio, N.; Padělková, Z.; Černošek, Z.; Císařová, I.; Růžička, A., Reactions of C,N-chelated Tin(II) and Lead(II) Compounds with Zirconocene Dichloride Derivatives. *Organometallics* **2009,** *28*, 3105-3108.

(56) Schneider, J. J.; Czap, N.; Bläser, D.; Boese, R.; Ensling, J.; Gütlich, P.; Janiak, C., Experimental and Theoretical Investigations on the Synthesis, Structure, Reactivity, and Bonding of the Stannylene-Iron Complex Bis{{bis(2-tert-butyl-4,5,6-trimethyl-phenyl)}Sn}Fe(η^6-toluene). *Chem. Eur. J.* **2000,** *6*, 468-474.

(57) Ellis, B. D.; Atkins, T. M.; Peng, Y.; Sutton, A. D.; Gordon, J. C.; Power, P. P., Synthesis and thermolytic behavior of tin(IV) formates: in search of recyclable metal–hydride systems. *Dalton Trans.* **2010,** *39*, 10659-10663.

(58) Sokolovicz, Y. C. A.; Nieto Faza, O.; Specklin, D.; Jacques, B.; López, C. S.; dos Santos, J. H. Z.; Schrekker, H. S.; Dagorne, S., Acetate-catalyzed hydroboration of CO_2 for the selective formation of methanol-equivalent products. *Catal. Sci. Technol.* **2020,** *10*, 2407-2414.

(59) Cao, X.; Wang, W.; Lu, K.; Yao, W.; Xue, F.; Ma, M., Magnesium-catalyzed hydroboration of organic carbonates, carbon dioxide and esters. *Dalton Trans.* **2020,** *49*, 2776-2780.

(60) Kircher, P.; Huttner, G.; Heinze, K.; Schiemenz, B.; Zsolnai, L.; Büchner, M.; Driess, A., Four-Coordinate Group-14 Elements in the Formal Oxidation State of Zero – Syntheses, Structures, and Dynamics of [{$(CO)_5Cr$}$_2$Sn(L_2)] and Related Species. *Eur. J. Inorg. Chem.* **1998,** *1998*, 703-720.

(61) Cotton, F. A.; Darensbourg, D. J.; Ilsley, W. H., .pi. Acidity of tris(2-cyanoethyl)phosphine. X-ray structural studies of $M(CO)_5P(CH_2CH_2CN)_3$ (M = chromium, molybdenum) and $Mo(CO)_5P(C_6H_5)_3$. *Inorg. Chem.* **1981,** *20*, 578-583.

(62) A. D. Becke, A new mixing of Hartree-Fock and local density-functional theories. *J. Chem. Phys.*, **1993**, 98, 1372-1377.

(63) C. Lee, W. Yang and R. G. Parr, Development of the Colle-Salvetti correlation-energy formula into a functional of the electron density. *Phys. Rev. B*, **1988**, 37, 785-789.

(64) S. H. Vosko, L. Wilk and M. Nusair, Accurate spin-dependent electron liquid correlation energies for local spin density calculations: a critical analysis. *Can. J. Phys.*, **1980**, 58, 1200-1211.

(65) P. J. Stephens, F. J. Devlin, C. F. Chabalowski and M. J. Frisch, *Ab Initio* Calculation of Vibrational Absorption and Circular Dichroism Spectra Using Density Functional Force Fields. *J. Phys. Chem.*, **1994**, 98, 11623-11627.

(66) F. Weigend and R. Ahlrichs, Balanced basis sets of split valence, triple zeta valence and quadruple zeta valence quality for H to Rn: Design and assessment of accuracy. *Phys. Chem Chem. Phys.*, **2005**, 7, 3297-3305.

(67) B. Metz, H. Stoll and M. Dolg, Small-core multiconfiguration-Dirac-Hartree-Fock-adjusted pseudopotentials for post-d main group elements: Application to PbH and PbO. *J. Chem. Phys.*, **2000**, 113, 2563-2569.

(68) S. Grimme, J. Antony, S. Ehrlich and H. Krieg, A consistent and accurate *ab initio* parametrization of density functional dispersion correction (DFT-D) for the 94 elements H-Pu, *J. Chem. Phys.*, **2010**, 132, 154104.

(69) S. Grimme, S. Ehrlich and L. Goerigk, Effect of the damping function in dispersion corrected density functional theory, *J. Comput. Chem.*, **2011**, 32, 1456-1465.

(70) F. Weigend, Accurate Coulomb-fitting basis sets for H to Rn, *Phys. Chem Chem. Phys.*, **2006**, 8, 1057-1065.

(71) A. Hellweg, C. Hättig, S. Höfener and W. Klopper, Optimized accurate auxiliary basis sets for RI-MP2 and Ri-CC2 calculations for the atoms Rb to Rn, *Theor. Chem. Acc.*, **2007**, 117, 587-597.

(72) F. Neese, The ORCA program system, *WIREs Comput. Mol. Sci.*, **2012**, 2, 73-78.

Chapter 4

Hydrostannylation of Olefins by a Hydridostannylene Tungsten Complex

This work is published in Organometallics, DOI: 10.1021/acs.organomet.2c00494

Zhu, Q.; Fettinger J. C.; Vasko, P.; Power, P. P. *Organometallics* **2022**, just accepted

4.1 Introduction

Divalent tin(II) hydrides have attracted increasing interest due to their potential catalytic applications in the hydrogenation of unsaturated molecules.[1-9] In 2000, the first stable tin(II) hydride, $\{Ar^{iPr6}Sn(\mu\text{-}H)\}_2$ (Ar^{iPr6} = -C_6H_3-2,6-(C_6H_2-2,4,6-$^i Pr_3$)$_2$) was reported.[10] This featured a dimeric hydrogen bridged structure. Shortly thereafter, Roesky and coworkers reported the monomeric tin(II) hydrides [{HC(CMeNAr)$_2$}SnH],[11] and [{ArN=C(Me)]$_2C_6H_3SnH$][12] (Ar = 2,6-i$Pr_2C_6H_3$) which featured terminal Sn-H bonds. Wesemann and coworkers have isolated several three-coordinate monomeric tin(II) hydrides with base-stabilization via reactions of tetravalent organotin trihydrides with Lewis bases.[13-15] Although numerous transition metal-complexed stannylene[16] compounds and their multiply bonded analogues[17-19] have been reported since the early 1970s, transition metal-complexes of hydridostannylenes remain scarce.[20-22] Successful synthetic routes to transition metal complexed hydridostannylenes include H/Cl exchange as exemplified by the "push-pull" complex, IPr·SnH_2·$W(CO)_5$, of Rivard and coworkers.[23] Similar "push-pull" complexes were also reported by Jambor and coworkers with the use of intramolecular base-stabilization.[24] In addition, hydrogen elimination reactions have been shown to be yield transition metal-stabilized hydridostannylenes, $[Cp_2Zr\{Sn(H)Ar\}]_2$.[25-26] In 2021, this group showed that the THF donor ligand in $[Mo(CO)_5THF]$ could be displaced by a hydridostannylene, $[Ar^{iPr6}SnH]$, to give $Mo(CO)_5\{Sn(Ar^{iPr6})H\}$.[27] This complex was then shown to effect facile

hydrostannylation of CO_2, and catalytic hydroboration of CO_2 was achieved with pinacolborane. These results were in contrast to the lack of catalytic activity for CO_2 reduction by the parent tin hydride, $\{Ar^{iPr6}Sn(\mu\text{-}H)\}_2$.[28]

The reactivity of $\{Ar^{iPr4}Sn(\mu\text{-}H)\}_2$, and $\{Ar^{iPr6}Sn(\mu\text{-}H)\}_2$ toward olefins has also been investigated, and both $\{Ar^{iPr4}Sn(\mu\text{-}H)\}_2$, and $\{Ar^{iPr6}Sn(\mu\text{-}H)\}_2$ were shown to effect facile hydrostannylation of ethylene at room temperature, where the steric properties of the ligands resulted in slightly different reactivity.[29-30] Moreover, it was also discovered that the aryltin(II) hydride $\{Ar^{iPr4}Sn(\mu\text{-}H)\}_2$ can exist in equilibrium with H_2 and the distannyne, $Ar^{iPr4}SnSnAr^{iPr4}$.[22] Notably, reversible reactions of ethylene with the distannynes were also reported, where cycloadducts $Ar^{iPr4}Sn(CH_2CH_2)_2SnAr^{iPr4}$, and $Ar^{iPr8}Sn(CH_2CH_2)_2SnAr^{iPr8}$ were isolated.[30] Jones and coworkers reported hydrostannylation reactions of $[LSn(\mu\text{-}H)]_2$ (L=-N(Ar)($SiPr^i_3$) Ar = $C_6H_2\{C(H)Ph_2\}_2Pr^i$-2,6,4) with a variety of alkenes, where the hydrostannylated products suggest equilibrium between the dimer, $[LSn(\mu\text{-}H)]_2$, and monomer LSnH.[31] However, no catalytic cycle has been achieved in the olefin hydrogenation using tin hydrides despite of the facile reactivity in hydrostannylation of olefins, whereas hydrosilylation reactions of olefins have been reported with silylene supported transition metal complexes.[32-33]

Herein, we report the reactions of $\{Ar^{iPr6}Sn(\mu\text{-}H)\}_2$ with $[W(CO)_5(THF)]$, to give $W(CO)_5\{Sn(Ar^{iPr6})H\}$, (**1**). Hydrostannylation by **1** of ethylene, or propylene resulted in the formation of $W(CO)_5\{Sn(Ar^{iPr6})(Et)\}$, (**2**), or $W(CO)_5\{Sn(Ar^{iPr6})(^nPr)\}$, (**3**) (Scheme 4.1). The Lewis acidic nature of the Sn atom in **1** was demonstrated by the formation and isolation of the Lewis acid-base complex $[(Ar^{iPr6})(H)Sn(dbu)\text{-}W(CO)_5]$, (**4)**, which resulted from the reaction of **1** and the weakly-nucleophilic base,[34] 1,8-diazabicycloundec-7-ene (dbu) (Scheme 4.2). The catalytic potential of **1** towards ethylene hydrosilylation was also investigated by reacting **2** with phenylsilane in C_6D_6, where limited conversion of **2** to **1** was observed. DFT calculation

suggests that the hydrostannylation reactions proceed via olefin insertion into the Sn-H bond by coordination of olefins at the tin atom. The limited conversion in reaction of **2** with phenylsilane in C_6D_6 can be accounted for in terms of the rate-determining step in the metathesis reaction between Sn-C/Si-H bond having a very high energy barrier of 71.3 kcal/mol.

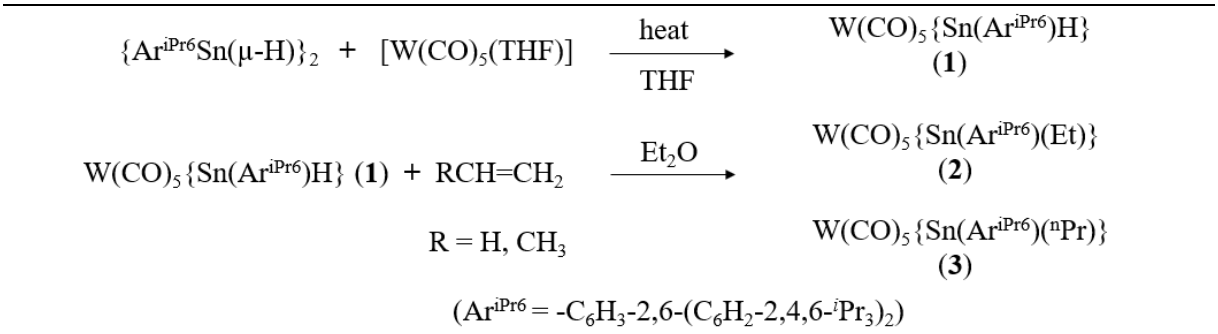

Scheme 4.1: Syntheses of **1-3**

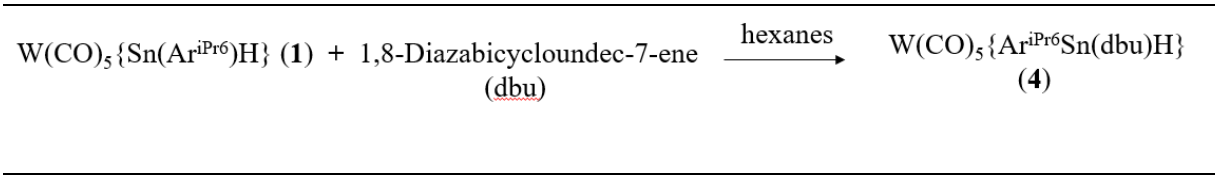

Scheme 4.2: Synthesis of **4**

4.2 Experimental Details

General considerations. All operations were carried out by using modified Schlenk techniques or in a Vacuum Atmospheres OMNI-Lab drybox under an atmosphere of dry argon or nitrogen. All solvents were dried over alumina columns and degassed prior to use.[35] The metal carbonyls were used as purchased without further purification. ^{1}H, $^{13}C\{^{1}H\}$, $^{29}Si\{^{1}H\}$, and $^{119}Sn\{^{1}H\}$ NMR spectra were collected on a Bruker 400 MHz Nanobay Avance III HD spectrometer. The ^{119}Sn NMR data were referenced to the external standard $SnMe_4$. UV-visible spectra were recorded in dilute hexane solutions in 3.5 mL quartz cuvettes using an Olis 17

Modernized Cary 14 UV-Vis/NIR spectrophotometer. Infrared spectra were collected on a Bruker Tensor 27 ATR-FTIR spectrometer. $\{Ar^{iPr6}Sn(\mu\text{-}H)\}_2$[10] and $[W(CO)_5(THF)]$[36] were synthesized by the literature methods. All synthesized compounds hydrolyzed rapidly in air, and therefore no elemental analysis was carried out.

Syntheses. $W(CO)_5\{Sn(Ar^{iPr6})H\}$ (1). A solution of $[W(CO)_5(THF)]$ (1.40 mmol, from 0.352 g $W(CO)_6$) in THF (ca. 40 mL) was added to a heavy-walled Teflon tapped Schlenk flask along with $\{Ar^{iPr6}SnH\}_2$ (0.705 g, 0.586 mmol) in THF (ca. 30 mL). Upon addition of $[W(CO)_5(THF)]$, the color of the solution changed from blue to green, and then to yellow orange after heating at 50 °C for 1 day, after which the reaction mixture was heated for 2 additional days. The solution was then cooled to room temperature, the solvent was removed under reduced pressure and the residue was extracted with ca. 50 mL of hexanes and filtered. Storage of the solution in a ca. -30 °C freezer for 2 weeks afforded crystals as pale yellow blocks that proved suitable for single crystal X-ray studies. Yield: 75.3% (0.817 g, 0.882 mmol). ^{1}H NMR (C_6D_6, 399.8 MHz, 298 K): δ 1.06 (d, 12 H, J_{HH} = 6.7 Hz, o-$CH(CH_3)_2$), 1.22 (d, 12 H, J_{HH} = 7.2 Hz, o-$CH(CH_3)_2$), 1.40 (d, 12 H, J_{HH} = 7.0 Hz, p-$CH(CH_3)_2$), 2.77 (sept., 2 H, J_{HH} = 6.8 Hz, p-$CH(CH_3)_2$), 3.09 (sept., 4 H, J_{HH} = 6.9 Hz, o-$CH(CH_3)_2$), 7.19 (s, 4H, m-C_6H_2), 7.28 (s, 3H, m-C_6H_3 and p-C_6H_3), 18.62 (s, 1 H, $J_{W\text{-}H}$ = 19 Hz, $J_{Sn\text{-}H}$ = 754 Hz, Sn-H); $^{13}C\{^1H\}$ NMR (C_6D_6, 100.5 MHz, 298 K): δ 23.39, 23.97, 26.28, 31.15, 34.76, 122.66, 128.83, 129.99, 133.61, 145.21, 150.72, 161.20, 196.80 ($J_{W\text{-}C}$ = 121 Hz), 201.28; $^{119}Sn\{^1H\}$ NMR (C_6D_6, 149.3 MHz, 298 K): δ 1159 (d, $J_{Sn\text{-}W}$ = 674 Hz). λ_{max} (ε): 397 nm (5.5×10^3 L mol^{-1} cm^{-1}). IR (ν, cm^{-1}): 2066 (m), 1915 (vs), 1757 (w).

$W(CO)_5\{Sn(Ar^{iPr6})(Et)\}$ (2). A solution of **1** (0.381 g, 0.410 mmol) in Et_2O (ca. 40 mL) was added to a heavy-walled Teflon tapped Schlenk flask. The flask was frozen by immersion in liquid nitrogen, evacuated under reduced pressure, and refilled with ethylene at room temperature, whereupon the reaction was stirred at room temperature for additional 15

min. The solvent was concentrated under reduced pressure to ca. 5 mL. Storage of the solution in a ca. -30 °C freezer for 1 week afforded yellow-orange blocks that were suitable for single crystal X-ray diffraction studies. Yield: 27.2% (0.107 g, 0.111 mmol). ^{1}H NMR (C_6D_6, 399.8 MHz, 298 K): δ 0.89-1.09 (m, 5 H, Sn-CH_2CH_3, 1.06 (d, 12 H, J_{HH} = 6.7 Hz, o-$CH(CH_3)_2$), 1.21 (d, 12 H, J_{HH} = 6.3 Hz, o-$CH(CH_3)_2$), 1.37 (d, 12 H, J_{HH} = 6.3 Hz, p-$CH(CH_3)_2$), 2.76 (sept., 2 H, J_{HH} = 7.0 Hz, p-$CH(CH_3)_2$), 3.11 (br, 4 H, o-$CH(CH_3)_2$), 7.19 (s, 4H, m-C_6H_2), 7.28-7.33 (m, 3H, m-C_6H_3 and p-C_6H_3); ^{13}C{^{1}H} NMR (C_6D_6, 100.5 MHz, 298 K): δ 8.66, 22.73, 23.93, 26.89, 30.98, 34.80, 40.49, 122.45, 128.41, 131.05, 135.48, 144.56, 147.13, 150.29, 165.41, 197.82, 201.47; ^{119}Sn{^{1}H} NMR (C_6D_6, 149.3 MHz, 298 K): δ 1455. λ_{max} (ε): 311 nm (shoulder, 4.6 × 10^3 L mol^{-1} cm^{-1}), 394 nm (4.4 × 10^3 L mol^{-1} cm^{-1}). IR (ν, cm^{-1}): 2059 (m), 1920 (vs).

$W(CO)_5${Sn(Ar^{iPr6})(^{n}Pr)} (3). A procedure similar to that used for the preparation of **2** was carried out using propylene, and 0.269 g (0.291 mmol) of **1**. Storage of the solution in a ca. -30 °C freezer for 1 week afforded yellow needle crystals. Yield: 30.2% (0.085 g, 0.088 mmol). ^{1}H NMR (C_6D_6, 399.8 MHz, 298 K): δ 0.80-0.91 (m, 2 H, Sn-CH_2**CH_2**CH_3), 0.99 (t, 2 H, J_{HH} = 7.1 Hz, Sn-**CH_2**CH_2CH_3), 1.07 (d, 12 H, J_{HH} = 6.7 Hz, o-$CH(CH_3)_2$), 1.22 (d, 12 H, J_{HH} = 7.1 Hz, o-$CH(CH_3)_2$), 1.23-1.29 (m, 3 H, Sn-CH_2CH_2**CH_3**), 1.39 (d, 12 H, J_{HH} = 6.7 Hz, p-$CH(CH_3)_2$), 2.77 (sept., 2 H, J_{HH} = 7.1 Hz, p-$CH(CH_3)_2$), 3.13 (br, 4 H, o-$CH(CH_3)_2$), 7.19 (s, 4H, m-C_6H_2), 7.24-7.34 (m, 3H, m-C_6H_3 and p-C_6H_3); ^{13}C{^{1}H} NMR (C_6D_6, 100.5 MHz, 298 K): δ 18.75, 19.04, 22.75, 23.96, 26.92, 30.93, 34.80, 51.13, 122.45, 128.41, 131.05, 135.68, 144.64, 147.09, 150.27, 165.32, 197.96 (J_{W-C} = 121 Hz), 201.54; ^{119}Sn{^{1}H} NMR (C_6D_6, 149.3 MHz, 298 K): δ 1443. λ_{max} (ε): 307 nm (shoulder, 6.5×10^3 L mol^{-1} cm^{-1}), 394 nm (6.3 × 10^3 L mol^{-1} cm^{-1}). IR (ν, cm^{-1}): 2059 (m), 1920 (vs).

$W(CO)_5${Sn(Ar^{iPr6})(dbu)H} (4). To a Schlenk flask charged with **1** (0.259 g, 0.280 mmol) and dbu (44 μL, 0.295 mmol), ca. 50 mL of hexanes were added. Upon addition of

solvent, the color of the solution lightened from yellow-orange to pale yellow. Then, the solution was stirred overnight, and concentrated under reduced pressure to ca. 10 mL. Storage of the solution in a ca. -30 °C freezer for 2 weeks afforded colorless blocks that were suitable for single crystal X-ray studies. Yield: 46.4% (0.141 g, 0.130 mmol). ^{1}H NMR (C_6D_6, 399.8 MHz, 298 K): δ 0.70-0.99 (m, 4 H, dbu), 1.15 (d, 12 H, J_{HH} = 6.7 Hz, o-CH(CH_3)$_2$), 1.19-1.24 (m, 3 H, dbu), 1.29 (d, 12 H, J_{HH} = 6.7 Hz, o-CH(CH_3)$_2$), 1.33 (d, 6 H, J_{HH} = 6.6 Hz, p-CH(CH_3)$_2$), 1.38-1.54 (m, 2 H, dbu), 1.59 (d, 6 H, J_{HH} = 6.7 Hz, p-CH(CH_3)$_2$), 1.99-2.14 (m, 2 H, dbu), 2.23-2.38 (m, 2 H, dbu), 2.63-2.76 (m, 1 H, dbu), 2.89 (sept., 2 H, J_{HH} = 6.9 Hz, o-CH(CH_3)$_2$ and 1H, dbu), 2.97 (sept., 2 H, J_{HH} = 6.6 Hz, o-CH(CH_3)$_2$), 3.02-3.12 (m, 1 H, dbu), 3.32 (sept., 2 H, J_{HH} = 6.6 Hz, p-CH(CH_3)$_2$), 7.08-7.14 (m, 3H, m-C_6H_3 and p-C_6H_3), 7.20 (s, 2H, m-C_6H_2), 7.26 (s, 2H, m-C_6H_2), 10.12 (s, 1H, $J_{W\text{-}H}$ = 19 Hz, $J^{119}_{Sn\text{-}H}$ = 1093 Hz, $J^{117}_{Sn\text{-}H}$ = 1045 Hz, $J_{W\text{-}H}$ = 12 Hz, Sn-H); ^{13}C{^{1}H} NMR (C_6D_6, 100.5 MHz, 298 K): δ 23.47, 23.61, 23.84, 24.31, 24.60, 26.01, 26.31, 26.58, 30.98, 31.42, 34.98, 48.44, 53.10, 121.46, 126.20, 131.86, 140.11, 146.99, 147.63, 148.67, 150.35, 167.51, 201.95, 202.77,; ^{119}Sn{^{1}H} NMR (C_6D_6, 149.3 MHz, 298 K): δ not detected. λ_{max} (ε): 357 nm (shoulder, 2.4 × 10^3 L mol^{-1} cm^{-1}). IR (ν, cm^{-1}): 2050 (m), 1963 (m), 1916 (s), 1887 (vs), 1793 (w), 1575 (m).

Catalytic Studies. To a J. Young's tube containing ca. 0.02 g of **2**, was added 0.6 mL of C_6D_6, then 280 μL (ca. ten equivalents) of Ph_3SiH was added to the tube. The reactions were monitored by ^{1}H, and ^{29}Si NMR spectroscopies, and ^{1}H and ^{29}Si NMR spectra were recorded after a brief sonication of the mixture. Additional ^{1}H NMR spectra of the mixture of **2** and Ph_3SiH in C_6D_6 were taken 12 h, 24 h, and 72 h after mixing in glove box, separately. No color change was observed upon addition of Ph_3SiH to the C_6D_6 solution of **2**, however, a minor color change from bright yellow to yellow-orange was observed upon heating mixture solution at ca. 65°C after ca. 60 h (see SI).

4.3 Results and Discussion

Syntheses. Compound **1** was synthesized by a similar procedure to that described in a previous publication,[27] it was offerred by gently heating 1 equivalent of THF solution of $\{Ar^{iPr6}Sn(\mu\text{-}H)\}_2$[10] with 2 equivalents of $[W(CO)_5(THF)]$,[36] and isolated with good yield, 75%. (Scheme 4.1) Alternatively, Jambor and coworkers demonstrated that transition metal complexed hydridostannylene can be synthesized via halide elimination reaction of $L^2(Cl)Sn{\cdot}W(CO)_5$ (L^2 = 2-Et_2NCH_2-4,6-tBu_2-C_6H_2) with KEt_3BH.[24] However, this synthetic route is inapplicable for terphenyl ligand supported species as shown previously. The oxidative addition of organolead(II) bromide with $[W(CO)_5THF]$ forms a bridged plumbylyne complex instead of formation of a plumbylene coordination transition metal complex.[37] Wesemann and coworkers have also successfully isolated transition metal complexed hydridostannylene via different synthetic routes, such as H_2 elimination from a organotin trihydride[26], or reaction of a low valent aryl tin cation with transition metal hydrides.[25] For the synthesis of **2** and **3** (Scheme 4.1), a solution of **1** in Et_2O was frozen, and the flask was evacuated under reduced pressure. The reaction flask was then allowed to warm to room temperature, and refilled with ethylene, or propylene, whereupon the color of the solution changed from yellow-orange to bright yellow. Stirring of the resultant solution for 30 min afforded a quantitative conversion based on the ^1H NMR spectrum of the crude product. Concentration of the solution, followed by storage in a ca. -30 ℃ freezer for 1 week afforded yellow crystals of **2** or **3** in moderate yield. Jones and coworkers have also reported the facile hydrostannylation reactions of unactivated alkenes with $[LSn(\mu\text{-}H)]_2$ (L = N(Ar)($SiPr^i_3$), Ar = $C_6H_2\{C(H)Ph_2\}_2Pr^i$-2,6,4) at low temperature (ca. -80℃) due to the mild thermal instability of the tin hydride species at room temperature, nevertheless these products were isolated in good yields.[38] Wesemann and coworkers reported hydrostannylation of styrene at slightly elevated temperature (ca. 75℃)

with $[Cp_2W(H)=SnHAr^{iPr6}]^+$ to afford $[Cp_2W(H)]Sn(CH_2CH_2Ph)Ar^{iPr6}]^+$ possibly due to the increased steric bulk from the phenyl group of styrene.[25]

Initial attempts to add dbu, a known weakly nucleophilic base,[34] to a solution of **1** was for the purpose of pKa determination of the complex reported in previous work of this group.[27] However, the ^1H NMR spectrum of the crude product showed quantitative coordination reaction rather than a Brønsted–Lowry acid–base reaction between the tin hydride species and dbu. Compound **4** was synthesized by addition of slight excess of dbu (1.05 equivalents) into a solution of **1** in hexanes at room temperature. The mixture was stirred overnight, whereupon the color of the solution changed from yellow-orange to very pale yellow. Concentration of the resultant solution followed by storage in a ca. -30 °C freezer for 2 weeks afforded colorless crystals of **4** in moderate yield.

Structures. The molecular structures of **1**, **2**, and **4** are shown in Figures 4.1-4.3, respectively.

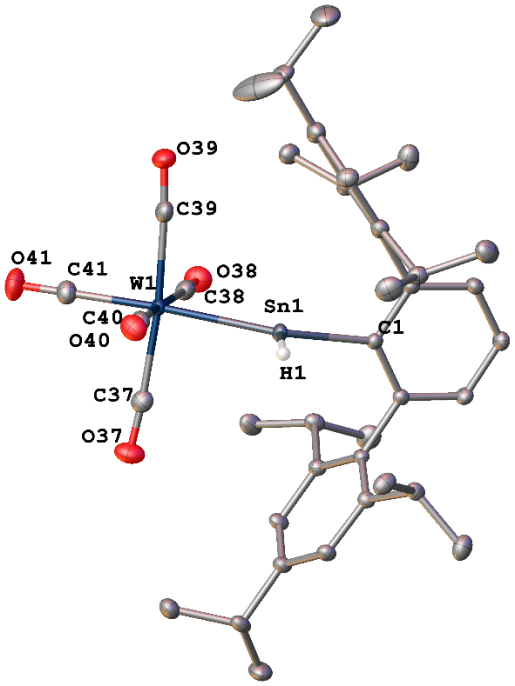

Figure 4.1: Solid-state molecular structure of **1** (hydrogen atoms, except for tin bound H1, and ligand disorder are not shown for clarity). Thermal ellipsoids are shown at 30% probability. Selected bond lengths

(Å) and angles (degrees): Sn(1)-C(1) 2.1518(19), Sn(1)-W(1) 2.7150(2), Sn(1)-H(1) 2.06(3), W(1)-C(37) 2.051(2), W(1)-C(38) 2.049(2), W(1)-C(39) 2.047(2), W(1)-C(40) 2.041(2), W(1)-C(41) 2.006(2), C(37)-O(37) 1.138(3), C(38)-O(38) 1.136(3), C(39)-O(39) 1.140(3), C(40)-O(40) 1.143(3), C(41)-O(41) 1.137(3); C(1)-Sn(1)-W(1) 141.34 (5), C(1)-Sn(1)-H(1) 107.9(7), W(1)-Sn(1)-H(1) 110.7(7).

The molecular structure of **1** shows that the tin atom is three-coordinate, and is bound to the Ar^{iPr6} ligand via C(1), a hydrogen atom, and a [$W(CO)_5$] fragment. Compound **1** displays similar structural features to those of $Mo(CO)_5\{Sn(Ar^{iPr6})H\}$[27] reported earlier by this group, where the hydridostannylene, [$Ar^{iPr6}SnH$] forms Lewis acid-base complex with [$W(CO)_5$] to afford almost planar coordination geometry at the tin atom, and distorted octahedral geometry at the tungsten atom, respectively. The sum of C(1)-Sn(1)-W(1), C(1)-Sn(1)-H(1), and W(1)-Sn(1)-H(1) angles around tin in complex **1** is 359.9(7)°. The almost planar coordination geometry at Sn that is imposed by the ligands agrees with the presence of a vacant p orbital oriented perpendicular to the coordination plane in the structure of **1**, which can be further demonstrated in the DFT calculations of optimized structure of **1** in gas phase (see ESI). In the structure of **1**, the C(1)-Sn(1)-H(1) unit is almost coplanar with that of tungsten and the three carbonyl groups of C(38), C(40), and C(41). The Sn(1)-W(1)-C(41) array is almost linear (176.23(7)°). The coordination reaction of dbu with compound **1** affords compound **4**. The molecular structure of **4** features Lewis acid-base complex with a four-coordinate tin atom to which dbu is also coordinated. This structure of **4** represents the first structurally characterized Sn-dbu coordination species. The Lewis acid-base reaction is likely to proceed via coordination of dbu to the vacant p orbital at the tin atom, located perpendicular to the tin coordination plane in the structure of **1**. However, the Sn(1)-N(1) bond vector in the structure of **4** is not perpendicular to the coordination plane, as shown by the bond angles of N(1)-Sn(1)-H(1), 96.5(9)°; N(1)-Sn(1)-C(1), 105.21(7)°; and N(1)-Sn(1)-W(1), 105.12(5)°. The sum of the angles at tin associated with the hydride and terphenyl ligand in **4**, C(1)-Sn(1)-H(1), C(1)-

Sn(1)-W(1), and W(1)-Sn(1)-H(1), is 344.6(9)°. The Sn(1)-N(1) distance is 2.2261(16) Å in **4**, which is slightly longer than the sum of covalent radii of Sn (1.40 Å) and N (0.71 Å).[39] The Sn(1)-N(1) distance in **4** is in close agreement with that in the four-coordinate transition metal complexed hydridostannylene, (Sn-N 2.292(3) Å) in $L^2(H)Sn{\cdot}W(CO)_5$ (L^2 = 2-Et_2NCH_2-4,6-tBu_2-C_6H_2), which was reported by Jambor and coworkers.[24] The Sn(1)-N(1) distance in **4** is also similar to [{$HC(CMeNAr)_2$}SnH] (Ar = 2,6-$iPr_2C_6H_3$), reported by Roesky and coworkers.[11] In comparison to Sn-N distances of bis(amido)stannylene, such as $Sn\{N(SiMe_3)_2\}_2$[40] and of N-heterocyclic stannylenes,[41,42] **4** displays a longer Sn-N distance likely due to the dative N→Sn bond coordination. Other examples of Sn-N dative bond coordination include [2,6-(Me_2-NCH_2)$_2$$C_6H_3(Cl)SnW(CO)_5$], reported by Jurkschat and coworkers, with Sn-N distances of 2.543(3) Å and 2.5526(3) Å, and shortening to 2.264(2) Å upon displacing chloride with aqua-coordination in [2,6-(Me_2-NCH_2)$_2$$C_6H_3$($H_2O$)$SnW(CO)_5$]$^+$[$CB_{11}H_{12}$]$^-$.[43] The positions of the hydrogen atoms bound to the tin atoms in both **1** and **4** were located in the Fourier difference map and refined isotropically. The Sn-H distance is 2.09 Å in **1**, may be compared to the Sn-H distance 1.93(2) Å in the previously reported $Mo(CO)_5${$Sn(Ar^{iPr6})H$}.[27] The Sn-H distance is 1.68(3) Å in **4**, which is similar to the Sn-H, 1.82(6) Å, in $Mo(CO)_5${$Sn(Ar^{iPr4})$(THF)H}.[27] These values may be compared to that of the terminal Sn-H bond, 1.74(3) Å, in [{$HC(CMeNAr)_2$}SnH][11] reported by Roesky and coworkers, 1.797(2) Å in L^2(Cl)Sn·$W(CO)_5$[24] reported by Jambor and coworkers, 1.81(11) Å in IPr·SnH_2·$W(CO)_5$[23] reported by Rivard and coworkers, and Sn-H bonds in $Cp_2M(Ar^{iPr6}SnH)_2$ (M = Ti, Zr, and Hf)[26] complexes reported by Wesemann and coworkers, which range from 1.69(2) to 1.776(18) Å.

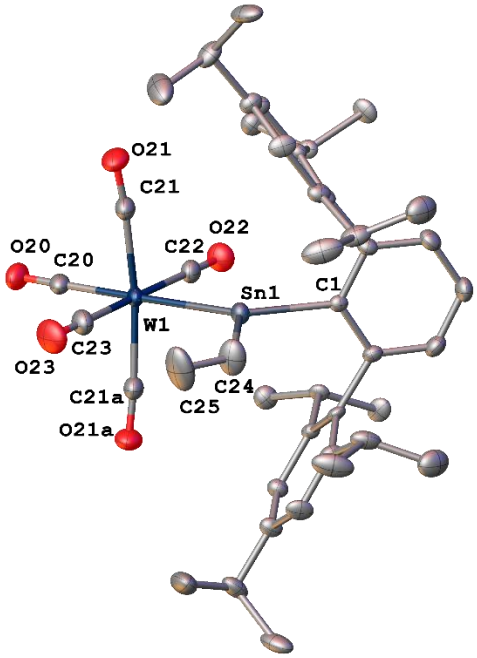

Figure 4.2: Solid-state molecular structure of **2** (hydrogen atoms and ligand disorder are not shown for clarity. Thermal ellipsoids are shown at 30% probability). Selected bond lengths (Å) and angles (degrees): Sn(1)-C(1) 2.166(3), Sn(1)-W(1) 2.7286(3), Sn(1)-C(24) 2.180(6), W(1)-C(20) 2.007(4), W(1)-C(21) 2.042(3), W(1)-C(22) 2.061(5), W(1)-C(23) 2.023(5), C(20)-O(20) 1.146(5), C(21)-O(21) 1.143(4), C(22)-O(22) 1.131(5), C(23)-O(23) 1.145(5), C(24)-C(25) 1.42(2); C(1)-Sn(1)-W(1) 135.13(8), C(1)-Sn(1)-C(24) 105.68(19), W(1)-Sn(1)-C(24) 118.68(18).

Insertion of ethylene, or propylene, into the Sn-H bond in **1** yielded compound **2** or **3**, respectively. The molecular structure of **2** shows little variation from the structure of **1**, as the tin atom in **2** remains three-coordinate. The Sn-C(alkyl) distance in **2** is 2.180(6) Å. This distance is comparable to the literature Sn-alkyl distances which range from 2.145(7) to 2.187(8) Å.[29, 38] The sum of the angles around tin is 359.5(2)°. The structure of **2** also displays coplanar coordination to the metal carbonyl fragment, where the C(1)-Sn(1)-alkyl unit is almost coplanar with that of tungsten and the three carbonyl groups. The Sn(1)-W(1) bond is almost co-linear with the carbonyl group C(20)-O(20) in trans position to the stannylene, 178.07(12)°.

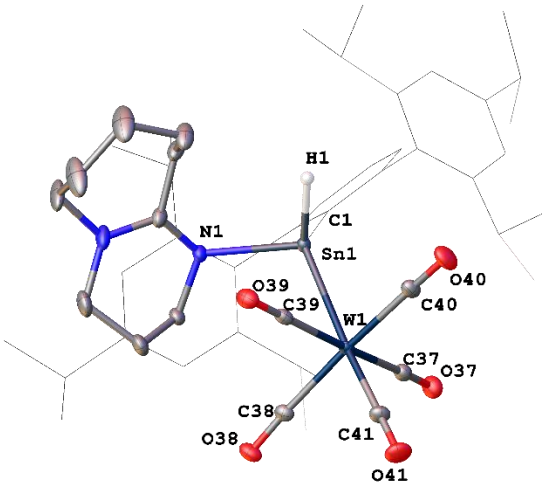

Figure 4.3: Solid-state molecular structure of **4** (Ar^{iPr6} substituent is shown as wireframe, and hydrogen atoms except for the tin bound H1, and ligand disorder are not shown for clarity). Thermal ellipsoids are shown at 30% probability. Selected bond lengths (Å) and angles (degrees): Sn(1)-C(1) 2.2031(18), Sn(1)-N(1) 2.2261(16), Sn(1)-W(1) 2.8063(2), Sn(1)-H(1) 1.68(3), W(1)-C(37) 2.046(2), W(1)-C(38) 2.023(3), W(1)-C(39) 2.024(2), W(1)-C(40) 2.043(2), W(1)-C(41) 1.983(2), C(37)-O(37) 1.142(3), C(38)-O(38) 1.147(3), C(39)-O(39) 1.148(3), C(40)-O(40) 1.141(3), C(41)-O(41) 1.155(3); C(1)-Sn(1)-W(1) 131.31(5), C(1)-Sn(1)-H(1) 101.6(9), C(1)-Sn(1)-N(1) 105.21(7), W(1)-Sn(1)-H(1) 111.7(9).

In the structures of **1**, **2**, and **4**, the average W-CO bond lengths of four carbonyls that are in cis positions relative to the stannylene ligand are slightly longer than those of the trans-positioned carbonyl group, suggesting a stronger π-backbonding for the trans W-CO bond. However, in the structure of **4**, the average bond length of W-CO for the four carbonyls that are in cis positions to the stannylene are slightly shortened to 2.034(3) Å, and the trans W-CO bond is shortened to 1.983(2) Å when compared to trans W-CO bonds in **1** and **2**. In turn, these bonds are comparable to the trans W-CO bond shortening with THF coordination in $Mo(CO)_5\{Sn(Ar^{iPr4})(THF)H\}$.[27] This is likely a result of the increased electron density at tungsten due to the coordination of dbu and disrupting of π-backbonding between the hydridostannylene and $W(CO)_5$, and therefore stronger π-backbonding between the tungsten atom and the trans carbonyl group. The Sn-W distances for **1**, **2**, and **4** range from 2.7150(2) Å to 2.8063(2) Å. These values are in close agreement with the sum of the covalent radii of Sn

(1.40 Å) and W (1.37 Å).[39] The Sn-W distances are comparable to the reported singly bonded stannylene-$W(CO)_5$ complexes.[24, 43-47] The Sn=W double bond in $[Cp_2W(H)=SnHAr^{iPr6}]^+$ was reported to be 2.6221(2) Å by Wesemann and coworkers,[25] in comparison to the Sn-W triple bonds[48] in stannylyne complexes, such as trans-$[Cl(dppe)_2W{\equiv}Sn\text{-}C_6H_3\text{-}2,6\text{-}Mes_2]$ and $[(dppe)_2W{\equiv}Sn\text{-}C_6H_3\text{-}2,6\text{-}Mes_2]^+[PF_6]^-$ (dppe = $Ph_2PCH_2CH_2PPh_2$, Mes = C_6H_2-2,4,6-Me_3) that were reported by Filippou and coworkers.[17-18] Nonetheless, the Sn-W distances reported here are shorter than those of metallostannylene complexes of tungsten such as $[Cp^*(CO)_3W\text{-}SnCl(Idipp)]$[49] (2.9514(4) Å) (Idipp = $C[N(C_6H_3\text{-}2,6\text{-}^iPr_2)CH]_2$) reported by Filippou and coworkers, or $Ar^{Me6}Sn\text{-}WCp(CO)_3$ (2.9107(10) Å) (Ar^{Me6} = -C_6H_3-2,6-(C_6H_2-2,4,6-Me_3)$_2$) and $Ar^{iPr6}Sn\text{-}WCp(CO)_3$ (2.9030(8) Å) reported by this group.[50-51]

NMR Spectroscopy. All ^1H, $^{13}C\{^1H\}$, and $^{119}Sn\{^1H\}$ NMR spectroscopic data are listed in greater detail in the Supporting Information. The solution ^1H NMR spectra of **1**-**4** displayed signals corresponding to the Ar^{iPr6} ligands with diastereotopic isopropyl methyl groups and septet methine proton signals, and showed small changes with respect to those reported for $Mo(CO)_5\{Sn(Ar^{iPr6})H\}$[27] or $\{Ar^{iPr6}Sn(\mu\text{-}H)\}_2$[10]. The Sn-H signal for **1** was observed at δ = 18.62 ppm. This is flanked by the $^{117/119}Sn$ satellites $^1J_{Sn\text{-}H}$ = 754 Hz, and coupling to tungsten ^{183}W, $^2J_{W\text{-}H}$ = 19 Hz, which is consistent with the Sn-H signal observed in the ^1H NMR spectrum of $Mo(CO)_5\{Sn(Ar^{iPr6})H\}$, δ = 18.00 ppm.[27] The chemical shift of the Sn-H signal and the observed coupling constant of **1** are in close agreement with the reported values for tantalum and tungsten coordinated hydridostannylenes, $[Cp_2W(H)=SnHAr^{iPr6}]^+[Al(OC\{CF_3\}_3)_4]$, δ = 15.13 ppm $^1J_{Sn\text{-}H}$ = 1040 Hz, and $^2J_{W\text{-}H}$ = 32 Hz, and $[Cp_2TaH_2\text{-}SnHAr^{iPr6}]^+[Al(OC\{CF_3\}_3)_4]^-$, δ = 15.55 ppm, and $^1J_{Sn\text{-}H}$ = 1165 Hz.[38] The Sn-H signal for **4** was observed at δ = 10.12 ppm, flanked by the respective $^{117/119}Sn$ satellites $^1J^{119}_{Sn\text{-}H}$ = 1093 Hz, $^1J^{117}_{Sn\text{-}H}$ = 1045 Hz, and ^{183}W $^2J_{W\text{-}H}$ = 12 Hz, which is much further upfield than the Sn-H signals for **1**, $Mo(CO)_5\{Sn(Ar^{iPr6})H\}$, and δ = 17.09 ppm for

$Mo(CO)_5\{Sn(Ar^{iPr4})(THF)H\}$.[27] Relevant species also includes the hydridostannylene complex, $Cp^*(^iPr_3P)(H)Os{=}SnH(trip)$ (trip = 2,4,6-triisopropylphenyl) with a resonance at δ=19.4 ppm, by Tilley and coworkers.[52] Compared to **1**, the upfield shift of the Sn-H signal in **4** can be attributed to the increased electron density at the tin atom due to dbu coordination at the tin atom, and that dbu is a better σ-donor than THF. The calculated ^{1}H NMR chemical shift of the Sn-H hydrogen of the hypothetical monomeric unit of $\{Ar^{iPr6}Sn(\mu\text{-}H)\}_2$ is δ=25.4 ppm,[53] and the reported chemical shifts of N-heterocyclic carbene (NHC) coordinated three-coordinate hydridostannylenes range from δ = 6.91 to δ = 7.23 ppm, with $^1J_{Sn\text{-}H}$ coupling constants of 192 Hz to 237 Hz.[14-15] In comparison to these NHC-coordinated hydridostannylenes, the Sn-H chemical shift of **4** can be explained by reduced electron density at the tin atom which should result in a downfield shift due to coordination of transition metal carbonyl moiety.[16] The chemical shift of Sn-H signal and coupling constant of **4** is comparable to the reported values for $L^2(H)Sn{\cdot}W(CO)_5$ (L^2 = 2-Et_2NCH_2-4,6-tBu_2-C_6H_2), δ = 10.25 ppm $^1J_{Sn\text{-}H}$ = 1091 Hz, and $^1J_{W\text{-}H}$ = 15.6 Hz, reported by Jambor and coworkers.[24] Diffusion-ordered spectroscopy (DOSY) ^{1}H NMR spectroscopy of **4** afforded a diffusion coefficient of 4.42×10^{-10} m^2/s, which suggested that no dissociation of the dbu molecule occurred in the C_6D_6 solution of **4**. The ^{1}H NMR spectrum of **2** showed broad resonances at δ = 0.89–1.09 ppm for the corresponding ethyl group, which agrees with the shifts from the ethyl group in the ^{1}H NMR spectrum of $\{Ar^{iPr6}Sn(\mu\text{-}Et)\}_2$ reported by this group.[29] The ^{1}H NMR spectra of **3** showed two broad resonances at δ = 0.80–0.91 ppm and δ = 1.23–1.29 ppm, separately, and a resolved triplet signal attributable to the two α-protons of the n-propyl group. One-dimensional nuclear Overhauser effect spectroscopy of ^{1}H NMR spectra of **2** and **3** with selective excitation of δ = 7.20–7.34 ppm showed transfer of nuclear spin polarization to the isopropyl substituents on the flanking rings due to the close contacts between these isopropyl groups and aromatic signals

on the central phenyl ring, therefore explaining NOE-coupled multiplets of aromatic signals in **2** and **3**.

The purity of the samples of **1**-**4** can be better represented by the $^{13}C\{^{1}H\}$ NMR spectra, in comparison to the ^{1}H NMR spectra, where restricted rotations and NOE-couplings were present throughout the structures of **1**-**4**. The $^{13}C\{^{1}H\}$ NMR spectra of **1**-**4** displayed two distinct chemical shifts for the carbonyl resonances in an approximate 1:4 ratio, which is consistent with their structural data (vide supra). The ^{13}C-$^{117/119}Sn$ coupling was not observed in all of the recorded $^{13}C\{^{1}H\}$ NMR spectra, while ^{13}C-^{183}W couplings were observed in the $^{13}C\{^{1}H\}$ NMR spectra of **1** and **3** for the four equatorial carbonyl groups. The ^{13}C-^{183}W coupling constants are $^{1}J_{W\text{-}C}$ = 122 Hz, and $^{1}J_{W\text{-}C}$ = 121 Hz for **1** and **3**, respectively, which is close to the reported values for $L^{2}(H)Sn{\cdot}W(CO)_5$ (L^{2} = 2-Et_2NCH_2-4,6-tBu_2-C_6H_2), $^{1}J_{W\text{-}C}$ = 122 Hz.[24] The 1:4 ratio of carbonyl resonances suggests free rotation around W-Sn bond in **1**-**4**. This suggests that hydridostannylene is a weak π-acceptor despite the presence of an empty p-orbital on the Sn atom, which is further demonstrated in calculations (vide infra). Compared to the $^{13}C\{^{1}H\}$ NMR spectrum of **1**, $^{13}C\{^{1}H\}$ NMR spectra of **2** and **3** showed additional signals attributable to the ethyl or n-propyl group coordinated at the tin atom which are similar to the reported values for tin-alkyls.[29, 38]

The $^{119}Sn\{^{1}H\}$ NMR spectra of **1**-**3** were recorded in C_6D_6 and referenced to the external standard $SnMe_4$ in $CDCl_3$. The ^{119}Sn signal of **1** appeared at δ = 1159 ppm, which is slightly further upfield than δ = 1324 ppm, the previously reported for $Mo(CO)_5\{Sn(Ar^{iPr6})H\}$.[27] The ^{119}Sn signal of **1** agrees well with the ^{119}Sn NMR chemical shift of $Cp_2M(Ar^{iPr6}SnH)_2$ (M = Ti, Zr, and Hf) complexes reported by Wesemann and coworkers, which ranged from 1060 to 1250 ppm.[26] The $^{119}Sn\{^{1}H\}$ NMR spectra of **2** and **3** displayed signals at δ = 1455 ppm, and δ = 1443 ppm, respectively. Unfortunately, no ^{119}Sn signal was

observed for **4**. Other reported ^{119}Sn chemical shifts of three-coordinate tin-transition metal complexes range from 673 to 1231 ppm.[45, 54-58]

IR spectroscopy. Compounds **1**-**4** were further characterized by FT-IR spectroscopy. Compounds **1**-**3** displayed ν_{CO} stretching bands that agree well with the previously reported complexes,[27] showing a characteristic pattern for a [LM(CO)$_5$] species.[59] Compared to **1**, FT-IR spectra of **2** and **3** showed similar ν_{CO} stretching bands, and disappearance of the weak absorption at 1757 cm^{-1} attributed to the Sn-H stretching frequencies, as a result of olefin insertion reaction into the Sn-H bond. However, the FT-IR spectrum of **4** displayed slightly different ν_{CO} stretching bands, 2050 cm^{-1} (m), 1963 cm^{-1} (m), 1916 cm^{-1} (s), and 1887 cm^{-1} (vs), and a weak absorption at 1793 cm^{-1} for the Sn-H stretching. DFT calculations suggest similar stretching frequencies of Sn-H to the experimental values (see SI). The FT-IR spectrum of **4** is in close agreement with the values of L^2(H)Sn·W(CO)$_5$ (L^2 = 2-Et$_2$NCH$_2$-4,6-tBu$_2$-C$_6$H$_2$) (2056, 1937, 1915, 1889 (CO), and 1781 cm^{-1}(Sn-H)), reported by Jambor and coworkers.[24] The observed Sn-H stretching frequencies can also be compared to the reported values of the bridged-hydride Sn(II) species, {Ar^{iPr6}Sn(μ-H)}$_2$ (ν_{Sn-H}=1828, and 1771 cm^{-1}), which are due to the asymmetric isomeric {Ar^{iPr6}SnSn(H)$_2$Ar^{iPr6}},[10, 20] and terminally bound tin hydride species reported by Roesky and coworkers, as well as to [{HC(CMeNAr)$_2$}SnH] (Ar = 2,6-iPr$_2$C$_6$H$_3$) ν_{Sn-H}= 1849 cm^{-1},[11] [{2,6-iPr$_2$C$_6$H$_3$NCMe}$_2$C$_6$H$_3$SnH] ν_{Sn-H}= 1826 cm^{-1},[12] and Cp$_2$M(Ar^{iPr6}SnH)$_2$ (M = Ti, Zr, and Hf) complexes reported by Wesemann and coworkers, with ν_{Sn-H} ranging from 1741 to 1749 cm^{-1}.[26]

Computational Analyses. The structures of **1**, **2** and **4** were further probed computationally at the DFT level of theory and greater details are listed in the supporting information. Overall, the calculated gas-phase structures agreed well with the solid-state molecular structures of **1**, **2**, and **4**. In more detail, we investigated the potential reaction pathways for the ethylene insertion to complex **1** (Figure 4.4a), the limited hydrosilylation

reaction of **2** (Figure 4.4b) and the dbu adduct formation **4** (Figure 4.5). First, for the ethylene insertion to **1**, it is suggested that the reaction proceeds via the initial face-on coordination of the olefin to the tin atom in **1**, the transition state for this insertion was found to be 17.1 kcal/mol. The ethylene inserted product **2** was then found to be 17.4 kcal/mol more stable than the starting materials **1** and C_2H_4, and therefore the overall reaction is exergonic which agrees well with the experimental findings.

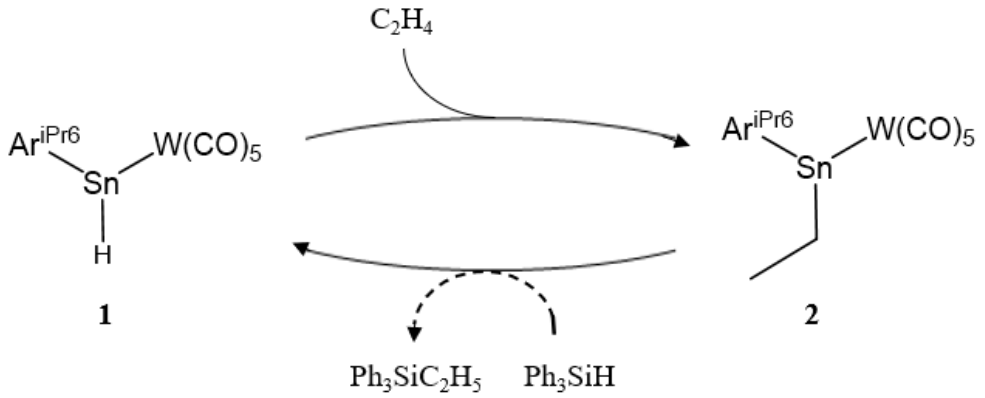

Scheme 4.3. Hypothetical Catalytic Hydrosilylation of Ethylene with **1**

We investigated the catalytic potential of **1** towards hydrogenation of ethylene using NMR spectroscopy and DFT calculations, as **1** readily effects facile hydrostannylation of ethylene. Initial attempts using dihydrogen gas as the hydrogen source in the regeneration of **1** were unsuccessful, however, using phenylsilane as the hydrogen source resulted in limited conversion of **2** to **1**. The ^{1}H and $^{29}Si\{^{1}H\}$ NMR spectra of the mixture of **2** and phenylsilane showed signals attributable to the unreacted species, 5 min after mixing the reagents in the glove box. After 72 h at ca. 65 °C, the ^{1}H NMR spectrum indicated limited conversion of **2** to **1**, as evidenced by the appearance of the 18.62 ppm signal of the Sn-H in **1**. The $^{29}Si\{^{1}H\}$ NMR spectrum of the reaction mixture showed only a signal for phenylsilane even after heating for 72 h at ca. 65 °C. The DFT calculations suggest that the rate determining step in this transformation is the metathesis reaction between Sn-C/Si-H bond for which there is an energy

barrier of 71.3 kcal/mol, despite the overall reaction being exergonic, albeit by just 4.9 kcal/mol. Taken together the high barrier and close to thermoneutral reaction energetics, it is not surprising that the experimental conversion is limited.

Finally, the reaction of **1** with dbu was also investigated computationally. Previously, both proton abstraction and coordination reactions have been reported to occur for dbu.[22, 60-62] However, in the case of **1** with dbu, coordination of dbu to the tin atom in **1** was the sole reaction observed both structurally and spectroscopically. DFT calculations suggest that the proton abstraction in this system is overall endergonic by 3.9 kcal/mol (compared to the free reagents **1** and dbu), yet the coordination reaction is overall exergonic by -14.3 kcal/mol. In addition, the proton abstraction transition state is at 25.4 kcal/mol (compared to the adduct **4**), therefore favoring the coordination product instead of proton abstraction.

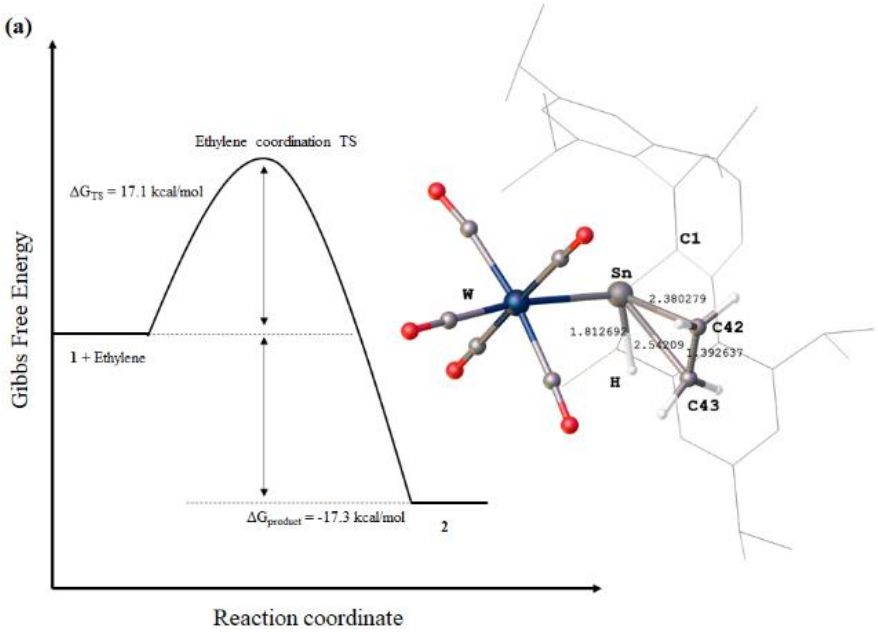

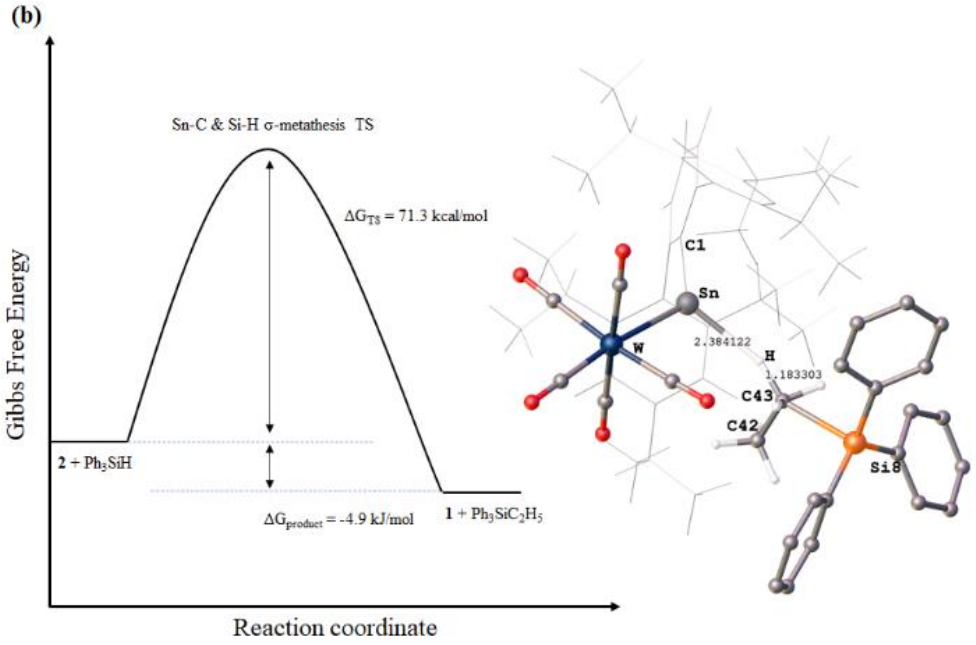

Figure 4.4: (a) DFT calculated reaction coordinate diagram of **1** + C_2H_4, with calculated gas-phase structure of the transition state; Ar^{iPr6} is shown as wireframe. (b) DFT calculated reaction coordinate diagram of **2** + Ph_3SiH, with calculated gas-phase structure of the transition state; Ar^{iPr6} is shown as wireframe.

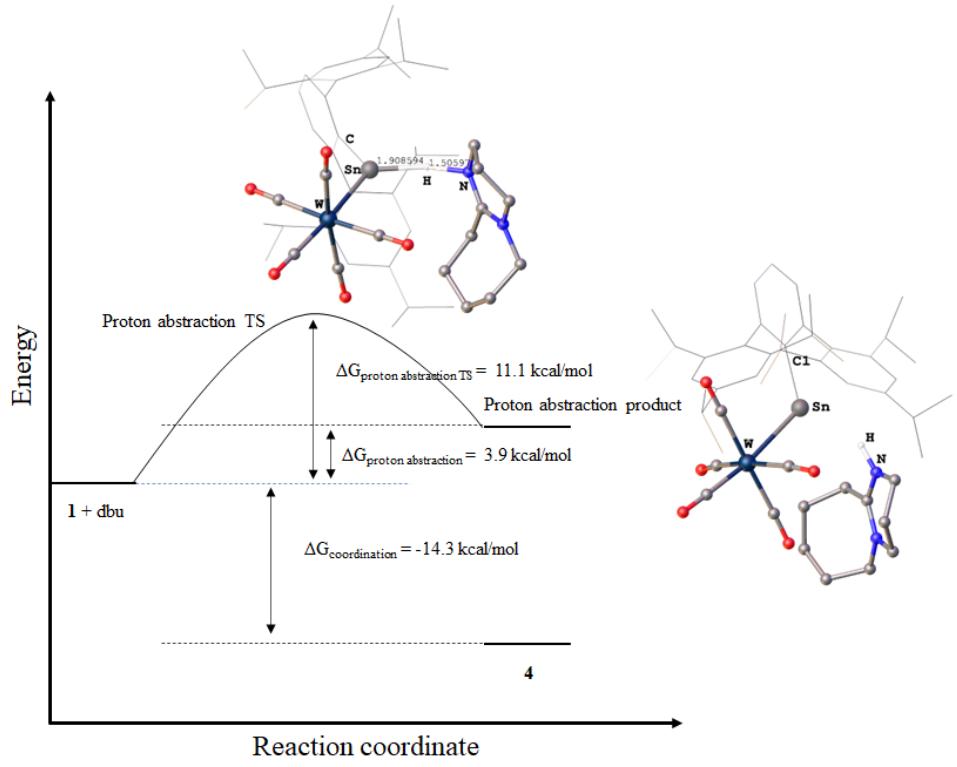

Figure 4.5: DFT calculated reaction coordinate diagram of **1** + dbu, with the calculated gas-phase structure of the transition state for proton abstraction, and calculated gas-phase structure of the proton abstraction products; Ar^{iPr6} is shown as wireframe.

4.4 Conclusions

Herein, we reported the synthesis of $W(CO)_5\{Sn(Ar^{iPr6})H\}$ (**1**) via a reaction of $\{Ar^{iPr6}Sn(\mu\text{-}H)\}_2$ with $[W(CO)_5(THF)]$. Compound **1** effects facile hydrostannylation of ethylene, or propylene, which yielded $W(CO)_5\{Sn(Ar^{iPr6})(Et)\}$, (**2**), or $W(CO)_5\{Sn(Ar^{iPr6})(^nPr)\}$, (**3**). The addition of dbu, a weakly-nucleophilic base, to a solution of **1** afforded the Lewis acid-base complex $[(Ar^{iPr6})(H)Sn(dbu)\text{-}W(CO)_5]$, (**4)**, which demonstrated the Lewis acidic nature of the Sn atom in **1**. Investigation of the catalytic potential of **1** towards ethylene hydrosilylation by reacting **2** with $PhSiH_3$ in C_6D_6 at elevated temperature revealed limited conversion of **2** to **1**, which was monitored by NMR spectroscopy. DFT calculations suggest that the mechanism of hydrostannylation reactions proceed via olefin insertion into the Sn-H bond by coordination of the olefin at the tin atom. The limited conversion in reaction of **2** with $PhSiH_3$ in C_6D_6 can be associated with that the calculated rate-determining step is the metathesis reaction between Sn-C/Si-H bond with an energy barrier of 71.3 kcal/mol.

4.5 Supporting Information

Computational details. The geometry optimizations were done with Gaussian16 Rev.C.01[63] using PBE1PBE[64-66] hybrid exchange functional and Def2-TZVP basis set.[67,68] For W and Sn ECPs were used. In addition, Grimme's empirical dispersion correction (GD3BJ)[69] and ultrafine integration grid were applied. Full frequency calculations were performed to ensure the identities of the stationary points found on the potential energy surface (no

imaginary frequencies for minima and one for transition states). Calculations were done in gas phase and energies represent the relative Gibbs free energies.

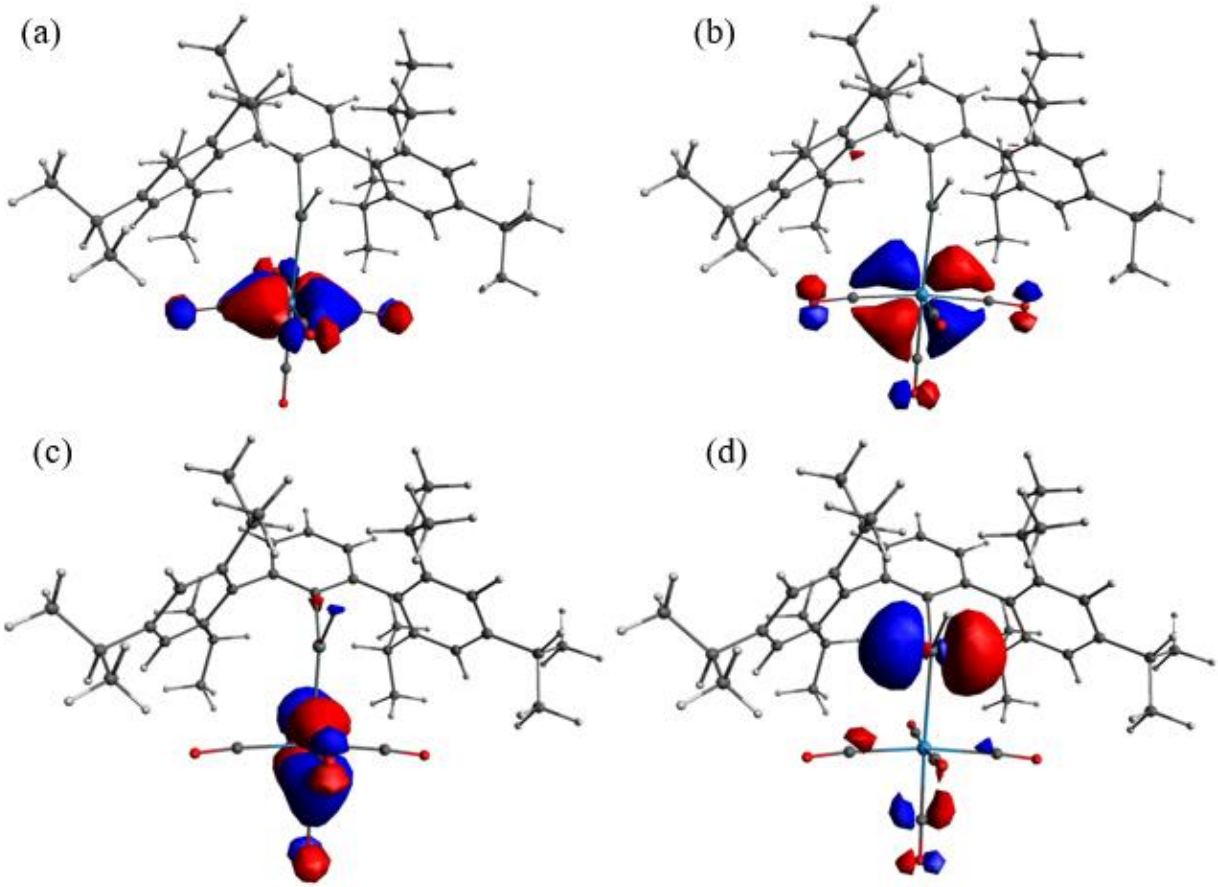

Figure 4.S1: Calculated HOMO-2 (a), HOMO-1 (b), HOMO (c) and LUMO (d) of **1**. Isosurface value set at ±0.05 a.u.

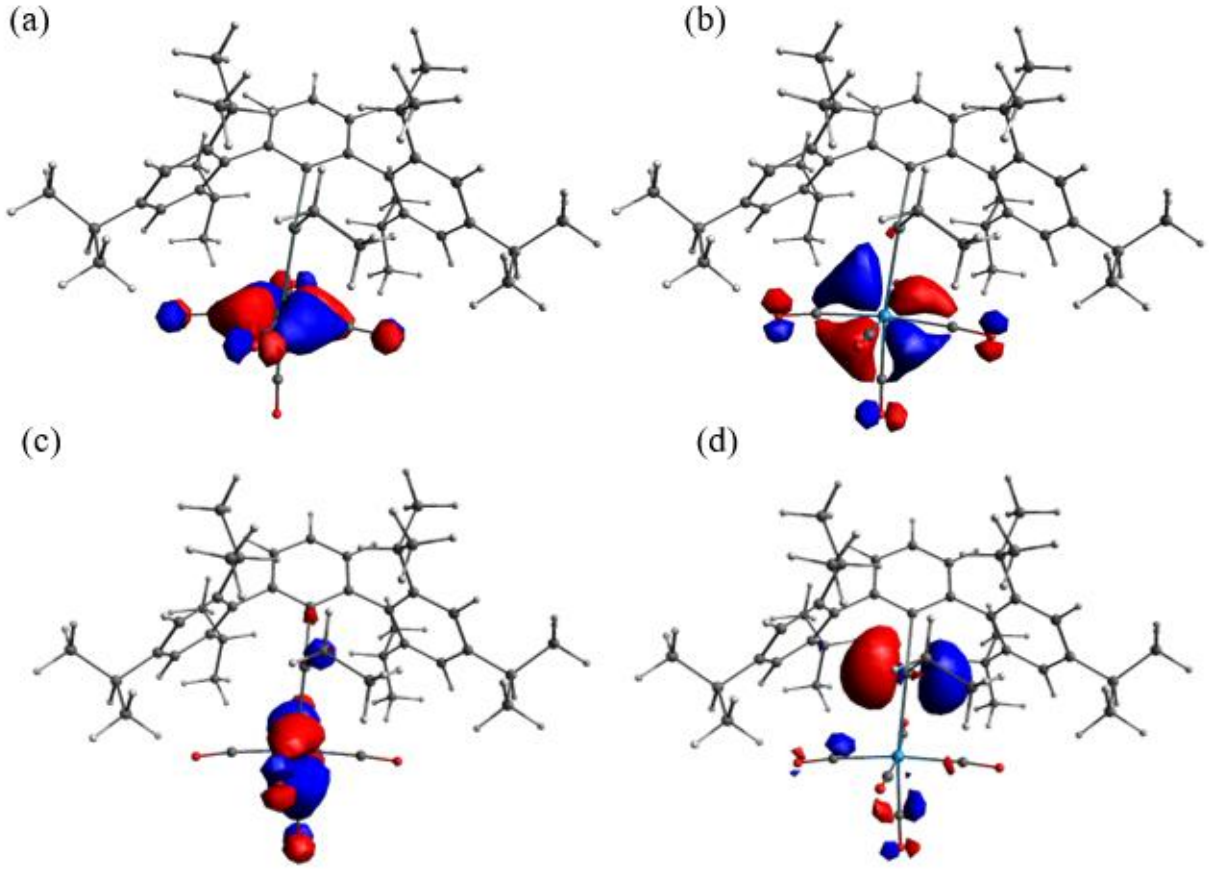

Figure 4.S2: Calculated HOMO-2 (a), HOMO-1 (b), HOMO (c) and LUMO (d) of **2**. Isosurface value set at ±0.05 a.u.

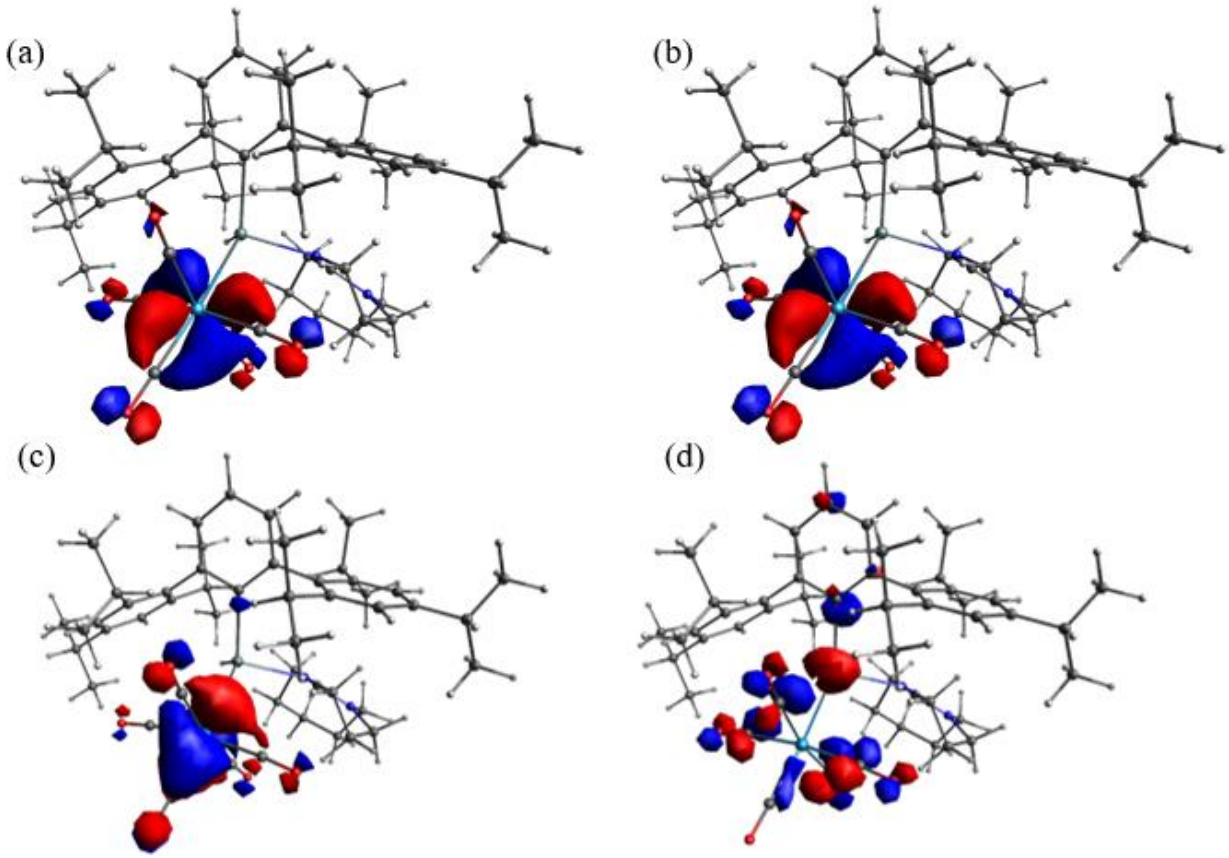

Figure 4.S3: Calculated HOMO-2 (a), HOMO-1 (b), HOMO (c) and LUMO (d) of **4**. Isosurface value set at ±0.05 a.u.

Compound	**1**	**2**	**4**
HOMO (eV)	-6.308 (W d-orbital)	-6.192	-5.800
LUMO (eV)	-2.262 (Sn empty p-orbital)	-2.061	-0.969 (CO π*-orbitals)
HOMO-LUMO gap (eV)	4.046	4.131	4.831
Mulliken charge W	-0.085141	-0.102010	-0.010447
Mulliken charge Sn	0.615324	0.877780	0.434631
UV-Vis			
HOMO-LUMO transition	430 nm (f = 0.0001)	417 nm (f = 0.0001)	351 nm (f = 0.0001) (multiple transitions)
HOMO-x – LUMO	388.90 nm (f = 0.0042) (HOMO-1 and HOMO-2 to LUMO)	375.16 nm (f = 0.0019) (HOMO-1 and HOMO-2 to LUMO)	
IR frequencies(scaled by 0.95)[70]			
Sn-H (cm^{-1})	1731		1777
W-CO (cm^{-1})	1948, 1954, 1963, 1983, 2057	1941, 1944, 1957, 1974, 2050	1911, 1922, 1941, 1961, 2042

Table 4.S1: Computational data for optimized structures **1**, **2**, and **4**

Reaction mechanisms

	Gibbs free energy G (a.u.)	ΔG (kJ/mol)	ΔG (kcal/mol)
1	-2248.0208		
ethylene	-78.485167		
1+ethylene	-2326.5059	0	0
TS	-2326.4787	71.5	17.1
product **2**	-2326.5336	-72.6	-17.4

Table 4.S2: Transition state energy calculation for **1** + ethylene → **2**

	G (a.u.)	ΔG (kJ/mol)	ΔG (kcal/mol)
2	-2326.5336		
Ph_3SiH	-984.16213		
2+ Ph_3SiH	-3310.69569	0	0
TS	-3310.5819	298.6	71.4
product 1+ $Ph_3Si(CH_2CH_3)$	-3310.70359	-20.7	-4.9

Table 4.S3: Transition state energy calculation for **2** + Ph_3SiH → **1** + $Ph_3Si(CH_2CH_3)$

	G (a.u.)	ΔG (kJ/mol)	ΔG (kcal/mol)
1	-2248.0208		
DBU	-461.52206		
1+DBU	-2709.54281	0	0
4	-2709.5656	-59.9	-14.3
TS	-2709.5251	106.3	25.4
Proton abstraction product	-2709.5365	76.4	18.3

Table 4.S4: Transition state energy calculation for **1** + DBU → **4**

Compound	**1**	**2**	**4**
Empirical formula	$C_{41}H_{50}WO_5Sn$	$C_{43}H_{54}WO_5Sn$	$C_{50}H_{66}WN_2O_5Sn$
Formula weight	923.35	953.40	881.45
Temperature	90(2) K	190(2) K	90(2) K
Wavelength	0.71073 Å	0.71073 Å	0.71073 Å
Crystal system	Monoclinic	Orthorhombic	Monoclinic

Space group	$P2_1/n$	Pnma	$P2_1/c$
Crystal color and habit	Yellow block	Yellow block	Colorless block
a(Å)	15.6352(9)	14.6411(10)	13.1439(10)
b(Å)	17.9970(10)	18.7801(13)	19.0998(14)
c(Å)	15.7333(9)	15.4255(11)	19.3889(14)
α(°)	90	90	90
β(°)	115.4750(7)	90	94.5851(19)
γ(°)	90	90	90
Density (calculated) (Mg/m^3)	1.538	1.493	1.475
F(000)	1840	1904	2176
Crystal size(mm^3)	0.420 x 0.400 x 0.186	0.328 x 0.294 x 0.178	0.244 x 0.190 x 0.163
θ range(°)	1.826 to 30.737°	1.708 to 27.540°	1.925 to 30.631°
Reflections collected	47481	26245	56450
Independent reflections	12433 [R(int) = 0.0223]	5022 [R(int) = 0.0239]	14892 [R(int) = 0.0181]
Observed reflections ($I > 2\sigma(I)$)	10630	4455	13646
Completeness to $2\theta = 25.242°$	99.9 %	100.0 %	99.9 %
Goodness-of-fit on F^2	1.050	1.052	1.091
Final R indices ($I>2\sigma(I)$)	R1 = 0.0225, wR2 = 0.0518	R1 = 0.0233, wR2 = 0.0541	R1 = 0.0218, wR2 = 0.0478
R indices (all data)	R1 = 0.0289, wR2 = 0.0545	R1 = 0.0284, wR2 = 0.0564	R1 = 0.0250, wR2 = 0.0492

Table 4.S5: Selected X-ray Crystallographic data for **1**, **2**, and **4**.

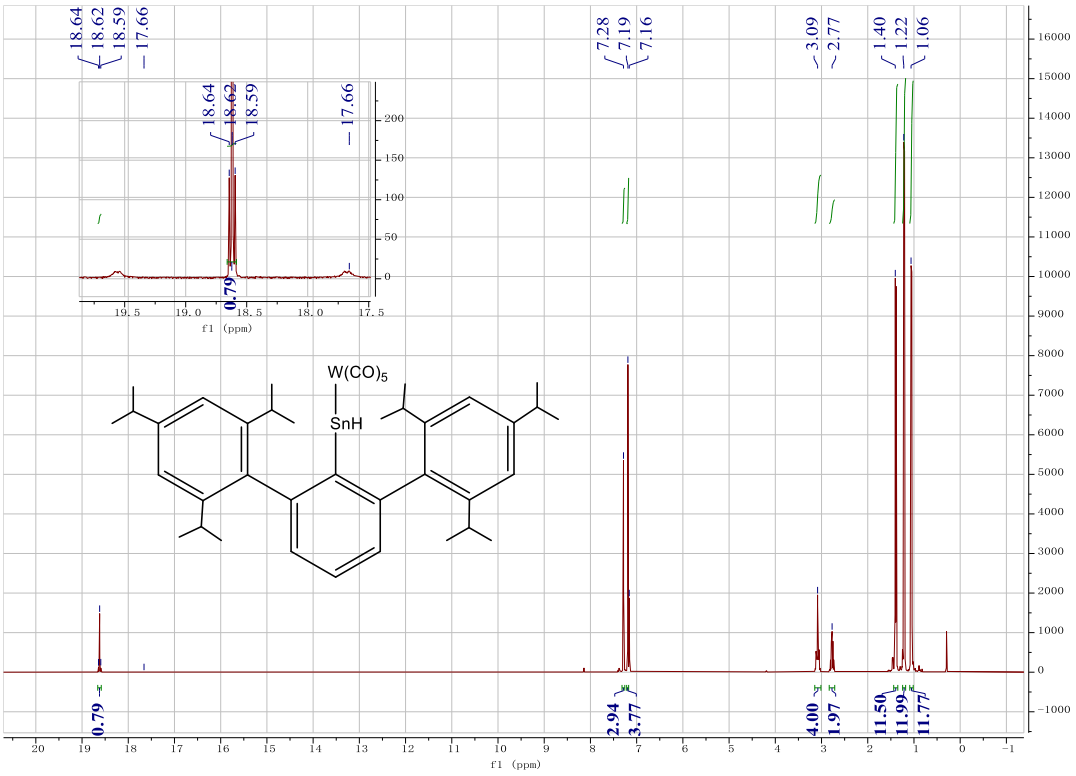

Figure 4.S4: ^{1}H NMR spectrum of **1** in C_6D_6 at 298K.

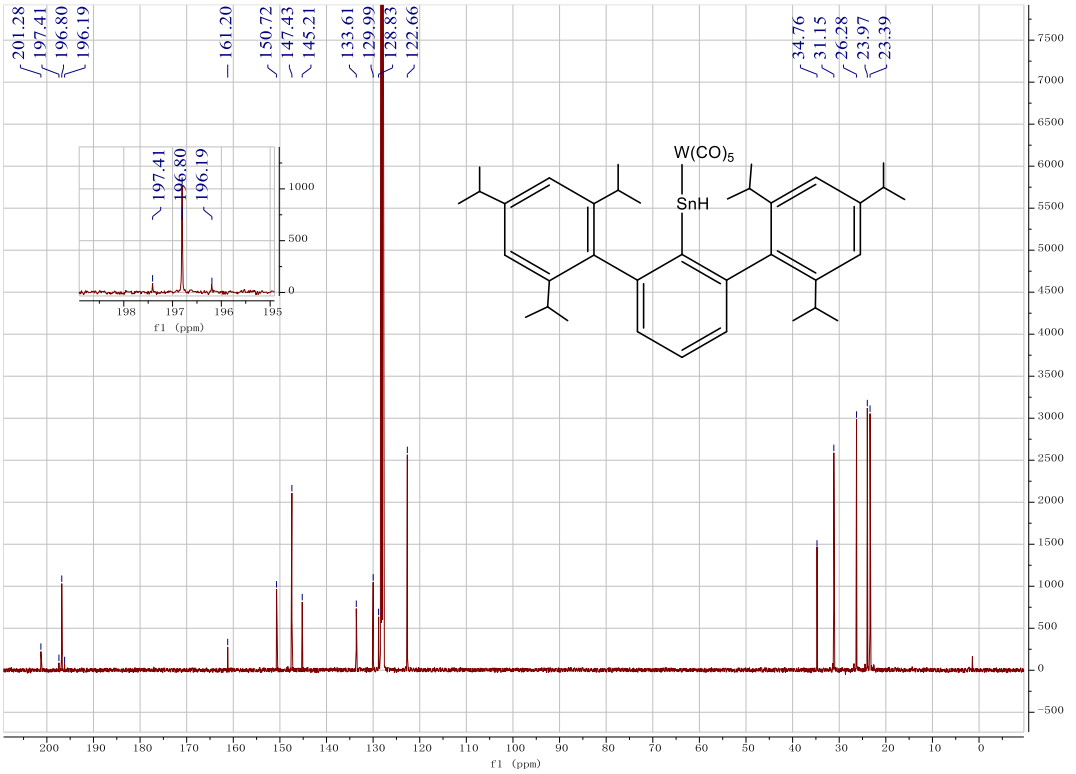

Figure 4.S5: $^{13}C\{^{1}H\}$ NMR spectrum of **1** in C_6D_6 at 298K.

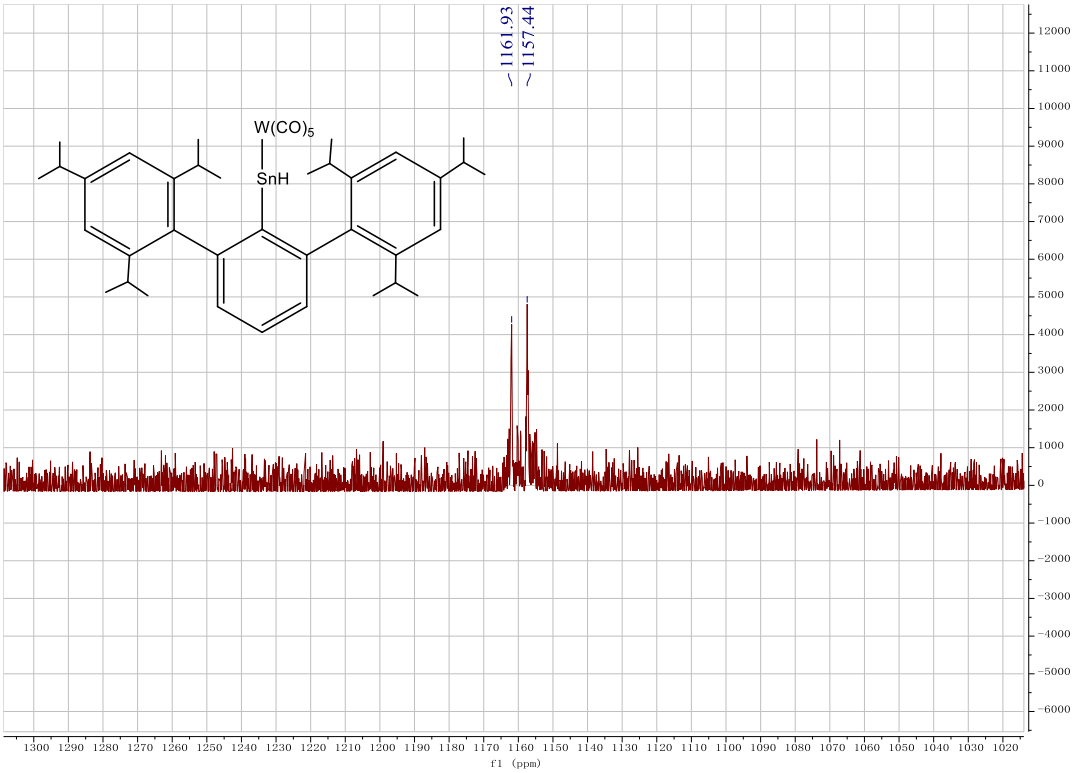

Figure 4.S6: $^{119}Sn\{^{1}H\}$ NMR spectrum of **1** in C_6D_6 at 298K.

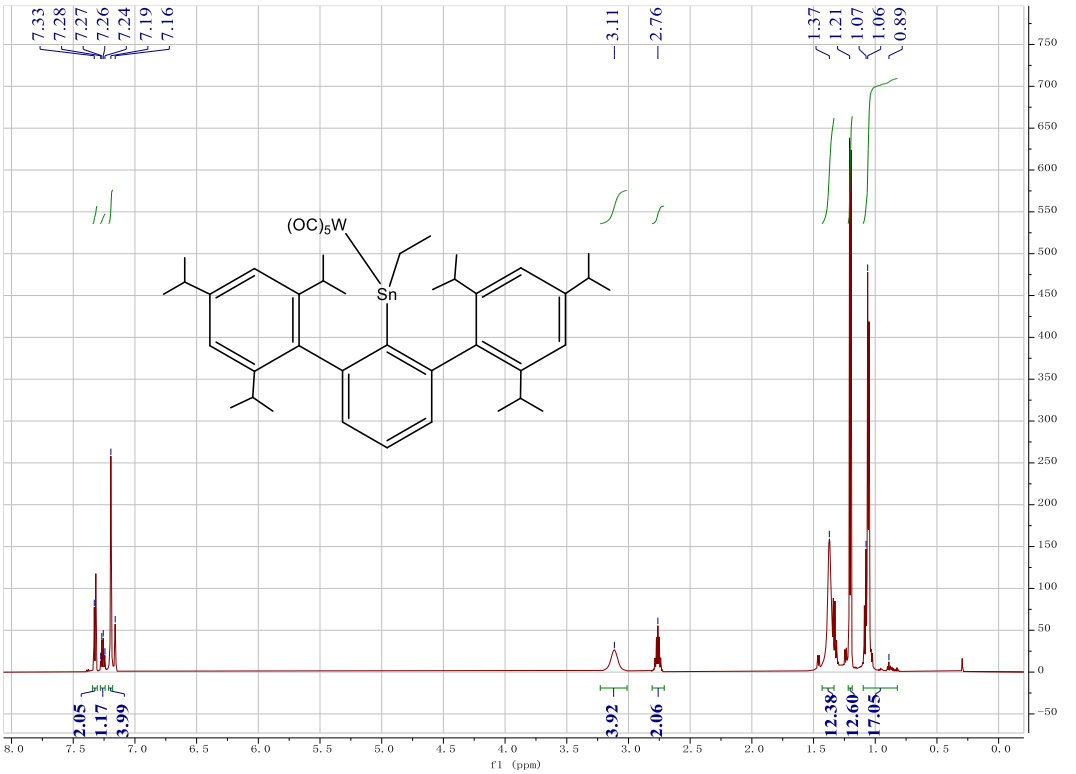

Figure 4.S7: ^{1}H NMR spectrum of **2** in C_6D_6 at 298K.

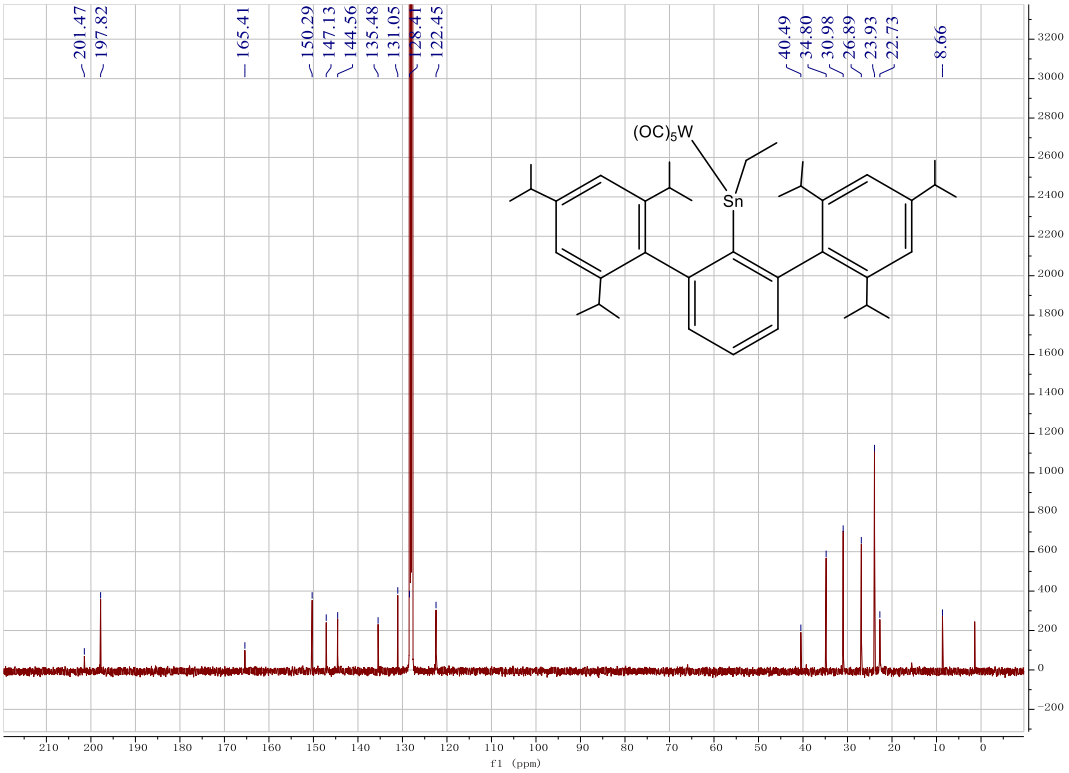

Figure 4.S8: $^{13}C\{^{1}H\}$ NMR spectrum of **2** in C_6D_6 at 298K.

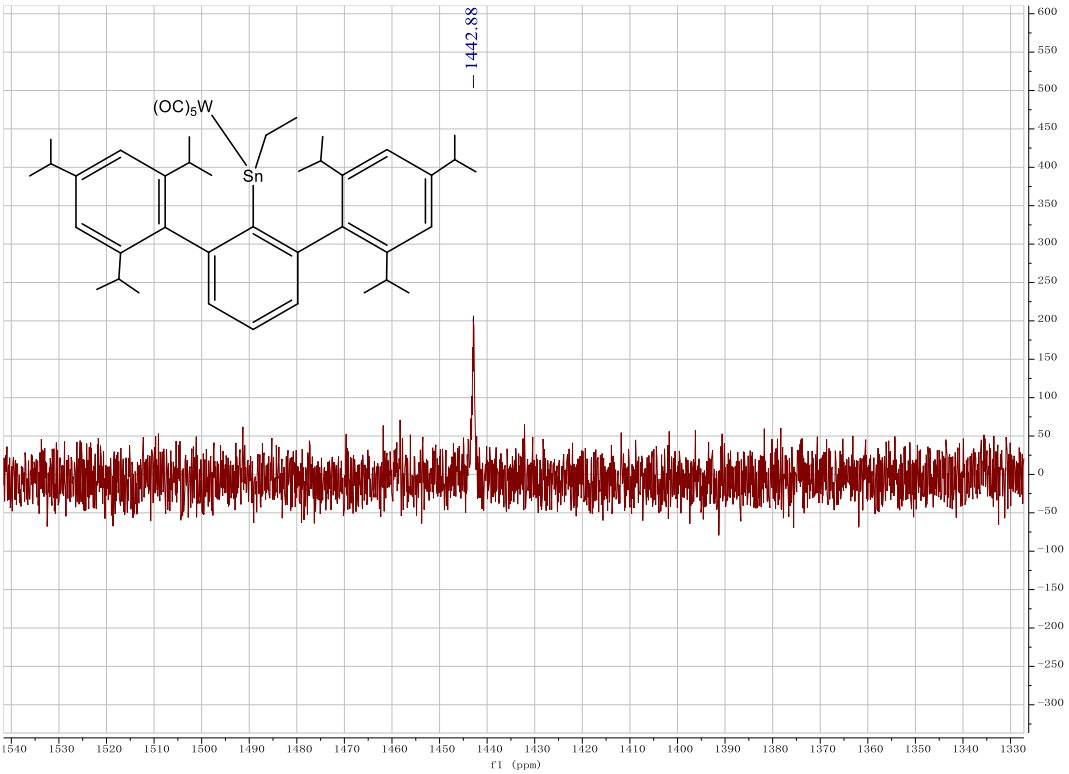

Figure 4.S9: $^{119}Sn\{^{1}H\}$ NMR spectrum of **2** in C_6D_6 at 298K.

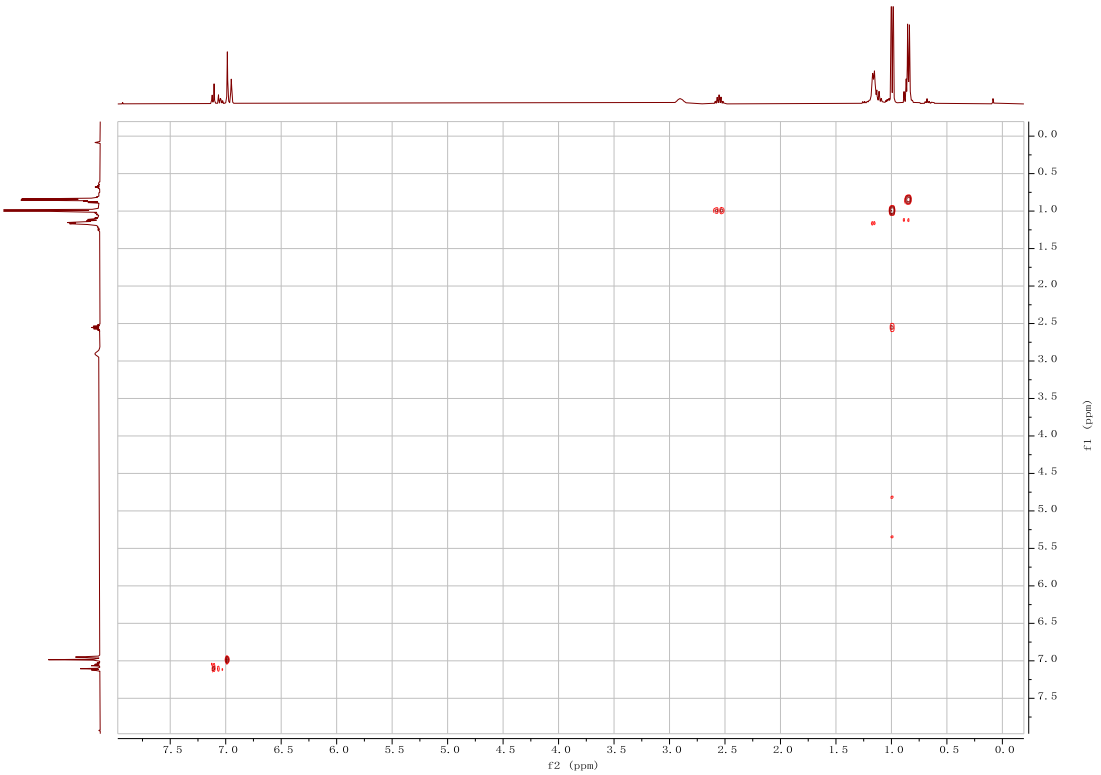

Figure 4.S10: ^{1}H-^{1}H COSY NMR spectrum of **2** in C_6D_6 at 298K.

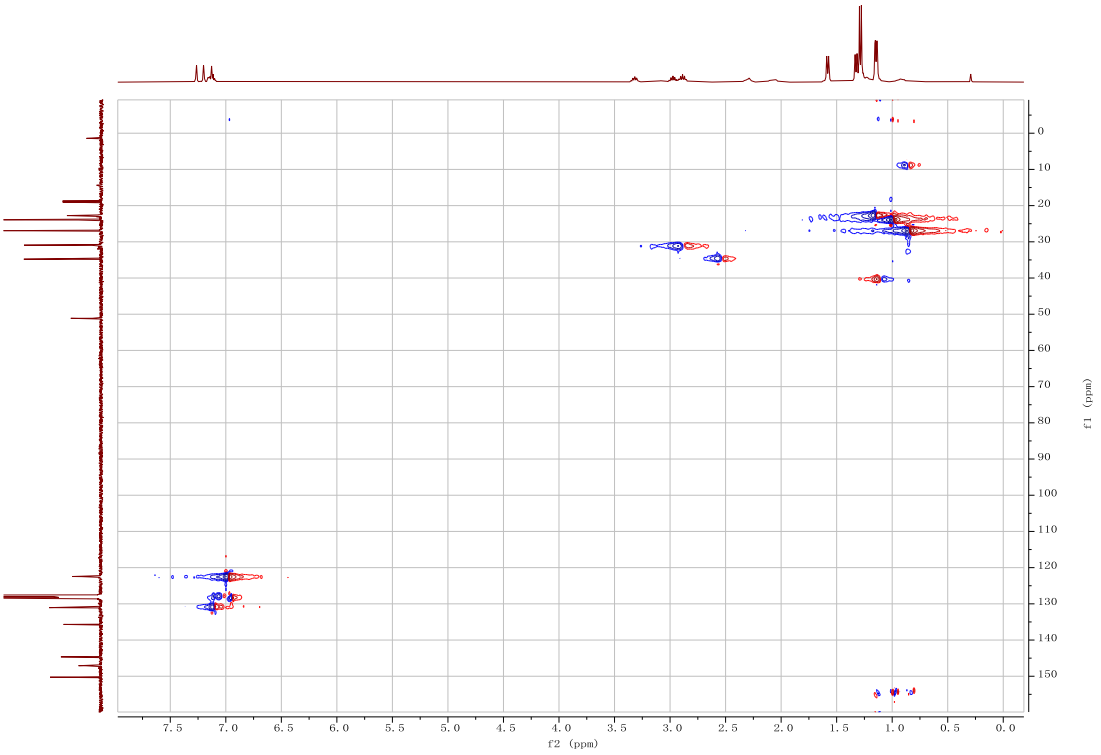

Figure 4.S11: ^{1}H-^{13}C HSQC NMR spectrum of **2** in C_6D_6 at 298K.

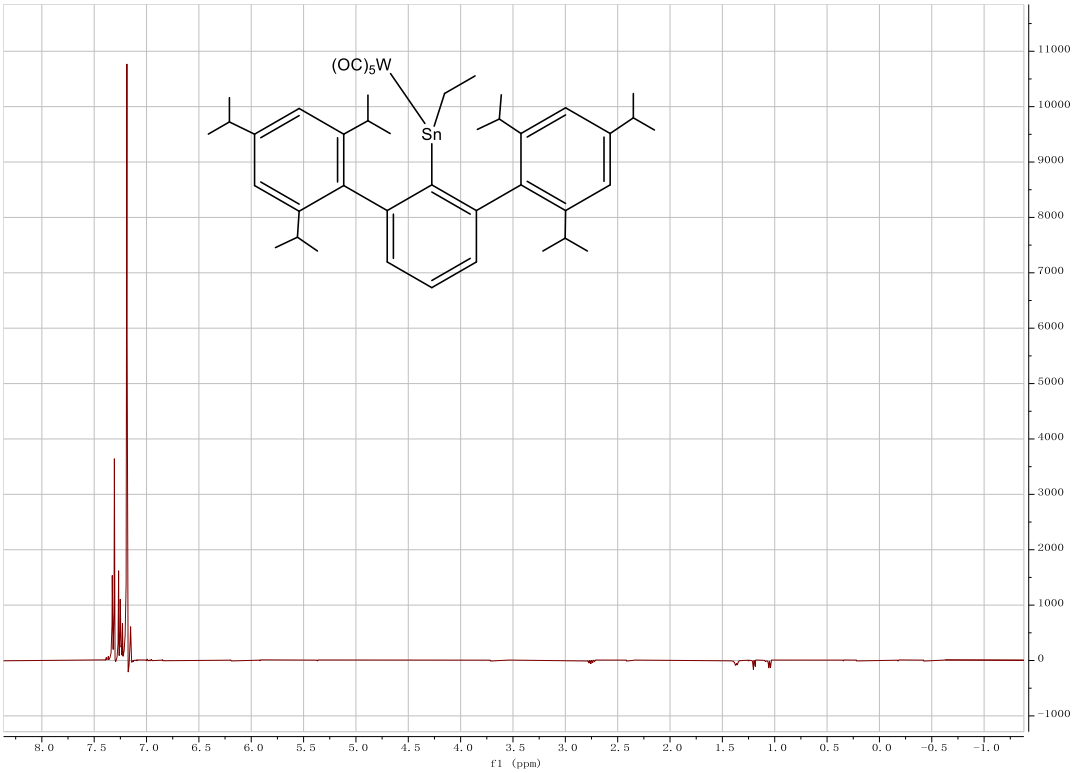

Figure 4.S12: 1D ^{1}H NOESY NMR spectrum of **2** in C_6D_6 at 298K.

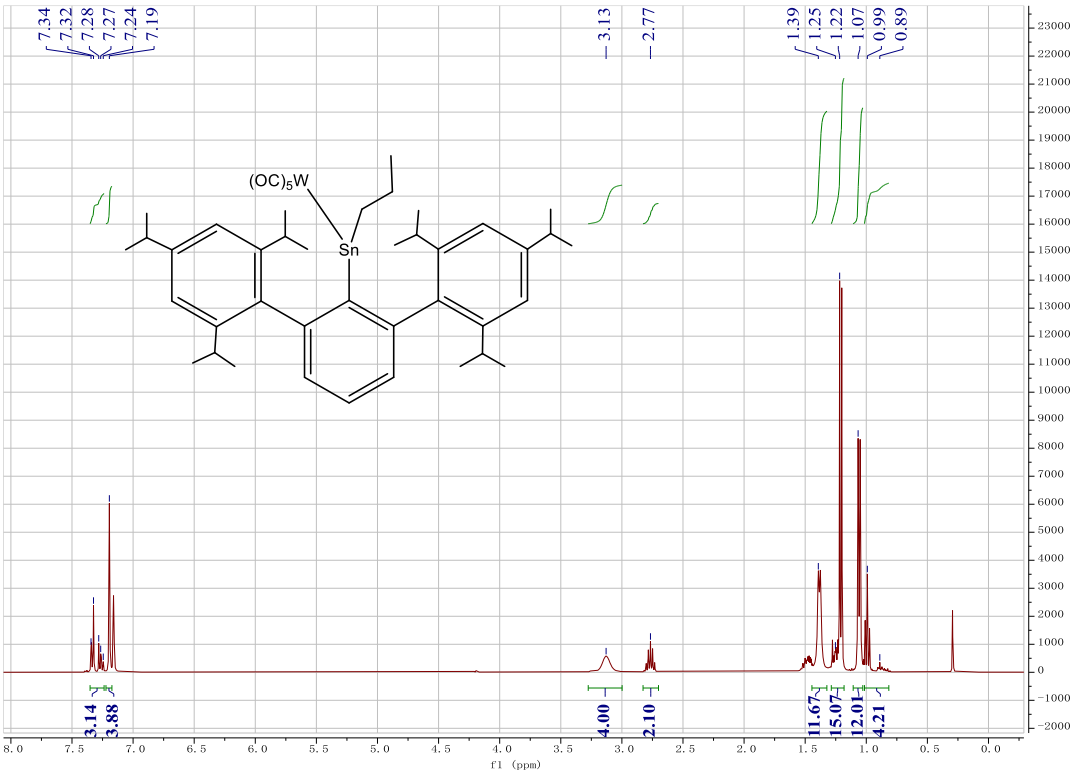

Figure 4.S13: ^{1}H NMR spectrum of **3** in C_6D_6 at 298K.

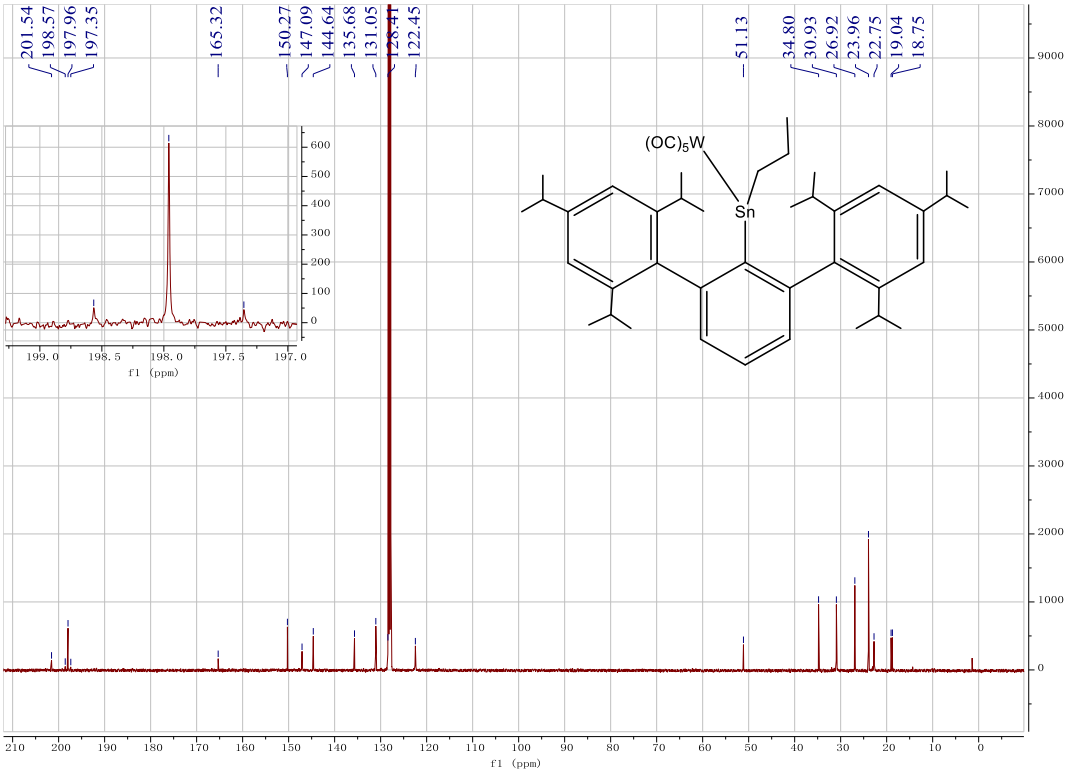

Figure 4.S14: $^{13}C\{^{1}H\}$ NMR spectrum of **3** in C_6D_6 at 298K.

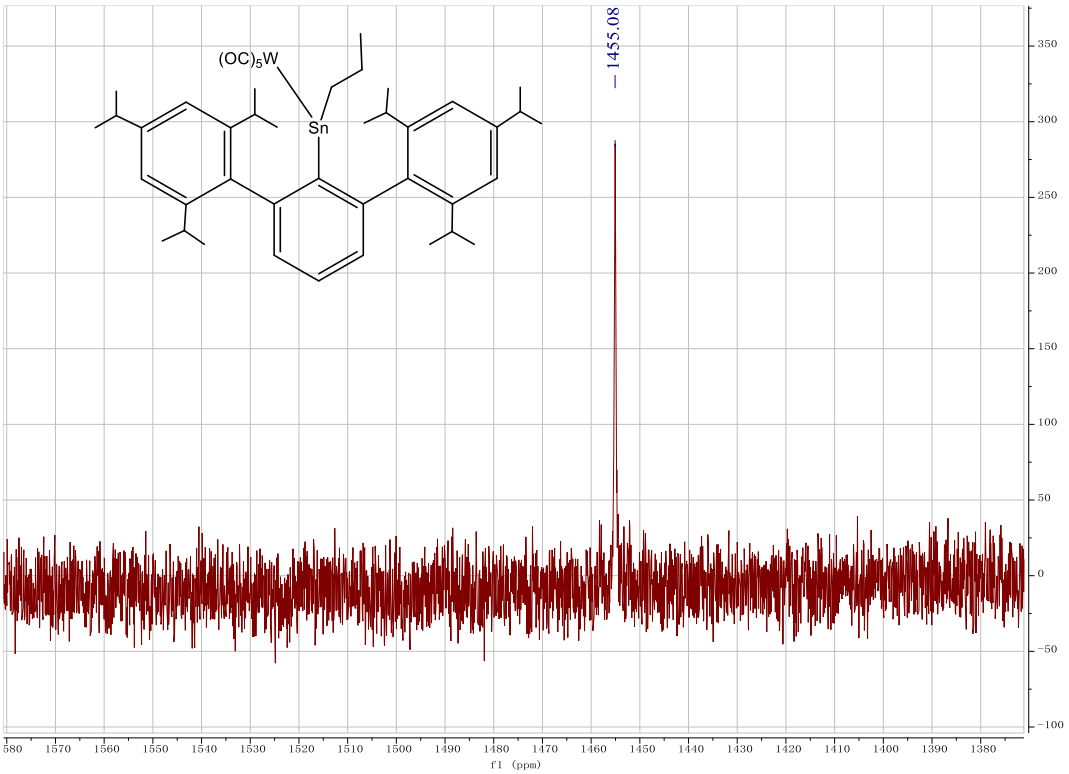

Figure 4.S15: $^{119}Sn\{^{1}H\}$ NMR spectrum of **3** in C_6D_6 at 298K.

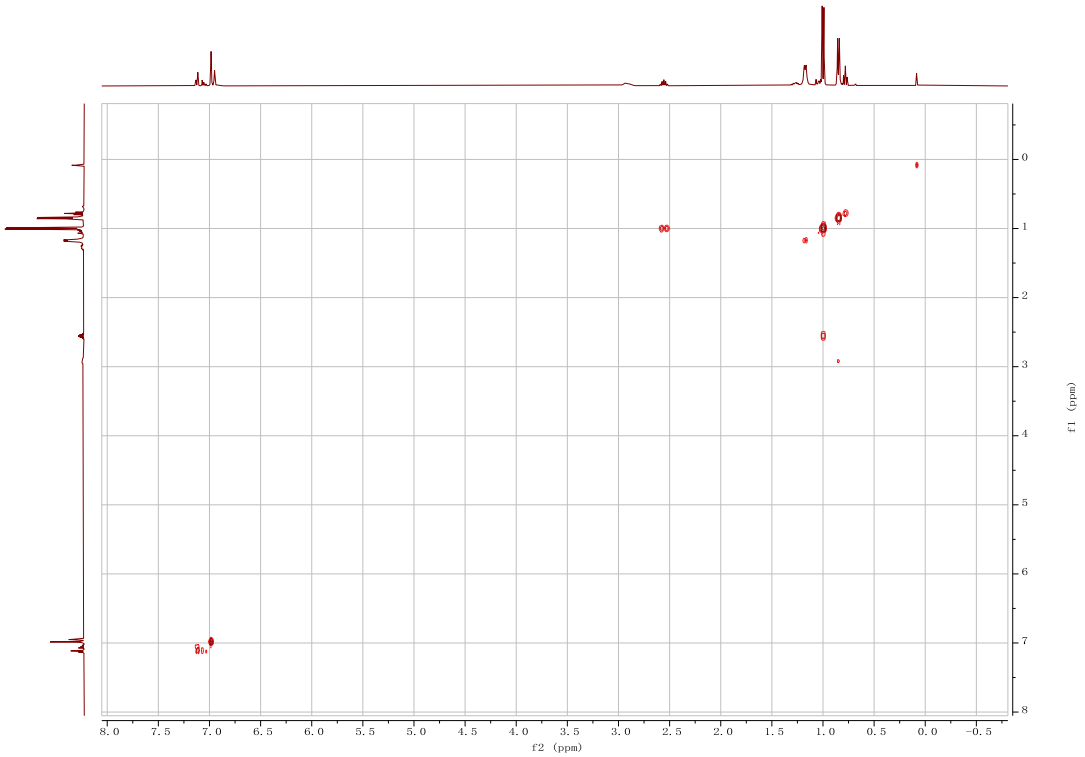

Figure 4.S16: ^{1}H-^{1}H COSY NMR spectrum of **3** in C_6D_6 at 298K.

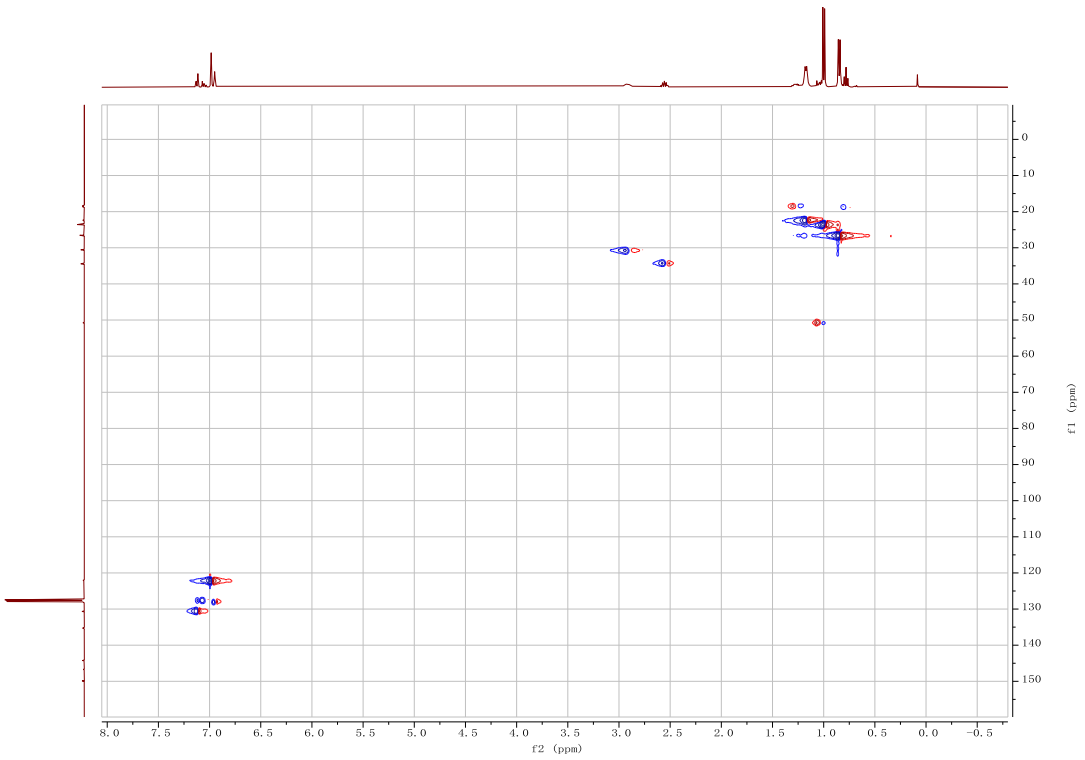

Figure 4.S17: ^{1}H-^{13}C HSQC NMR spectrum of **3** in C_6D_6 at 298K.

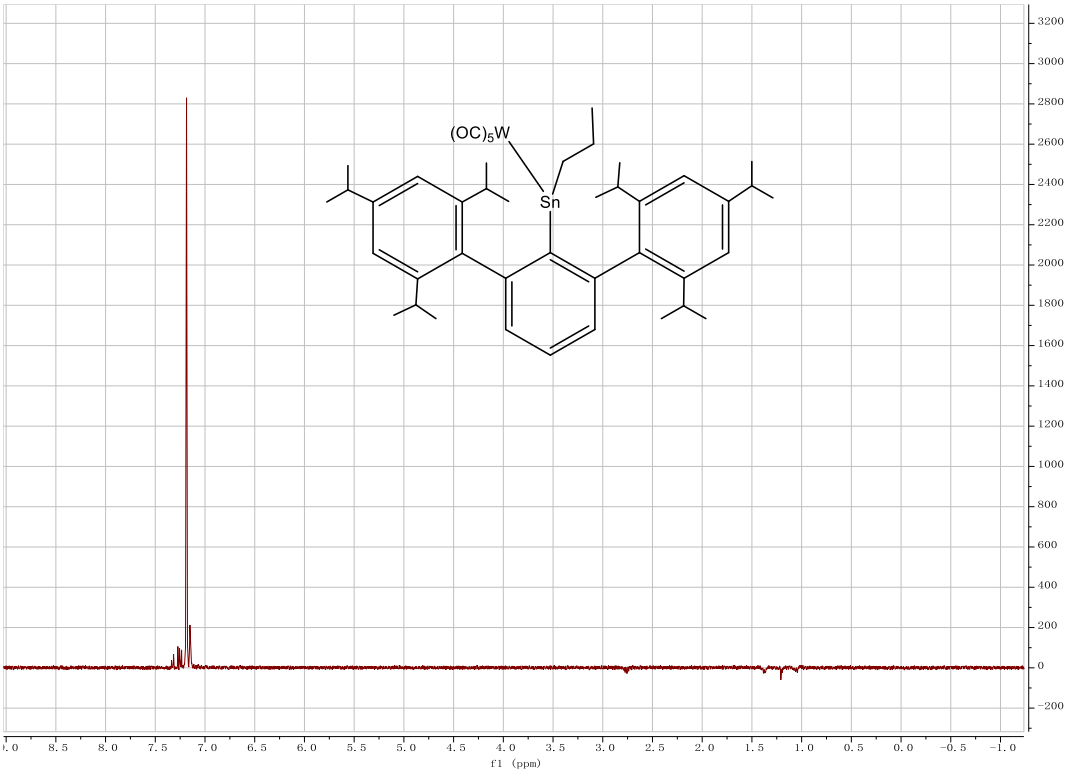

Figure 4.S18: 1D ^{1}H NOESY NMR spectrum of **3** in C_6D_6 at 298K.

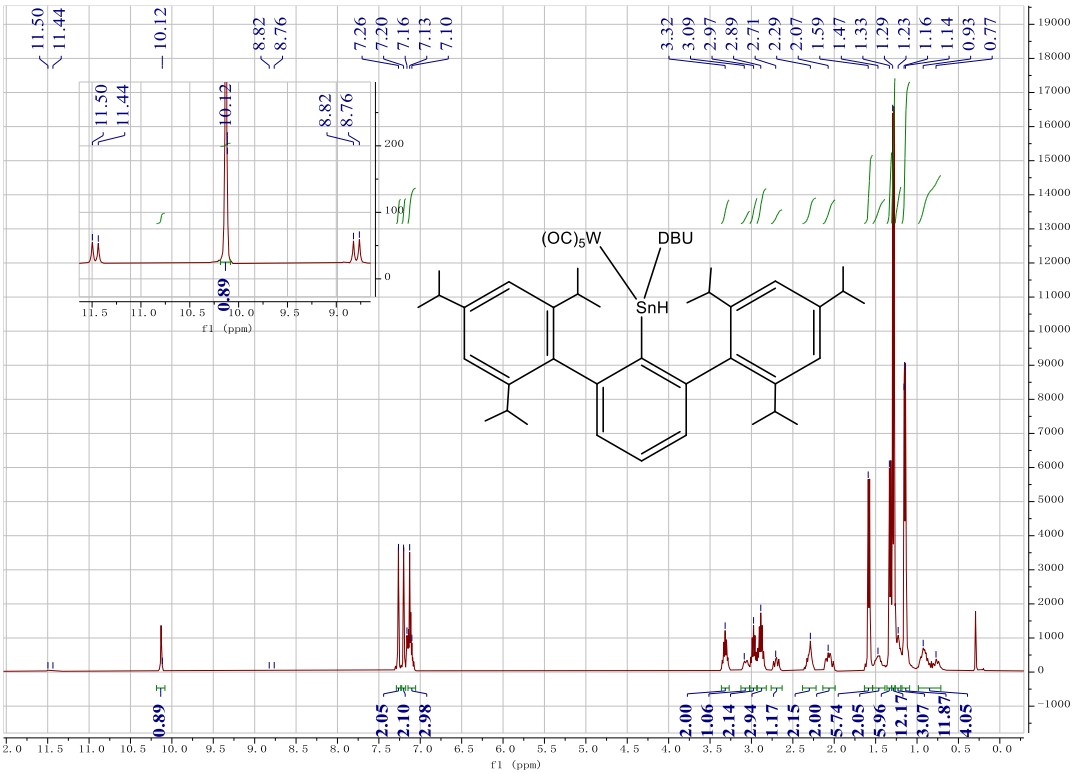

Figure 4.S19: ^{1}H NMR spectrum of **4** in C_6D_6 at 298K.

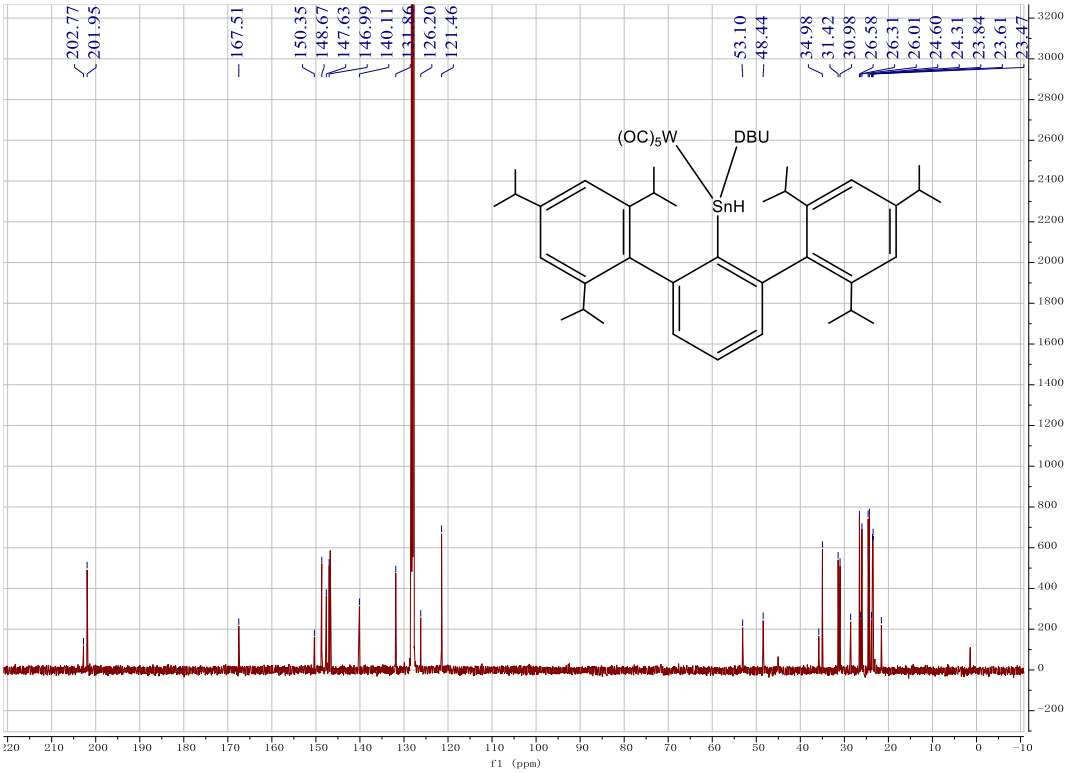

Figure 4.S20: $^{13}C\{^{1}H\}$ NMR spectrum of **4** in C_6D_6 at 298K.

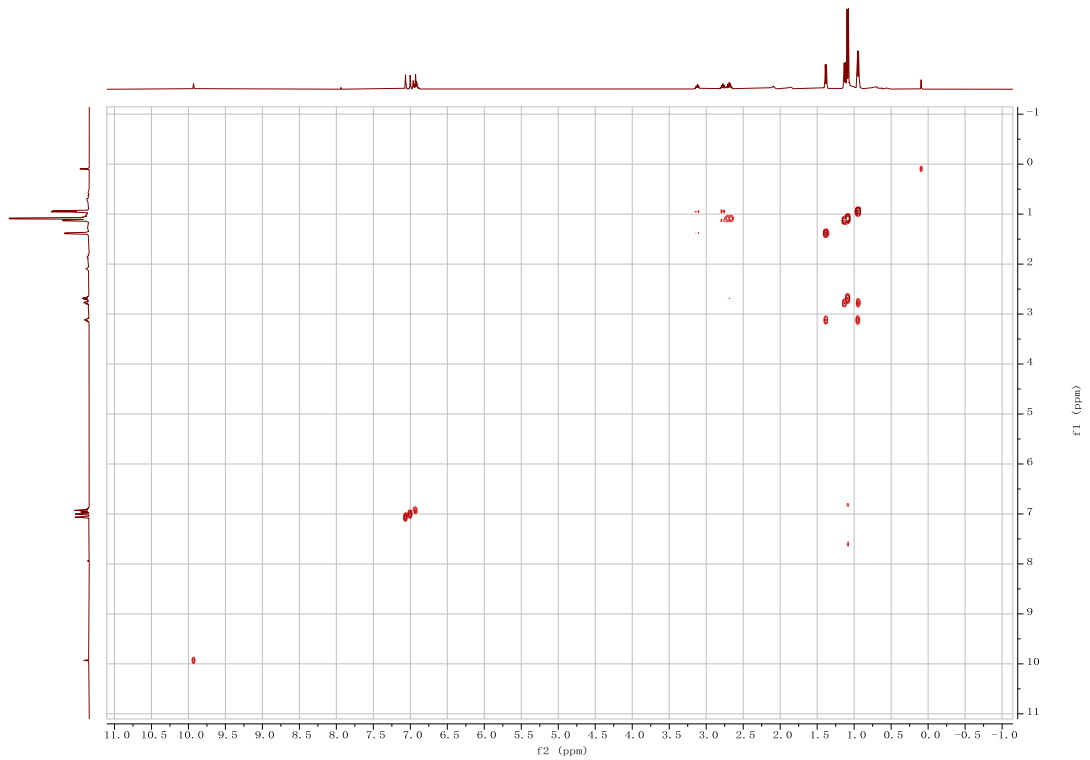

Figure 4.S21: ^{1}H-^{1}H COSY NMR spectrum of **4** in C_6D_6 at 298K.

Figure 4.S22: ^{1}H-^{13}C HSQC NMR spectrum of **4** in C_6D_6 at 298K.

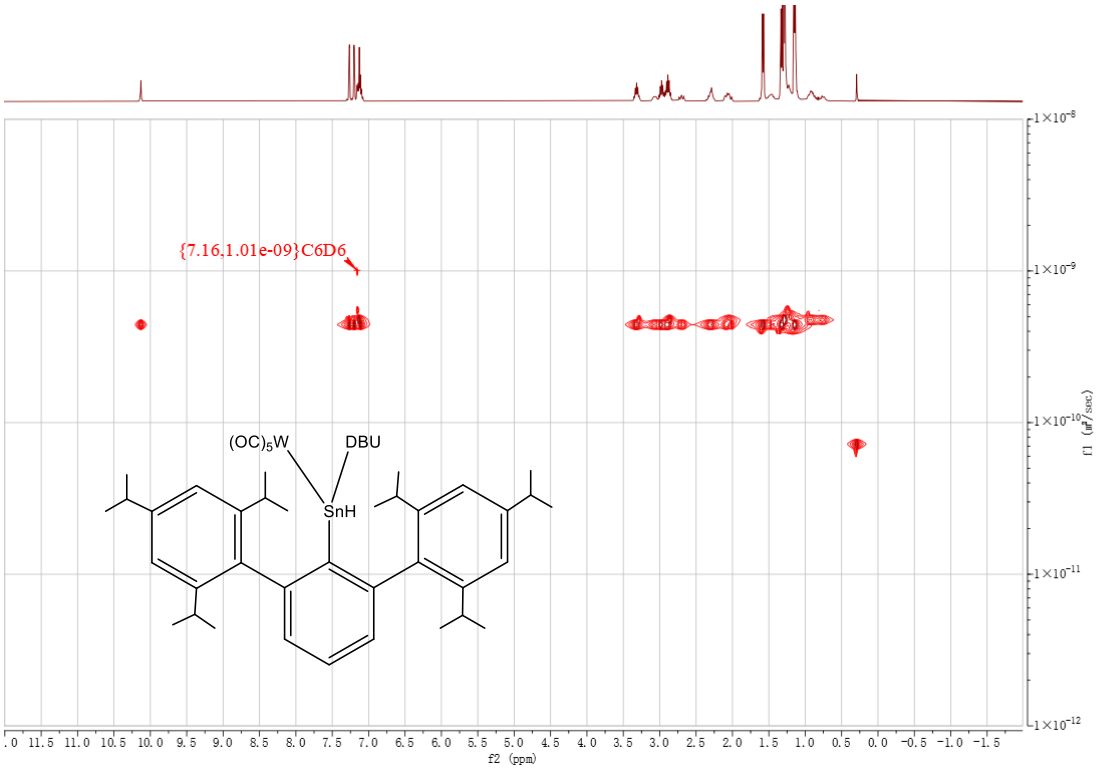

Figure 4.S23: ^{1}H-^{1}H DOSY NMR spectrum of **4** in C_6D_6 at 298K. DOSY coefficient = 4.42 * 10^{-10} m^2/s. other species is grease.

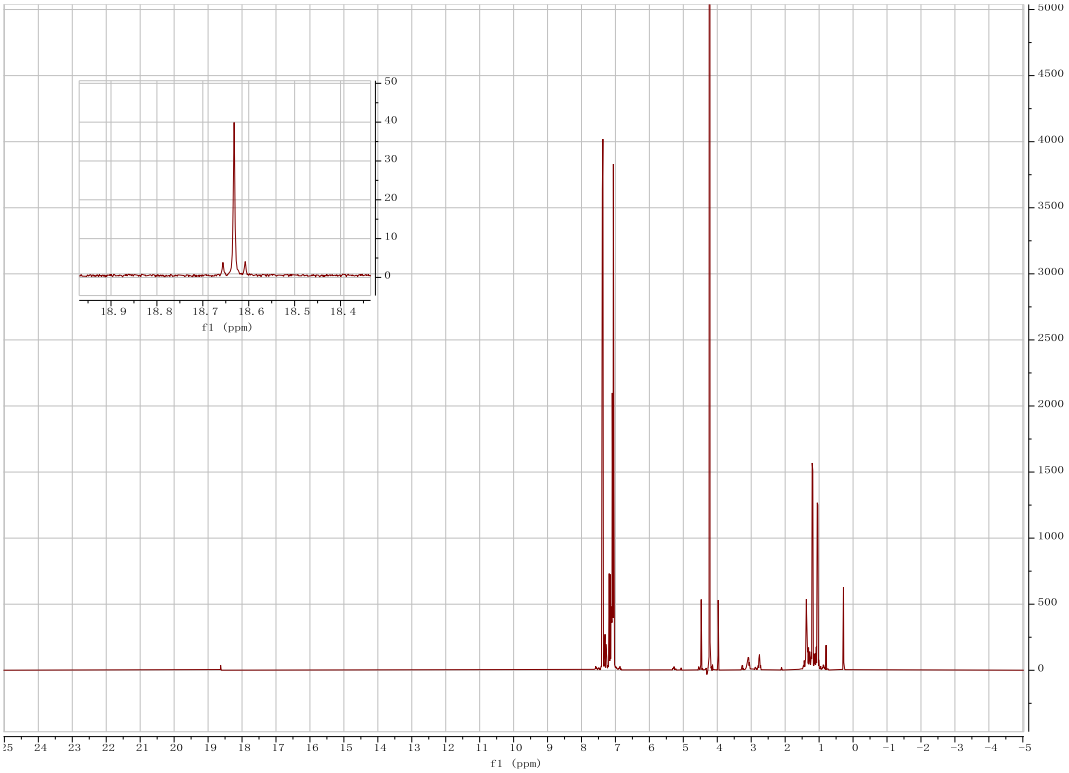

Figure 4.S24: ^{1}H NMR spectrum of **2** and excess of $PhSiH_3$ (after 72 hours of heating at 60°C) in C_6D_6 at 298K.

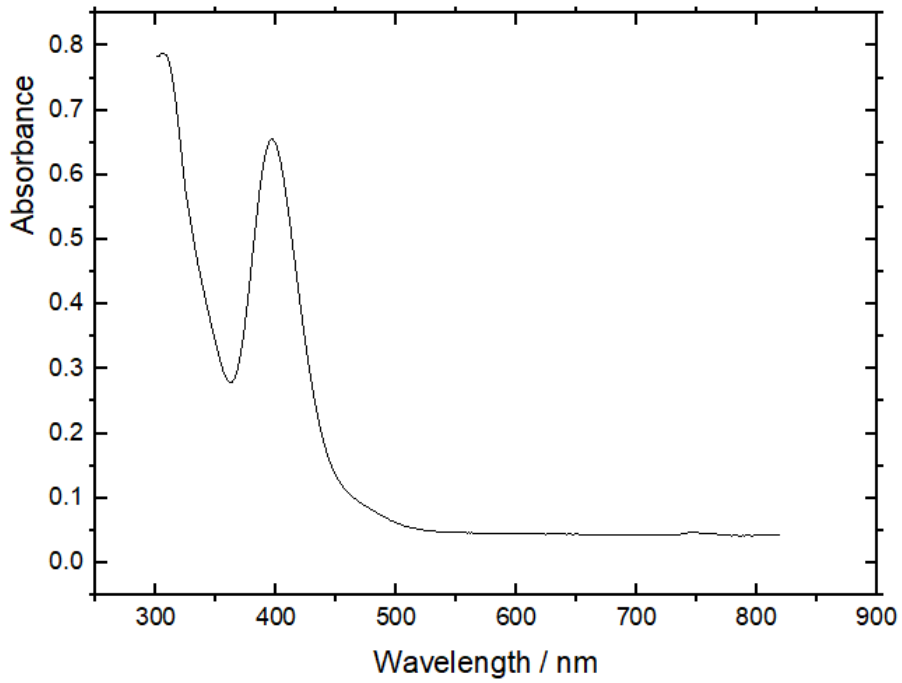

Figure 4.S25: UV-vis spectrum of **1** in hexanes ($1.2*10^{-4}$ M) at 298K.

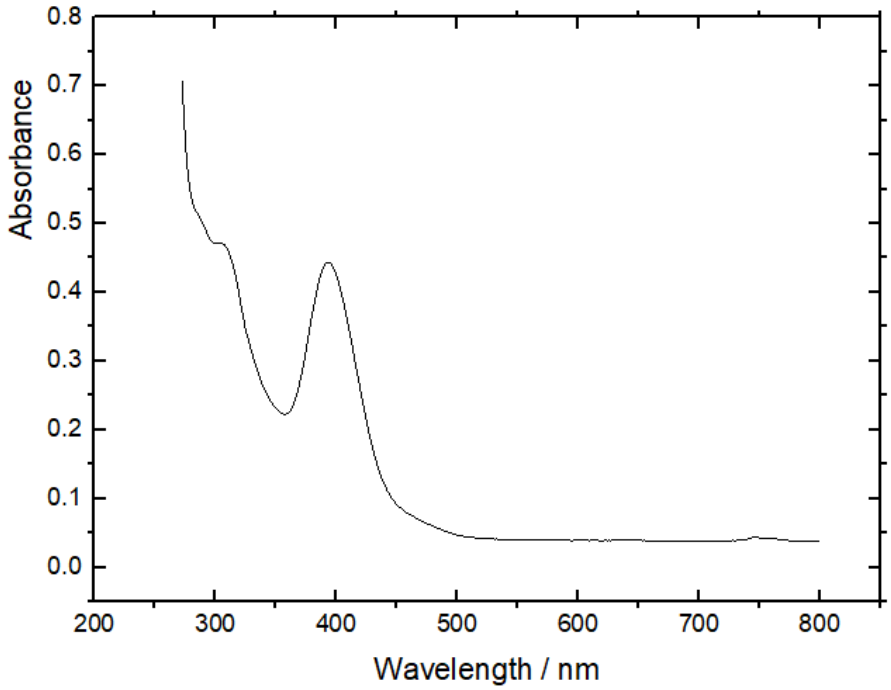

Figure 4.S26: UV-vis spectrum of **2** in hexanes ($1.0*10^{-4}$ M) at 298K.

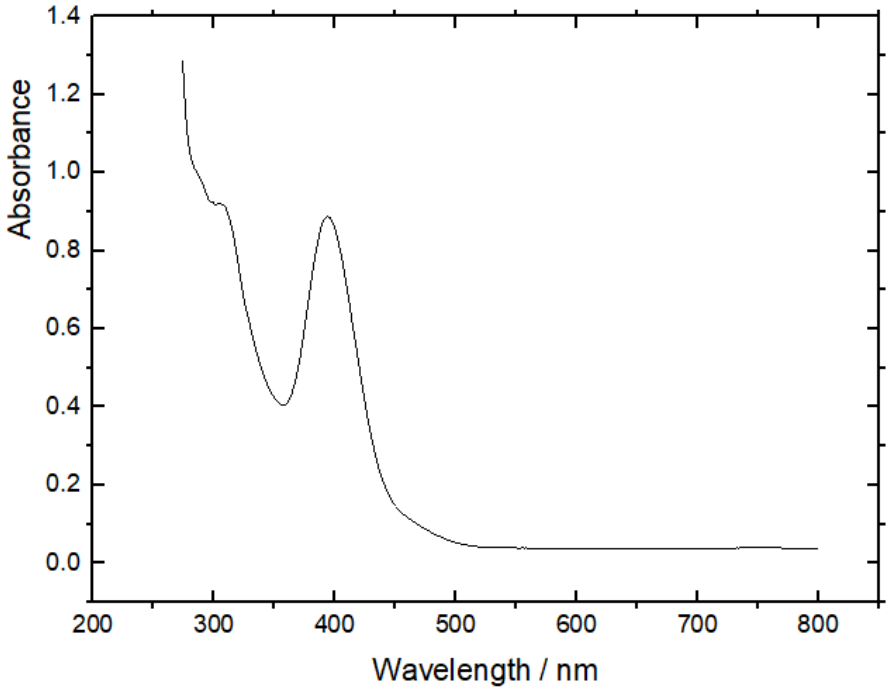

Figure 4.S27: UV-vis spectrum of **3** in hexanes ($1.4*10^{-4}$ M) at 298K.

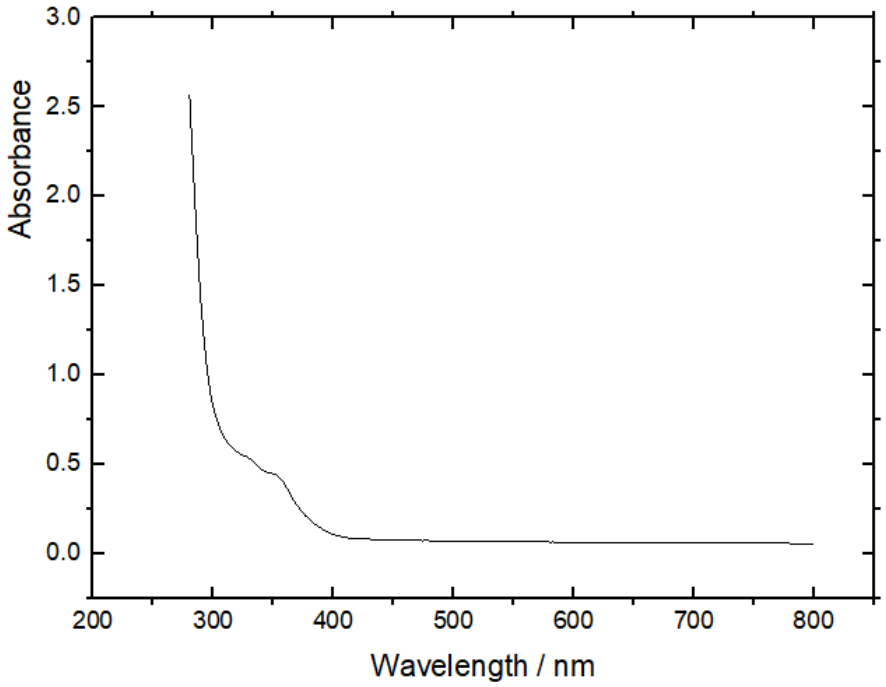

Figure 4.S28: UV-vis spectrum of **4** in hexanes ($1.7*10^{-4}$ M) at 298K.

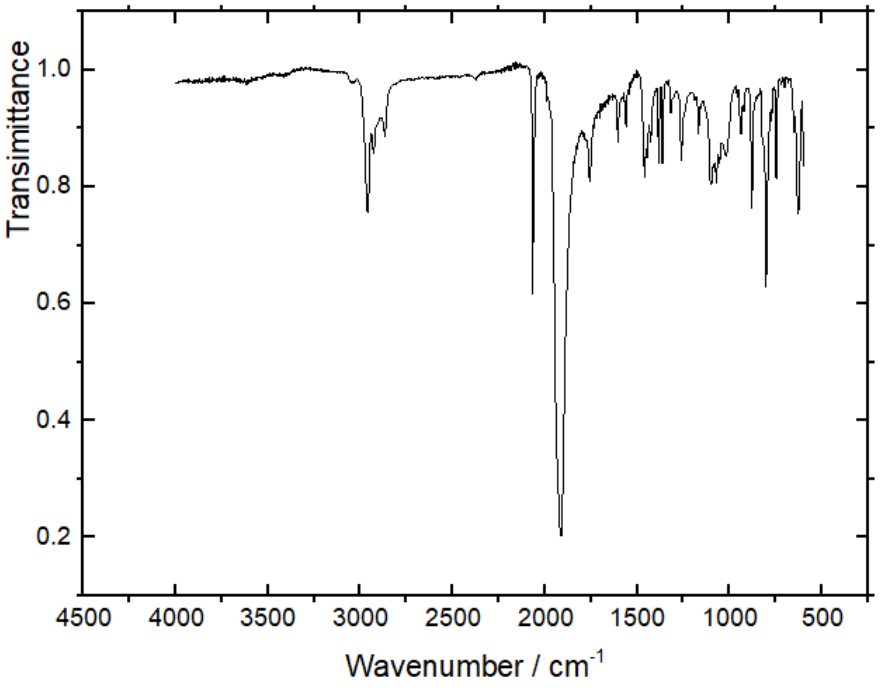

Figure 4.S29: ATR-FTIR spectrum of **1** at 298K.

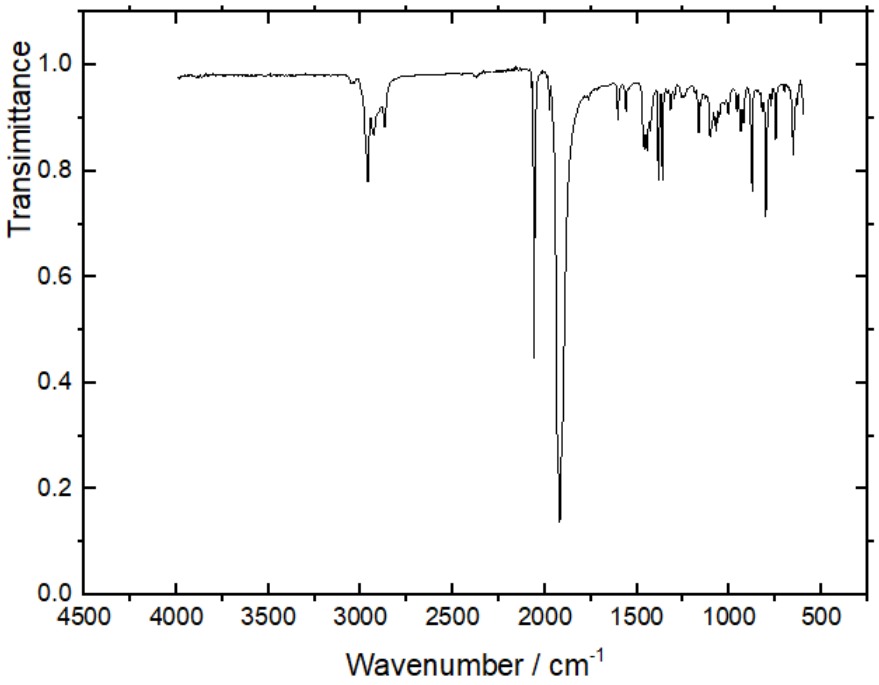

Figure 4.S30: ATR-FTIR spectrum of **2** at 298K.

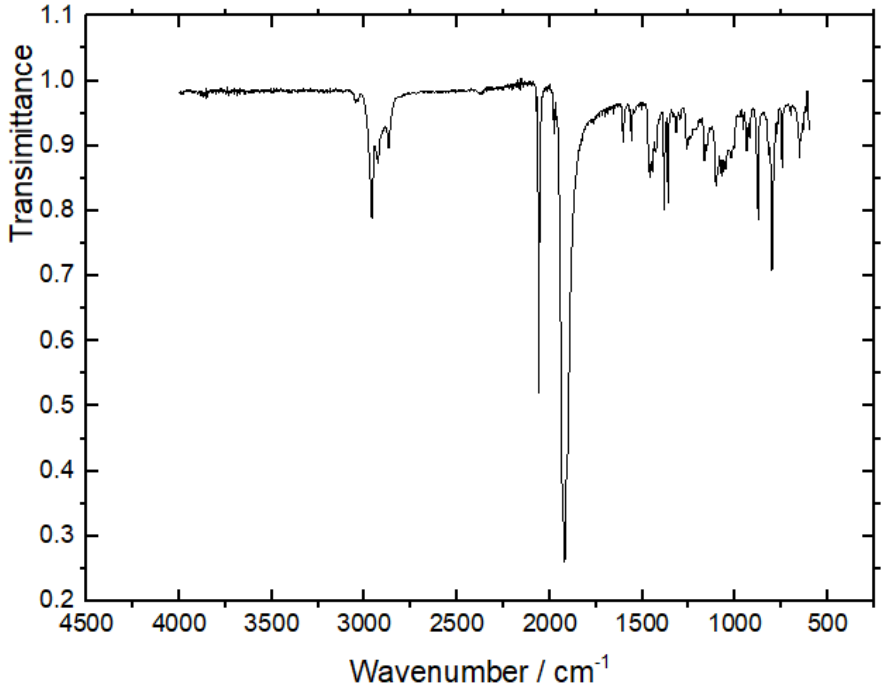

Figure 4.S31: ATR-FTIR spectrum of **3** at 298K.

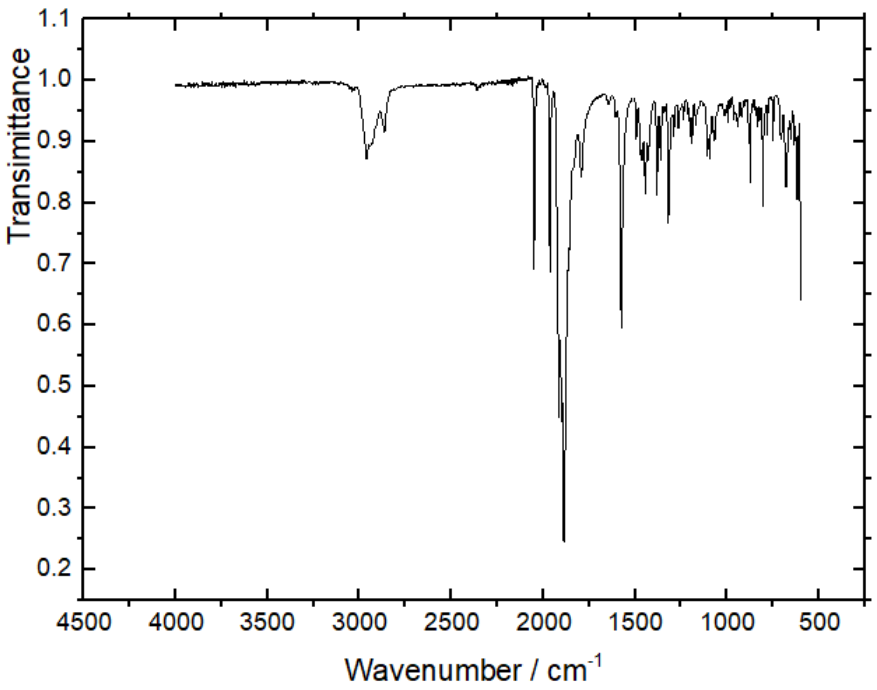

Figure 4.S32: ATR-FTIR spectrum of **4** at 298K.

Optimized xyz-coordinates

98
Compound 1

W	0.22748	-2.53436	-0.15280
Sn	0.08051	0.14577	-0.58216
O	3.40951	-2.70439	0.04039
O	0.52126	-2.78899	-3.31779
O	0.28185	-5.65358	0.30797
O	-2.92361	-2.90243	-0.49328
C	-1.38657	2.35034	1.04454
O	-0.05830	-1.92622	2.96426
C	-0.13136	1.84320	0.71922
C	-4.81714	0.52287	-0.78117
C	-2.58676	1.71448	0.43087
C	0.94662	3.57892	1.97694
H	1.84539	4.08039	2.31694
C	-2.25173	3.21185	-1.59934
H	-1.23269	3.25832	-1.20662
C	-2.96940	2.09797	-0.86724
C	-2.91942	4.55224	-1.29563
H	-3.95396	4.55286	-1.64965
H	-2.38862	5.36817	-1.79316
H	-2.92998	4.75699	-0.22390
C	-6.03111	-0.09645	-1.42896

H	-6.14361	0.37793	-2.41033
C	3.06803	0.97990	1.43194
C	-0.30015	4.07607	2.32945
H	-0.36853	4.95553	2.95949
C	1.03987	2.45495	1.16395
C	4.19246	0.39012	0.86792
H	4.76444	-0.32389	1.44891
C	-2.93820	0.32142	2.52728
H	-1.85799	0.46604	2.63179
C	-4.41305	0.14979	0.49493
H	-4.96992	-0.61806	1.01851
C	-3.31378	0.72384	1.11757
C	2.58290	4.63633	-1.08223
H	3.64681	4.69445	-1.32765
H	2.47083	4.83075	-0.01472
H	2.06304	5.42758	-1.62849
C	-4.07876	1.48901	-1.44493
H	-4.38549	1.78166	-2.44317
C	-1.45969	3.47517	1.86133
H	-2.42672	3.89557	2.11343
C	4.59124	0.65051	-0.43457
C	2.27521	-2.58770	-0.01463
C	0.41501	-2.71416	-2.18321
C	0.26572	-4.52205	0.14032
C	2.09022	3.06587	-2.96895
H	1.44671	3.79477	-3.46658
H	1.75544	2.06825	-3.25945
H	3.10196	3.21539	-3.35472
C	-1.80415	-2.72290	-0.36140
C	3.84861	1.55525	-1.18021
H	4.15437	1.77989	-2.19489
C	2.72617	2.18959	-0.66140
C	5.80491	-0.02880	-1.01835
H	6.15133	-0.75486	-0.27513
C	0.04344	-2.15277	1.84864
C	-3.24816	-1.13439	2.84893
H	-4.32424	-1.30773	2.93047
H	-2.80198	-1.40552	3.80741
H	-2.85591	-1.81263	2.09109
C	2.02219	3.26576	-1.46206
H	0.96733	3.25470	-1.17493
C	-5.85370	-1.59449	-1.65145
H	-4.96769	-1.80503	-2.25278
H	-6.72503	-2.01081	-2.16336
H	-5.73793	-2.12310	-0.70235
C	2.32014	1.88327	0.65680

C	2.67519	0.66649	2.85858
H	1.58820	0.77762	2.92755
C	3.31022	1.67086	3.82016
H	4.40057	1.60826	3.76601
H	3.00842	1.45809	4.84883
H	3.02097	2.69553	3.58718
C	-3.62845	1.22960	3.54473
H	-3.36556	2.27702	3.39673
H	-3.34394	0.94896	4.56206
H	-4.71463	1.13811	3.45743
C	-2.15204	2.99346	-3.10292
H	-1.72533	2.01664	-3.33823
H	-1.51010	3.75819	-3.54664
H	-3.12630	3.06853	-3.59213
C	3.03043	-0.74956	3.29215
H	2.69357	-1.49364	2.57088
H	2.55918	-0.97326	4.25104
H	4.10863	-0.87130	3.42311
C	-7.29559	0.19145	-0.62494
H	-7.24559	-0.27378	0.36307
H	-8.17541	-0.20797	-1.13561
H	-7.43872	1.26461	-0.48177
C	5.46981	-0.79312	-2.29479
H	4.68140	-1.52692	-2.12024
H	6.35143	-1.32102	-2.66637
H	5.13320	-0.11627	-3.08446
C	6.93092	0.97316	-1.25879
H	6.63549	1.71984	-2.00102
H	7.82485	0.46699	-1.63173
H	7.19363	1.50187	-0.34007
H	0.02391	0.90111	-2.14374

104

Compound 2

C	-4.90914	-0.25104	-0.31692
C	-4.24250	-0.66860	0.82382
C	-3.21704	0.07557	1.39769
C	-2.83257	1.27964	0.78221
C	-3.51362	1.73544	-0.36210
C	-4.54084	0.96127	-0.88441
C	-1.68078	2.06797	1.30587
C	-0.39367	1.76952	0.85823
C	0.69974	2.54880	1.24439
C	0.50568	3.61430	2.11559
C	-0.76534	3.89275	2.59475
C	-1.85052	3.13238	2.18787

Sn	0.06471	0.10850	-0.44375
C	-0.56887	0.64678	-2.44483
C	-1.67374	-0.28898	-2.91815
C	2.01057	2.19270	0.63004
C	2.95315	1.42262	1.33251
C	4.08439	0.97695	0.65950
C	4.30576	1.25434	-0.68044
C	3.38864	2.05737	-1.34556
C	2.25272	2.55233	-0.71642
C	2.76079	1.10162	2.79798
C	3.36635	2.20743	3.66314
C	1.36084	3.55476	-1.42255
C	1.45433	3.51925	-2.94088
C	5.51545	0.70311	-1.39260
C	6.48920	1.81614	-1.76954
C	-2.58783	-0.37091	2.70089
C	-3.21825	0.38043	3.87455
C	-3.17248	3.06607	-1.00072
C	-3.37496	3.09670	-2.51119
C	-5.97225	-1.11825	-0.94392
C	-7.28236	-0.36908	-1.15709
W	0.78815	-2.50058	-0.04479
C	2.82062	-2.26066	0.10531
O	3.96124	-2.22359	0.15158
C	1.07477	-2.58181	-2.06557
O	1.26081	-2.60280	-3.19378
C	-1.18798	-2.96223	-0.32444
O	-2.26870	-3.28127	-0.51842
C	0.59056	-2.21926	1.97271
O	0.51768	-2.05312	3.10134
C	1.09300	-4.47059	0.18222
O	1.24889	-5.59718	0.31196
C	3.34158	-0.24243	3.21559
C	1.68485	4.96522	-0.92703
C	5.12165	-0.11865	-2.61582
C	-2.68769	-1.86773	2.95591
C	-3.98467	4.19040	-0.35834
C	-5.46573	-1.72659	-2.24961
H	1.34286	4.23610	2.41004
H	-0.91421	4.72023	3.27891
H	1.68292	1.07701	2.98711
H	4.80211	0.35677	1.18321
H	3.56674	2.31254	-2.38293
H	3.01783	-1.04759	2.55833
H	3.01886	-0.48642	4.22955
H	4.43432	-0.22619	3.21715

H	4.44501	2.26951	3.49461
H	3.19999	1.99762	4.72274
H	2.93703	3.18364	3.43851
H	0.32578	3.33929	-1.13938
H	4.43618	-0.92442	-2.34806
H	6.00576	-0.56329	-3.07893
H	4.63165	0.50371	-3.36928
H	6.02132	0.03381	-0.68885
H	6.03090	2.51161	-2.47808
H	7.38467	1.40238	-2.23992
H	6.79590	2.38821	-0.89133
H	1.54573	5.05549	0.14996
H	1.03794	5.69850	-1.41544
H	2.72288	5.21803	-1.15948
H	2.41682	3.90161	-3.29091
H	0.68005	4.15783	-3.37175
H	1.32189	2.51451	-3.34266
H	-2.84303	3.37215	2.55180
H	-1.52710	-0.10059	2.66774
H	-4.52962	-1.61195	1.27243
H	-5.05449	1.30420	-1.77484
H	-2.31824	-2.45617	2.11577
H	-2.09937	-2.13132	3.83586
H	-3.71941	-2.17059	3.15204
H	-4.28859	0.16353	3.92943
H	-2.75877	0.06776	4.81564
H	-3.09506	1.45877	3.78047
H	-2.11492	3.26335	-0.79833
H	-4.54822	-2.29593	-2.08819
H	-6.21456	-2.39568	-2.68129
H	-5.25145	-0.94451	-2.98360
H	-6.16466	-1.94018	-0.24565
H	-7.16189	0.44471	-1.87702
H	-8.04887	-1.04228	-1.54878
H	-7.64927	0.06199	-0.22321
H	-3.80429	4.25735	0.71418
H	-3.72851	5.15394	-0.80684
H	-5.05358	4.01761	-0.51065
H	-4.43580	3.09598	-2.77424
H	-2.94536	4.01275	-2.92358
H	-2.90709	2.24651	-3.00866
H	-1.98201	-0.05039	-3.94129
H	-1.34758	-1.33147	-2.91980
H	-2.56280	-0.22479	-2.28705
H	-0.88029	1.69039	-2.47035
H	0.31493	0.54558	-3.08052

125
Compound 4

C	-5.08538	0.43607	-1.47530
C	-4.63820	1.53720	-0.75477
C	-3.32961	1.99231	-0.84581
C	-2.43224	1.32383	-1.69733
C	-2.85827	0.20147	-2.42086
C	-4.17912	-0.21963	-2.29226
C	-1.08393	1.91297	-1.94899
C	0.09646	1.56402	-1.27525
C	1.28185	2.24953	-1.60262
C	1.26948	3.25523	-2.56585
C	0.10899	3.57741	-3.24241
C	-1.05581	2.90402	-2.93180
Sn	0.31385	-0.03463	0.20689
N	-1.63673	-0.01189	1.30194
C	-1.87120	0.44649	2.50119
N	-2.90808	0.03521	3.25289
C	-3.70475	-1.13959	2.91975
C	-3.06856	-1.92573	1.80341
C	-2.60936	-0.94555	0.75061
C	2.58591	1.97869	-0.92710
C	2.89289	2.65167	0.26942
C	4.12685	2.44122	0.86401
C	5.07020	1.58450	0.31159
C	4.75419	0.94248	-0.87289
C	3.53104	1.12248	-1.51239
C	-3.20445	0.62235	4.55071
C	-2.22760	0.22010	5.64753
C	-0.92689	1.00728	5.61738
C	-0.17220	0.94620	4.29845
C	-0.96765	1.47435	3.10234
C	1.90867	3.61768	0.89383
C	2.11513	5.03238	0.35595
C	-1.92204	-0.52656	-3.36159
C	-1.99064	0.06902	-4.76705
C	3.27122	0.43642	-2.83838
C	3.71306	1.32148	-4.00444
C	-2.89876	3.19965	-0.03863
C	-3.56287	3.26579	1.33288
C	6.39402	1.34068	0.99222
C	6.20153	0.66925	2.34903
C	-6.50171	-0.06530	-1.33550
C	-6.73820	-0.65073	0.05472
W	0.99714	-2.74645	0.00000

C	1.72657	-4.60520	0.02056
O	2.15917	-5.66774	0.04330
C	0.62816	-2.68996	1.99601
O	0.37464	-2.61306	3.11441
C	-0.83340	-3.59523	-0.25949
O	-1.83340	-4.14634	-0.37536
C	1.12961	-2.56096	-2.03519
O	1.14209	-2.45889	-3.17473
C	2.91511	-2.12966	0.38938
O	3.99265	-1.87014	0.66721
C	-2.17916	-2.02599	-3.42331
C	3.95264	-0.92024	-2.96591
C	-3.16794	4.50340	-0.78838
C	1.96020	3.62440	2.41595
C	7.20673	2.62456	1.12477
C	-7.52903	1.01458	-1.65552
H	-2.21382	-2.47600	-2.43047
H	-1.38381	-2.51477	-3.98749
H	-3.12135	-2.25328	-3.92864
H	-0.90427	-0.37648	-2.98889
H	5.03656	-0.81512	-3.05735
H	3.59909	-1.42809	-3.86466
H	3.74842	-1.56598	-2.11227
H	-1.97707	3.14501	-3.45058
H	2.19036	3.78622	-2.77783
H	-2.15487	-1.45706	-0.09398
H	-3.46039	-0.37856	0.36515
H	5.48363	0.26639	-1.30328
H	2.19045	0.28357	-2.92530
H	4.35863	2.95117	1.79203
H	-1.56216	2.34382	3.39859
H	-0.29112	1.81192	2.32261
H	-3.78470	-2.63559	1.38751
H	-2.21484	-2.49586	2.17528
H	-1.81797	3.11513	0.11197
H	0.11053	4.35072	-4.00205
H	-5.32867	2.05116	-0.09540
H	0.90652	3.29405	0.59555
H	-4.51472	-1.09014	-2.84481
H	0.15560	-0.07667	4.09034
H	0.73656	1.54537	4.38926
H	4.78324	1.53442	-3.93107
H	3.17914	2.27054	-4.02340
H	3.53271	0.81298	-4.95523
H	-2.62351	4.54644	-1.73063
H	-2.86430	5.36203	-0.18320

H	-4.23538	4.60168	-1.00526
H	-4.61241	3.56165	1.25630
H	-3.06550	4.01577	1.95302
H	-3.52731	2.30555	1.84927
H	-4.71387	-0.81457	2.64095
H	-3.79356	-1.74869	3.82438
H	7.36544	3.09449	0.15178
H	8.18328	2.41910	1.57094
H	6.69532	3.34835	1.76520
H	1.93799	2.60849	2.81466
H	1.10815	4.17772	2.81987
H	2.86438	4.11216	2.78892
H	6.95721	0.65023	0.35479
H	-7.46919	1.84121	-0.94262
H	-8.54288	0.60933	-1.60717
H	-7.37070	1.42461	-2.65490
H	3.12085	5.38725	0.59737
H	1.39423	5.72360	0.80177
H	1.99389	5.06927	-0.72696
H	-3.00169	-0.02886	-5.17272
H	-1.30363	-0.45741	-5.43439
H	-1.72286	1.12582	-4.77051
H	-4.21217	0.28985	4.80557
H	-3.25647	1.71145	4.46373
H	5.64927	1.32183	3.03106
H	7.16737	0.44594	2.80998
H	5.64181	-0.26219	2.24907
H	-6.03220	-1.45760	0.26553
H	-7.75095	-1.05222	0.14337
H	-6.61395	0.11759	0.82360
H	-0.27482	0.65552	6.42165
H	-1.15141	2.05770	5.84224
H	-2.71387	0.37118	6.61604
H	-2.02692	-0.85349	5.56094
H	1.18850	0.78482	1.45051
H	-6.62693	-0.87463	-2.06313

6
Ethylene

C	-0.00004	-0.66150	0.00000
C	-0.00004	0.66152	-0.00000
H	-0.92326	-1.23020	-0.00000
H	-0.92331	1.22999	0.00000
H	0.92301	1.23053	-0.00000
H	0.92405	-1.23048	-0.00000

104
TS (1 + ethylene --> 2)

C	-5.52505	-0.98200	0.15428
C	-4.64413	-1.03646	1.22556
C	-3.62796	-0.10502	1.39488
C	-3.47979	0.91491	0.44244
C	-4.37223	1.00386	-0.63824
C	-5.37874	0.05203	-0.75876
C	-2.40342	1.93058	0.59410
C	-1.04757	1.67236	0.33315
C	-0.11499	2.70619	0.49481
C	-0.53007	3.97526	0.89085
C	-1.86297	4.22370	1.15794
C	-2.78576	3.20290	1.01678
Sn	-0.17257	-0.26076	-0.19648
C	-0.93328	-0.29284	-2.45170
C	-1.91854	-1.07543	-1.85483
C	1.34032	2.45969	0.31288
C	2.12654	2.18514	1.43932
C	3.48879	1.97294	1.26383
C	4.08456	2.00738	0.01336
C	3.28356	2.28365	-1.08914
C	1.92318	2.52513	-0.96417
C	1.53104	2.12473	2.83046
C	2.12366	3.20514	3.72963
C	1.09915	2.93431	-2.16594
C	1.51138	2.24666	-3.45965
C	5.56859	1.77820	-0.13718
C	6.27266	3.05045	-0.60163
C	-2.73992	-0.16289	2.61872
C	-3.33287	0.69349	3.73672
C	-4.27814	2.10828	-1.67225
C	-4.29081	1.58709	-3.10623
C	-6.59954	-2.02747	-0.01455
C	-7.99479	-1.41192	-0.02800
W	1.89279	-2.18817	-0.12801
C	3.30027	-1.33805	1.10024
O	4.14850	-1.02034	1.79592
C	2.70325	-1.31909	-1.79435
O	3.13913	-0.86173	-2.74682
C	0.64981	-3.29639	-1.29604
O	-0.01743	-3.96589	-1.94377
C	1.00559	-2.97069	1.54304
O	0.51906	-3.41345	2.47714
C	3.16359	-3.70956	-0.23940
O	3.88670	-4.59682	-0.31655

C	1.68137	0.74447	3.46121
C	1.13953	4.45279	-2.33317
C	5.88053	0.61212	-1.06845
C	-2.46103	-1.57604	3.10892
C	-5.40084	3.12473	-1.47566
C	-6.35778	-2.86641	-1.26626
H	0.21187	4.75647	1.01370
H	-2.18307	5.20672	1.48385
H	0.46140	2.32621	2.74281
H	4.10683	1.75337	2.12809
H	3.73601	2.31914	-2.07340
H	1.23922	-0.03258	2.83223
H	1.18460	0.71562	4.43430
H	2.73105	0.48376	3.61225
H	3.19740	3.05764	3.87090
H	1.65128	3.18537	4.71503
H	1.97768	4.19886	3.30029
H	0.06058	2.66053	-1.95602
H	5.42234	-0.31283	-0.71532
H	6.95985	0.45310	-1.13134
H	5.51219	0.80078	-2.07970
H	5.95285	1.52442	0.85666
H	5.93143	3.34242	-1.59860
H	7.35375	2.89747	-0.65051
H	6.07336	3.88308	0.07640
H	0.77039	4.96099	-1.44092
H	0.52476	4.76431	-3.18189
H	2.16450	4.78816	-2.51317
H	2.49074	2.58697	-3.80458
H	0.79493	2.47988	-4.25116
H	1.56007	1.16326	-3.34738
H	-3.83180	3.38299	1.23664
H	-1.78028	0.28770	2.35028
H	-4.75823	-1.83607	1.94901
H	-6.06263	0.11712	-1.59839
H	-2.11018	-2.21973	2.30026
H	-1.69013	-1.55907	3.88226
H	-3.34905	-2.03659	3.54919
H	-4.31091	0.30710	4.03606
H	-2.68022	0.68511	4.61363
H	-3.46128	1.72931	3.41705
H	-3.32886	2.62746	-1.51907
H	-5.37103	-3.33402	-1.24312
H	-7.10849	-3.65565	-1.35562
H	-6.41424	-2.24838	-2.16655
H	-6.53514	-2.69381	0.85271

H	-8.12490	-0.74963	-0.88799
H	-8.75873	-2.19077	-0.09190
H	-8.17688	-0.82575	0.87507
H	-5.38372	3.55251	-0.47202
H	-5.31239	3.94180	-2.19625
H	-6.37682	2.65277	-1.61808
H	-5.24112	1.10848	-3.35462
H	-4.15192	2.41492	-3.80592
H	-3.49630	0.86059	-3.28499
H	-1.86398	-2.15511	-1.92267
H	-1.67691	-1.26769	-0.10211
H	-2.88649	-0.66251	-1.60048
H	-1.13588	0.74852	-2.66954
H	-0.13611	-0.76469	-3.01096

35

Ph_3SiH

Si	-0.00034	0.00006	-0.97160
C	-1.74973	0.26623	-0.36529
C	0.64368	-1.64790	-0.36538
C	1.10538	1.38148	-0.36514
H	-0.00030	0.00027	-2.46318
C	-2.28389	-0.49871	0.67193
C	-3.56759	-0.26405	1.14426
C	-4.33967	0.74173	0.58298
C	-3.82608	1.51152	-0.45174
C	-2.54315	1.27427	-0.91867
H	-1.68879	-1.29140	1.11395
H	-3.96653	-0.86913	1.95075
H	-5.34349	0.92526	0.94938
H	-4.42800	2.29689	-0.89501
H	-2.15304	1.88413	-1.72824
C	0.70900	2.22933	0.66938
C	1.55419	3.22398	1.14108
C	2.81250	3.38718	0.58208
C	3.22357	2.55449	-0.44998
C	2.37624	1.56223	-0.91664
H	-0.27626	2.11291	1.10912
H	1.22876	3.87428	1.94534
H	3.47346	4.16488	0.94803
H	4.20581	2.68107	-0.89135
H	2.71039	0.91691	-1.72382
C	1.57852	-1.72812	0.66732
C	2.01789	-2.95744	1.13866
C	1.52798	-4.12877	0.58166
C	0.59866	-4.06871	-0.44805

C	0.16312	-2.83890	-0.91500
H	1.97137	-0.81676	1.10632
H	2.74533	-3.00055	1.94158
H	1.87135	-5.08987	0.94758
H	0.21544	-4.98263	-0.88793
H	-0.56439	-2.80606	-1.72080

139

TS (2 + Ph_3SiH --> 1 + $Ph_3Si(CH_2CH_3)$)

C	-5.04432	-0.40214	2.44314
C	-5.57895	-0.26633	1.14676
C	-6.80084	-0.90018	0.86096
C	-7.45745	-1.65119	1.83398
C	-6.90778	-1.78111	3.10934
C	-5.69971	-1.15184	3.41390
Si	-4.65343	0.72821	-0.11639
C	-4.15584	2.41908	0.46894
C	-4.73003	2.94857	1.63840
C	-4.34012	4.19587	2.12396
C	-3.37302	4.93798	1.44593
C	-2.79460	4.42782	0.28291
C	-3.17415	3.17743	-0.19943
C	-2.22922	-5.61339	-0.58359
C	-0.73408	-5.92970	-0.55590
C	-0.46624	-7.32644	0.02368
C	0.09036	-4.89309	0.17874
C	1.37653	-4.59600	-0.27577
C	2.20808	-3.68204	0.37111
C	1.72016	-3.02200	1.52269
C	0.42421	-3.31633	2.00967
C	-0.36207	-4.25345	1.33178
C	2.51234	-1.95726	2.21261
C	2.36409	-0.63001	1.77731
C	2.89224	0.42207	2.54742
C	3.63223	0.13612	3.69927
C	3.83433	-1.18481	4.09310
C	3.26315	-2.22582	3.36313
C	2.57610	1.81612	2.12176
C	1.26004	2.30860	2.30813
C	0.93727	3.57777	1.80878
C	1.88531	4.38332	1.17749
C	3.18747	3.89464	1.05522
C	3.55702	2.62926	1.51113
C	0.25943	1.56357	3.18492
C	-1.19933	1.86566	2.85901
C	4.98299	2.12862	1.34670

C	6.02078	3.24317	1.27580
C	1.53548	5.74762	0.61756
C	0.57936	6.53615	1.50811
Sn	1.00331	-0.17572	0.13506
C	-2.50266	-0.27115	-0.03359
C	-2.66031	-1.68380	-0.55597
C	3.62608	-3.44352	-0.11620
C	4.63036	-4.18423	0.77243
C	-0.11577	-2.65506	3.26693
C	-1.48239	-2.00049	3.04390
C	3.84881	-3.82939	-1.57358
C	-0.14310	-3.63751	4.43577
W	1.64000	0.19555	-2.57045
C	3.54508	-0.52891	-2.32532
O	4.63685	-0.87042	-2.21349
C	1.89919	0.38062	-4.54586
O	2.04786	0.48230	-5.68403
C	2.44223	2.04596	-2.22207
O	2.91819	3.08084	-2.05536
C	-0.19728	1.04680	-2.68659
O	-1.23606	1.55935	-2.73509
C	0.85032	-1.67987	-2.80326
O	0.38129	-2.72595	-2.92859
C	5.09982	1.19793	0.14152
C	0.99657	5.62378	-0.80890
C	0.55478	1.85537	4.65842
C	-5.15342	0.52900	-1.88258
C	-5.01988	1.60717	-2.77990
C	-5.31665	1.45125	-4.13068
C	-5.75241	0.21657	-4.61454
C	-5.89365	-0.86229	-3.74027
C	-5.59535	-0.71104	-2.38865
H	4.03862	0.95581	4.29887
H	4.41235	-1.40308	4.99442
H	5.21167	1.52647	2.24024
H	3.93562	4.52842	0.57560
H	-0.07727	3.95439	1.94679
H	4.39336	0.36036	0.21579
H	6.11509	0.77862	0.06486
H	4.88465	1.74134	-0.79039
H	5.94307	3.81725	0.33878
H	7.03406	2.81395	1.30521
H	5.92489	3.94845	2.11595
H	0.41459	0.48540	3.02764
H	1.72359	5.13144	-1.46820
H	0.75712	6.61434	-1.22867

H	0.07984	5.01249	-0.82503
H	2.48082	6.31556	0.56267
H	-0.41399	6.06178	1.55762
H	0.43500	7.55387	1.11253
H	0.96110	6.61848	2.53739
H	1.57860	1.55851	4.92686
H	-0.14085	1.30362	5.31171
H	0.44473	2.93078	4.87207
H	-1.49422	2.88266	3.16177
H	-1.85969	1.16340	3.39475
H	-1.40032	1.76764	1.78205
H	3.37102	-3.25812	3.70711
H	3.82656	-2.36359	-0.01345
H	1.73139	-5.09406	-1.17962
H	-1.35917	-4.48049	1.71794
H	3.09956	-3.37996	-2.24000
H	4.83917	-3.48801	-1.90517
H	3.81287	-4.92188	-1.71048
H	4.44860	-5.27079	0.73709
H	5.65860	-3.99866	0.42544
H	4.56541	-3.86175	1.81989
H	0.58386	-1.84842	3.53096
H	-2.42192	-4.61846	-1.02405
H	-2.76475	-6.36218	-1.18833
H	-2.67534	-5.63296	0.42974
H	-0.37665	-5.92354	-1.60522
H	-0.78990	-7.37851	1.08078
H	-1.01289	-8.10012	-0.53950
H	0.60802	-7.57621	-0.00804
H	0.86063	-4.04212	4.63681
H	-0.50230	-3.14492	5.35379
H	-0.81008	-4.48912	4.22529
H	-2.28943	-2.74034	2.91918
H	-1.74335	-1.35768	3.89933
H	-1.44681	-1.38263	2.13473
H	-2.41528	-2.40848	0.23368
H	-3.66799	-1.91221	-0.93351
H	-1.95431	-1.85595	-1.38377
H	-1.37491	-0.13404	0.29745
H	-2.54516	0.52403	-0.79487
H	-5.49239	2.37853	2.17676
H	-4.79555	4.59059	3.03539
H	-3.06717	5.91724	1.82440
H	-2.03276	5.00321	-0.24738
H	-2.68249	2.79043	-1.09796
H	-4.68436	2.58275	-2.41667

H	-5.20501	2.29942	-4.81136
H	-5.98035	0.09538	-5.67666
H	-6.23324	-1.83120	-4.11548
H	-5.70447	-1.57097	-1.72260
H	-7.25198	-0.79653	-0.12893
H	-8.40854	-2.13451	1.59617
H	-7.42213	-2.37387	3.86920
H	-5.26479	-1.24883	4.41160
H	-4.09507	0.08430	2.69876
H	-2.94909	-0.05647	0.95472

41

$Ph_3Si(CH_2CH_3)$

C	2.06335	1.95130	0.68222
C	1.48014	0.89402	-0.01963
C	2.02388	0.55551	-1.26038
C	3.10766	1.24676	-1.78228
C	3.67260	2.29246	-1.06745
C	3.14862	2.64444	0.16816
Si	-0.02907	0.01039	0.65760
C	-0.08030	-1.72422	-0.05738
C	-1.25112	-2.25970	-0.59620
C	-1.28711	-3.55620	-1.08993
C	-0.14656	-4.34376	-1.05598
C	1.03047	-3.82858	-0.53112
C	1.06024	-2.53301	-0.03919
C	-1.57402	0.94139	0.14353
C	-1.54213	1.87334	-0.89513
C	-2.68935	2.54425	-1.29309
C	-3.89575	2.29487	-0.65620
C	-3.94950	1.37444	0.38069
C	-2.79904	0.70792	0.77432
C	0.05126	-0.05285	2.53516
H	-0.60290	2.08219	-1.39703
H	-2.64112	3.26538	-2.10146
H	-4.79322	2.81897	-0.96504
H	-4.88926	1.17772	0.88468
H	-2.86119	-0.00777	1.58855
H	-2.14795	-1.65038	-0.63946
H	-2.20733	-3.95068	-1.50638
H	-0.17199	-5.35616	-1.44324
H	1.92754	-4.43735	-0.50822
H	1.99275	-2.14034	0.35417
H	1.59535	-0.26566	-1.82594
H	3.51380	0.96703	-2.74799
H	4.52154	2.83221	-1.47178

H	3.58709	3.46046	0.73170
H	1.66437	2.24275	1.64889
C	1.25388	-0.79956	3.10157
H	1.26271	-0.77732	4.19437
H	1.24808	-1.84820	2.79524
H	2.19448	-0.36274	2.75567
H	0.02876	0.97885	2.90480
H	-0.87776	-0.51137	2.89177

27
DBU

N	-1.46075	-1.44180	-0.13943
C	-0.39631	-0.76273	-0.35368
C	0.88791	-1.52625	-0.51715
H	1.33380	-1.32526	-1.49875
H	0.59374	-2.57466	-0.50710
C	1.91731	-1.25498	0.58185
H	1.40007	-1.20956	1.54683
H	2.59331	-2.11316	0.63814
C	2.75637	-0.00243	0.37495
H	3.50509	0.06536	1.17047
H	3.31718	-0.11186	-0.56234
C	1.97163	1.29851	0.31391
H	1.49635	1.50474	1.27976
H	2.66714	2.12271	0.12325
C	0.89640	1.30630	-0.76671
H	1.30811	0.90593	-1.70002
H	0.60514	2.33616	-0.98632
N	-0.31734	0.60429	-0.41218
C	-1.44898	1.42633	-0.02951
H	-1.08217	2.26427	0.57425
H	-1.92027	1.85868	-0.92337
C	-2.45783	0.61712	0.75439
H	-2.06860	0.41531	1.75731
H	-3.38405	1.18590	0.86668
C	-2.68838	-0.70423	0.04329
H	-3.16008	-0.51976	-0.93308
H	-3.38687	-1.32811	0.60758

125
TS (proton abstraction from 4)

C	-4.65450	0.59628	-0.89106
C	-3.87844	0.31933	-2.00909
C	-3.02598	-0.77644	-2.05494
C	-2.93279	-1.61388	-0.92227
C	-3.76158	-1.39014	0.18849

C	-4.60441	-0.28441	0.17861
C	-1.87985	-2.66877	-0.91518
C	-0.56937	-2.24085	-0.68140
C	0.49557	-3.13534	-0.80861
C	0.23630	-4.46630	-1.12105
C	-1.06720	-4.89962	-1.31073
C	-2.12188	-4.00294	-1.22220
Sn	-0.21346	-0.13760	-0.22987
N	0.36221	2.37435	-2.36776
C	1.42991	3.03244	-2.04551
N	1.48093	4.36692	-1.86251
C	0.26860	5.16700	-1.90391
C	-0.95040	4.31470	-1.63200
C	-0.89884	3.06652	-2.48931
C	1.87683	-2.58558	-0.70123
C	2.43686	-1.94810	-1.82164
C	3.69062	-1.35203	-1.70295
C	4.39948	-1.37096	-0.51221
C	3.83645	-2.03265	0.57465
C	2.60013	-2.65611	0.50403
C	2.72814	5.07263	-1.62113
C	3.30412	4.87538	-0.22559
C	4.02029	3.54563	-0.04697
C	3.17755	2.32107	-0.35956
C	2.67703	2.23787	-1.80150
C	1.76193	-2.02994	-3.17579
C	2.32593	-3.22631	-3.94206
C	-3.78731	-2.36710	1.34242
C	-4.83784	-3.44668	1.07740
C	2.08175	-3.47807	1.66341
C	2.58617	-4.91634	1.53312
C	-2.32521	-1.15340	-3.34427
C	-1.85900	0.02099	-4.18878
C	5.76695	-0.74153	-0.35984
C	6.16573	0.17290	-1.50712
C	-5.52748	1.82535	-0.83569
C	-4.69087	3.09847	-0.92724
W	-0.18787	0.78401	2.39651
C	-0.18233	1.28708	4.33503
O	-0.18048	1.55829	5.44899
C	0.17004	2.69207	1.81907
O	0.35704	3.78695	1.51941
C	-2.15364	1.34737	2.28665
O	-3.21243	1.78051	2.24456
C	-0.58477	-1.17909	2.85416
O	-0.80803	-2.27169	3.10630

C	1.84545	0.57456	2.48955
O	2.98877	0.56686	2.56092
C	-4.04586	-1.72927	2.69994
C	2.44647	-2.93709	3.03769
C	-3.24454	-2.06758	-4.15486
C	1.85545	-0.76344	-4.01335
C	6.83060	-1.82070	-0.15835
C	-6.60927	1.80128	-1.91063
H	-3.35289	-0.91528	2.90807
H	-3.92769	-2.47800	3.48600
H	-5.06255	-1.33552	2.77599
H	-2.80914	-2.85396	1.37990
H	3.52217	-2.99135	3.22382
H	1.95343	-3.53336	3.80827
H	2.13394	-1.90240	3.16672
H	-3.13373	-4.33829	-1.41900
H	1.05908	-5.16205	-1.24038
H	-1.68728	2.36712	-2.18883
H	-1.08135	3.30959	-3.54322
H	4.38392	-2.05444	1.51030
H	0.99147	-3.49934	1.58858
H	4.12115	-0.87031	-2.57176
H	3.46450	2.54837	-2.49785
H	2.43919	1.20428	-2.04517
H	-1.85718	4.88986	-1.82963
H	-0.96259	4.02927	-0.57875
H	-1.43970	-1.73492	-3.07911
H	-1.26042	-5.93762	-1.55620
H	-3.94391	0.97056	-2.87350
H	0.70198	-2.22586	-3.00123
H	-5.22303	-0.08122	1.04503
H	2.31823	2.27374	0.31358
H	3.76352	1.42343	-0.15292
H	3.67754	-4.94273	1.59977
H	2.29890	-5.36213	0.58063
H	2.18058	-5.53743	2.33588
H	-3.53262	-2.94929	-3.57982
H	-2.74538	-2.40315	-5.06771
H	-4.15816	-1.53799	-4.43930
H	-2.69174	0.64197	-4.52941
H	-1.35039	-0.34918	-5.08208
H	-1.15471	0.64991	-3.64428
H	0.18601	5.66320	-2.88009
H	0.35728	5.94942	-1.14576
H	6.59430	-2.46400	0.69065
H	7.81111	-1.37073	0.01759

H	6.90055	-2.45400	-1.04712
H	1.38085	0.08501	-3.51802
H	1.34344	-0.91540	-4.96674
H	2.88989	-0.49634	-4.24524
H	5.73167	-0.13720	0.55598
H	-6.16868	1.81650	-2.91126
H	-7.26204	2.67349	-1.82170
H	-7.22452	0.90262	-1.83147
H	3.39311	-3.08948	-4.13853
H	1.81504	-3.34518	-4.90120
H	2.20564	-4.15074	-3.37416
H	-5.83541	-3.00115	1.02754
H	-4.83587	-4.18770	1.88090
H	-4.65743	-3.96541	0.13543
H	2.51532	6.13000	-1.78846
H	3.46729	4.78739	-2.37775
H	6.29899	-0.38949	-2.43561
H	7.11666	0.66116	-1.28334
H	5.42237	0.95162	-1.68935
H	-3.92939	3.12420	-0.14545
H	-5.32226	3.98445	-0.82111
H	-4.18690	3.16323	-1.89589
H	4.38799	3.47057	0.98032
H	4.90831	3.53357	-0.69263
H	4.00984	5.68863	-0.02856
H	2.49461	4.97245	0.50403
H	0.16693	1.05291	-1.67234
H	-6.02138	1.82145	0.14174

125

Proton abstraction product

C	-4.85096	-0.39378	-0.63209
C	-4.05407	-0.47816	-1.76686
C	-2.95152	-1.32255	-1.82815
C	-2.61664	-2.09724	-0.69642
C	-3.42757	-2.04244	0.44745
C	-4.52733	-1.19127	0.45239
C	-1.39670	-2.95586	-0.74017
C	-0.14370	-2.34607	-0.60766
C	1.01610	-3.11516	-0.75879
C	0.91672	-4.48352	-0.98844
C	-0.32694	-5.08971	-1.08179
C	-1.47869	-4.32592	-0.97014
Sn	0.00839	-0.16592	-0.44634
N	-0.82031	2.78986	-1.92326
C	0.10558	3.71312	-1.81931

N	-0.18611	4.95293	-1.47194
C	-1.52723	5.31820	-1.02056
C	-2.32013	4.11067	-0.56795
C	-2.21220	3.00118	-1.58965
C	2.33182	-2.41307	-0.73959
C	2.72522	-1.67077	-1.87436
C	3.91425	-0.95226	-1.83169
C	4.74037	-0.96782	-0.71571
C	4.35648	-1.73714	0.36993
C	3.16935	-2.46069	0.38533
C	0.81980	6.01187	-1.48854
C	1.86690	5.89996	-0.39148
C	2.95467	4.87867	-0.68836
C	2.46433	3.45921	-0.92115
C	1.51167	3.30179	-2.10601
C	1.95405	-1.78124	-3.17414
C	2.48021	-2.97078	-3.97667
C	-3.16995	-2.93495	1.64033
C	-4.06022	-4.17537	1.56689
C	2.83739	-3.32760	1.57861
C	3.57726	-4.66146	1.47878
C	-2.21875	-1.51687	-3.13975
C	-2.13946	-0.26896	-4.00500
C	6.02834	-0.18205	-0.68221
C	5.76791	1.31867	-0.76146
C	-6.04497	0.52791	-0.57643
C	-5.62603	1.99266	-0.65849
W	0.07313	0.74175	2.24837
C	0.07355	1.09803	4.21401
O	0.06940	1.28246	5.34752
C	0.14748	2.71260	1.86454
O	0.15965	3.85964	1.69339
C	-1.93256	1.03170	2.05573
O	-3.03263	1.33386	1.89886
C	-0.04159	-1.28015	2.62026
O	-0.11018	-2.39813	2.85462
C	2.10941	0.80027	2.08847
O	3.24108	0.95420	1.96169
C	-3.36722	-2.23645	2.97988
C	3.14206	-2.66617	2.91686
C	-2.86084	-2.66490	-3.91807
C	1.96621	-0.51795	-4.02016
C	6.99328	-0.63002	-1.77517
C	-7.07251	0.19143	-1.65199
H	-2.79326	-1.31229	3.04499
H	-3.03945	-2.89196	3.78963

H	-4.41776	-1.99458	3.16074
H	-2.13091	-3.26498	1.58453
H	4.21711	-2.54966	3.07645
H	2.75640	-3.28395	3.73083
H	2.68197	-1.68151	2.99714
H	-2.45072	-4.79480	-1.07868
H	1.81755	-5.07480	-1.11182
H	-2.60288	2.05830	-1.20135
H	-2.77054	3.23981	-2.50065
H	5.00003	-1.75892	1.24259
H	1.76627	-3.53579	1.54433
H	4.21615	-0.38423	-2.70468
H	1.87621	3.86855	-2.97045
H	1.47774	2.25342	-2.40691
H	-3.36317	4.39345	-0.42339
H	-1.93536	3.75874	0.38854
H	-1.19559	-1.81430	-2.90071
H	-0.39872	-6.15621	-1.26192
H	-4.31325	0.11107	-2.63977
H	0.91343	-1.99346	-2.92068
H	-5.14823	-1.13575	1.33980
H	1.98611	3.06110	-0.02398
H	3.32458	2.81572	-1.11283
H	4.65921	-4.50192	1.50082
H	3.33720	-5.18796	0.55384
H	3.31262	-5.30962	2.31837
H	-2.85396	-3.58666	-3.33464
H	-2.31964	-2.84856	-4.85032
H	-3.89932	-2.42771	-4.16616
H	-3.12090	0.04297	-4.37236
H	-1.51458	-0.46275	-4.88005
H	-1.69264	0.56186	-3.45507
H	-2.03854	5.84859	-1.83215
H	-1.40707	6.01634	-0.18979
H	7.19888	-1.70011	-1.70486
H	7.94180	-0.09180	-1.69896
H	6.57950	-0.43536	-2.76842
H	1.59174	0.33255	-3.44589
H	1.31791	-0.64632	-4.89039
H	2.96520	-0.27780	-4.39358
H	6.49861	-0.38573	0.28586
H	-6.65877	0.34354	-2.65265
H	-7.95574	0.82871	-1.55727
H	-7.39129	-0.85031	-1.57943
H	3.53119	-2.82237	-4.24044
H	1.90939	-3.09552	-4.90099

H	2.40302	-3.89536	-3.40238
H	-5.11596	-3.89238	1.61069
H	-3.85317	-4.84457	2.40609
H	-3.90236	-4.73149	0.64171
H	0.26641	6.94621	-1.38911
H	1.29642	6.03601	-2.47389
H	5.30703	1.57927	-1.71930
H	6.70242	1.88029	-0.67948
H	5.09963	1.63818	0.04034
H	-4.90853	2.23379	0.12829
H	-6.49277	2.65049	-0.55116
H	-5.16505	2.20759	-1.62751
H	3.66923	4.87034	0.13872
H	3.51458	5.20749	-1.57352
H	2.32921	6.88452	-0.27372
H	1.36825	5.66473	0.55188
H	-0.48611	1.80640	-1.92969
H	-6.51734	0.37447	0.39977

4.6 References

(1) Hadlington, T. J.; Driess, M.; Jones, C., Low-valent group 14 element hydride chemistry: towards catalysis. *Chem. Soc. Rev.* **2018,** *47*, 4176-4197.

(2) Hadlington, T. J.; Hermann, M.; Frenking, G.; Jones, C., Low Coordinate Germanium(II) and Tin(II) Hydride Complexes: Efficient Catalysts for the Hydroboration of Carbonyl Compounds. *J. Am. Chem. Soc.* **2014,** *136*, 3028-3031.

(3) Hadlington, T. J.; Kefalidis, C. E.; Maron, L.; Jones, C., Efficient Reduction of Carbon Dioxide to Methanol Equivalents Catalyzed by Two-Coordinate Amido–Germanium(II) and −Tin(II) Hydride Complexes. *ACS Catal.* **2017,** *7*, 1853-1859.

(4) Erickson, J. D.; Lai, T. Y.; Liptrot, D. J.; Olmstead, M. M.; Power, P. P., Catalytic dehydrocoupling of amines and boranes by an incipient tin(II) hydride. *Chem. Commun.* **2016,** *52*, 13656-13659.

(5) Schneider, J.; Sindlinger, C. P.; Freitag, S. M.; Schubert, H.; Wesemann, L., Diverse Activation Modes in the Hydroboration of Aldehydes and Ketones with Germanium, Tin, and Lead Lewis Pairs. *Angew. Chem. Int. Ed.* **2017,** *56*, 333-337.

(6) Villegas-Escobar, N.; Schaefer, H. F.; Toro-Labbé, A., Formation of Formic Acid Derivatives through Activation and Hydroboration of CO_2 by Low-Valent Group 14 (Si, Ge, Sn, Pb) Catalysts. *J. Phys. Chem. A* **2020,** *124*, 1121-1133.

(7) Rivard, E.; Power, P. P., Recent developments in the chemistry of low valent Group 14 hydrides. *Dalton Trans.* **2008**, 4336-4343.

(8) Aldridge, S.; Downs, A. J., Hydrides of the Main-Group Metals: New Variations on an Old Theme. *Chem. Rev.* **2001,** *101*, 3305-3366.

(9) Roy, M. M. D.; Omaña, A. A.; Wilson, A. S. S.; Hill, M. S.; Aldridge, S.; Rivard, E., Molecular Main Group Metal Hydrides. *Chem. Rev.* **2021,** *121*, 12784-12965.

(10) Eichler, B. E.; Power, P. P., $[2,6\text{-Trip}_2H_3C_6Sn(\mu\text{-}H)]_2$ (Trip = C_6H_2-2,4,6-i-Pr_3): Synthesis and Structure of a Divalent Group 14 Element Hydride. *J. Am. Chem. Soc.* **2000,** *122*, 8785-8786.

(11) Pineda, L. W.; Jancik, V.; Starke, K.; Oswald, R. B.; Roesky, H. W., Stable Monomeric Germanium(II) and Tin(II) Compounds with Terminal Hydrides. *Angew. Chem. Int. Ed.* **2006,** *45*, 2602-2605.

(12) Khan, S.; Samuel, P. P.; Michel, R.; Dieterich, J. M.; Mata, R. A.; Demers, J.-P.; Lange, A.; Roesky, H. W.; Stalke, D., Monomeric Sn(II) and Ge(II) hydrides supported by a tridentate pincer-based ligand. *Chem. Commun.* **2012,** *48*, 4890-4892.

(13) Maudrich, J.-J.; Sindlinger, C. P.; Aicher, F. S. W.; Eichele, K.; Schubert, H.; Wesemann, L., Reductive Elimination of Hydrogen from Bis(trimethylsilyl)methyltin Trihydride and Mesityltin Trihydride. *Chem. Eur. J.* **2017,** *23*, 2192-2200.

(14) Sindlinger, C. P.; Wesemann, L., Hydrogen abstraction from organotin di- and trihydrides by N-heterocyclic carbenes: a new method for the preparation of NHC adducts to tin(II) species and observation of an isomer of a hexastannabenzene derivative $[R_6Sn_6]$. *Chem. Sci.* **2014,** *5*, 2739-2746.

(15) Sindlinger, C. P.; Grahneis, W.; Aicher, F. S. W.; Wesemann, L., Access to Base Adducts of Low-Valent Organotin-Hydride Compounds by Controlled, Stepwise Hydrogen Abstraction from a Tetravalent Organotin Trihydride. *Chem. Eur. J.* **2016,** *22*, 7554-7566.

(16) Petz, W., Transition-metal complexes with derivatives of divalent silicon, germanium, tin, and lead as ligands. *Chem. Rev.* **1986,** *86*, 1019-1047.

(17) Filippou, A. C.; Philippopoulos, A. I.; Schnakenburg, G., Triple Bonding to Tin: Synthesis and Characterization of the Square-Pyramidal Stannylyne Complex Cation $[(dppe)_2W{\equiv}Sn{-}C_6H_3\text{-}2,6\text{-}Mes_2]^+$ (dppe = $Ph_2PCH_2CH_2PPh_2$, Mes = $C_6H_2\text{-}2,4,6\text{-}Me_3$). *Organometallics* **2003,** *22*, 3339-3341.

(18) Filippou, A. C.; Portius, P.; Philippopoulos, A. I.; Rohde, H., Triple Bonding to Tin: Synthesis and Characterization of the Stannylyne Complex trans-[Cl(PMe3)4W≡Sn-C6H3-2,6-Mes2]. *Angew. Chem. Int. Ed.* **2003,** *42*, 445-447.

(19) Queen, J. D.; Phung, A. C.; Caputo, C. A.; Fettinger, J. C.; Power, P. P., Metathetical Exchange between Metal-Metal Triple Bonds. *J. Am. Chem. Soc.* **2020,** *142*, 2233-2237.

(20) Rivard, E.; Fischer, R. C.; Wolf, R.; Peng, Y.; Merrill, W. A.; Schley, N. D.; Zhu, Z.; Pu, L.; Fettinger, J. C.; Teat, S. J.; Nowik, I.; Herber, R. H.; Takagi, N.; Nagase, S.; Power, P. P., Isomeric Forms of Heavier Main Group Hydrides: Experimental and Theoretical Studies of the $[Sn(Ar)H]_2$ (Ar = Terphenyl) System. *J. Am. Chem. Soc.* **2007,** *129*, 16197-16208.

(21) Rivard, E.; Steiner, J.; Fettinger, J. C.; Giuliani, J. R.; Augustine, M. P.; Power, P. P., Convergent syntheses of $[Sn_7\{C_6H_3\text{-}2,6\text{-}(C_6H_3\text{-}2,6\text{-}^iPr_2)_2\}_2]$: a cluster with a rare pentagonal bipyramidal motif. *Chem. Commun.* **2007**, 4919-4921.

(22) Wang, S.; Sherbow, T. J.; Berben, L. A.; Power, P. P., Reversible Coordination of H_2 by a Distannyne. *J. Am. Chem. Soc.* **2018,** *140*, 590-593.

(23) Al-Rafia, S. M. I.; Malcolm, A. C.; Liew, S. K.; Ferguson, M. J.; Rivard, E., Stabilization of the Heavy Methylene Analogues, GeH_2 and SnH_2, within the Coordination Sphere of a Transition Metal. *J. Am. Chem. Soc.* **2011,** *133*, 777-779.

(24) Novák, M.; Dostál, L.; Růžičková, Z.; Mebs, S.; Beckmann, J.; Jambor, R., From Monomeric Tin(II) Hydride to Nonsymmetric Distannyne. *Organometallics* **2019,** *38*, 2403-2407.

(25) Widemann, M.; Jeggle, S.; Auer, M.; Eichele, K.; Schubert, H.; Sindlinger, C. P.; Wesemann, L., Hydridotetrylene [Ar*EH] (E = Ge, Sn, Pb) coordination at tantalum, tungsten, and zirconium. *Chem. Sci.* **2022**, 13, 3999-4009.

(26) Maudrich, J.-J.; Widemann, M.; Diab, F.; Kern, R. H.; Sirsch, P.; Sindlinger, C. P.; Schubert, H.; Wesemann, L., Hydridoorganostannylene Coordination: Group 4 Metallocene Dichloride Reduction in Reaction with Organodihydridostannate Anions. *Chem. Eur. J.* **2019,** *25*, 16081-16087.

(27) Zhu, Q.; Fettinger, J. C.; Power, P. P., Hydrostannylation of carbon dioxide by a hydridostannylene molybdenum complex. *Dalton Trans.* **2021,** *50*, 12555-12562.

(28) Weiß, S.; Widemann, M.; Eichele, K.; Schubert, H.; Wesemann, L., Low valent lead and tin hydrides in reactions with heteroallenes. *Dalton Trans.* **2021,** *50*, 4952-4958.

(29) Wang, S.; McCrea-Hendrick, M. L.; Weinstein, C. M.; Caputo, C. A.; Hoppe, E.; Fettinger, J. C.; Olmstead, M. M.; Power, P. P., Dynamic Behavior and Isomerization Equilibria of Distannenes Synthesized by Tin Hydride/Olefin Insertions: Characterization of the Elusive Monohydrido Bridged Isomer. *J. Am. Chem. Soc.* **2017,** *139*, 6586-6595.

(30) Peng, Y.; Ellis, B. D.; Wang, X.; Fettinger, J. C.; Power, P. P., Reversible Reactions of Ethylene with Distannynes Under Ambient Conditions. *Science* **2009,** *325*, 1668-1670.

(31) Hadlington, T. J.; Hermann, M.; Li, J.; Frenking, G.; Jones, C., Activation of H_2 by a Multiply Bonded Amido–Digermyne: Evidence for the Formation of a Hydrido–Germylene. *Angew. Chem. Int. Ed.* **2013,** *52*, 10199-10203.

(32) Lücke, M.-P.; Yao, S.; Driess, M., Boosting homogeneous chemoselective hydrogenation of olefins mediated by a bis(silylenyl)terphenyl-nickel(0) pre-catalyst. *Chem. Sci.* **2021,** *12*, 2909-2915.

(33) Glaser, P. B.; Tilley, T. D., Catalytic Hydrosilylation of Alkenes by a Ruthenium Silylene Complex. Evidence for a New Hydrosilylation Mechanism. *J. Am. Chem. Soc.* **2003,** *125*, 13640-13641.

(34) Wu, J.; Thiyagarajan, S.; Fonseca Guerra, C.; Eduard, P.; Lutz, M.; Noordover, B. A. J.; Koning, C. E.; van Es, D. S., Isohexide Dinitriles: A Versatile Family of Renewable Platform Chemicals. *ChemSusChem* **2017,** *10*, 3202-3211.

(35) Pangborn, A. B.; Giardello, M. A.; Grubbs, R. H.; Rosen, R. K.; Timmers, F. J., Safe and Convenient Procedure for Solvent Purification. *Organometallics* **1996,** *15*, 1518-1520.

(36) Boylan, M. J.; Braterman, P. S.; Fullarton, A., Metal carbonyl photolysis and its reversal;probable spurious nature of "trigonal bipyramidal $Mo(CO)_5$". *J. Organomet. Chem.* **1971,** *31*, C29-C30.

(37) Pu, L.; Twamley, B.; Power, P. P., Terphenyl Ligand Stabilized Lead(II) Derivatives of Simple Organic Groups: Characterization of $Pb(R)C_6H_3$-2,6-$Trip_2$ (R = Me, t-Bu, or Ph; Trip = C_6H_2-2,4,6-i-Pr_3), $\{Pb(\mu\text{-}Br)C_6H_3\text{-}2,6\text{-}Trip_2\}_2$, py·$Pb(Br)C_6H_3$-2,6-$Trip_2$ (py = Pyridine), and the Bridged Plumbylyne Complex $[\{W(CO)_4\}_2(\mu\text{-}Br)(\mu\text{-}PbC_6H_3\text{-}2,6\text{-}Trip_2)]$. *Organometallics* **2000,** *19*, 2874-2881.

(38) Hadlington, T. J.; Hermann, M.; Frenking, G.; Jones, C., Two-coordinate group 14 element(II) hydrides as reagents for the facile, and sometimes reversible,

hydrogermylation/hydrostannylation of unactivated alkenes and alkynes. *Chem. Sci.* **2015,** *6*, 7249-7257.

(39) Pyykkö, P.; Atsumi, M., Molecular Single-Bond Covalent Radii for Elements 1–118. *Chem. Eur. J.* **2009,** *15*, 186-197.

(40) Lappert, M. F.; Power, P. P.; Slade, M. J.; Hedberg, L.; Hedberg, K.; Schomaker, V., Monomeric bivalent group 4B metal dialkylamides $M[NCMe_2(CH_2)_3CMe_2]_2$ (M = Ge or Sn), and the structure of a gaseous disilylamide, $Sn[N(SiMe_3)_2]_2$, by gas electron diffraction. *J. Chem. Soc., Chem. Commun.* **1979**, 369-370.

(41) Mansell, S. M.; Russell, C. A.; Wass, D. F., Synthesis and Structural Characterization of Tin Analogues of N-Heterocyclic Carbenes. *Inorg. Chem.* **2008,** *47*, 11367-11375.

(42) Mansell, S. M.; Herber, R. H.; Nowik, I.; Ross, D. H.; Russell, C. A.; Wass, D. F., Coordination Chemistry of N-Heterocyclic Stannylenes: A Combined Synthetic and Mössbauer Spectroscopy Study. *Inorg. Chem.* **2011,** *50*, 2252-2263.

(43) Jambor, R.; Kašná, B.; Koller, S. G.; Strohmann, C.; Schürmann, M.; Jurkschat, K., $[\{2,6\text{-}(Me_2NCH_2)_2C_6H_3(H_2O)Sn\}W(CO)_5]^+\text{-}CB_{11}H_{12}^-$: Aqua Complex of a Transition-Metal-Bound Organotin(II) Cation versus an Ammonium-Type Structure. *Eur. J. Inorg. Chem.* **2010,** 902-908.

(44) Balch, A. L.; Oram, D. E., Four- and five-coordinate tin(II) (stannylene) compounds: crystal and molecular structures of $W(CO)_5\{SnCl_2(OC_4H_8)\}$ and $W(CO)_5\{SnCl_2(OC_4H_8)_2\}$. *Organometallics* **1988,** *7*, 155-158.

(45) Weidenbruch, M.; Stilter, A.; Schlaefke, J.; Peters, K.; Schnering, H. G. v., Compounds of germanium and tin XIV. Rearrangement of bis(2,4,6-tri-tert-butylphenyl)stannylene: synthesis and structure of a donor-free alkylarylstannylene-tungsten complex. *J. Organomet. Chem.* **1995,** *501*, 67-70.

(46) Kašná, B.; Jambor, R.; Schürman, M.; Jurkschat, K., Synthesis and characterization of novel intramolecularly O,C,O-coordinated heteroleptic organostannylenes and their tungstenpentacarbonyl complexes. *J. Organomet. Chem.* **2008,** *693*, 3446-3450.

(47) Jambor, R.; Herres-Pawlis, S.; Schürmann, M.; Jurkschat, K., [{2,6-$(Me_2NCH_2)_2C_6H_3$}Sn(μ-OH)$W(CO)_5]_2$: A Transition-Metal-Coordinated Organotin(II) Hydroxide. *Eur. J. Inorg. Chem.* **2011,** 344-348.

(48) Hashimoto, H.; Nagata, K., Transition-metal Complexes with Triple Bonds to Si, Ge, Sn, and Pb and Relevant Complexes. *Chem. Lett.* **2021,** *50*, 778-787.

(49) Lebedev, Y. N.; Das, U.; Schnakenburg, G.; Filippou, A. C., Coordination Chemistry of $[E(Idipp)]^{2+}$ Ligands (E = Ge, Sn): Metal Germylidyne $[Cp^*(CO)_2W{\equiv}Ge(Idipp)]^+$ and Metallotetrylene $[Cp^*(CO)_3W–E(Idipp)]^+$ Cations. *Organometallics* **2017,** *36*, 1530-1540.

(50) Eichler, B. E.; Phillips, A. D.; Haubrich, S. T.; Mork, B. V.; Power, P. P., Synthesis, Structures, and Spectroscopy of the Metallostannylenes $(\eta^5\text{-}C_5H_5)(CO)_3M{-}\ddot{S}n{-}C_6H_3\text{-}2,6\text{-}Ar_2$ (M = Cr, Mo, W; Ar = C_6H_2-2,4,6-Me_3, C_6H_2-2,4,6-Pr^i_3). *Organometallics* **2002,** *21*, 5622-5627.

(51) McCrea-Hendrick, M. L.; Caputo, C. A.; Linnera, J.; Vasko, P.; Weinstein, C. M.; Fettinger, J. C.; Tuononen, H. M.; Power, P. P., Cleavage of Ge–Ge and Sn–Sn Triple Bonds in Heavy Group 14 Element Alkyne Analogues $(EAr^{iPr4})_2$ (E = Ge, Sn; Ar^{iPr4} = C_6H_3-2,6(C_6H_3-2,6-$^iPr_2)_2$) by Reaction with Group 6 Carbonyls. *Organometallics* **2016,** *35*, 2759-2767.

(52) Hayes, P. G.; Gribble, C. W.; Waterman, R.; Tilley, T. D., A Hydrogen-Substituted Osmium Stannylene Complex: Isomerization to a Metallostannylene Complex via an Unusual α-Hydrogen Migration from Tin to Osmium. *J. Am. Chem. Soc.* **2009,** *131*, 4606-4607.

(53) Vícha, J.; Marek, R.; Straka, M., High-Frequency 1H NMR Chemical Shifts of SnII and PbII Hydrides Induced by Relativistic Effects: Quest for PbII Hydrides. *Inorg. Chem.* **2016,** *55*, 10302-10309.

(54) Weidenbruch, M.; Stilter, A.; Peters, K.; von Schnering, H. G., Verbindungen des Germainums und Zinns. Alkylarylstannylen-Komplexe des Chroms und Molybdäns ohne Donorstabilisierung. *Z. Anorg. Allg. Chem.* **1996,** *622*, 534-538.

(55) Weidenbruch, M.; Stilter, A.; Saak, W.; Peters, K.; von Schnering, H. G., An octahedral stannylmanganese stannylene complex. *J. Organomet. Chem.* **1998,** *560*, 125-129.

(56) Schneider, J. J.; Czap, N.; Bläser, D.; Boese, R., Metal Atom Synthesis of (η^6-Toluene)(η^2-ethene)iron(σ^1-stannandiyls): Unusual Iron(0) Complexes. *J. Am. Chem. Soc.* **1999,** *121*, 1409-1410.

(57) Bareš, J.; Richard, P.; Meunier, P.; Pirio, N.; Padělková, Z.; Černošek, Z.; Císařová, I.; Růžička, A., Reactions of C,N-chelated Tin(II) and Lead(II) Compounds with Zirconocene Dichloride Derivatives. *Organometallics* **2009,** *28*, 3105-3108.

(58) Schneider, J. J.; Czap, N.; Bläser, D.; Boese, R.; Ensling, J.; Gütlich, P.; Janiak, C., Experimental and Theoretical Investigations on the Synthesis, Structure, Reactivity, and Bonding of the Stannylene-Iron Complex Bis{{bis(2-tert-butyl-4,5,6-trimethyl-phenyl)}Sn}Fe(η^6-toluene). *Chem. Eur. J.* **2000,** *6*, 468-474.

(59) Kircher, P.; Huttner, G.; Heinze, K.; Schiemenz, B.; Zsolnai, L.; Büchner, M.; Driess, A., Four-Coordinate Group-14 Elements in the Formal Oxidation State of Zero – Syntheses, Structures, and Dynamics of [{$(CO)_5Cr$}$_2$Sn(L_2)] and Related Species. *Eur. J. Inorg. Chem.* **1998,** 703-720.

(60) Wang, P.; Zhang, M.; Zhu, C., Synthesis, Characterization, and Reactivity of a Pincer-Type Aluminum(III) Complex. *Organometallics* **2020,** *39*, 2732-2738.

(61) Sole, R. D.; Luca, A. D.; Mele, G.; Vasapollo, G., First evidence of formation of stable DBU Zn-phthalocyanine complexes: synthesis and characterization. *J. Porphyr. Phthalocyanines* **2005,** *09*, 519-527.

(62) Agou, T.; Ikeda, S.; Sasamori, T.; Tokitoh, N., Synthesis and Structure of Lewis Base-Coordinated Phosphanylalumanes Bearing P–H and Al–Br Moieties. *Eur. J. Inorg. Chem.* **2018,** 1984-1987.

(63) Frisch, M. J.; Trucks, G. W.; Schlegel, H. B.; Scuseria, G. E.; Robb, M. A.; Cheeseman, J. R.; Scalmani, G.; Barone, V.; Petersson, G. A.; Nakatsuji, H.; Li, X.; Caricato, M.; Marenich, A. V.; Bloino, J.; Janesko, B. G.; Gomperts, R.; Mennucci, B.; Hratchian, H. P.; Ortiz, J. V.; Izmaylov, A. F.; Sonnenberg, J. L.; Williams; Ding, F.; Lipparini, F.; Egidi, F.; Goings, J.; Peng, B.; Petrone, A.; Henderson, T.; Ranasinghe, D.; Zakrzewski, V. G.; Gao, J.; Rega, N.; Zheng, G.; Liang, W.; Hada, M.; Ehara, M.; Toyota, K.; Fukuda, R.; Hasegawa, J.; Ishida, M.; Nakajima, T.; Honda, Y.; Kitao, O.; Nakai, H.; Vreven, T.; Throssell, K.; Montgomery Jr., J. A.; Peralta, J. E.; Ogliaro, F.; Bearpark, M. J.; Heyd, J. J.; Brothers, E. N.; Kudin, K. N.; Staroverov, V. N.; Keith, T. A.; Kobayashi, R.; Normand, J.; Raghavachari, K.; Rendell, A. P.; Burant, J. C.; Iyengar, S. S.; Tomasi, J.; Cossi, M.; Millam, J. M.; Klene, M.; Adamo, C.; Cammi, R.; Ochterski, J. W.; Martin, R. L.; Morokuma, K.; Farkas, O.; Foresman, J. B.; Fox, D. J. Gaussian 16 Rev. C.01, 2016.

(64) Perdew, J. P.; Burke, K.; Ernzerhof, M. Generalized Gradient Approximation Made Simple. *Phys. Rev. Lett.* **1996**, *77*, 3865–3868. https://doi.org/10.1103/PhysRevLett.77.3865.

(65) Perdew, J. P.; Burke, K.; Ernzerhof, M. Generalized Gradient Approximation Made Simple [Phys. Rev. Lett. 77, 3865 (1996)]. *Phys. Rev. Lett.* **1997**, *78*, 1396–1396. https://doi.org/10.1103/PhysRevLett.78.1396.

(66) Adamo, C.; Barone, V. Toward Reliable Density Functional Methods without Adjustable Parameters: The PBE0 Model. *J. Chem. Phys.* **1999**, *110*, 6158–6170. https://doi.org/10.1063/1.478522.

(67) Weigend, F.; Ahlrichs, R. Balanced Basis Sets of Split Valence, Triple Zeta Valence and Quadruple Zeta Valence Quality for H to Rn: Design and Assessment of Accuracy. *Phys. Chem. Chem. Phys.* **2005**, *7*, 3297–3305. https://doi.org/10.1039/B508541A.

(68) Weigend, F. Accurate Coulomb-Fitting Basis Sets for H to Rn. *Phys. Chem. Chem. Phys.* **2006**, *8*, 1057–1065. https://doi.org/10.1039/B515623H.

(69) Grimme, S.; Ehrlich, S.; Goerigk, L. Effect of the Damping Function in Dispersion Corrected Density Functional Theory. *J. Comput. Chem.* **2011**, *32*, 1456–1465. https://doi.org/10.1002/jcc.21759.

(70) Alecu, I. M.; Zheng, J.; Zhao, Y.; Truhlar, D. G. Computational Thermochemistry: Scale Factor Databases and Scale Factors for Vibrational Frequencies Obtained from Electronic Model Chemistries. *J. Chem. Theory Comput.* **2010**, *6*, 2872–2887. https://doi.org/10.1021/ct100326h.